

arXiv:1803.06478v1 [hep-ph] 17 Mar 2018

Exploring physics beyond the Standard Electroweak Model in the light of supersymmetry

Thesis Submitted to
The University of Calcutta
for The Degree of
Doctor of Philosophy (Science)

By

Pradipta Ghosh

Advisers: Sourov Roy & Utpal Chattopadhyay



**Department of Theoretical Physics
Indian Association for the Cultivation of Science
Kolkata, India**

2011

Abstract

Weak scale supersymmetry has perhaps become the most popular choice for explaining new physics beyond the standard model. An extension beyond the standard model was essential to explain issues like gauge-hierarchy problem or non-vanishing neutrino mass. With the initiation of the large hadron collider era at CERN, discovery of weak-scale supersymmetric particles and, of course, Higgs boson are envisaged. In this thesis we try to discuss certain phenomenological aspects of an R_p -violating non-minimal supersymmetric model, called $\mu\nu$ SSM. We show that $\mu\nu$ SSM can provide a solution to the μ -problem of supersymmetry and can simultaneously accommodate the existing three flavour global data from neutrino experiments even at the tree level with the simple choice of flavour diagonal neutrino Yukawa couplings. We show that it is also possible to achieve different mass hierarchies for light neutrinos at the tree level itself. In $\mu\nu$ SSM, the effect of R -parity violation together with a seesaw mechanism with TeV scale right-handed neutrinos are instrumental for light neutrino mass generation. We also analyze the stability of tree level neutrino masses and mixing with the inclusion of one-loop radiative corrections. In addition, we investigate the sensitivity of the one-loop corrections to different light neutrino mass orderings. Decays of the lightest supersymmetric particle were also computed and ratio of certain decay branching ratios was observed to correlate with certain neutrino mixing angle. We extend our analysis for different natures of the lightest supersymmetric particle as well as with various light neutrino mass hierarchies. We present estimation for the length of associated displaced vertices for various natures of the lightest supersymmetric particle which can act as a discriminating feature at a collider experiment. We also present an unconventional signal of Higgs boson in supersymmetry which can lead to a discovery, even at the initial stage of the large hadron collider running. Besides, we show that a signal of this kind can also act as a probe to the seesaw scale. Certain other phenomenological issues have also been addressed.

To a teacher who is like the pole star to me and many others

Dr. Ranjan Ray

1949 - 2001

Acknowledgment

I am grateful to the Council of Scientific and Industrial Research, Government of India for providing me the financial assistance for the completion of my thesis work (Award No. 09/080(0539)/2007-EMR-I (Date 12.03.2007)). I am also thankful to my home institute for a junior research fellowship that I had enjoyed from August, 2006 to January, 2007.

I have no words to express my gratitude to the members of theoretical high energy physics group of the Department of Theoretical Physics of my home institute, particularly Dr. Utpal Chattopadhyay and Dr. Sourov Roy. Their gratuitous infinite patience for my academic and personal problems, unconditional affection to me, heart-rending analysis of my performance, cordial pray for my success, spontaneous and constant motivations for facing new challenges were beyond the conventional teacher-student relation. I am also grateful to Dr. Dilip Kumar Ghosh, Dr. Pushan Majumdar, Dr. Koushik Ray, Prof. Siddhartha Sen and Prof. Soumitra SenGupta of the same group for their encouragement, spontaneous affection, crucial guidance and of course criticism, in academics and life beyond it. It is also my pleasure to thank Dr. Shudhanshu Sekhar Mandal and Dr. Krishnendu Sengupta of the condensed matter group. It is an honour for me to express my respect to Prof. Jayanta Kumar Bhattacharjee not only for his marvelous teaching, but also for explaining me a different meaning of academics.

I sincerely acknowledge the hard efforts and sincere commitments of my collaborators Dr. Priyotosh Bandopadhyay and Dr. Paramita Dey to the research projects. I am thankful to them for their level of tolerance to my infinite curiosity in spite of their extreme busy schedules. I learned several new techniques and some rare insights of the subjects from them. In the course of scientific collaboration I have been privileged to work with Prof. Biswarup Mukhopadhyaya, who never allowed me to realize the two decades of age difference between us. Apart from his precious scientific guidance (I was also fortunate enough to attend his teaching), his affection and inspiration for me has earned an eternal mark in my memory just like his signature smile.

It is my duty to express my sincere gratitude to all of my teachers, starting from the very basic level till date. It was their kind and hard efforts which help me to reach here. I am especially grateful to Ms. Anuradha SenSarma and Mr. Malay Ghosh for their enthusiastic efforts and selfless sacrifices during my school days. I have no words to express my respect to Prof. Anirban Kundu and Prof. Amitava Raychaudhuri for their precious guidance and unconventional teaching during my post-graduate studies. I am really fortunate enough to receive their affection and guidance till date. In this connection I express my modest gratitude to some of the renowned experts of the community for their valuable advise and encouragement. They were always very generous to answer even some of my stupid questions, in spite of their extremely busy professional schedules. I am particularly grateful to Dr. Satyaki Bhattacharya, Prof. Debajyoti Choudhury, Dr. Anindya Datta, Dr. Aseshkrishna Datta, Dr. Manas Maity, Prof. Bruce Mellado, Dr. Sujoy Poddar, Dr. Subhendu Rakshit and Prof. Sreerup Raychaudhuri for many useful suggestions and very helpful discussions.

I also express my humble thanks to my home institute, Indian Association for the Cultivation of Science, for providing all the facilities like high-performance personal desktop, constant and affluent access to high-speed internet, a homely atmosphere and definitely a world class library. I am also thankful to all the non-teaching staff members of my department (Mr. Subrata Balti, Mr. Bikash Darji, Mr. Bhudeb Ghosh, Mr. Tapan Moulik and Mr. Suresh Mondal) who were always there to assist us. It is my honour to thank the Director of my home institute, Prof. Kankan Bhattacharyya for the encouragement I received from him.

It is a pleasure to express my thanks to my colleagues and friends who were always there to cheer me up when things were not so smooth either in academics or in personal life. My cordial and special thanks to Dr. Naba Kumar Bera, Dr. Debottam Das, Sudipto Paul Chowdhury, Dwipesh Majumder and Joydip Mitra who were not just my colleagues but were, are and always will be my brothers. I am really thankful to them and also to Dr. Shyamal Biswas, Amit Chakraborty, Dr. Dipanjan Chakrabarti, Manimala Chakraborty, Sabyasachi Chakraborty, Anirban Datta, Ashmita Das, Sanjib Ghosh, Dr. R. S. Hundi, Dr. Ratna Koley, Dr. Debaprasad Maity, Sourav Mondal, Subhadeep Mondal, Sanhita Modak, Shreyoshi Mondal, Dr. Soumya Prasad Mukherjee, Sutirtha Mukherjee, Tapan Naskar, Dr. Himadri Sekhar Samanta, Kush Saha, Ipsita Saha and Ankur Sensharma for making my office my second home.

It is definitely the worst injustice to acknowledge the support of my family as without them I believe it is just like getting lost in crowd.

I cannot resist myself to show my humble tribute to three personalities, who by the philosophy of their lives and works have influenced diverse aspects of my life. The scientist who was born long before his time, Richard P. Feynman, the writer who showed that field of expertise is not really a constraint, Narayan Sanyal and my old friend, Mark.

Pradipta Ghosh

List of Publications

In refereed journals.

- **Radiative contribution to neutrino masses and mixing in $\mu\nu$ SSM.**
Pradipta Ghosh, Paramita Dey, Biswarup Mukhopadhyaya, Sourov Roy.
Journal of High Energy Physics 05 (2010) 087, [arXiv:1002.2705 \[hep-ph\]](#).
- **Neutrino masses and mixing, lightest neutralino decays and a solution to the μ problem in supersymmetry.**
Pradipta Ghosh, Sourov Roy.
Journal of High Energy Physics 04 (2009) 069, [arXiv:0812.0084 \[hep-ph\]](#).

Preprints.

- **An unusual signal of Higgs boson in supersymmetry at the LHC.**
Priyotosh Bandyopadhyay, Pradipta Ghosh, Sourov Roy.
Phys. Rev. D 84 (2011) 115022, [arXiv:1012.5762 \[hep-ph\]](#)¹.

In proceedings.

- **Neutrino masses and mixing in $\mu\nu$ SSM.**
2010 J. Phys.: Conf. Ser. 259 012063, [arXiv:1010.2578 \[hep-ph\]](#), PASCOS 2010
- **Neutrino masses and mixing in a supersymmetric model and characteristic signatures at the LHC.**
Proceedings of the XVIII DAE-BRNS symposium, Vol. 18, 2008, 140-143.

¹Now published as “Unusual Higgs boson signal in R-parity violating nonminimal supersymmetric models at the LHC” in *Phys. Rev. D* 84 (2011) 115022.

Motivation and plan of the thesis

The standard model of the particle physics is extremely successful in explaining the elementary particle interactions, as has been firmly established by a host of experiments. However, unfortunately there exist certain issues where the standard model is an apparent failure, like unnatural fine tuning associated with the mass of the hitherto unseen Higgs boson or explaining massive neutrinos, as confirmed by neutrino oscillation experiments. A collective approach to address these shortcomings requires extension beyond the standard model framework. The weak scale supersymmetry has been a very favourite choice to explain physics beyond the standard model where by virtue of the construction, the mass of Higgs boson is apparently free from fine-tuning problem. On the other hand, violation of a discrete symmetry called R -parity is an intrinsically supersymmetric way of accommodating massive neutrinos. But, in spite of all these successes supersymmetric theories are also not free from drawbacks and that results in a wide variety of models. Besides, not a single supersymmetric particle has been experimentally discovered yet. Nevertheless, possibility of discovering weak scale supersymmetric particles as well as Higgs boson are highly envisaged with the initiation of the large hadron collider experiment at CERN.

In this thesis we plan to study a few phenomenological aspects of a particular variant of R -parity violating supersymmetric model, popularly known as the $\mu\nu$ SSM. This model offers a solution for the μ -problem of the minimal supersymmetric standard model and simultaneously accommodate massive neutrinos with the use of a common set of right-handed neutrino superfields. Initially, we aimed to accommodate massive neutrinos in this model consistent with the three flavour global neutrino data with tree level analysis for different schemes of light neutrino masses. Besides, as the lightest supersymmetric particle is unstable due to R -parity violation, we also tried to explore the possible correlations between light neutrino mixing angles with the branching ratios of the decay modes of the lightest supersymmetric particle (which is usually the lightest neutralino for an appreciable region of the parameter space) as a possible check of this model in a collider experiment. Later on we looked forward to re-investigate the tree level analysis with the inclusion of one-loop radiative corrections. We were also keen to study the sensitivity of our one-loop corrected results to the light neutrino mass hierarchy. Finally, we proposed an unconventional background free signal for Higgs boson in $\mu\nu$ SSM which can concurrently act as a probe to the seesaw scale. A signal of this kind not only can lead to an early discovery, but also act as an unique collider signature of $\mu\nu$ SSM.

This thesis is organized as follows, we start with a brief introduction of the standard model in chapter 1, discuss the very basics of mathematical formulations and address the apparent successes and shortcomings. We start our discussion in chapter 2 by studying how the quadratic divergences in the standard model Higgs boson mass can be handled in a supersymmetric theory. We also discuss the relevant mathematical formulations, address the successes and drawbacks of the minimal supersymmetric standard model with special attentions on the μ -problem and the R -parity. A small discussion on the next-to-minimal supersymmetric standard model has also been addressed. We devote chapter 3 for neutrinos. The issues of neutrino mass generation both in supersymmetric and non-supersymmetric models have been addressed for tree level as well as for one-loop level analysis. Besides, implications of neutrino physics in a collider analysis has been discussed. Light neutrino masses and mixing in $\mu\nu$ SSM both for tree level and one-loop level analysis are given in chapter 4. The $\mu\nu$ SSM model has been discussed more extensively in this chapter. We present the results of correlation study between the neutrino mixing angles and the branching ratios of the decay modes of the lightest neutralino in $\mu\nu$ SSM in chapter 5. Our results are given for different natures of the lightest neutralino with different hierarchies in light neutrino masses. Finally, in chapter 6 we present an unusual background

free signal for Higgs boson in $\mu\nu$ SSM, which can lead to early discovery. We list our conclusions in chapter 7. Various technical details, like different mass matrices, couplings, matrix element squares of the three-body decays of the lightest supersymmetric particle, Feynman diagrams etc. are relegated to the appendices.

Contents

1	The Standard Model and beyond...	1
1.1	The Standard Model	1
1.2	Apparent successes and the dark sides	6
2	Supersymmetry	13
2.1	Waking up to the idea	13
2.2	Basics of supersymmetry algebra	14
2.3	Constructing a supersymmetric Lagrangian	16
2.4	SUSY breaking	18
2.5	Minimal Supersymmetric Standard Model	20
2.6	The R -parity	25
2.7	Successes of supersymmetry	27
2.8	The μ -problem	28
2.9	Next-to-Minimal Supersymmetric Standard Model	29
3	Neutrinos	41
3.1	Neutrinos in the Standard Model	41
3.2	Neutrino oscillation	42
3.3	Models of neutrino mass	47
3.3.1	Mass models I	48
3.3.2	Mass models II	50
3.4	Testing neutrino oscillation at Collider	58
4	$\mu\nu$SSM: neutrino masses and mixing	73
4.1	Introducing $\mu\nu$ SSM	73
4.2	The model	73
4.3	Scalar sector of $\mu\nu$ SSM	76
4.4	Fermions in $\mu\nu$ SSM	78
4.5	Neutrinos at the tree level	81
4.5.1	Neutrino masses at the tree level	82
4.5.2	Neutrino mixing at the tree level	83
4.6	Neutrinos at the loop level	86
4.7	Analysis of neutrino masses and mixing at one-loop	88
4.8	One-loop corrections and mass hierarchies	91
4.8.1	Normal hierarchy	92
4.8.2	Inverted hierarchy	98
4.8.3	Quasi-degenerate spectra	100
4.9	Summary	102
5	$\mu\nu$SSM: decay of the LSP	109
5.1	A decaying LSP	109
5.2	Different LSP scenarios in $\mu\nu$ SSM	109
5.3	Decays of the lightest neutralino in $\mu\nu$ SSM	110
5.4	Light neutrino mixing and the neutralino decay	112

5.4.1	Bino dominated lightest neutralino	113
5.4.2	Higgsino dominated lightest neutralino	115
5.4.3	Right-handed neutrino dominated lightest neutralino	116
6	$\mu\nu$SSM: Unusual signal of Higgs boson at LHC	125
6.1	Higgs boson in $\mu\nu$ SSM	125
6.2	The Signal	125
6.3	Collider analysis and detection	127
6.4	Correlations with neutrino mixing angles	130
6.5	Invariant mass	131
7	Summary and Conclusion	135
A		139
A.1	Scalar mass squared matrices in MSSM	139
A.2	Fermionic mass matrices in MSSM	139
B		141
B.1	Scalar mass squared matrices in $\mu\nu$ SSM	141
B.2	Quark mass matrices in $\mu\nu$ SSM	146
C		147
C.1	Details of expansion matrix ξ	147
C.2	Tree level analysis with perturbative calculation	147
C.3	See-saw masses with n generations	149
D		151
D.1	Feynman rules	151
E		155
E.1	The $\tilde{\Sigma}_{ij}^V$ function	155
E.2	The $\tilde{\Pi}_{ij}^V$ function	156
F		157
F.1	The \mathbf{B}_0 , \mathbf{B}_1 functions	157
G		159
G.1	Feynman diagrams for the tree level $\tilde{\chi}_1^0$ decay	159
H		161
H.1	Feynman rules	161
H.2	Squared matrix elements for $h^0 \rightarrow \tilde{\chi}_i^0 \tilde{\chi}_j^0, b\bar{b}$	163
I		165
I.1	Three body decays of the $\tilde{\chi}_1^0$ LSP	165
I.2	Process $\tilde{\chi}_1^0 \rightarrow q\bar{q}\nu$	165
I.3	Process $\tilde{\chi}_1^0 \rightarrow \ell_i^+ \ell_j^- \nu_k$	170
I.4	Process $\tilde{\chi}_1^0 \rightarrow \nu_i \bar{\nu}_j \nu_k$	179
I.5	Process $\tilde{\chi}_1^0 \rightarrow \bar{u}_i d_j \ell_k^+$	180
I.6	Process $\tilde{\chi}_1^0 \rightarrow u_i \bar{d}_j \ell_k^-$	184

Chapter 1

The Standard Model and beyond...

1.1 The Standard Model

The quest for explaining diverse physical phenomena with a single “supreme” theory is perhaps deeply embedded in the human mind. The journey was started long ago with *Michael Faraday* and later with *James Clerk Maxwell* with the unification of the electric and the magnetic forces as the electromagnetic force. The inspiring successful past has finally led us to the Standard Model (SM) (see reviews [1, 2] and [3–6]) of elementary Particle Physics. In the SM three of the four fundamental interactions, namely electromagnetic, weak and strong interactions are framed together. The first stride towards the SM was taken by *Sheldon Glashow* [7] by unifying the theories of electromagnetic and weak interactions as the electroweak theory. Finally, with pioneering contributions from *Steven Weinberg* [8] and *Abdus Salam* [9] and including the third fundamental interaction of nature, namely the strong interaction the Standard Model of particle physics emerged in its modern form. Ever since, the SM has successfully explained host of experimental results and precisely predicted a wide variety of phenomena. Over time and through many experiments by many physicists, the Standard Model has become established as a well-tested physics theory.

✠ *The quarks and leptons*

The SM contains elementary particles which are the basic ingredients of all the matter surrounding us. These particles are divided into two broad classes, namely, *quarks* and *leptons*. These particles are called *fermions* since they are spin $\frac{1}{2}$ particles. Each group of quarks and leptons consists of six members, which are “paired up” or appear in *generations*. The lightest and most stable particles make up the first generation, whereas the heavier and less stable particles belong to the second and third generations. The six quarks are paired in the three generations, namely the ‘up quark (u)’ and the ‘down quark (d)’ form the first generation, followed by the second generation containing the ‘charm quark (c)’ and ‘strange quark (s)’, and finally the ‘top quark (t)’ and ‘bottom quark (b)’ of the third generation. The leptons are similarly arranged in three generations, namely the ‘electron (e)’ and the ‘electron-neutrino (ν_e)’, the ‘muon (μ)’ and the ‘muon-neutrino (ν_μ)’, and the ‘tau (τ)’ and the ‘tau-neutrino (ν_τ)’.

✠ *There are gauge bosons too*

Apart from the quarks and leptons the SM also contains different types of *spin-1* bosons, responsible for mediation of the electromagnetic, weak and the strong interaction. These force mediators essentially emerge as a natural consequence of the theoretical fabrication of the SM, which relies on the principle of local gauge invariance with the gauge group $SU(3)_C \times SU(2)_L \times U(1)_Y$. The force mediator gauge bosons are $\mathbf{n}^2 - 1$ in number for an $SU(n)$ group and belong to the adjoint representation of the group.

The group $SU(3)_C$ is associated with the *colour* symmetry in the quark sector and under this group one obtains the so-called colour triplets. Each quark (q) can carry a *colour charge* under the $SU(3)_C$ group¹ (very similar to electric charges under $U(1)_{em}$ symmetry). Each quark carries one of the three

¹The colour quantum number was introduced for quarks [10] to save the *Fermi* statistics. These are some hypothetical charges having no connection with the real life colour of light.

fundamental colours ($\mathbf{3}$ representation), namely, red (R), green (G) and blue (B). In a similar fashion an anti-quark (\bar{q}) has the complementary colours ($\bar{\mathbf{3}}$ representation), cyan (\bar{R}), magenta (\bar{G}) and yellow (\bar{B}). The accompanying eight force mediators are known as gluons (G_μ^a). The gluons belong to the adjoint representation of $SU(3)_C$. However, all of the hadrons (bound states of quarks) are colour singlet. Three weak bosons (W_μ^a) are the force mediators for $SU(2)_L$ group, under which left-chiral quark and lepton fields transform as doublets. The remaining gauge group $U(1)_Y$ provides hypercharge quantum number (Y) to all the SM particles and the corresponding gauge boson is denoted by B_μ . In describing different gauge bosons the index ' μ ' ($= 1, \dots, 4$) has been used to denote *Lorentz* index. The index ' a ' appears for the non-Abelian gauge groups² and they take values $1, \dots, 8$ for $SU(3)_C$ and $1, 2, 3$ for $SU(2)_L$.

Different transformations for the SM fermions and gauge bosons under the gauge group $SU(3)_C \times SU(2)_L \times U(1)_Y$ are shown below³

$$\begin{aligned} L_{i_L} &= \begin{pmatrix} \nu_{\ell_i} \\ \ell_i \end{pmatrix}_L \sim (\mathbf{1}, \mathbf{2}, -1), \quad \ell_{i_R} \sim (\mathbf{1}, \mathbf{1}, -2), \\ Q_{i_L} &= \begin{pmatrix} u_i \\ d_i \end{pmatrix}_L \sim (\mathbf{3}, \mathbf{2}, \frac{1}{3}), \quad u_{i_R} \sim (\mathbf{3}, \mathbf{1}, \frac{4}{3}), \quad d_{i_R} \sim (\mathbf{3}, \mathbf{1}, -\frac{2}{3}), \\ G_\mu^a &\sim (\mathbf{8}, \mathbf{0}, \mathbf{0}), \quad W_\mu^a \sim (\mathbf{1}, \mathbf{3}, \mathbf{0}), \quad B_\mu \sim (\mathbf{1}, \mathbf{1}, \mathbf{0}), \end{aligned} \quad (1.1)$$

where $\ell_i = e, \mu, \tau$, $u_i = u, c, t$ and $d_i = d, s, b$. The singlet representation is given by $\mathbf{1}$.

✂ Massive particles in the SM ?

Principle of gauge invariance demands for massless gauge bosons which act as the force mediators. In addition, all of the SM fermions (quarks and leptons) are supposed to be exactly massless, as a consequence of the gauge invariance. But these are in clear contradiction to observational facts. In reality one encounters with massive fermions. Also, the short range nature of the weak interaction indicates towards some massive mediators. This apparent contradiction between gauge invariance and massive gauge boson was resolved by the celebrated method of *spontaneous breaking of gauge symmetry* [12–16]. The initial SM gauge group after spontaneous symmetry breaking (SSB) reduces to $SU(3)_C \times U(1)_{em}$, leaving the colour and electric charges to be conserved in nature. Consequently, the corresponding gauge bosons, gluons and photon, respectively remain massless ensuing gauge invariance, whereas the weak force mediators (W^\pm and Z bosons) become massive. Symbolically,

$$SU(3)_C \times SU(2)_L \times U(1)_Y \xrightarrow{SSB} SU(3)_C \times U(1)_{em}. \quad (1.2)$$

Since $SU(3)_C$ is unbroken in nature, all the particles existing freely in nature are forced to be colour neutral. In a similar fashion unbroken $U(1)_{em}$ implies that any charged particles having free existence in nature must have their charges as integral multiple of that of an electron or its antiparticle. It is interesting to note that quarks have fractional charges but they are not free in nature since $SU(3)_C$ is unbroken.

◆ Spontaneous symmetry breaking

Let us consider a Hamiltonian H_0 which is invariant under some symmetry transformation. If this symmetry of H_0 is not realized by the particle spectrum, the symmetry is spontaneously broken. A more illustrative example is shown in figure 1.1. Here the minima of the potential lie on a circle (white dashed) rather than being a specific point. Each of these points are equally eligible for being the minimum and whenever the red ball chooses a specific minimum, the symmetry of the ground state (the state of minimum energy) is spontaneously broken. In other words, when the symmetry of H_0 is not respected by the ground state, the symmetry is spontaneously broken. It turns out that the degeneracy in the ground state is essential for spontaneous symmetry breaking.

²Yang and Mills [11].

³We choose $Q = T_3 + \frac{Y}{2}$, where Q is the electric charge, T_3 is the third component of the weak isospin ($\pm \frac{1}{2}$ for an $SU(2)$ doublet) and Y is the weak hypercharge.

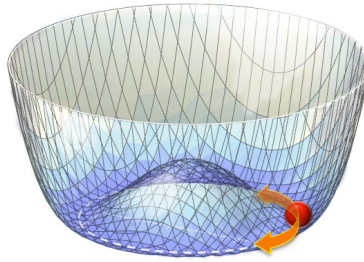


Figure 1.1: Spontaneous breaking of symmetry through the choice of a specific degenerate ground state.

Everything seems to work fine with the massive gauge bosons. But the demon lies within the method of spontaneous symmetry breaking itself. The *spontaneous breakdown of a continuous symmetry* implies the existence of *massless, spinless particles* as suggested by *Goldstone theorem*.⁴ They are known as *Nambu-Goldstone* or simply *Goldstone bosons*. So the SSB apart from generating gauge boson masses also produces massless scalars which are not yet experimentally detected. This is the crisis point when the celebrated “Higgs-mechanism”⁵ resolves the crisis situation. The unwanted massless scalars are now eaten up by the gauge boson fields and they turn out to be the badly needed longitudinal polarization mode for the “massive” gauge bosons. So this is essentially the reappearance of three degrees of freedom associated with three massless scalars in the form of three longitudinal polarization modes for the massive gauge bosons. This entire mechanism happens without breaking the gauge invariance of the theory explicitly. This mechanism for generating gauge boson masses is also consistent with the renormalizability of a theory with massive gauge bosons.⁶ The fermion masses also emerge as a consequence of Higgs mechanism.

✦ *Higgs sector of the SM and mass generation*

So the only scalar (spin-0) in the SM is the Higgs boson. Higgs mechanism is incorporated in the SM through a complex scalar doublet Φ with the following transformation properties under the SM gauge group.

$$\Phi = \begin{pmatrix} \phi^+ \\ \phi^0 \end{pmatrix} \sim (\mathbf{1}, \mathbf{2}, \mathbf{1}). \quad (1.3)$$

The potential for Φ is written as

$$V(\Phi) = \mu^2 \Phi^\dagger \Phi + \lambda (\Phi^\dagger \Phi)^2, \quad (1.4)$$

with $\mu^2 < 0$ and $\lambda > 0$ (so that the potential is bounded from below). Only a colour and charge (electric) neutral component can acquire a vacuum expectation value (VEV), since even after SSB the theory remains invariant under $SU(3)_C \times U(1)_{em}$ (see eqn.(1.2)). Now with a suitable choice of gauge (“unitary gauge”), so that the Goldstone bosons disappear one ends up with

$$\Phi = \frac{1}{\sqrt{2}} \begin{pmatrix} 0 \\ v + h^0 \end{pmatrix}, \quad (1.5)$$

where h^0 is the physical Higgs field and ‘ v ’ is the VEV for $\mathcal{R}e(\phi^0)$ (all other fields acquire zero VEVs) with $v^2 = -\frac{\mu^2}{\lambda}$. At this moment it is apparent that eqn.(1.2) can be recasted as

$$SU(2)_L \times U(1)_Y \xrightarrow{SSB} U(1)_{em}, \quad (1.6)$$

⁴Initially by Nambu [17], Nambu and Jona-Lasino. [18,19]. General proof by Goldstone [20,21].

⁵The actual name should read as Brout-Englert-Higgs-Guralnik-Hagen-Kibble mechanism after all the contributors. Brout and Englert [13], Higgs [14,15], Guralnik, Hagen and Kibble [16].

⁶Veltman and ‘t Hooft, [22,23].

which is essentially the breaking of the electroweak symmetry since the $SU(3)_C$ sector remains unaffected. Thus the phenomena of SSB in the context of the SM is identical with the electroweak symmetry breaking (EWSB). The weak bosons, W_μ^a and $U(1)_Y$ gauge boson B_μ now mix together and finally yield three massive vector bosons (W_μ^\pm, Z_μ^0) and one massless photon (A_μ^0):

$$\begin{aligned} W_\mu^\pm &= \frac{W_\mu^1 \mp iW_\mu^2}{\sqrt{2}}, \\ Z_\mu^0 &= \cos\theta_W W_\mu^3 - \sin\theta_W B_\mu, \\ A_\mu^0 &= \sin\theta_W W_\mu^3 + \cos\theta_W B_\mu, \end{aligned} \quad (1.7)$$

where θ_W is the *Weinberg* angle or weak mixing angle.⁷ In terms of the $SU(2)_L$ and $U(1)_Y$ gauge couplings (g_2, g_1) one can write

$$g_2 \sin\theta_W = g_1 \cos\theta_W. \quad (1.8)$$

The W_μ^\pm, Z_μ^0 boson masses are given by

$$M_W = \frac{g_2 v}{2}, \quad M_Z = \frac{v}{2} \sqrt{g_1^2 + g_2^2}, \quad (1.9)$$

with $v^2 = -\frac{\mu^2}{\lambda}$. The mass of physical Higgs boson (h^0) is given by $m_{h^0}^2 = 2v^2\lambda$. Note that $m_{h^0} > 0$ since $\mu^2 < 0$. Interestingly, ratio of the quantities M_W^2 and $M_Z^2 \cos^2\theta_W$ is equal to one at the tree level (see eqns. (1.8) and (1.9)). This ratio is defined as the ρ -parameter, which is an important parameter for electroweak precision test:

$$\rho = \frac{M_W^2}{M_Z^2 \cos^2\theta_W} = 1. \quad (1.10)$$

There exists an alternative realization of the ρ -parameter. The ρ -parameter specifies the relative strength of the neutral current (mediated through Z -bosons) to the charged current (mediated through W^\pm -boson) weak interactions.

For the purpose of fermion mass generation consider the Lagrangian containing interactions between Higgs field and matter fermions.

$$-\mathcal{L}_{\text{Yukawa}} = y_{\ell_i} \bar{L}_i \Phi e_i + y_{d_i} \bar{Q}_i \Phi d_i + y_{u_i} \bar{Q}_i \tilde{\Phi} u_i + \text{Hermitian conjugate}, \quad (1.11)$$

where y_{ℓ_i, u_i, d_i} are the *Yukawa* couplings for the charged leptons, up-type quarks and down-type quarks, respectively. The $SU(2)_L$ doublet and singlet quark and lepton fields are shown in eqn.(1.1). The field $\tilde{\Phi}$ is used to generate masses for the up-type quarks and it is given by

$$\tilde{\Phi} = -i\sigma_2 \Phi^* = i \begin{pmatrix} 0 & -i \\ i & 0 \end{pmatrix} \begin{pmatrix} \phi^- \\ \phi^{0*} \end{pmatrix} = \begin{pmatrix} -\phi^{0*} \\ \phi^- \end{pmatrix}. \quad (1.12)$$

The fermion masses and their interactions with Higgs field emerge after the EWSB using eqn.(1.11). For example considering the *electron* these terms are as follows

$$\mathcal{L}_{\text{Yukawa}}^{\text{electron}} = -\frac{y_e(v+h^0)}{\sqrt{2}} (\bar{e}_L e_R + \bar{e}_R e_L), \quad (1.13)$$

where $e_L = P_L L_e$ (see eqn.(1.1)).

So with four component spinor e as $\begin{pmatrix} e_L \\ e_R \end{pmatrix}$, eqn.(1.13) can be rewritten as

$$\mathcal{L}_{\text{Yukawa}}^{\text{electron}} = -m_e \bar{e} e - \frac{m_e}{v} \bar{e} e h^0, \quad (1.14)$$

with $m_e = \frac{Y_e v}{\sqrt{2}}$ as mass of the electron. The particle spectrum of the SM can be written in a tabular form as shown in table 1.1.

⁷ At present $\sin^2\theta_W = 0.231$ (evaluated at M_Z with renormalization scheme \overline{MS}) [24].

Particle	mass in GeV	Spin	Electric Charge	Colour charge
electron (e)	5.109×10^{-4}	$\frac{1}{2}$	-1	0
muon (μ)	0.105	$\frac{1}{2}$	-1	0
tau (τ)	1.776	$\frac{1}{2}$	-1	0
neutrinos ($\nu_{e,\mu,\tau}$)	0	$\frac{1}{2}$	0	0
up-quark (u)	2.49×10^{-3}	$\frac{1}{2}$	$\frac{2}{3}$	yes
down-quark (d)	5.05×10^{-3}	$\frac{1}{2}$	$-\frac{1}{3}$	yes
charm-quark (c)	1.27	$\frac{1}{2}$	$\frac{2}{3}$	yes
strange-quark (s)	0.101	$\frac{1}{2}$	$-\frac{1}{3}$	yes
top-quark (t)	172.0	$\frac{1}{2}$	$\frac{2}{3}$	yes
bottom-quark (b)	4.19	$\frac{1}{2}$	$-\frac{1}{3}$	yes
W-boson (W^\pm)	80.399	1	± 1	0
Z-boson (Z^0)	91.187	1	0	0
photon (γ)	0	1	0	0
gluon (g)	0	1	0	yes
Higgs (h^0)	?	0	0	0

Table 1.1: The particle spectrum of the SM [24]. Each of the charged particles are accompanied by charge conjugate states of equal mass. The charge neutral particles act as their own antiparticles with all charge like quantum numbers as opposite to that of the corresponding particles. Evidence for Higgs boson is yet experimentally missing and thus Higgs mass is denoted as ‘?’. The neutrinos are presented with zero masses since we are considering the SM only (see section 1.2).

✂ SM interactions

Based on the discussion above, the complete Lagrangian for the SM can be written as

$$\mathcal{L}_{SM} = \mathcal{L}_1 + \mathcal{L}_2 + \mathcal{L}_3 + \mathcal{L}_4, \quad (1.15)$$

where

1. \mathcal{L}_1 is the part of the Lagrangian which contains kinetic energy terms and self-interaction terms for the gauge bosons. After the EWSB these gauge bosons are known as W^\pm, Z^0 , gluons and photon. So we have

$$\mathcal{L}_1 = \sum_{\mu,\nu=1}^4 \left[-\frac{1}{4} \sum_{a=1}^8 G_{\mu\nu}^a G_a^{\mu\nu} - \frac{1}{4} \sum_{i=1}^3 W_{\mu\nu}^i W_i^{\mu\nu} - \frac{1}{4} B_{\mu\nu} B^{\mu\nu} \right], \quad (1.16)$$

where

$$\begin{aligned} G_{\mu\nu}^a &= \partial_\mu G_\nu^a - \partial_\nu G_\mu^a - g_3 f_{abc} G_\mu^b G_\nu^c, \\ W_{\mu\nu}^i &= \partial_\mu W_\nu^i - \partial_\nu W_\mu^i - g_2 \epsilon_{ijk} W_\mu^j W_\nu^k, \\ B_{\mu\nu} &= \partial_\mu B_\nu - \partial_\nu B_\mu, \end{aligned} \quad (1.17)$$

with f_{abc} and ϵ_{ijk} as the structure constants of the respective non-Abelian groups. g_3 is the coupling constant for $SU(3)_C$ group.

2. Kinetic energy terms for quarks and leptons belong to \mathcal{L}_2 . This part of the Lagrangian also contains the interaction terms between the elementary fermions and gauge bosons. Symbolically,

$$\mathcal{L}_2 = i\overline{\chi}_L \not{D}\chi_L + i\overline{\chi}_R \not{D}\chi_R, \quad (1.18)$$

where $\not{D} = \gamma^\mu D_\mu$ with D_μ as the covariant derivative.⁸ The quantity χ_L stands for lepton and quark $SU(2)_L$ doublets whereas χ_R denotes $SU(2)_L$ singlet fields (see eqn.(1.1)). The covariant

⁸Replacement of ordinary derivative (∂_μ) by D_μ is essential for a gauge transformation, so that $D_\mu\psi$ transforms covariantly under gauge transformation, similar to the matter field, ψ .

derivative D_μ for different fermion fields are written as (using eqn.(1.1))

$$\begin{aligned}
D_\mu Q_i &= \left[\partial_\mu + ig_1 \frac{1}{6} B_\mu + i \sum_{i=1}^3 g_2 \frac{1}{2} \sigma_i \cdot W_\mu^i \right] Q_i, \\
D_\mu u_i &= \left[\partial_\mu + ig_1 \frac{2}{3} B_\mu \right] u_i, \\
D_\mu d_i &= \left[\partial_\mu - ig_1 \frac{1}{3} B_\mu \right] d_i, \\
D_\mu L_i &= \left[\partial_\mu - ig_1 \frac{1}{2} B_\mu + i \sum_{i=1}^3 g_2 \frac{1}{2} \sigma_i \cdot W_\mu^i \right] L_i, \\
D_\mu e_i &= [\partial_\mu - ig_1 B_\mu] e_i.
\end{aligned} \tag{1.19}$$

But these are the information for $SU(2)_L \times U(1)_Y$ only. What happens to the $SU(3)_C$ part? Obviously, for the leptons there will be no problem since they are $SU(3)_C$ singlet after all (see eqn.(1.1)). For the quarks the $SU(3)_C$ part can be taken care of in the following fashion,

$$D_\mu \begin{pmatrix} q_{iR} \\ q_{iG} \\ q_{iB} \end{pmatrix} = \left[\partial_\mu + i \sum_{a=1}^8 g_3 \frac{1}{2} \lambda_a \cdot G_\mu^a \right] \begin{pmatrix} q_{iR} \\ q_{iG} \\ q_{iB} \end{pmatrix}, \tag{1.20}$$

where R, G and B are the three types of colour charge and λ_a 's are eight Gell-Mann matrices. q_i is triplet under $SU(3)_C$, where ' i ' stands for different types of left handed or right handed (under $SU(2)_L$) quark flavours, namely u, d, c, s, t and b .

3. The terms representing physical Higgs mass and Higgs self-interactions along with interaction terms between Higgs and the gauge bosons are in housed in \mathcal{L}_3

$$\mathcal{L}_3 = (D^\mu \Phi)^\dagger (D_\mu \Phi) - V(\Phi). \tag{1.21}$$

The expressions for Φ and $V(\Phi)$ are given in eqns.(1.3) and (1.4), respectively. For Φ the covariant derivative D_μ is given by

$$D_\mu \Phi = \left[\partial_\mu + ig_1 \frac{1}{2} B_\mu + i \sum_{i=1}^3 g_2 \frac{1}{2} \sigma_i \cdot W_\mu^i \right] \Phi. \tag{1.22}$$

4. The remaining Lagrangian \mathcal{L}_4 contains lepton and quark mass terms and their interaction terms with Higgs field (h^0) (after EWSB). The expression for \mathcal{L}_4 is shown in eqn.(1.11). The elementary fermions get their masses through respective Yukawa couplings, which are *free parameters* of the theory. It turns out that in the SM the flavour states are not necessarily the mass eigenstates, and it is possible to relate them through an *unitary transformation*. In case of the quarks this matrix is known as the CKM (Cabibbo-Kobayashi-Maskawa) [25, 26] matrix. This 3×3 unitary matrix contains three mixing angles and one phase. The massless neutrinos in the SM make the corresponding leptonic mixing matrix a trivial one (Identity matrix). All possible interactions of the SM are shown in figure 1.2. The loops represent self-interactions like $h^0 h^0 h^0$, $h^0 h^0 h^0 h^0$ (from the choice of potential, see eqn. (1.4)) $W^\pm W^\pm W^\mp W^\mp$, ggg or $gggg$ (due to non-Abelian interactions) and also interactions like $W^\pm W^\mp ZZ$, $W^\pm W^\mp \gamma\gamma$, $W^\pm W^\mp Z$, $W^\pm W^\mp \gamma$ etc.

1.2 Apparent successes and the dark sides

The SM is an extremely successful theory to explain a host of elementary particle interactions. Masses of the W^\pm and Z bosons as predicted by the SM theory are very close to their experimentally measured values. The SM also predicted the existence of the charm quark from the requirement to suppress

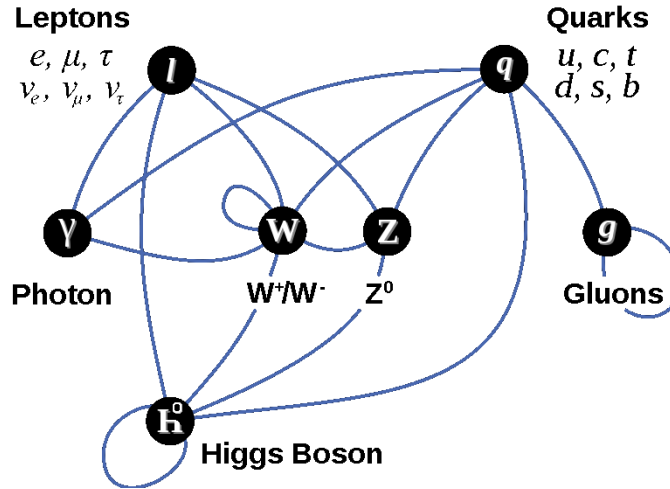


Figure 1.2: Interactions of the Standard Model. See text for more details.

flavour changing neutral current (FCNC)⁹ before it was actually discovered in 1974. In a similar fashion the SM also predicted the mass of the heavy top quark in the right region before its discovery. Besides, all of the SM particles except Higgs boson have been discovered already and their masses are also measured very precisely [24]. Indeed, apart from Higgs sector, rest of the SM has been already analysed for higher order processes and their spectacular accuracy as revealed by a host of experiments has firmly established the success of the SM.

Unfortunately, the so-called glorious success of the SM suffers serious threat from various theoretical and experimental perspective. One of the main stumbling blocks is definitely the Higgs boson, yet to be observed in an experiment and its mass. Some of these shortcomings are listed below.

1. The SM has a large number of free parameters (**19**). The parameters are **9** Yukawa couplings (or elementary fermion masses) + **3** angles and **one** phase of CKM matrix + **3** gauge couplings g_1, g_2, g_3 ¹⁰ + **2** parameters (μ, λ) from scalar potential (see eqn.(1.4)) + **one** vacuum angle for quantum chromodynamics (QCD). The number of free parameters is rather large for a fundamental theory.
2. There are no theoretical explanation why there exist only three generations of quarks and leptons. Also the huge mass hierarchy between different generations (from first to third), that is to say why mass of the top quark (m_t) \gg mass of the up-quark (m_u) (see table 1.1), is unexplained.
3. The single phase of CKM matrix accounts for many Charge-Parity (CP) violating processes. However, one needs additional source of CP-violation to account for the large matter-anti matter asymmetry of the universe.
4. The most familiar force in our everyday lives, gravity, is not a part of the SM. Since the effect of gravity dominates near the “*Planck Scale* (M_P)”, ($\sim 10^{19}$ GeV) the SM still works fine despite its reluctant exclusion of the gravitational interaction. In conclusion, the Standard Model cannot be a theory which is valid for all energy scales.
5. There is no room for a cold Dark Matter candidate inside the SM framework, which has been firmly established by now from the observed astrophysical and cosmological evidences.
6. Neutrinos are exactly massless in the Standard Model as a consequence of the particle content, gauge invariance, renormalizability and Lorentz invariance. However, the experimental results from atmospheric, solar and reactor neutrino experiments suggest that the neutrinos do have non-zero masses with non-trivial mixing among different neutrino flavours [28, 29]. In order to

⁹Glashow, Iliopoulos and Maiani [27].

¹⁰An alternate set could be g_3, e (the unit of electric charge) and the Weinberg angle θ_W .

generate masses and mixing for the neutrinos, one must extend the SM framework by introducing additional symmetries or particles or both.

But in reality the consequence of a massive neutrino is far serious than asking for an extension of the SM. As written earlier, the massive neutrinos trigger a non-trivial mixing in the charged lepton sector just like the CKM matrix¹¹, but with large off-diagonal entries. It remains to explain why the structure of the mixing matrix for the leptons are so different from the quarks?

7. Perhaps the severe most of all the drawbacks is associated with Higgs boson mass. In the Standard Model, Higgs boson mass is totally unprotected by any symmetry argument. In other words putting $m_{h^0} = 0$, does not enhance any symmetry of the theory.¹² Higgs mass can be as large as the “Grand Unified Theory (GUT)” scale (10^{16} GeV) or the “Planck Scale” (10^{19} GeV) when radiative corrections are included. This is the so called *gauge hierarchy problem*. However, from several theoretical arguments [30–47] and various experimental searches [24, 48, 49] Higgs boson mass is expected to be in the range of a few hundreds of GeV, which requires unnatural fine tuning of parameters (\sim one part in 10^{38}) for all orders in perturbation theory. Different one-loop diagrams contributing to the radiative correction to Higgs boson mass are shown in figure 1.3.

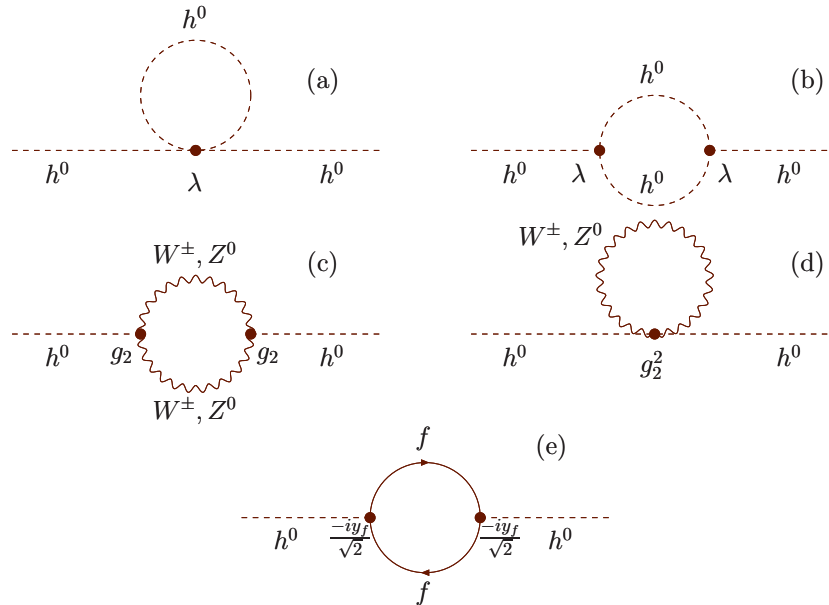


Figure 1.3: One-loop radiative corrections to the Higgs boson mass from (a) and (b) self-interactions (c) and (d) interactions with gauge bosons and (e) interactions with fermions (f).

It is clear from figure 1.3, the contribution from the fermion loop is proportional to the squared Yukawa couplings (y_f^2). As a corollary these contributions are negligible except when heavy quarks are running in the loop. Contributions from the diagrams (b) and (c) are *logarithmically divergent* which is well under control due to the behaviour of *log* function. The contributions from diagrams (a), (d) and (e) are *quadratically divergent*, which are the sources of the hierarchy problem.

◆ Loop correction and divergences

Consider the diagram (e) of figure 1.3, which represents the fermionic loop contribution to the scalar two point function. Assuming the loop momentum to be ‘ k ’ and the momentum for the external leg to be ‘ p ’ this contribution can be written as

¹¹Known as the PMNS matrix, will be addressed in chapter 3 in more details.

¹²Note that putting zero for fermion or gauge boson mass however enhances the symmetry of the Lagrangian. In this case the chiral and gauge symmetry, respectively.

$$\begin{aligned}
\Pi_{h^0 h^0}^f(p^2 = 0) &= (-1) \int \frac{d^4 k}{(2\pi)^4} \left(\frac{-iy_f}{\sqrt{2}}\right)^2 \text{Tr} \left[\frac{i}{\not{k} - m_f} \frac{i}{\not{k} - m_f} \right], \\
&= \left(-\frac{y_f^2}{2}\right) \int \frac{d^4 k}{(2\pi)^4} \text{Tr} \left[\frac{(\not{k} + m_f)(\not{k} + m_f)}{(k^2 - m_f^2)^2} \right], \\
&= (-2y_f^2) \int \frac{d^4 k}{(2\pi)^4} \left[\frac{(k^2 + m_f^2)}{(k^2 - m_f^2)^2} \right], \\
&= -2y_f^2 \int \frac{d^4 k}{(2\pi)^4} \left[\frac{1}{(k^2 - m_f^2)} + \frac{2m_f^2}{(k^2 - m_f^2)^2} \right],
\end{aligned} \tag{1.23}$$

where the (-1) factor appears for closed fermion loop and ‘ i ’ comes from the *Feynman* rules (see eqn.(1.11)). Fermion propagator is written as $i/(\not{k} - m_f)$. Here some of the properties of Dirac Gamma matrices have been used.

Now in eqn.(1.23) Higgs mass appears nowhere which justifies the fact that setting $m_{h^0} = 0$ does not increase any symmetry of the Lagrangian. From naive power counting argument the second term of eqn.(1.23) is logarithmically divergent whereas the first term is quadratically divergent. Suppose the theory of the SM is valid upto Planck scale and the cut off scale Λ (scale upto which a certain theory is valid) lies there, then the correction to the Higgs boson mass goes as (using eqn.(1.23)),

$$\delta m_{h^0}^2 \approx -\frac{y_f^2}{8\pi^2} \Lambda^2 + \text{logarithmic terms.} \tag{1.24}$$

The renormalized Higgs mass squared is then given by

$$\tilde{m}_{h^0}^2 = m_{h^0, \text{bare}}^2 + \delta m_{h^0}^2, \tag{1.25}$$

and looking at eqn.(1.24) the requirement of fine tuning for a TeV scale Higgs mass is apparent. Note that mass generation for all of the SM particles solely depend on Higgs. So in a sense the entire mass spectrum of the SM will be driven towards a high scale with the radiative correction in Higgs boson mass.

The list of drawbacks keep on increasing with issues like unification of gauge couplings at a high scale and a few more. To summarize, all of these unanswered questions have opened up an entire new area of physics, popularly known as ‘‘Beyond the Standard Model (BSM)’’ physics. Some of the well-known candidates are *supersymmetry*¹³ [50–54], *theories with extra spatial dimensions* [55–57] and many others. In this proposed thesis we plan to study some of the problems mentioned earlier in the context of a supersymmetric theory and look for signatures of such a theory at the ongoing Large Hadron Collider (LHC) experiment.

¹³First proposed in the context of hadronic physics, by Hironari Miyazawa (1966).

Bibliography

- [1] Abers E S and Lee B W 1973 *Phys. Rept.* **9** 1–141
- [2] Beg M A B and Sirlin A 1982 *Phys. Rept.* **88** 1
- [3] Halzen F and Martin A D ISBN-9780471887416
- [4] Cheng T P and Li L F Oxford, UK: Clarendon (1984) 536 P. (Oxford Science Publications)
- [5] Griffiths D J New York, USA: Wiley (1987) 392p
- [6] Burgess C P and Moore G D Cambridge, UK: Cambridge Univ. Pr. (2007) 542 p
- [7] Glashow S L 1961 *Nucl. Phys.* **22** 579–588
- [8] Weinberg S 1967 *Phys. Rev. Lett.* **19** 1264–1266
- [9] Salam A Originally printed in *Svartholm: Elementary Particle Theory, Proceedings Of The Nobel Symposium Held 1968 At Lerum, Sweden*, Stockholm 1968, 367-377
- [10] Greenberg O W 1964 *Phys. Rev. Lett.* **13** 598–602
- [11] Yang C N and Mills R L 1954 *Phys. Rev.* **96** 191–195
- [12] Anderson P W 1958 *Phys. Rev.* **112** 1900–1916
- [13] Englert F and Brout R 1964 *Phys. Rev. Lett.* **13** 321–322
- [14] Higgs P W 1964 *Phys. Lett.* **12** 132–133
- [15] Higgs P W 1964 *Phys. Rev. Lett.* **13** 508–509
- [16] Guralnik G S, Hagen C R and Kibble T W B 1964 *Phys. Rev. Lett.* **13** 585–587
- [17] Nambu Y 1960 *Phys. Rev.* **117** 648–663
- [18] Nambu Y and Jona-Lasinio G 1961 *Phys. Rev.* **122** 345–358
- [19] Nambu Y and Jona-Lasinio G 1961 *Phys. Rev.* **124** 246–254
- [20] Goldstone J 1961 *Nuovo Cim.* **19** 154–164
- [21] Goldstone J, Salam A and Weinberg S 1962 *Phys. Rev.* **127** 965–970
- [22] 't Hooft G 1971 *Nucl. Phys.* **B35** 167–188
- [23] 't Hooft G and Veltman M J G 1972 *Nucl. Phys.* **B44** 189–213
- [24] Nakamura K *et al.* (Particle Data Group) 2010 *J. Phys.* **G37** 075021
- [25] Cabibbo N 1963 *Phys. Rev. Lett.* **10** 531–533
- [26] Kobayashi M and Maskawa T 1973 *Prog. Theor. Phys.* **49** 652–657

- [27] Glashow S L, Iliopoulos J and Maiani L 1970 *Phys. Rev.* **D2** 1285–1292
- [28] Schwetz T, Tortola M A and Valle J W F 2008 *New J. Phys.* **10** 113011
- [29] Gonzalez-Garcia M C, Maltoni M and Salvado J 2010 *JHEP* **04** 056
- [30] Cornwall J M, Levin D N and Tiktopoulos G 1973 *Phys. Rev. Lett.* **30** 1268–1270
- [31] Cornwall J M, Levin D N and Tiktopoulos G 1974 *Phys. Rev.* **D10** 1145
- [32] Llewellyn Smith C H 1973 *Phys. Lett.* **B46** 233–236
- [33] Lee B W, Quigg C and Thacker H B 1977 *Phys. Rev.* **D16** 1519
- [34] Dashen R F and Neuberger H 1983 *Phys. Rev. Lett.* **50** 1897
- [35] Lindner M 1986 *Zeit. Phys.* **C31** 295
- [36] Stevenson P M 1985 *Phys. Rev.* **D32** 1389–1408
- [37] Hasenfratz P and Nager J 1988 *Z. Phys.* **C37** 477
- [38] Luscher M and Weisz P 1987 *Nucl. Phys.* **B290** 25
- [39] Hasenfratz A, Jansen K, Lang C B, Neuhaus T and Yoneyama H 1987 *Phys. Lett.* **B199** 531
- [40] Luscher M and Weisz P 1988 *Nucl. Phys.* **B295** 65
- [41] Kuti J, Lin L and Shen Y 1988 *Phys. Rev. Lett.* **61** 678
- [42] Sher M 1989 *Phys. Rept.* **179** 273–418
- [43] Lindner M, Sher M and Zaglauer H W 1989 *Phys. Lett.* **B228** 139
- [44] Callaway D J E 1988 *Phys. Rept.* **167** 241
- [45] Ford C, Jones D R T, Stephenson P W and Einhorn M B 1993 *Nucl. Phys.* **B395** 17–34
- [46] Sher M 1993 *Phys. Lett.* **B317** 159–163
- [47] Choudhury S R and Mamta 1997 *Int. J. Mod. Phys.* **A12** 1847–1859
- [48] Abbiendi G *et al.* (OPAL) 1999 *Eur. Phys. J.* **C7** 407–435
- [49] Barate R *et al.* (LEP Working Group for Higgs boson searches) 2003 *Phys. Lett.* **B565** 61–75
- [50] Gervais J L and Sakita B 1971 *Nucl. Phys.* **B34** 632–639
- [51] Golfand Y A and Likhtman E P 1971 *JETP Lett.* **13** 323–326
- [52] Volkov D V and Akulov V P 1973 *Phys. Lett.* **B46** 109–110
- [53] Wess J and Zumino B 1974 *Nucl. Phys.* **B70** 39–50
- [54] Wess J and Zumino B 1974 *Phys. Lett.* **B49** 52
- [55] Arkani-Hamed N, Dimopoulos S and Dvali G R 1998 *Phys. Lett.* **B429** 263–272
- [56] Arkani-Hamed N, Dimopoulos S and Dvali G R 1999 *Phys. Rev.* **D59** 086004
- [57] Randall L and Sundrum R 1999 *Phys. Rev. Lett.* **83** 3370–3373

Chapter 2

Supersymmetry

2.1 Waking up to the idea

The effect of radiative correction drives the “natural” Higgs mass, and therefore the entire SM particle spectra to some ultimate cutoff of the theory, namely, the Planck scale. A solution to this hierarchy problem could be that, either the Higgs boson is some sort of composite particle rather than being a fundamental particle or the SM is an effective theory valid upto a certain energy scale so that the cutoff scale to the theory lies far below the Planck scale. It is also a viable alternative that there exists no Higgs boson at all and we need some alternative mechanism to generate masses for the SM particles¹. However, it is also possible that even in the presence of quadratic divergences the Higgs boson mass can be in the range of a few hundreds of GeV to a TeV provided different sources of radiative corrections cancel the quadratic divergent pieces. It is indeed possible to cancel the total one-loop quadratic divergences (shown in chapter 1, section 1.2) by explicitly canceling contributions between bosonic and fermionic loop with some postulated relation between their masses. However, this cancellation is not motivated by any symmetry argument and thus a rather accidental cancellation of this kind fails for higher order loops.

Driven by this simple argument let us assume that there are two additional complex scalar fields \tilde{f}_L and \tilde{f}_R corresponding to a fermion f which couples to field Φ (see eqn.(1.3)) in the following manner

$$\begin{aligned} \mathcal{L}_{\tilde{f}\tilde{f}h^0} &= \tilde{\lambda}_f |\Phi|^2 (|\tilde{f}_L|^2 + |\tilde{f}_R|^2), \\ \underline{EW\!SB} &\frac{1}{2} \tilde{\lambda}_f h^0{}^2 (|\tilde{f}_L|^2 + |\tilde{f}_R|^2) + v \tilde{\lambda}_f h^0 (|\tilde{f}_L|^2 + |\tilde{f}_R|^2) + \dots, \end{aligned} \quad (2.1)$$

where h^0 is the physical Higgs field (see eqn.(1.5)). A Lagrangian of the form of eqn.(2.1) will yield additional one-loop contributions to Higgs mass. Note that in order to get a potential bounded from below, $\tilde{\lambda}_f < 0$. The additional contributions to the two point function for Higgs mass via the loops

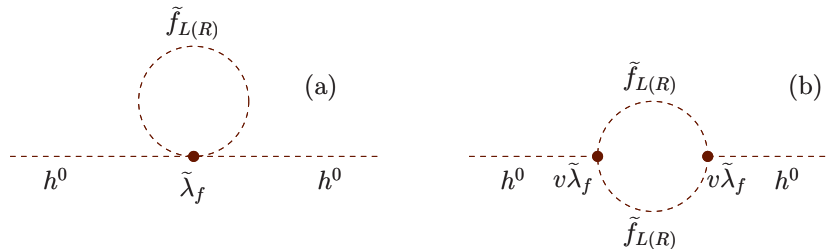


Figure 2.1: New diagrams contributing to Higgs mass correction from Lagrangian $\mathcal{L}_{\tilde{f}\tilde{f}h^0}$ (eqn.(2.1)).

(figure 2.1) can be written as

¹These issues are well studied in the literature and beyond the theme of this thesis.

$$\begin{aligned} \Pi_{h^0 h^0}^{\tilde{f}}(p^2 = 0) &= -\tilde{\lambda}_f \int \frac{d^4 k}{(2\pi)^4} \left(\frac{1}{k^2 - m_{\tilde{f}_L}^2} + \frac{1}{k^2 - m_{\tilde{f}_R}^2} \right) \\ &+ (v\tilde{\lambda}_f)^2 \int \frac{d^4 k}{(2\pi)^4} \left(\frac{1}{(k^2 - m_{\tilde{f}_L}^2)^2} + \frac{1}{(k^2 - m_{\tilde{f}_R}^2)^2} \right). \end{aligned} \quad (2.2)$$

Eqn.(2.2) contains two types of divergences, (a) the first line which is quadratically divergent and (b) second line, which is logarithmically divergent. Following similar procedure to that of deriving eqn.(1.24), one can see that the total two point function $\Pi_{h^0 h^0}^{\tilde{f}}(p^2 = 0) + \Pi_{h^0 h^0}^f(p^2 = 0)$ (see eqn.(1.23)) is *completely* free from quadratic divergences, provided

$$\tilde{\lambda}_f = -y_f^2. \quad (2.3)$$

It is extremely important to note that eqn.(2.3) is *independent* of mass of f , \tilde{f}_L and \tilde{f}_R , namely $m_f, m_{\tilde{f}_L}$ and $m_{\tilde{f}_R}$ respectively. The remaining part of $\Pi_{h^0 h^0}^{\tilde{f}}(p^2 = 0) + \Pi_{h^0 h^0}^f(p^2 = 0)$, containing logarithmic divergences can be explicitly written as (using eqn.(2.3) and dropping p^2)

$$\begin{aligned} \Pi_{h^0 h^0}^{\tilde{f}}(0) + \Pi_{h^0 h^0}^f(0) &= \frac{iy_f^2}{16\pi^2} \left[-2m_f^2 \left(1 - \ln \frac{m_f^2}{\mu_R^2}\right) + 4m_f^2 \ln \frac{m_f^2}{\mu_R^2} \right] \\ &+ \frac{iy_f^2}{16\pi^2} \left[+2m_f^2 \left(1 - \ln \frac{m_f^2}{\mu_R^2}\right) - 4m_f^2 \ln \frac{m_f^2}{\mu_R^2} \right], \end{aligned} \quad (2.4)$$

with $m_{\tilde{f}_L} = m_{\tilde{f}_R} = m_{\tilde{f}}$. μ_R is the scale of renormalization. If further one considers $m_{\tilde{f}} = m_f$ then from eqn.(2.4), $\Pi_{h^0 h^0}^{\tilde{f}}(0) + \Pi_{h^0 h^0}^f(0) = 0$, i.e. sum of the two point functions via the loop vanishes! This theory is absolutely free from hierarchy problem. However, in order to achieve a theory free from quadratic divergences, such cancellation between fermionic and bosonic contributions must persists for all higher orders also. This is indeed a unavoidable feature of a theory, if there exists a symmetry relating fermion and boson masses and couplings².

2.2 Basics of supersymmetry algebra

A symmetry which transforms a fermionic state into a bosonic one is known as supersymmetry (SUSY) [1–23] (also see references of [17]). The generator (Q) of SUSY thus satisfies

$$Q|Boson\rangle = |Fermion\rangle, \quad Q|Fermion\rangle = |Boson\rangle. \quad (2.5)$$

In eqn.(2.5) spin of the left and right hand side differs by *half-integral* number and thus Q must be a *spinorial* object in nature and hence follows anti-commutation relation. Corresponding Hermitian conjugate (\bar{Q}) is also another viable generator since spinors are complex objects. It is absolutely important to study the space-time property of Q , because they change the spin (and hence statistics also) of a particle and spin is related to the behaviour under *spatial rotations*.

Let us think about an unitary operator \mathcal{U} , representing a rotation by 360° about some axis in configuration space, then

$$\begin{aligned} \mathcal{U}Q|Boson\rangle &= \mathcal{U}Q\mathcal{U}^{-1}\mathcal{U}|Boson\rangle = \mathcal{U}|Fermion\rangle, \\ \mathcal{U}Q|Fermion\rangle &= \mathcal{U}Q\mathcal{U}^{-1}\mathcal{U}|Fermion\rangle = \mathcal{U}|Boson\rangle. \end{aligned} \quad (2.6)$$

However, under a rotation by 360° (see ref. [24])

$$\mathcal{U}|Boson\rangle = |Boson\rangle, \quad \mathcal{U}|Fermion\rangle = -|Fermion\rangle. \quad (2.7)$$

²The hint of such a symmetry is evident from $m_{\tilde{f}} = m_f$.

Combining eqns.(2.6), (2.7) one ends up with

$$\mathcal{U}Q\mathcal{U}^{-1} = -Q, \quad \Rightarrow \{Q, \mathcal{U}\} = 0. \quad (2.8)$$

Extending this analysis for any Lorentz transformations it is possible to show that Q does not commute with the generators of Lorentz transformation. On the contrary, under space-time translation,

$$P_\mu |Boson\rangle = |Boson\rangle, \quad P_\mu |Fermion\rangle = |Fermion\rangle. \quad (2.9)$$

Eqns.(2.9) and (2.5) together imply that Q (also \bar{Q}) is invariant under space-time translations. that is

$$[Q, P^\mu] = [\bar{Q}, P^\mu] = 0. \quad (2.10)$$

It is obvious from eqns.(2.8) and (2.10), that supersymmetry is indeed a space-time symmetry. In fact now the largest possible space-time symmetry is no longer *Poincaré* symmetry but the supersymmetry itself with larger number of generators,³ $M^{\mu\nu}$ (Lorentz transformation \Rightarrow spatial rotations and boosts), P^μ (Poincaré transformation \Rightarrow translations) and Q, \bar{Q} (SUSY transformations). It has been argued earlier that the SUSY generators Q, \bar{Q} are *anti-commuting* rather than being commutative. So what is $\{Q, \bar{Q}\}$? Since Q, \bar{Q} are spinorial in nature, then expression for $\{Q, \bar{Q}\}$ must be bosonic in nature and definitely has to be another symmetry generator of the larger group. In general, one can expect that $\{Q, \bar{Q}\}$ should be a combination of P^μ and $M^{\mu\nu}$ (with appropriate index contraction), However, after a brief calculation one gets

$$\{Q, \bar{Q}\} \propto P^\mu. \quad (2.11)$$

Eqn.(2.11) is the basic of the SUSY algebra which contains generators of the SUSY transformations (Q, \bar{Q}) on the left hand side and generator for space-time translations, P^μ on the other side. This suggests that successive operation of two finite SUSY transformations will induce a space-time translation on the states under operation. The quantity $\{Q, \bar{Q}\}$ is a Hermitian operator with positive definite eigenvalue, that is

$$\langle \dots | \{Q, \bar{Q}\} | \dots \rangle = |Q| \dots \rangle|^2 + |\bar{Q}| \dots \rangle|^2 \geq 0. \quad (2.12)$$

Summing over all the SUSY generators and using eqns.(2.11) and (2.12) one gets

$$\sum_Q \{Q, \bar{Q}\} \propto P^0, \quad (2.13)$$

where P^0 is the total energy of the system or the eigenvalue of the Hamiltonian, thus Hamiltonian of supersymmetric theory contains no negative eigenvalues.

If $|0\rangle$ denotes the *vacuum* or the lowest energy state of any supersymmetric theory then following eqns.(2.12) and (2.13) one obtains $P^0|0\rangle = 0$. This is again true if $Q|0\rangle = 0$ and $\bar{Q}|0\rangle = 0$ for all Q, \bar{Q} . This implies that any one-particle state with non-zero energy cannot be invariant under SUSY transformations. So there must be one or more supersymmetric partners (*superpartners*) $Q|1\rangle$ or $\bar{Q}|1\rangle$ for every one-particle state $|1\rangle$. Spin of superpartner state differs by $\frac{1}{2}$ unit from that of $|1\rangle$. The state $|1\rangle$ together with its superpartner state said to form a *supermultiplet*. In a supermultiplet different states are connected in between through one or more SUSY transformations. Inside a supermultiplet the number of fermionic degrees of freedom (n_F) must be equal to that for bosonic one (n_B). A supermultiplet must contain at least one boson and one fermion state. This simple most supermultiplet is known as the *chiral* supermultiplet which contains a Weyl spinor (two degrees of freedom) and one complex scalar (two degrees of freedom). It is important to note that the translational invariance of SUSY generators (see eqn.(2.10)) imply *All states in a supermultiplet must have same mass*⁴. It must be emphasized here that throughout the calculation indices for Q and \bar{Q} have been suppressed. In reality $Q \equiv Q_a^i$ where ' $i = 1, 2, \dots, N$ ' is the number of supercharges and ' a ' is the spinor index. To be specific one should explicitly write (for $i = 1$), $Q_\alpha, \bar{Q}_{\dot{\alpha}}$, where $\alpha, \dot{\alpha}$ are spinorial indices belonging to two different representations of the Lorentz group. We stick to $i = 1$ for this thesis. Details of SUSY algebra is given in refs. [27, 28].

³This statement is consistent with the statement of *Coleman-Mandula* theorem [25] and *Haag-Lopuszanski-Sohnius* theorem [26].

⁴It is interesting to note that supercharge Q satisfies $[Q, P^2] = 0$ but $[Q, W^2] \neq 0$, where $W^\mu (= \frac{1}{2}\epsilon^{\mu\nu\rho\sigma} M_{\nu\rho} P_\sigma)$ is the *Pauli-Lubanski* vector. Note that eigenvalue of $W^2 \propto s(s+1)$ where s is spin of a particle. Thus in general members of a supermultiplet should have same mass but different spins, which is the virtue of supersymmetry.

2.3 Constructing a supersymmetric Lagrangian

Consider a supersymmetric Lagrangian with a single Weyl fermion, ψ (contains two helicity states, $\Rightarrow n_F = 2$) and a complex scalar, ϕ ($\Rightarrow n_B = 2$) without any interaction terms. This two component Weyl spinor and the associated complex scalar are said to form a chiral supermultiplet. The free Lagrangian, which contains only kinetic terms is written as

$$\mathcal{L}^{susy} = -\partial_\mu \phi^* \partial^\mu \phi + i\psi^\dagger \bar{\sigma}^\mu \partial_\mu \psi, \quad (2.14)$$

where $\bar{\sigma}^\mu = \mathbf{1}, -\sigma_i$. Eqn.(2.14) represents a massless, non-interacting supersymmetric model known as *Wess-Zumino* model [5]. The action $\mathcal{S}^{susy} (= \int d^4x \mathcal{L}^{susy})$ is invariant under the set of transformations, given as

$$\begin{aligned} \delta\phi &= \epsilon_\alpha \psi^\alpha \equiv \epsilon\psi, & \Rightarrow \delta\phi^* &= \epsilon^\dagger \psi^\dagger, \\ \delta\psi_\alpha &= -i(\sigma^\mu \epsilon^\dagger)_\alpha \partial\phi, & \Rightarrow \delta\psi_\alpha^\dagger &= i(\epsilon\sigma^\mu)_{\dot{\alpha}} \partial\phi^*, \end{aligned} \quad (2.15)$$

where ϵ^α parametrizes infinitesimal SUSY transformation. It is clear from eqn.(2.15), on the basis of dimensional argument that ϵ^α must be spinorial object and hence anti-commuting in nature. They have mass dimension $[M]^{-\frac{1}{2}}$. It is important to note that $\partial_\mu \epsilon^\alpha = 0$ for global SUSY transformation.

✧ *Is supersymmetry algebra closed?*

It has already been stated that \mathcal{S}^{susy} is invariant under SUSY transformations (eqn.(2.15)). But does it also indicate that the SUSY algebra is closed? In other words, is it true that two successive SUSY transformations (parametrized by ϵ_1, ϵ_2) is indeed another symmetry of the theory? In reality one finds

$$[\delta_{\epsilon_2}, \delta_{\epsilon_1}]X = -i(\epsilon_1 \sigma_\mu \epsilon_2^\dagger - \epsilon_2 \sigma_\mu \epsilon_1^\dagger) \partial^\mu X, \quad (2.16)$$

where $X = \phi, \psi_\alpha$, which means that commutator of two successive supersymmetry transformations is equivalent to the space-time translation of the respective fields.

This is absolutely consistent with our realization of eqn.(2.11). But there is a *flaw* in the above statement. In order to obtain eqn.(2.16) one has to use the equation of motion for the massless fermions and therefore the SUSY algebra closes only in on-shell limit. So how to close SUSY algebra even in off-shell. A more elucidate statement for this problem should read as how to match the bosonic degrees of freedom to that of a fermionic one in off-shell? The remedy of this problem can come from adding some auxiliary field, F (with mass dimension 2) in the theory which can provide the required extra bosonic degrees of freedom. Being auxiliary, F cannot possess a kinetic term ($\mathcal{L}_{auxiliary} = F^* F$, Euler-Lagrange equation is $F = F^* = 0$). So the modified set of transformations read as

$$\begin{aligned} \delta\phi &= \epsilon\psi, & \Rightarrow \delta\phi^* &= \epsilon^\dagger \psi^\dagger, \\ \delta\psi_\alpha &= -i(\sigma^\mu \epsilon^\dagger)_\alpha \partial\phi + \epsilon_\alpha F, & \Rightarrow \delta\psi_\alpha^\dagger &= i(\epsilon\sigma^\mu)_{\dot{\alpha}} \partial\phi^* + \epsilon_\alpha^\dagger F^* \\ \delta F &= -i\epsilon^\dagger \bar{\sigma}^\mu \partial_\mu \psi & \Rightarrow \delta F^* &= i\partial_\mu \psi^\dagger \bar{\sigma}^\mu \epsilon. \end{aligned} \quad (2.17)$$

Eqn.(2.14) also receives modification and for ‘ i ’ number of chiral supermultiplets is given by

$$\mathcal{L}^{chiral} = -\underbrace{\partial_\mu \phi^{i*} \partial^\mu \phi_i}_{\mathcal{L}_{scalar}} + \underbrace{i\psi^{i\dagger} \bar{\sigma}^\mu \partial_\mu \psi_i}_{\mathcal{L}_{fermion}} + \underbrace{F^{i*} F_i}_{\mathcal{L}_{auxiliary}}. \quad (2.18)$$

✧ *Gauge bosons*

Theory of the SM also contains different types of gauge bosons. So in order to supersymmetrize the SM one must consider some “fermionic counterparts” also to complete the set. The massless spin one gauge boson (A_μ^a) and the accompanying spin $\frac{1}{2}$ supersymmetric partner (two component Weyl spinor, called *gauginos* (λ^a)) also belong to the same multiplet, known as the gauge supermultiplet. The index ‘ a ’ runs over adjoint representation of the associated SU(N) group. It is interesting to note that since gauge bosons belong to the adjoint representation, hence a gauge supermultiplet is a real

representation. Just like the case of chiral supermultiplet one has to rely on some auxiliary fields D^a to close off-shell SUSY algebra. The corresponding Lagrangian is written as

$$\mathcal{L}^{gauge} = - \frac{F_{\mu\nu}^a = \partial_\mu A_\nu^a - \partial_\nu A_\mu^a + gf^{abc} A_\mu^b A_\nu^c}{\frac{1}{4} F_{\mu\nu}^a F_a^{\mu\nu}} + \underbrace{i\lambda^{a\dagger} \bar{\sigma}^\mu D_\mu \lambda^a}_{D_\mu \lambda^a = \partial_\mu \lambda^a + gf^{abc} A_\mu^b \lambda^c} + \frac{1}{2} D^a D^a, \quad (2.19)$$

where $F_{\mu\nu}^a$ is the Yang-Mills field strength and $D_\mu \lambda^a$ is the covariant derivative for gaugino field, λ^a . The set of SUSY transformations which leave the action $\mathcal{S}^{gauge} (= \int d^4x \mathcal{L}^{gauge})$ invariant are written as

$$\begin{aligned} \delta A_\mu^a &= -\frac{1}{\sqrt{2}} (\epsilon^\dagger \bar{\sigma}_\mu \lambda^a + \lambda^{a\dagger} \bar{\sigma}_\mu \epsilon), \\ \delta \lambda_\alpha^a &= \frac{i}{2\sqrt{2}} (\sigma^\mu \bar{\sigma}^\nu \epsilon)_\alpha F_{\mu\nu}^a + \frac{1}{\sqrt{2}} \epsilon_\alpha D^a, \\ \delta D^a &= -\frac{i}{\sqrt{2}} (\epsilon^\dagger \bar{\sigma}_\mu D_\mu \lambda^a - D_\mu \lambda^{a\dagger} \bar{\sigma}_\mu \epsilon). \end{aligned} \quad (2.20)$$

✂ Interactions in a supersymmetric theory

A supersymmetrize version of the SM should include an interaction Lagrangian invariant under SUSY transformations. From the argument of renormalizability and naive power counting the most general interaction Lagrangian (without gauge interaction) appears to be

$$\mathcal{L}^{int} = \underbrace{-\frac{1}{2} W^{ij} \psi_i \psi_j}_{[W^{ij}] = [mass]^1} + \underbrace{W^i F_i}_{[W^i] = [mass]^2} + \underbrace{x^{ij} F_i F_j}_{[x^{ij}] = [mass]^0} + c.c. - \underbrace{U}_{[U] = [mass]^4}, \quad (2.21)$$

where x^{ij}, W^{ij}, W^i, U all are polynomials of ϕ, ϕ^* (scalar fields) with degrees 0, 1, 2, 4. However, invariance under SUSY transformations restricts the form of eqn. (2.21) as

$$\mathcal{L}^{int} = \left(-\frac{1}{2} W^{ij} \psi_i \psi_j + W^i F_i\right) + c.c. \quad (2.22)$$

It turns out that in order to maintain the interaction Lagrangian invariant under supersymmetry transformations, the quantity W^{ij} must to be analytic function of ϕ_i and thus cannot contain a ϕ_i^* . It is convenient to define a quantity W such that $W^{ij} = \frac{\partial W}{\partial \phi_i \partial \phi_j}$ and $W^i = \frac{\partial W}{\partial \phi_i}$. The entity W in most general form looks like

$$W = h_i \phi_i + \frac{1}{2} M^{ij} \phi_i \phi_j + \frac{1}{3!} f^{ijk} \phi_i \phi_j \phi_k. \quad (2.23)$$

First term of eqn.(2.23) vanishes for the supersymmetric version of the SM as $h^i = 0$ in the absence of a gauge singlet scalar field. It is important to note that in an equivalent language, the quantity W is said to be a function of the chiral superfields [7, 29]. A superfield is a single object that contains as components all of the bosonic, fermionic, and auxiliary fields within the corresponding supermultiplet. That is

$$\begin{aligned} \Phi &\supset (\phi, \psi, F), \text{ or,} \\ \Phi(y^\mu, \theta) &= \phi(y^\mu) + \theta \psi(y^\mu) + \theta \theta F(y^\mu) \text{ and,} \\ \Phi^\dagger(\bar{y}^\mu, \bar{\theta}) &= \phi^*(\bar{y}^\mu) + \bar{\theta} \bar{\psi}(\bar{y}^\mu) + \bar{\theta} \bar{\theta} F(\bar{y}^\mu), \end{aligned} \quad (2.24)$$

where $y^\mu (= x^\mu - i\theta\sigma^\mu\bar{\theta})$ and $\bar{y}^\mu (= \bar{x}^\mu + i\theta\sigma^\mu\bar{\theta})$ represent left and right chiral superspace coordinates, respectively. It is important to note that in case of the (3 + 1) dimensional field theory x^μ represents the set of coordinates. However, for implementation of SUSY with (3 + 1) dimensional field theory one needs to consider *superspace* with supercoordinate $(x^\mu, \theta^\alpha, \bar{\theta}_{\dot{\alpha}})$. $\theta^\alpha, \bar{\theta}_{\dot{\alpha}}$ are spinorial coordinates spanning the fermionic subspace of the superspace. Any superfield, which is a function of y and θ

(\bar{y} and $\bar{\theta}$) only, would be known as a left(right) chiral superfield. Alternatively, if one defines chiral covariant derivatives \mathcal{D}_A and $\bar{\mathcal{D}}_{\bar{A}}$ as

$$\mathcal{D}_A \bar{y}^\mu = 0, \quad \bar{\mathcal{D}}_{\bar{A}} y^\mu = 0, \quad (2.25)$$

then a left and a right chiral superfield is defined as

$$\mathcal{D}_A \Phi = 0 \quad \text{and} \quad \bar{\mathcal{D}}_{\bar{A}} \Phi^\dagger = 0, \quad (2.26)$$

The gauge quantum numbers and the mass dimension of a chiral superfield are the same as that of its scalar component, thus in the superfield formulation, eqn.(2.23) can be recasted as

$$W = h_i \Phi_i + \frac{1}{2} M^{ij} \Phi_i \Phi_j + \frac{1}{3!} f^{ijk} \Phi_i \Phi_j \Phi_k. \quad (2.27)$$

The quantity W is now called a superpotential. The superpotential W now not only determines the scalar interactions of the theory, but also determines fermion masses as well as different Yukawa couplings. Note that $W(W^\dagger)$ is an analytical function of the left(right) chiral superfield.

Coming back to interaction Lagrangian, using the equation of motion for F and F^* finally one ends up with

$$\mathcal{L}^{int} = -\frac{1}{2} (W^{ij} \psi_i \psi_j + W_i^* \psi^{\dagger i} \psi^{\dagger j}) - 2W^i W_i^*. \quad (2.28)$$

The last and remaining interactions are coming from the interaction between gauge and chiral supermultiplets. In presence of the gauge interactions SUSY transformations of eqn.(2.17) suffer the following modification, $\Rightarrow \partial_\mu \rightarrow D_\mu$. It is also interesting to know that in presence of interactions, Euler-Lagrange equations for D^a modify as $D^a = -g(\phi^{i*} T^a \phi^i)$ with T^a as the generator of the group.

So finally with the help of eqns.(2.18), (2.19), (2.28) and including the effect of gauge interactions the complete supersymmetric Lagrangian looks like

$$\begin{aligned} \mathcal{L}^{total} &= -\partial_\mu \phi^{i*} \partial^\mu \phi_i + i \psi^{i\dagger} \bar{\sigma}^\mu \partial_\mu \psi_i - \frac{1}{4} F_{\mu\nu}^a F_a^{\mu\nu} + i \lambda^{a\dagger} \bar{\sigma}^\mu D_\mu \lambda^a \\ &- \left[\frac{1}{2} (W^{ij} \psi_i \psi_j + \sqrt{2} g (\phi_i^* T_{ij}^a \psi_j) \lambda^a) + h.c \right] \\ &- V(\phi, \phi^*) \left\{ \underbrace{\Rightarrow W_i^* W^i}_{F_i^* F^i} + \frac{1}{2} \overbrace{\sum_a g_a^2 (\phi^{i*} T^a \phi_i)^2}^{\sum \frac{1}{2} D^a D^a} \right\}. \end{aligned} \quad (2.29)$$

In eqn.(2.29) index 'a' runs over three of the SM gauge group, $SU(3)_C \times SU(2)_L \times U(1)_Y$. Potential $V(\phi, \phi^*)$, by definition (see eqn.(2.29)) is bounded from below with minima at the origin.

2.4 SUSY breaking

In a supersymmetric theory fermion and boson belonging to the same supermultiplet must have equal mass. This statement can be re-framed in a different way. Consider the supersymmetric partner of electron (called selectron, \tilde{e}), then SUSY invariance demands, $m_e = m_{\tilde{e}} = 5.109 \times 10^{-4} \text{ GeV}$ (see table 1.1), where $m_{\tilde{e}}$ is mass of the selectron. But till date there exists no experimental evidence (see ref. [30]) for a selectron. That simply indicates that supersymmetry is a broken symmetry in nature. The immediate question arises then what is the pattern of SUSY breaking? Is it a spontaneous or an explicit breaking? With the successful implementation of massive gauge bosons in the SM, it is naturally tempting to consider a spontaneous SUSY breaking first.

◆ *Spontaneous breaking of SUSY*

In the case of spontaneous SUSY breaking the supersymmetric Lagrangian remains unchanged, however, vacuum of the theory is no longer symmetric under SUSY transformations. This will in turn cause splitting in masses between fermionic and bosonic states within the same multiplet connected by supersymmetry transformation. From the argument given in section 2.2 it is evident that the spontaneous breaking of supersymmetry occurs when the supercharges Q, \bar{Q} (the SUSY generators) fail to annihilate the vacuum of the theory. In other words if supersymmetry is broken spontaneously (see figure 2.2), the vacuum must have positive energy, i.e. $\langle 0|\mathcal{H}^{susy}|0\rangle \equiv \langle \mathcal{H}^{susy} \rangle > 0$ (see eqn.(2.12)). \mathcal{H}^{susy} is the SUSY Hamiltonian. Neglecting the space-time effects one gets

$$\langle 0|\mathcal{H}^{susy}|0\rangle = \langle 0|\mathcal{V}^{susy}|0\rangle, \quad (2.30)$$

where \mathcal{V}^{susy} is given by $V(\phi, \phi^*)$ (see eqn.(2.29)). Therefore spontaneous breaking of SUSY implies

$$\underbrace{\langle F \rangle \neq 0}_{\text{F-type breaking}} \quad \text{or} \quad \underbrace{\langle D \rangle \neq 0}_{\text{D-type breaking}}. \quad (2.31)$$

It is interesting to note that eqn.(2.31) does not contain D^a because if the theory is gauge invariant then $\langle D \rangle = 0$ holds for Abelian vector superfield only. It is informative to note that the spontaneous breaking of a supersymmetric theory through F -term is known as *O'raifeartaigh* mechanism [31] and the one from D -term as *Fayet-Iliopoulos* mechanism [32, 33]. In the case of global ⁵ SUSY breaking, the broken generator is Q , and hence the Nambu-Goldstone particle must be a massless neutral spin $\frac{1}{2}$ Weyl fermion (known as *goldstino*). The goldstino is not the supersymmetric partner of Goldstone boson, but a Goldstone fermion itself.

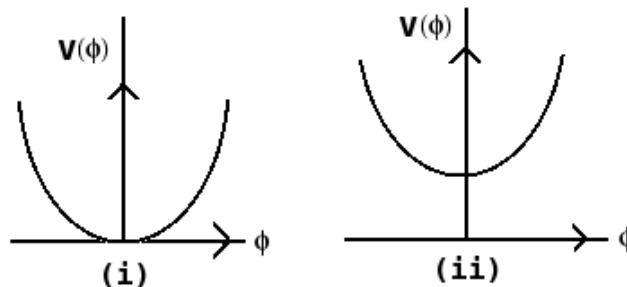


Figure 2.2: Vacua of a supersymmetric theory. (i) exactly supersymmetric and (ii) SUSY is spontaneously broken.

But there are drawbacks with this simple approach. The supersymmetric particle spectrum is known to follow certain sum rules, known as the supertrace sum rules which must vanish. The supertrace of the tree-level squared-mass eigenvalues is defined with a weighted sum over all particles with spin j as $\text{STr}(m^2) \equiv \sum (-1)^j (2j+1) \text{Tr}(m_j^2) = 0$ [34, 35]. This theorem holds for sets of states having same quantum numbers.

But, a vanishing supertrace indicates that some of the supersymmetric particles must be lighter compared to that of the SM, which is of course not observed experimentally so far. However, this relation holds true at the tree level and for renormalizable theories. So supersymmetry can be spontaneously broken in some “hidden sector” which only couples to the “visible” or “observable” SM sector through loop mediated or through non-renormalizable interactions. These intermediate states which appear in loops or are integrated out to produce non-renormalizable interactions are known as the “messengers” or “mediators”. Some of the well-motivated communication schemes are *supergravity*, *anomaly mediation*, *gauge mediation*, *gaugino mediation* and many others (see review [36, 37]). In all of these scenario SUSY is spontaneously broken at some hidden or secluded sector, containing fields singlet under the SM gauge group at some distinct energy scale and the information of breaking is

⁵The infinitesimal SUSY transformation parameter ϵ_α is a space-time independent quantity.

communicated to the observable minimal sector via some messenger interaction. A discussion on these issues is beyond the scope of this thesis.

◆ *Explicit SUSY breaking and soft-terms*

It is now well understood that with the minimal field content SUSY has to be broken explicitly. But what happens to Higgs mass hierarchy if SUSY is broken in nature? It turns out that in order to have a theory free from quadratic divergence as well as to have the desired convergent behaviour of supersymmetric theories at high energies along with the nonrenormalization of its superpotential couplings, the explicit SUSY breaking terms must be soft [38–41]. The word soft essentially implies that all field operators occurring in explicit SUSY breaking Lagrangian must have a mass dimension less than four.

The possible most general [9, 40] soft supersymmetry breaking terms in housed in \mathcal{L}_{soft} are⁶

$$\begin{aligned} \mathcal{L}_{soft} &= - \left(\frac{1}{2} M_a \lambda^a \lambda^a + \frac{1}{3!} a^{ijk} \phi_i \phi_j \phi_k + \frac{1}{2} b^{ij} \phi_i \phi_j + t^i \phi_i \right) + c.c. \\ &\quad - (m^2)_j^i \phi^{j*} \phi_i. \end{aligned} \quad (2.32)$$

In eqn.(2.32) terms like $t^i \phi_i$ are possible only if there exist gauge singlet superfields and thus these terms are absent from the minimal supersymmetric version of the SM. M_a 's are the gaugino soft mass terms, $(m^2)_i^j$ are the coefficients for scalar squared mass terms and b^{ij} , a^{ijk} are the couplings for quadratic and cubic scalar interactions.

◆ *Higgs mass hierarchy and \mathcal{L}_{soft}*

The form of eqn.(2.32) indicates modification of Lagrangian shown in eqn.(2.1). Adding a possible interaction term of the form $\frac{\lambda_f A_{\tilde{f}}}{\sqrt{2}} \tilde{f}_L \tilde{f}_R^* h^0 + h.c$ (scalar cubic interaction) in eqn.(2.1) in turn modifies the two-point function via the loop (see eqn.(2.4)) as

$$\begin{aligned} \Pi_{h^0 h^0}^{\tilde{f}}(0) + \Pi_{h^0 h^0}^f(0) &= - \frac{iy_{\tilde{f}}^2}{16\pi^2} \left[4\delta^2 + (2\delta^2 + |A_{\tilde{f}}|^2) \ln \frac{m_{\tilde{f}}^2}{\mu_R^2} \right] \\ &\quad + \text{higher orders}, \end{aligned} \quad (2.33)$$

where $\delta^2 = m_{\tilde{f}}^2 - m_f^2$ and we assume $|\delta|, |A_{\tilde{f}}| \ll m_f$. The most important observation about eqn.(2.33) is that, in the exact supersymmetric limit

$$m_{\tilde{f}}^2 = m_f^2, \quad A_{\tilde{f}} = 0, \quad (2.34)$$

that is, entire one loop renormalization of the Higgs self energy vanishes⁷. It is also clear from eqn.(2.33) that Higgs self energy is linearly proportional to the SUSY breaking parameters $(\delta^2, |A_{\tilde{f}}|^2)$. Thus supersymmetric theories are free from quadratic divergences, unless $m_{\tilde{f}}^2 \gg m_f^2$. This is an extremely important relation, which indicates that in order to have a TeV scale Higgs boson mass (theoretical limit) the soft terms ($A_{\tilde{f}}$) and the sparticle masses ($m_{\tilde{f}}$) must lie in the same energy scale (reason why we are dreaming to discover SUSY at the large hadron collider experiment).

2.5 Minimal Supersymmetric Standard Model

We are now well equipped to study the Minimal Supersymmetric Standard Model or MSSM (see reviews [10, 13, 17]). It is always illuminating to start with a description of the particle content. Each

⁶It is interesting to note that terms like $-\frac{1}{2} c_i^{jk} \phi^{i*} \phi_j \phi_k + c.c$ are also viable candidates for \mathcal{L}_{soft} , however they can generate quadratic divergence from the loop in the presence of gauge singlet chiral superfields. A term like this becomes soft [41] in the absence of singlet superfields. One more important lesson is that the mass dimension of any coupling in \mathcal{L}_{soft} has to be less than four is a necessary but not sufficient condition for the softness of any operator.

⁷Actually this condition is true for all orders of perturbation theory and is a consequence of the nonrenormalization theorem [6, 42–45].

of the SM fermions have their bosonic counterparts, known as sfermions. Fermionic counterpart for a gauge boson is known as a gaugino. Higgsino is the fermionic counter part for a Higgs boson. It is important to re-emphasize that since a superpotential is invariant under supersymmetry transformation it cannot involve an chiral and a anti-chiral superfield at the same time. In other words a superpotential (W) is an analytical functions of chiral superfields only (W^\dagger contains anti-chiral superfields only) and thus two Higgs doublets are essential for MSSM. In addition, the condition for anomaly cancellation in the higgsino sector, which is a requirement of renormalizability also asks for two Higgs doublets, H_u and H_d . It must be remembered that each of the supersymmetric particle (*sparticle*) has same set of gauge quantum numbers under the SM gauge group as their SM counterpart, as shown in eqn.(1.1). The Higgs doublet H_u behaves like eqn.(1.3), whereas the other doublet H_d under $SU(3)_C \times SU(2)_L \times U(1)_Y$ transforms as,

$$H_d = \begin{pmatrix} H_d^0 \\ H_d^- \end{pmatrix} \sim (1, 2, -1). \quad (2.35)$$

The particle content of the MSSM is shown in figure 2.3. Every lepton (ℓ) and quark (q) of the SM

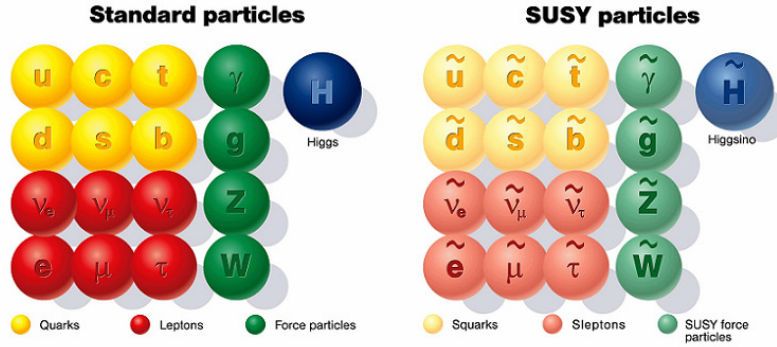


Figure 2.3: particle content of the MSSM.

(spin $\frac{1}{2}$) is accompanied by a *slepton* ($\tilde{\ell}$) and *squark* (\tilde{q}) (spin 0). Corresponding to two Higgs fields H_u and H_d (denoted as H in figure 2.3) there exist two *Higgsino* fields (\tilde{H}_u, \tilde{H}_d) as well (denoted as \tilde{H} in figure 2.3). The electroweak gauge bosons W, Z , gluons (g) and photon (γ) are associated with their superpartner states, namely, *wino* (\tilde{W}), *zino* (\tilde{Z}), *gluino* (\tilde{g}) and *photino* ($\tilde{\gamma}$)⁸. Without further clarification we will concentrate first on the MSSM superpotential and then on the soft terms. We will not talk about the kinetic terms i.e, the free Lagrangian and the gauge interactions (see ref. [22] for an extensive discussions).

✂ MSSM superpotential and soft terms

The superpotential for the MSSM is written as

$$W^{MSSM} = \epsilon_{ab}(Y_u^{ij} \hat{H}_u^b \hat{Q}_i^a \hat{u}_j^c + Y_d^{ij} \hat{H}_d^a \hat{Q}_i^b \hat{d}_j^c + Y_e^{ij} \hat{H}_d^a \hat{L}_i^b \hat{e}_j^c - \mu \hat{H}_d^a \hat{H}_u^b), \quad (2.36)$$

where \hat{H}_d and \hat{H}_u are the down-type and up-type Higgs superfields, respectively. The \hat{Q}_i are $SU(2)_L$ doublet quark superfields, \hat{u}_j^c [\hat{d}_j^c] are $SU(2)_L$ singlet up-type [down-type] quark superfields. The \hat{L}_i are the doublet lepton superfields, and the \hat{e}_j^c are the singlet charged lepton superfields. Here a, b are $SU(2)$ indices, and $\epsilon_{12} = -\epsilon_{21} = 1$. Note that $u_i^c, d_i^c, e_i^c \equiv u_{i_R}^*, d_{i_R}^*, \ell_{i_R}^*$ (see eqn.(1.1)). The only coupling of the superpotential W , that has a positive mass dimension is the μ -parameter.

⁸Another alternative set in lieu of Z, γ could be B, W^3 , where B and W^3 are the $U(1)_Y$ and $SU(2)_L$ gauge bosons, respectively. Correspondingly on the right hand side one should have $\tilde{W}_3, \tilde{B} \iff \tilde{\gamma}, \tilde{Z}$.

The corresponding soft SUSY breaking Lagrangian can be written as

$$\begin{aligned}
-\mathcal{L}_{\text{soft}}^{MSSM} &= (m_{\tilde{Q}}^2)^{ij} \tilde{Q}_i^a \tilde{Q}_j^a + (m_{\tilde{u}^c}^2)^{ij} \tilde{u}_i^c \tilde{u}_j^c + (m_{\tilde{d}^c}^2)^{ij} \tilde{d}_i^c \tilde{d}_j^c - \epsilon_{ab} B_\mu \hat{H}_d^a \hat{H}_u^b \\
&+ (m_{\tilde{L}}^2)^{ij} \tilde{L}_i^a \tilde{L}_j^a + (m_{\tilde{e}^c}^2)^{ij} \tilde{e}_i^c \tilde{e}_j^c + m_{H_d}^2 H_d^a H_d^a + m_{H_u}^2 H_u^a H_u^a \\
&+ \left[\epsilon_{ab} \left\{ (A_u Y_u)^{ij} H_u^b \tilde{Q}_i^a \tilde{u}_j^c + (A_d Y_d)^{ij} H_d^a \tilde{Q}_i^b \tilde{d}_j^c \right. \right. \\
&\left. \left. + (A_e Y_e)^{ij} H_d^a \tilde{L}_i^b \tilde{e}_j^c \right\} - \frac{1}{2} \sum_{i=1}^3 M_i \tilde{\lambda}_i + \text{h.c.} \right]. \tag{2.37}
\end{aligned}$$

In eqn.(2.37), the first two lines consist of squared-mass terms of squarks, sleptons and Higgses along with a bilinear term $(\epsilon_{ab} B_\mu \hat{H}_d^a \hat{H}_u^b)$ in two Higgs superfields. The next line contains the trilinear scalar couplings. Finally, in the last line $M_3, M_2,$ and M_1 are Majorana masses corresponding to $SU(3)_c, SU(2)_L$ and $U(1)_Y$ gauginos $\tilde{\lambda}_3, \tilde{\lambda}_2,$ and $\tilde{\lambda}_1,$ respectively.

The tree level scalar potential is given by (see eqn.(2.29))

$$V_{\text{scalar}}^{MSSM} = V_{\text{soft}}^{MSSM} + \frac{1}{2} D^a D^a + \left| \frac{\partial W^{MSSM}}{\partial \phi^{MSSM}} \right|^2, \tag{2.38}$$

where V_{soft}^{MSSM} contains only the scalar couplings of eqn.(2.37) and Φ^{MSSM} represents scalar component of any of the MSSM chiral superfields. Only the neutral scalar fields develop vacuum expectation values while minimizing the scalar potential V_{scalar}^{MSSM} as follows

$$\langle H_d^0 \rangle = v_1, \quad \langle H_u^0 \rangle = v_2. \tag{2.39}$$

It is evident from eqns.(2.36) and (2.37) that the MSSM has a very rich particle spectra. Note that the matrices associated with bilinear terms in fields (particles or sparticles) are often appear with off-diagonal entries after EWSB (see chapter 1). Clearly entries of these matrices cannot represent any physical masses. So in general these off-diagonal matrices of the gauge or flavour basis can be rotated in a diagonal basis using suitable unitary or bi-unitary transformations. All the scalar mass squared matrices are in housed in V_{scalar}^{MSSM} .

✂ Gauge versus Mass eigen-basis

- The squarks (\tilde{q}) and sleptons (\tilde{l})

The squark and slepton mass square matrices in the flavour basis are bilinears in $\tilde{f}_L^* \tilde{f}_L, \tilde{f}_R^* \tilde{f}_R$ and $\tilde{f}_L^* \tilde{f}_R + \text{c.c}$ where $\tilde{f} \equiv \tilde{l}/\tilde{q}$. It is always possible to rotate them into another basis \tilde{f}_1, \tilde{f}_2 where only combination like $\tilde{f}_1^* \tilde{f}_1, \tilde{f}_2^* \tilde{f}_2$ exists. The basis $\tilde{f}_{1,2}$ is known as the mass basis for squarks and sleptons. The orthogonal mixing matrix relating $\tilde{f}_{L,R}$ and $\tilde{f}_{1,2}$ contains an angle ' θ ' which depends on the ratio of the off-diagonal entry in $\tilde{f}_{L,R}$ basis and the difference in diagonal entries in the same basis. It can be shown (see for example ref. [22]) that for the first two generations of squark and charged slepton the effect of off diagonal mixing is negligible and to a very good approximation $\tilde{f}_{L,R}$ can be treated as the mass basis. So we conclude that

Gauge or flavour basis	Mass basis
$\tilde{e}_L, \tilde{e}_R, \tilde{\mu}_L, \tilde{\mu}_R$	$\tilde{e}_L, \tilde{e}_R, \tilde{\mu}_L, \tilde{\mu}_R$
$\tilde{u}_L, \tilde{u}_R, \tilde{d}_L, \tilde{d}_R$	$\tilde{u}_L, \tilde{u}_R, \tilde{d}_L, \tilde{d}_R$
$\tilde{c}_L, \tilde{c}_R, \tilde{s}_L, \tilde{s}_R$	$\tilde{c}_L, \tilde{c}_R, \tilde{s}_L, \tilde{s}_R$

However, this simple minded approach fails for the third family of slepton and squark due to relatively large Yukawa coupling. This is because, it is the effect of Yukawa coupling which controls the size of the off-diagonal term. Summing up, for the third family

Gauge or flavour basis	Mass basis
$\tilde{\tau}_L, \tilde{\tau}_R$	$\tilde{\tau}_1, \tilde{\tau}_2$
$\tilde{b}_L, \tilde{b}_R, \tilde{t}_L, \tilde{t}_R$	$\tilde{b}_1, \tilde{b}_2, \tilde{t}_1, \tilde{t}_2$

It remains to talk about the left sneutrinos which do not have any right handed counter part. The degenerate squared mass for all three generations of left sneutrino is given by

$$M_{\tilde{\nu}}^2 = m_{\tilde{L}}^2 + \frac{1}{2}M_Z^2 \cos 2\beta, \quad (2.40)$$

where $\tan\beta = \frac{v_2}{v_1}$ is the ratio of two Higgs VEVs and M_Z is the Z boson mass given by $M_Z^2 = \frac{1}{2}(g_1^2 + g_2^2)(v_1^2 + v_2^2)$. Mass for the W^\pm -bosons are given by $M_W^2 = \frac{g_2^2}{2}(v_1^2 + v_2^2)$.

- The neutral and charged supersymmetric fermions

The neutral supersymmetric fermions $(-i\tilde{B}^0, -i\tilde{W}_3^0, \tilde{H}_d^0, \tilde{H}_u^0)$ are known to form a 4×4 symmetric matrix in the flavour basis. This symmetric matrix is diagonalizable using a single unitary matrix N and the corresponding four mass eigenstates are known as neutralinos, χ_i^0 (two-component spinor). Mathematically,

$$\chi_i^0 = N_{i1}\tilde{B}^0 + N_{i2}\tilde{W}_3^0 + N_{i3}\tilde{H}_d^0 + N_{i4}\tilde{H}_u^0, \quad (2.41)$$

with N_{ij} as the elements of the matrix N .

The charged fermions $\psi^+ = -i\tilde{W}^+, \tilde{H}_u^+$ and $\psi^- = -i\tilde{W}^-, \tilde{H}_d^-$ on the other hand form a 4×4 mass matrix in the Lagrangian as follows

$$\mathcal{L}_{MSSM}^{chargino} = -\frac{1}{2} \begin{pmatrix} \psi^+ & \psi^- \end{pmatrix} \begin{pmatrix} 0 & (M_{MSSM}^{chargino})_{2 \times 2}^T \\ (M_{MSSM}^{chargino})_{2 \times 2} & 0 \end{pmatrix} \begin{pmatrix} \psi^+ \\ \psi^- \end{pmatrix} + h.c. \quad (2.42)$$

The 2×2 non-symmetric matrix $(M_{MSSM}^{chargino})_{2 \times 2}$ (see appendix A) requires a bi-unitary transformation to go the two-component physical charged fermion eigenstates, known as charginos, χ_i^\pm . If U, V are the two required transformation matrices, then

$$\begin{aligned} \chi_i^+ &= V_{i1}\tilde{W}^+ + V_{i2}\tilde{H}_u^+, \\ \chi_i^- &= U_{i1}\tilde{W}^- + U_{i2}\tilde{H}_d^-. \end{aligned} \quad (2.43)$$

It is important to re-emphasize that all the charged and neutral spinors considered here are two-component Weyl spinors. They can be used further to construct the corresponding four-component spinors. The neutralino and chargino mass matrices for MSSM are given in appendix A.

- The neutral and the charged leptons and the quarks are treated in MSSM similar to that of the SM.
- The gauge bosons are also treated in similar fashion.
- Higgs bosons in MSSM

Let us write down two Higgs doublet of the MSSM in the real (\Re) and imaginary (\Im) parts as follows

$$\begin{aligned} H_d &= \begin{pmatrix} H_d^0 \\ H_d^- \end{pmatrix} = \begin{pmatrix} \Re H_d^0 + i\Im H_d^0 \\ \Re H_d^- + i\Im H_d^- \end{pmatrix} = \begin{pmatrix} h_1 + ih_2 \\ h_3 + ih_4 \end{pmatrix}, \\ H_u &= \begin{pmatrix} H_u^+ \\ H_u^0 \end{pmatrix} = \begin{pmatrix} \Re H_u^+ + i\Im H_u^+ \\ \Re H_u^0 + i\Im H_u^0 \end{pmatrix} = \begin{pmatrix} h_5 + ih_6 \\ h_7 + ih_8 \end{pmatrix}, \end{aligned} \quad (2.44)$$

Out of this eight Higgs field (h_i), only the neutral real fields can develop a *non-zero* VEV which are (recasting eqn.(2.39))

$$\langle \Re H_d^0 \rangle = v_1, \quad \langle \Re H_u^0 \rangle = v_2. \quad (2.45)$$

These eight Higgs fields are further classifiable into three groups, namely (1) CP-even (h_1, h_7), (2) CP-odd (h_2, h_8) and (3) charged (h_{3-6}). In the mass basis these give five physical Higgs states, h^0, H^0, A^0, H^\pm and three Goldstone bosons (G^0, G^\pm). In terms of mathematical relations,

$$\begin{aligned} H^0 &= \sqrt{2} \left((\Re H_d^0 - v_1) \cos \alpha + (\Re H_u^0 - v_2) \sin \alpha \right), \\ h^0 &= \sqrt{2} \left(-(\Re H_d^0 - v_1) \sin \alpha + (\Re H_u^0 - v_2) \cos \alpha \right), \\ H^- &= \left((\Re H_d^- + i \Im H_d^-) \sin \beta + (\Re H_u^+ + i \Im H_u^+)^\dagger \cos \beta \right), \\ A^0 &= \sqrt{2} \left(-\Im H_d^0 \sin \beta + \Im H_u^0 \cos \beta \right), \\ G^0 &= \sqrt{2} \left(\Im H_d^0 \cos \beta - \Im H_u^0 \sin \beta \right), \\ G^- &= \left((\Re H_d^- + i \Im H_d^-) \cos \beta - (\Re H_u^+ + i \Im H_u^+)^\dagger \sin \beta \right), \\ H^+ &= (H^-)^\dagger, \quad G^+ = (G^-)^\dagger, \end{aligned} \quad (2.46)$$

where α is a mixing angle relating the gauge and mass basis of CP-even Higgs fields. Scalar (CP-even), pseudoscalar (CP-odd) and charged scalar mass squared matrices in the flavour basis for MSSM Higgs fields are given in appendix A. Physical Higgs boson squared masses are given by (using eqns.(2.36),(2.37))

$$\begin{aligned} m_{A^0}^2 &= \frac{2B_\mu}{\sin 2\beta}, \\ m_{H^0}^2 &= \frac{1}{2} \left[m_{A^0}^2 + M_Z^2 + \sqrt{(m_{A^0}^2 + M_Z^2)^2 - 4m_{A^0}^2 M_Z^2 \cos^2 2\beta} \right], \\ m_{h^0}^2 &= \frac{1}{2} \left[m_{A^0}^2 + M_Z^2 - \sqrt{(m_{A^0}^2 + M_Z^2)^2 - 4m_{A^0}^2 M_Z^2 \cos^2 2\beta} \right], \\ m_{H^\pm}^2 &= m_{A^0}^2 + M_W^2. \end{aligned} \quad (2.47)$$

From eqn.(2.47) one can achieve a theoretical upper limit of the lightest Higgs boson mass [46,47], (m_{h^0}) at the tree level after a bit of algebraic exercise as [48–50],

$$m_{h^0} \leq M_Z |\cos 2\beta|. \quad (2.48)$$

The lightest Higgs mass can however, receive significant radiative corrections from higher order processes, which are capable of altering the lightest Higgs mass bound drastically. Note that the value for angle β is between 0 to $\frac{\pi}{2}$. Thus it is easy to conclude that m_{h^0} at the tree level can be at most of the order of the Z -boson mass. But this is already ruled out by the LEP experiment [30,51]. So it is evident that inclusion of loop correction [52–57] (see also ref. [58] and references therein) to lightest Higgs boson mass in MSSM is extremely important. The dominant contribution arises from top-stop loop and assuming masses for sparticles below 1 TeV we get $m_{h^0} \leq 135$ GeV⁹.

The conditions for the tree level Higgs potential to be bounded from below (in the direction $v_1 = v_2$) as well as the condition for EWSB are

$$\begin{aligned} m_{H_d}^2 + m_{H_u}^2 + 2|\mu|^2 &\geq 2|B_\mu|, \\ (m_{H_d}^2 + |\mu|^2)(m_{H_u}^2 + |\mu|^2) &< B_\mu^2. \end{aligned} \quad (2.49)$$

It is extremely important to note that if $B_\mu, m_{H_d}^2, m_{H_u}^2$ all are zero, i.e. there exist no soft SUSY breaking terms, the EWSB turns out to be impossible. So in a sense SUSY breaking is somehow related to the EWSB.

⁹This limit can be further relaxed to $m_{h^0} \leq 150$ GeV, assuming all couplings in the theory remain perturbative up to the unification scale [59,60].

We conclude the description of the MSSM with a note on the corresponding set of Feynman rules. The number of vertices are extremely large for a supersymmetric theory even in the minimal version, and consequently there exist a huge number of Feynman rules. The rules are far more complicated compared to the SM because of the presence of Majorana particles (particles, that are antiparticles of their own, neutralinos for example). For a complete set of Feynman rules for the MSSM see references [12, 48, 50, 61, 62]. A detailed analysis for the Higgs boson in supersymmetry and related phenomenology are addressed in a series of references [50, 63–65].

2.6 The R -parity

The superpotential for MSSM was shown in eqn.(2.36). This superpotential is gauge (the SM gauge group) invariant, Lorentz invariant and maintains renormalizability. However, it is natural to ask that what is preventing the following terms to appear in W^{MSSM} , which are also gauge and Lorentz invariant and definitely renormalizable:

$$W^{extra} = \epsilon_{ab}(-\varepsilon^i \hat{L}_i^a \hat{H}_u^b + \frac{1}{2} \lambda_{ijk} \hat{L}_i^a \hat{L}_j^b \hat{e}_k^c + \lambda'_{ijk} \hat{L}_i^a \hat{Q}_j^b \hat{d}_k^c + \frac{1}{2} \lambda''_{ijk} \hat{u}_i^c \hat{d}_j^c \hat{d}_k^c). \quad (2.50)$$

Of course, all of these terms violate either lepton (L) [66, 67] or baryon (B) [66, 68] number by odd units. The second and the third terms of eqn.(2.50) violate lepton number by one unit whereas the fourth term violates baryon number by one unit.

Now it is well known that in the SM, lepton and baryon numbers are conserved at the perturbative level. In the SM, L and B are the accidental symmetry of the Lagrangian, that is to say that these are not symmetries imposed on the Lagrangian, rather they are consequence of the gauge and Lorentz invariance, renormalizability and, of course, particle content of the SM. Moreover, these numbers are no way related to any fundamental symmetries of nature, since they are known to be violated by non-perturbative electroweak effects [69]. So it is rather difficult to drop these terms from a general MSSM superpotential unless one assumes B, L conservation as a postulate for the MSSM. However, in the presence of these terms there exists new contribution to the proton decay process ($p \rightarrow \ell^+ \pi^0$ with $\ell^+ = e^+, \mu^+$) as shown in figure 2.4. This process (see figure 2.4) will yield a proton life time $\approx 10^{-9}$ sec,

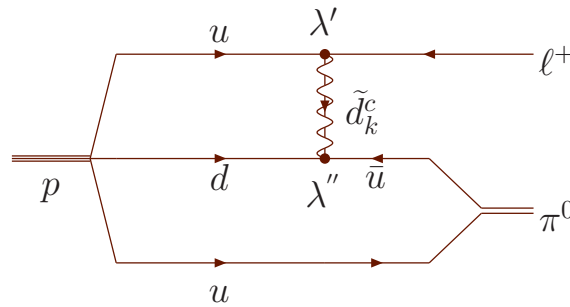


Figure 2.4: Feynman diagrams for the process $p \rightarrow \ell^+ \pi^0$ with $\ell^+ = e^+, \mu^+$.

assuming $\lambda', \lambda'' \sim \mathcal{O}(10^{-1})$ and TeV scale squark masses. However, the known experimental bound for proton lifetime is $> 10^{32}$ years [30, 70]. So in order to explain proton stability either these new couplings ($\lambda, \lambda', \lambda''$) are extremely small (which again requires explanation) or their products (appear in the decay width for the process $p \rightarrow \ell^+ \pi^0$) are very small or these terms are somehow forbidden from the MSSM superpotential. In fact, to avoid very fast proton decay mediated through squarks of masses of the order of the electroweak scale, simultaneous presence of λ', λ'' type couplings must be forbidden unless the product $\lambda' \lambda''$ is severely constrained (see figure 2.4). The λ type of operators are not so stringently suppressed, and therefore still a lot of freedom remains (see ref. [71] and references therein).

It turns out that since these new terms (see eqn.(2.50)) violate either lepton or baryon number by odd units it is possible to restrict them from appearing in W^{MSSM} by imposing a discrete symmetry called R -parity (R_p),¹⁰ [66,72–74] defined as,

$$R_p = (-1)^{3(B-L)+2s}, \quad (2.51)$$

where s is the spin of the particle. Since L is an integer, an alternative expression for R_p is also given by

$$R_p = (-1)^{3B+L+2s}. \quad (2.52)$$

It is interesting to note that since different states within a supermultiplet have different spins, they must have different R_p . It turns out that by construction all the SM particles have $R_p = +1$ and for all superpartners, $R_p = -1$. This is a discrete Z_2 symmetry and multiplicative in nature. It is important to note that R_p conservation would require (1) even number of sparticles at each interaction vertex, and (2) the lightest supersymmetric particle (LSP) has no lighter $R_p = -1$ states to decay and thus it is absolutely stable (see figure 2.5). Thus the LSP for a supersymmetric model with conserved R_p can act as a natural dark matter candidate. It must be remembered that the soft supersymmetry breaking Lagrangian will also contain R_p violating terms [75,76].

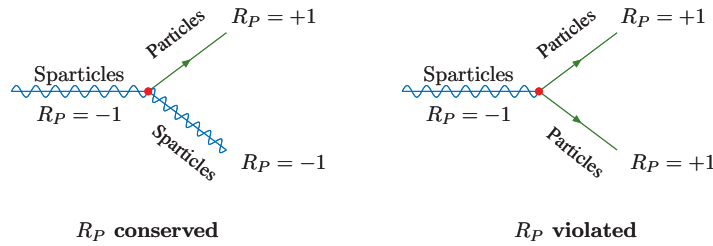


Figure 2.5: With R_p conservation the LSP is forced to be stable due to unavailability of any lighter sparticle states (*left*), whereas for the R_p -violating scenario the LSP can decay into SM particles (*right*).

Looking at eqn.(2.50) it is clear that sources for R_p violation (\mathcal{R}_p) (see references [77–89]) are either bilinear (ϵ) [90–102] or trilinear ($\lambda, \lambda', \lambda''$) [76,81,84,97,103–106] in nature. The simple most example of \mathcal{R}_p turns out to be bilinear. It is interesting to note that these bilinear terms are removable from superpotential by using field redefinitions, however they reappear as trilinear couplings both in superpotential and in soft SUSY breaking Lagrangian [67,107,108] along with the original bilinear R_p -violating terms, that were in the soft SUSY breaking Lagrangian to start with. The effect of rotating away $L_i H_u$ term from the superpotential by a redefinition of the lepton and Higgs superfields are bound to show up via the scalar potential [92]. Also even if bilinear terms are rotated away at one energy scale, they reappear in some other energy scale as the couplings evolve radiatively [109]. The trilinear couplings can also give rise to bilinear terms in one-loops (see figure 2.6) [76]. Note that \mathcal{R}_p can be either explicit (like eqn.(2.50)) [67,77,107,108] or spontaneous [77,78,110–116].

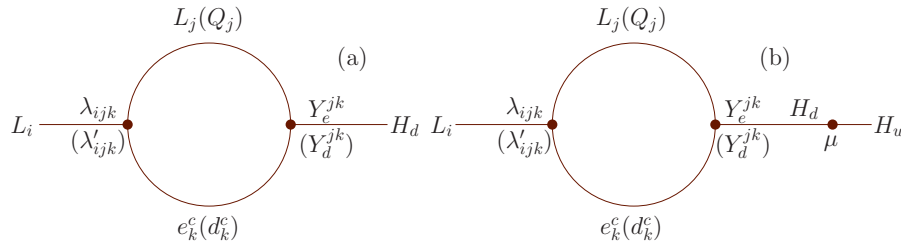


Figure 2.6: One loop diagrams contributing to bilinear terms like $L_i H_u, L_i H_d$ using the trilinear couplings λ, λ' .

¹⁰See also matter parity [38,66,72,73].

Here as a digression it should be mentioned that R_p can be embedded into a larger continuous group (see, for example, ref. [117] and references therein) which is finally abandoned for phenomenological reasons¹¹. However, its Z_2 subgroup could still be retained, which is the R_p .

To summarize, it seems that R_p violation is a natural feature for supersymmetric theories, since R_p -violating terms (see eqn.(2.50)) are not forbidden to appear in the MSSM superpotential by the arguments of gauge and Lorentz invariance or renormalizability. On the contrary, assumption of R_p -conservation to prevent proton decay appears to be an ad hoc one. Besides, models with R_p -violation are also phenomenologically very rich. Of course, it is natural to ask about the fate of the proton. But considering either lepton or baryon number violation at a time proton stability can be achieved.

It is true that with \mathcal{R}_p the LSP is no longer stable and can decay into the SM particles. The stable LSP (in case it is colour and charge neutral) can be a natural candidate for the Dark matter [118, 119]. However, there exist other viable dark matter candidates even for a theory with \mathcal{R}_p , namely, gravitino [120–122], axion [123, 124] and axino [125, 126] (supersymmetric partner of axion).

It is important to note that a decaying LSP has very different and enriched implications in a collider study. Unlike models with R_p conservation, which yield large missing energy signature at the end of any supersymmetric process, effect of \mathcal{R}_p can often produce interesting visible final states detectable in a collider experiments. Models with bilinear \mathcal{R}_p are especially interesting concerning collider studies [122, 127–140], as they admit direct mixing between neutrino and neutralinos.

Finally, it remains to be mentioned the most important aspect of R_p violation, namely, generation of the neutrino mass. It is impossible to generate neutrino masses in a supersymmetric model with R_p conservation along with minimal field content (see eqn.(2.36)). It is rather important to clarify the importance of \mathcal{R}_p in neutrino mass generation. There are other ways to generate light neutrino masses, both in supersymmetric or non-supersymmetric models like adding extra particles or enhancing the gauge group (left-right symmetric models [141] for example) and many others. But generating massive neutrinos with \mathcal{R}_p is a pure supersymmetric phenomenon without any SM analog. More on the issue of light neutrino mass generation and \mathcal{R}_p will be addressed in the next chapter.

To complete the discussion, it is important to mention that these \mathcal{R}_p couplings are highly constrained by experimental limits on different physical processes, like neutron-anti neutron scattering [142–145], neutrinoless double beta decay [103, 146–150], precision measurements of Z decay [151–153], proton decay [154–156], Majorana masses for neutrinos [105, 157–161] etc. Discussion on different supersymmetric models with and without R_p conservation, proposed in the literature is given in a recent review [162].

2.7 Successes of supersymmetry

So far, we tried to formulate the theory of MSSM step by step starting from the very basics. It is perhaps the appropriate place to discuss the success of the supersymmetric theories over most of the shortcomings of the SM (see section 1.2). We are about to discuss all the seven points made in section 1.2 but in reverse order.

1. The last point deals with Higgs mass hierarchy in the SM. It has been shown earlier that how a supersymmetric theory can predict a finite Higgs mass without any *quadratic divergences* even though SUSY is broken in nature.
2. It is true that MSSM with R_p conservation predicts massless neutrinos similar to the SM. However, as argued in the earlier section, supersymmetric theories are capable of accommodating massive neutrinos if R_p is broken. Just for the sake of completeness, let us mention that there exist also certain non-minimal supersymmetric models, which can account for the neutrino masses with seesaw mechanism. Such models include e.g. right-handed neutrinos or other very heavy particles. In the next chapter these possibilities will be explored in detail.
3. The SM hardly offers any room for a suitable dark matter candidate. But as described in section 2.6 the lightest supersymmetric particle is a good candidate for the dark matter in a supersymmetric model with R_p conservation. Nevertheless, as stated in section 2.6, there exist other viable dark matter candidates (gravitino, axion etc.) even for an R_p -violating supersymmetric theory.

¹¹A continuous symmetry would prefer massless gauginos, which is already ruled out by experiments.

4. The apparent exclusion of gravitational interaction from the SM is still maintained in supersymmetric theories, so long one considers global supersymmetry. A locally supersymmetric theory together with the theory of general relativity can incorporate gravitational interaction in SUSY. This theory is popularly known as supergravity theory.
5. Concerning point no.(3) of section 1.2, there are other sources of CP-violation in the MSSM itself, which can account for the large matter-anti matter asymmetry of the universe. In general, apart from one CKM phase there exist many different phases in the MSSM, particularly in the soft supersymmetry breaking sector. However, some of these are subjected to strong phenomenological constraints.
6. It is true that the number of free parameters in a general MSSM theory is larger (> 100) [163,164] compared to that of the SM. However, there are models where most of these parameters can be achieved through evolution of a fewer number of parameters at a higher scale. For example in minimal supergravity [10,165] theory the number of free parameters is just five.

It has to be emphasized here, that this will be a rather incorrect statement that supersymmetric theories are free from any drawbacks. It is definitely true that they provide explanations to some of the shortcomings of the SM in a few occasions, but not always. As an example supersymmetric theories are more prone to FCNC through the sparticle mediated processes [163,166–171]. This problem can be removed using clever tricks, but a related discussion is beyond the scope of this thesis. Another, well known problem of MSSM, the μ -problem will be addressed in the following section.

The main stumbling block for any supersymmetric theory is that there are no experimental evidence for supersymmetry till date. All the experimental bounds on different phenomenological processes with supersymmetric effects are basically exclusion limit.

2.8 The μ -problem

The μ -parameter, associated with the bilinear term in Higgs superfields (see eqn.(2.36)) is the only coupling in the MSSM superpotential having a non-zero positive mass dimension. The problem appears when one consider the EWSB condition, which is given by

$$\frac{1}{2}M_Z^2 = \frac{m_{H_d}^2 - m_{H_u}^2 \tan^2 \beta}{\tan^2 \beta - 1} - |\mu^2|, \quad (2.53)$$

where $m_{H_d}^2, m_{H_u}^2$ are given by eqn.(2.37), $\tan \beta = \frac{v_2}{v_1}$ and M_Z is the Z boson mass. The Z boson mass is very precisely measured to be 91.187 GeV (see table 1.1). So it is expected that all the entries of the right hand side of eqn.(2.53) (without any fine cancellation) should have the same order of magnitudes. But how could this happen? $m_{H_d}^2, m_{H_u}^2$ are coming from the soft supersymmetric breaking sector with entries at the TeV scale. On the other hand, μ belongs to SUSY invariant W^{MSSM} (eqn.(2.36)), which naturally can be as large as the Planck scale. So why these two scales appear to be of the same order of magnitude without having any a priori connection in between? This defines the μ -problem [172]. An alternative statement could be why $\mu^2 \sim m_{soft}^2$ and not $\sim M_{Planck}^2$.

It seems easy to solve this problem by starting with $\mu = 0$ at W^{MSSM} and then use the favour of radiative corrections to generate a non-zero μ term. But there are some phenomenological problems of this approach and moreover $\mu = 0$ will give zero VEV for H_d along with the presence of unwanted Weinberg-Wilczek axion [173,174]. So it is apparent that one needs to consider either $\mu \neq 0$ or require extra fields. The requirement of additional fields often lead to other problems and consequently do not predict satisfactory models [175–179]. There exist indeed various solutions to the μ -problem where in most of the occasions the μ -term is absent at the tree level and a TeV or electroweak scale μ -term arises from the VEV(s) of new fields. These VEVs are obtained by minimizing the potential which also involves soft SUSY breaking terms. Thus, the fact $\mu^2 \sim m_{soft}^2$ turns out to be rather natural. Different solutions to the μ -problem have been addressed in references [180–191]. Some of these mechanisms are operational at very high energies and thus are hardly testable experimentally.

Perhaps the simple most dynamical solution to the μ -problem is offered by next-to minimal supersymmetric standard model or NMSSM (see review [192] and references therein). In NMSSM the

bilinear term $\epsilon_{ab}\hat{H}_d^a\hat{H}_u^b$ gets replaced by $\epsilon_{ab}\lambda\hat{S}\hat{H}_d^a\hat{H}_u^b$. The superfield \hat{S} is singlet [193–198] under the SM gauge group. After the EWSB an effective μ term is given by

$$\mu = \lambda v_s, \quad (2.54)$$

where $v_s = \langle S \rangle$, is the VEV acquired by the scalar component of the superfield \hat{S} . The VEV calculation invokes the soft SUSY breaking terms and hence in general the VEVs are at the TeV scale. It is now clear that the μ -term of eqn.(2.54) is of the right order of magnitude and it is indeed connected to m_{soft}^2 . The NMSSM superpotential assumes a Z_3 symmetry which forbids any bilinear term in superpotential.

It is important to note that any term in the superpotential with a non-zero positive mass dimension suffers the similar fate. In fact the bilinear R_p terms (see eqn.(2.50)) are also associated with similar kind of problem known as the ϵ -problem [96]. A common origin for the ϵ_i (to account for the neutrino oscillation data), and the μ -term can be achieved using a horizontal family symmetry as suggested in ref. [199].

2.9 Next-to-Minimal Supersymmetric Standard Model

It is perhaps logical and consistent with the theme of this thesis to give a brief introduction of the NMSSM. The NMSSM superpotential, is given by (see review [192, 200])

$$W^{NMSSM} = W'^{MSSM} - \epsilon_{ab}\lambda\hat{S}\hat{H}_d^a\hat{H}_u^b + \frac{1}{3}\kappa\hat{S}^3, \quad (2.55)$$

where W'^{MSSM} is the MSSM superpotential (eqn.(2.36)) without the μ -term. In a similar fashion if $\mathcal{L}_{soft}^{NMSSM}$ denotes $\mathcal{L}_{soft}^{MSSM}$ without the B_μ term (see eqn.(2.37)), then

$$-\mathcal{L}_{soft}^{NMSSM} = -\mathcal{L}_{soft}^{MSSM} + (m_{\tilde{S}}^2)\tilde{S}\tilde{S} - \epsilon_{ab}(A_\lambda\lambda)\tilde{S}H_d^aH_u^b + \frac{1}{3}(A_\kappa\kappa)\tilde{S}^3 + h.c. \quad (2.56)$$

However, even in NMSSM, if R_p is conserved, light neutrinos are exactly massless. NMSSM models of neutrino mass generation will be discussed in the next chapter.

Particle spectrum for NMSSM will be enlarged over that of the MSSM due to extra particle content. However, \hat{S} being SM gauge singlet only the neutralino sector and the neutral Higgs sector receives modifications. The neutralino mass matrix is now a 5×5 symmetric matrix and there will be one more CP-odd and CP-even neutral scalar states, compared to that of the MSSM. The phenomenology of NMSSM is definitely much enriched compared to the MSSM. This is essentially due to the admixture of new singlet states with MSSM fields. For example, theoretical lower bound on the lightest Higgs mass is now given by [201] (For Higgs sector in NMSSM also see references [52, 202–229])

$$m_{h^0}^2 \leq M_Z^2 \left[\cos^2 2\beta + \frac{2\lambda^2 \cos^2 \theta_w}{g_2^2} \sin^2 2\beta \right]. \quad (2.57)$$

which is clearly different from eqn.(2.48). It is interesting to note that the lower limit of tree level lightest Higgs boson mass in NMSSM depends on λ and hence it is in general difficult to put some upper bound on $m_{h^0}^2$ without constraining λ .

The last term in eqn.(2.55) with coefficient κ is included in order to avoid an unacceptable axion associated to the breaking of a global U(1) symmetry [202]. This term is perfectly allowed by all symmetry. However, the discrete Z_3 symmetry of the NMSSM superpotential (see section 2.8) when spontaneously broken leads to three degenerate vacua. Casually disconnected parts of the Universe then would have randomly chosen one of these three equivalent minima leading to the formation of the dangerous cosmological domain wall [230–232]. However, solutions to this problem exist [233–235], but these issues are beyond the scope of this thesis¹². Another major problem of the NMSSM theories are associated with the stability of gauge hierarchy arising from the *tadpole* contribution of the singlet field.

¹²One solution of this problem is to put $\kappa = 0$ in the NMSSM superpotential by some symmetry argument. This simplified version is known as Minimally NMSSM or MNMSSM.

Diverse phenomenological aspects of NMSSM models are discussed in references [214, 225, 236–253, 253–299].

The prime focus of this thesis remains the issues of neutrino masses and mixing in supersymmetric theories. It has been already argued that massive neutrinos can be accommodated in supersymmetric theories either through R_p or using seesaw mechanism with non-minimal field contents. Besides, mass generation is possible both with the tree level and loop level analysis. However, even before it is important to note the evidences as well as the basics of the neutrino oscillation. It is also interesting to note the implications of the massive neutrinos in an accelerator experiment. We aim to discuss these issues in details in the next chapter along with other phenomenological implications.

Bibliography

- [1] Gervais J L and Sakita B 1971 *Nucl. Phys.* **B34** 632–639
- [2] Neveu A and Schwarz J H 1971 *Nucl. Phys.* **B31** 86–112
- [3] Ramond P 1971 *Phys. Rev.* **D3** 2415–2418
- [4] Aharonov Y, Casher A and Susskind L 1971 *Phys. Lett.* **B35** 512–514
- [5] Wess J and Zumino B 1974 *Nucl. Phys.* **B70** 39–50
- [6] Wess J and Zumino B 1974 *Phys. Lett.* **B49** 52
- [7] Ferrara S, Wess J and Zumino B 1974 *Phys. Lett.* **B51** 239
- [8] Iwasaki Y and Kikkawa K 1973 *Phys. Rev.* **D8** 440–449
- [9] Fayet P and Ferrara S 1977 *Phys. Rept.* **32** 249–334
- [10] Nilles H P 1984 *Phys. Rept.* **110** 1–162
- [11] Gates S J, Grisaru M T, Rocek M and Siegel W 1983 *Front. Phys.* **58** 1–548
- [12] Haber H E and Kane G L 1985 *Phys. Rept.* **117** 75–263
- [13] Sohnius M F 1985 *Phys. Rept.* **128** 39–204
- [14] Drees M 1996 (*Preprint hep-ph/9611409*)
- [15] Lykken J D 1996 (*Preprint hep-th/9612114*)
- [16] Dine M 1996 (*Preprint hep-ph/9612389*)
- [17] Martin S P 1997 (*Preprint hep-ph/9709356*)
- [18] Bilal A 2001 (*Preprint hep-th/0101055*)
- [19] Wess J and Bagger J Princeton, USA: Univ. Pr. (1992) 259 p
- [20] Bailin D and Love A Bristol, UK: IOP (1994) 322 p. (Graduate student series in physics)
- [21] Weinberg S Cambridge, UK: Univ. Pr. (2000) 419 p
- [22] Drees M, Godbole R and Roy P Hackensack, USA: World Scientific (2004) 555 p
- [23] Baer H and Tata X Cambridge, UK: Univ. Pr. (2006) 537 p
- [24] Feynman R P and Weinberg S Cambridge, USA: Univ. PR. (1987) 110p
- [25] Coleman S R and Mandula J 1967 *Phys. Rev.* **159** 1251–1256
- [26] Haag R, Lopuszanski J T and Sohnius M 1975 *Nucl. Phys.* **B88** 257
- [27] Muller-Kirsten H J W and Wiedemann A Print-86-0955 (Kaiserslautern)

- [28] Simonsen I 1995 (*Preprint hep-ph/9506369*)
- [29] Salam A and Strathdee J A 1974 *Nucl. Phys.* **B76** 477–482
- [30] Nakamura K *et al.* (Particle Data Group) 2010 *J. Phys.* **G37** 075021
- [31] O’Raifeartaigh L 1975 *Nucl. Phys.* **B96** 331
- [32] Fayet P and Iliopoulos J 1974 *Phys. Lett.* **B51** 461–464
- [33] Fayet P 1976 *Nuovo Cim.* **A31** 626
- [34] Ferrara S Invited talk given at Sanibel Symp. on Fundamental Problems of Quantum Field Theory, Palm Coast, Fla., Feb 25 - Mar 2, 1979
- [35] Ferrara S, Girardello L and Palumbo F 1979 *Phys. Rev.* **D20** 403
- [36] Kolda C F 1998 *Nucl. Phys. Proc. Suppl.* **62** 266–275
- [37] Intriligator K A and Seiberg N 2007 *Class. Quant. Grav.* **24** S741–S772
- [38] Dimopoulos S and Georgi H 1981 *Nucl. Phys.* **B193** 150
- [39] Sakai N 1981 *Zeit. Phys.* **C11** 153
- [40] Girardello L and Grisaru M T 1982 *Nucl. Phys.* **B194** 65
- [41] Hall L J and Randall L 1990 *Phys. Rev. Lett.* **65** 2939–2942
- [42] Iliopoulos J and Zumino B 1974 *Nucl. Phys.* **B76** 310
- [43] Ferrara S, Iliopoulos J and Zumino B 1974 *Nucl. Phys.* **B77** 413
- [44] Zumino B 1975 *Nucl. Phys.* **B89** 535
- [45] Grisaru M T, Siegel W and Rocek M 1979 *Nucl. Phys.* **B159** 429
- [46] Casas J A, Espinosa J R, Quiros M and Riotto A 1995 *Nucl. Phys.* **B436** 3–29
- [47] Casas J A, Espinosa J R and Quiros M 1995 *Phys. Lett.* **B342** 171–179
- [48] Gunion J F, Haber H E, Kane G L and Dawson S 2000 *Front. Phys.* **80** 1–448
- [49] Gunion J F, Haber H E, Kane G L and Dawson S 1992 (*Preprint hep-ph/9302272*)
- [50] Gunion J F and Haber H E 1986 *Nucl. Phys.* **B272** 1
- [51] Barate R *et al.* (LEP Working Group for Higgs boson searches) 2003 *Phys. Lett.* **B565** 61–75
- [52] Haber H E and Hempfling R 1991 *Phys. Rev. Lett.* **66** 1815–1818
- [53] Okada Y, Yamaguchi M and Yanagida T 1991 *Prog. Theor. Phys.* **85** 1–6
- [54] Okada Y, Yamaguchi M and Yanagida T 1991 *Phys. Lett.* **B262** 54–58
- [55] Ellis J R, Ridolfi G and Zwirner F 1991 *Phys. Lett.* **B257** 83–91
- [56] Ellis J R, Ridolfi G and Zwirner F 1991 *Phys. Lett.* **B262** 477–484
- [57] Espinosa J R and Quiros M 1991 *Phys. Lett.* **B266** 389–396
- [58] Chankowski P H, Pokorski S and Rosiek J 1994 *Nucl. Phys.* **B423** 437–496
- [59] Kane G L, Kolda C F and Wells J D 1993 *Phys. Rev. Lett.* **70** 2686–2689
- [60] Espinosa J R and Quiros M 1993 *Phys. Lett.* **B302** 51–58

- [61] Rosiek J 1990 *Phys. Rev.* **D41** 3464
- [62] Rosiek J 1995 (*Preprint hep-ph/9511250*)
- [63] Gunion J F and Haber H E 1986 *Nucl. Phys.* **B278** 449
- [64] Gunion J F and Haber H E 1988 *Nucl. Phys.* **B307** 445
- [65] Gunion J F and Haber H E 1992 (*Preprint hep-ph/9301205*)
- [66] Weinberg S 1982 *Phys. Rev.* **D26** 287
- [67] Hall L J and Suzuki M 1984 *Nucl. Phys.* **B231** 419
- [68] Zwirner F 1983 *Phys. Lett.* **B132** 103–106
- [69] 't Hooft G 1976 *Phys. Rev. Lett.* **37** 8–11
- [70] Nishino H *et al.* (Super-Kamiokande) 2009 *Phys. Rev. Lett.* **102** 141801
- [71] Dreiner H K, Kramer M and O'Leary B 2007 *Phys. Rev.* **D75** 114016
- [72] Sakai N and Yanagida T 1982 *Nucl. Phys.* **B197** 533
- [73] Dimopoulos S, Raby S and Wilczek F 1982 *Phys. Lett.* **B112** 133
- [74] Farrar G R and Fayet P 1978 *Phys. Lett.* **B76** 575–579
- [75] Allanach B C, Dedes A and Dreiner H K 2004 *Phys. Rev.* **D69** 115002
- [76] de Carlos B and White P L 1996 *Phys. Rev.* **D54** 3427–3446
- [77] Ellis J R, Gelmini G, Jarlskog C, Ross G G and Valle J W F 1985 *Phys. Lett.* **B150** 142
- [78] Ross G G and Valle J W F 1985 *Phys. Lett.* **B151** 375
- [79] Dawson S 1985 *Nucl. Phys.* **B261** 297
- [80] Barbieri R and Masiero A 1986 *Nucl. Phys.* **B267** 679
- [81] Barger V D, Giudice G F and Han T 1989 *Phys. Rev.* **D40** 2987
- [82] Ibanez L E and Ross G G 1992 *Nucl. Phys.* **B368** 3–37
- [83] Bhattacharyya G 1997 *Nucl. Phys. Proc. Suppl.* **52A** 83–88
- [84] Dreiner H K 1997 (*Preprint hep-ph/9707435*)
- [85] Bhattacharyya G 1997 (*Preprint hep-ph/9709395*)
- [86] Barbier R *et al.* 1998 (*Preprint hep-ph/9810232*)
- [87] Allanach B *et al.* (R parity Working Group) 1999 (*Preprint hep-ph/9906224*)
- [88] Barbier R *et al.* 2005 *Phys. Rept.* **420** 1–202
- [89] Chemtob M 2005 *Prog. Part. Nucl. Phys.* **54** 71–191
- [90] Joshipura A S and Nowakowski M 1995 *Phys. Rev.* **D51** 5271–5275
- [91] Joshipura A S and Nowakowski M 1995 *Phys. Rev.* **D51** 2421–2427
- [92] de Campos F, Garcia-Jareno M A, Joshipura A S, Rosiek J and Valle J W F 1995 *Nucl. Phys.* **B451** 3–15
- [93] Smirnov A Y and Vissani F 1996 *Nucl. Phys.* **B460** 37–56

- [94] Nowakowski M and Pilaftsis A 1996 *Nucl. Phys.* **B461** 19–49
- [95] Hempfling R 1996 *Nucl. Phys.* **B478** 3–30
- [96] Nilles H P and Polonsky N 1997 *Nucl. Phys.* **B484** 33–62
- [97] de Carlos B and White P L 1997 *Phys. Rev.* **D55** 4222–4239
- [98] Roy S and Mukhopadhyaya B 1997 *Phys. Rev.* **D55** 7020–7029
- [99] Diaz M A, Romao J C and Valle J W F 1998 *Nucl. Phys.* **B524** 23–40
- [100] Akeroyd A G, Diaz M A, Ferrandis J, Garcia-Jareno M A and Valle J W F 1998 *Nucl. Phys.* **B529** 3–22
- [101] Hirsch M, Diaz M A, Porod W, Romao J C and Valle J W F 2000 *Phys. Rev.* **D62** 113008
- [102] Restrepo Quintero D A 2001 (*Preprint* hep-ph/0111198)
- [103] Enqvist K, Masiero A and Riotto A 1992 *Nucl. Phys.* **B373** 95–116
- [104] Choudhury D and Raychaudhuri S 1997 *Phys. Lett.* **B401** 54–61
- [105] Rakshit S, Bhattacharyya G and Raychaudhuri A 1999 *Phys. Rev.* **D59** 091701
- [106] Raychaudhuri S 1999 (*Preprint* hep-ph/9905576)
- [107] Lee I H 1984 *Phys. Lett.* **B138** 121
- [108] Lee I H 1984 *Nucl. Phys.* **B246** 120
- [109] Barger V D, Berger M S, Phillips R J N and Woehrmann T 1996 *Phys. Rev.* **D53** 6407–6415
- [110] Aulakh C S and Mohapatra R N 1982 *Phys. Lett.* **B119** 136
- [111] Santamaria A and Valle J W F 1987 *Phys. Lett.* **B195** 423
- [112] Santamaria A and Valle J W F 1988 *Phys. Rev. Lett.* **60** 397–400
- [113] Santamaria A and Valle J W F 1989 *Phys. Rev.* **D39** 1780–1783
- [114] Masiero A and Valle J W F 1990 *Phys. Lett.* **B251** 273–278
- [115] Nogueira P, Romao J C and Valle J W F 1990 *Phys. Lett.* **B251** 142–149
- [116] Romao J C, Santos C A and Valle J W F 1992 *Phys. Lett.* **B288** 311–320
- [117] Joshipura A S, Vaidya R D and Vempati S K 2000 *Phys. Rev.* **D62** 093020
- [118] Goldberg H 1983 *Phys. Rev. Lett.* **50** 1419
- [119] Ellis J R, Hagelin J S, Nanopoulos D V, Olive K A and Srednicki M 1984 *Nucl. Phys.* **B238** 453–476
- [120] Borgani S, Masiero A and Yamaguchi M 1996 *Phys. Lett.* **B386** 189–197
- [121] Takayama F and Yamaguchi M 2000 *Phys. Lett.* **B485** 388–392
- [122] Hirsch M, Porod W and Restrepo D 2005 *JHEP* **03** 062
- [123] Kim J E 1987 *Phys. Rept.* **150** 1–177
- [124] Raffelt G G Chicago, USA: Univ. Pr. (1996) 664 p
- [125] Chun E J and Kim H B 1999 *Phys. Rev.* **D60** 095006
- [126] Chun E J and Kim H B 2006 *JHEP* **10** 082

- [127] Guchait M and Roy D P 1996 *Phys. Rev.* **D54** 3276–3282
- [128] Huitu K, Maalampi J and Puolamaki K 1999 *Eur. Phys. J.* **C6** 159–166
- [129] Bar-Shalom S, Eilam G and Soni A 1998 *Phys. Rev. Lett.* **80** 4629–4632
- [130] Choudhury D and Raychaudhuri S 1998 (*Preprint hep-ph/9807373*)
- [131] Mukhopadhyaya B, Roy S and Vissani F 1998 *Phys. Lett.* **B443** 191–195
- [132] Choi S Y, Chun E J, Kang S K and Lee J S 1999 *Phys. Rev.* **D60** 075002
- [133] Ghosh D K, Godbole R M and Raychaudhuri S 1999 (*Preprint hep-ph/9904233*)
- [134] Hikasa K i, Yang J M and Young B L 1999 *Phys. Rev.* **D60** 114041
- [135] Chiappetta P *et al.* 2000 *Phys. Rev.* **D61** 115008 (*Preprint hep-ph/9910483*)
- [136] Lebedev O, Loinaz W and Takeuchi T 2000 *Phys. Rev.* **D62** 015003
- [137] Moreau G, Perez E and Polesello G 2001 *Nucl. Phys.* **B604** 3–31
- [138] Ghosh D K and Roy S 2001 *Phys. Rev.* **D63** 055005
- [139] Choudhury D, Godbole R M and Polesello G 2002 *JHEP* **08** 004
- [140] Li P Y, Lu G R, Yang J M and Zhang H 2007 *Eur. Phys. J.* **C51** 163–168
- [141] Pati J C and Salam A 1974 *Phys. Rev.* **D10** 275–289
- [142] Bastero-Gil M and Brahmachari B 1997 *Phys. Rev.* **D56** 6912–6918
- [143] Bastero-Gil M, Brahmachari B and Mohapatra R N 1996
- [144] Brahmachari B and Roy P 1994 *Phys. Rev.* **D50** R39
- [145] Goity J L and Sher M 1995 *Phys. Lett.* **B346** 69–74
- [146] Hirsch M, Klapdor-Kleingrothaus H V and Kovalenko S G 1995 *Phys. Rev. Lett.* **75** 17–20
- [147] Hirsch M, Klapdor-Kleingrothaus H V and Kovalenko S G 1996 *Phys. Rev.* **D53** 1329–1348
- [148] Faessler A, Kovalenko S, Simkovic F and Schwieger J 1997 *Phys. Rev. Lett.* **78** 183–186
- [149] Faessler A, Kovalenko S and Simkovic F 1998 *Phys. Rev.* **D58** 055004
- [150] Hirsch M and Valle J W F 1999 *Nucl. Phys.* **B557** 60–78
- [151] Bhattacharyya G, Choudhury D and Sridhar K 1995 *Phys. Lett.* **B355** 193–198
- [152] Lebedev O, Loinaz W and Takeuchi T 2000 *Phys. Rev.* **D62** 015003
- [153] Takeuchi T, Lebedev O and Loinaz W 2000 (*Preprint hep-ph/0009180*)
- [154] Smirnov A Y and Vissani F 1996 *Phys. Lett.* **B380** 317–323
- [155] Bhattacharyya G and Pal P B 1998 *Phys. Lett.* **B439** 81–84
- [156] Bhattacharyya G and Pal P B 1999 *Phys. Rev.* **D59** 097701
- [157] Dimopoulos S and Hall L J 1988 *Phys. Lett.* **B207** 210
- [158] Godbole R M, Roy P and Tata X 1993 *Nucl. Phys.* **B401** 67–92
- [159] Drees M, Pakvasa S, Tata X and ter Veldhuis T 1998 *Phys. Rev.* **D57** 5335–5339
- [160] Borzumati F and Lee J S 2002 *Phys. Rev.* **D66** 115012

- [161] Bhattacharyya G, Klapdor-Kleingrothaus H V and Pas H 1999 *Phys. Lett.* **B463** 77–82
- [162] Munoz C 2007 (*Preprint* 0705.2007)
- [163] Dimopoulos S and Sutter D W 1995 *Nucl. Phys.* **B452** 496–512
- [164] Giudice G F and Rattazzi R 1999 *Phys. Rept.* **322** 419–499
- [165] Nath P, Arnowitt R L and Chamseddine A H Lectures given at Summer Workshop on Particle Physics, Trieste, Italy, Jun 20 - Jul 29, 1983
- [166] Hall L J, Kostelecky V A and Raby S 1986 *Nucl. Phys.* **B267** 415
- [167] Dine M, Leigh R G and Kagan A 1993 *Phys. Rev.* **D48** 4269–4274
- [168] Dine M 1993 (*Preprint* hep-ph/9306328)
- [169] Hagelin J S, Kelley S and Tanaka T 1994 *Nucl. Phys.* **B415** 293–331
- [170] Sutter D W 1995 (*Preprint* hep-ph/9704390)
- [171] Haber H E 1998 *Nucl. Phys. Proc. Suppl.* **62** 469–484
- [172] Kim J E and Nilles H P 1984 *Phys. Lett.* **B138** 150
- [173] Weinberg S 1978 *Phys. Rev. Lett.* **40** 223–226
- [174] Wilczek F 1978 *Phys. Rev. Lett.* **40** 279–282
- [175] Polchinski J and Susskind L 1982 *Phys. Rev.* **D26** 3661
- [176] Nilles H P, Srednicki M and Wyler D 1983 *Phys. Lett.* **B124** 337
- [177] Lahanas A B 1983 *Phys. Lett.* **B124** 341
- [178] Ferrara S, Nanopoulos D V and Savoy C A 1983 *Phys. Lett.* **B123** 214
- [179] Alvarez-Gaume L, Polchinski J and Wise M B 1983 *Nucl. Phys.* **B221** 495
- [180] Giudice G F and Masiero A 1988 *Phys. Lett.* **B206** 480–484
- [181] Kim J E and Nilles H P 1991 *Phys. Lett.* **B263** 79–85
- [182] Chun E J, Kim J E and Nilles H P 1992 *Nucl. Phys.* **B370** 105–122
- [183] Casas J A and Munoz C 1993 *Phys. Lett.* **B306** 288–294
- [184] Giudice G F and Roulet E 1993 *Phys. Lett.* **B315** 107–112
- [185] Kim J E and Nilles H P 1994 *Mod. Phys. Lett.* **A9** 3575–3584
- [186] Yanagida T 1997 *Phys. Lett.* **B400** 109–111
- [187] Dimopoulos S, Dvali G R and Rattazzi R 1997 *Phys. Lett.* **B413** 336–341
- [188] Kim J E 1999 *Phys. Lett.* **B452** 255–259
- [189] Langacker P, Polonsky N and Wang J 1999 *Phys. Rev.* **D60** 115005
- [190] Choi K and Kim H D 2000 *Phys. Rev.* **D61** 015010
- [191] Mafi A and Raby S 2001 *Phys. Rev.* **D63** 055010
- [192] Ellwanger U, Hugonie C and Teixeira A M 2010 *Phys. Rept.* **496** 1–77
- [193] Fayet P 1975 *Nucl. Phys.* **B90** 104–124

- [194] Kaul R K and Majumdar P 1982 *Nucl. Phys.* **B199** 36
- [195] Barbieri R, Ferrara S and Savoy C A 1982 *Phys. Lett.* **B119** 343
- [196] Nilles H P, Srednicki M and Wyler D 1983 *Phys. Lett.* **B120** 346
- [197] Frere J M, Jones D R T and Raby S 1983 *Nucl. Phys.* **B222** 11
- [198] Derendinger J P and Savoy C A 1984 *Nucl. Phys.* **B237** 307
- [199] Mira J M, Nardi E, Restrepo D A and Valle J W F 2000 *Phys. Lett.* **B492** 81–90
- [200] Maniatis M 2010 *Int. J. Mod. Phys.* **A25** 3505–3602
- [201] Drees M 1989 *Int. J. Mod. Phys.* **A4** 3635
- [202] Ellis J R, Gunion J F, Haber H E, Roszkowski L and Zwirner F 1989 *Phys. Rev.* **D39** 844
- [203] Binetruy P and Savoy C A 1992 *Phys. Lett.* **B277** 453–458
- [204] Espinosa J R and Quiros M 1992 *Phys. Lett.* **B279** 92–97
- [205] Pietroni M 1993 *Nucl. Phys.* **B402** 27–45
- [206] Moroi T and Okada Y 1992 *Phys. Lett.* **B295** 73–78
- [207] Elliott T, King S F and White P L 1993 *Phys. Lett.* **B314** 56–63
- [208] Elliott T, King S F and White P L 1994 *Phys. Rev.* **D49** 2435–2456
- [209] Pandita P N 1993 *Z. Phys.* **C59** 575–584
- [210] Pandita P N 1993 *Phys. Lett.* **B318** 338–346
- [211] Wu Y Y 1995 *Phys. Rev.* **D51** 5276–5284
- [212] Franke F and Fraas H 1995 *Phys. Lett.* **B353** 234–242
- [213] King S F and White P L 1996 *Phys. Rev.* **D53** 4049–4062
- [214] Franke F and Fraas H 1997 *Int. J. Mod. Phys.* **A12** 479–534
- [215] Choudhury S R, Mamta and Dutta S 1998 *Pramana* **50** 163–171
- [216] Ham S W, Oh S K and Kim B R 1996 *J. Phys.* **G22** 1575–1584
- [217] Daikoku Y and Suematsu D 2000 *Prog. Theor. Phys.* **104** 827–833
- [218] Ellwanger U and Hugonie C 2000 (*Preprint hep-ph/0006222*)
- [219] Panagiotakopoulos C and Pilaftsis A 2001 *Phys. Rev.* **D63** 055003
- [220] Davies A T, Froggatt C D and Usai A 2001 *Phys. Lett.* **B517** 375–382
- [221] Ellwanger U, Gunion J F and Hugonie C 2001 (*Preprint hep-ph/0111179*)
- [222] Ellwanger U, Gunion J F, Hugonie C and Moretti S 2004 (*Preprint hep-ph/0401228*)
- [223] Ham S W, OH S K, Kim C M, Yoo E J and Son D 2004 *Phys. Rev.* **D70** 075001
- [224] Ellwanger U, Gunion J F and Hugonie C 2005 *JHEP* **02** 066
- [225] Ellwanger U and Hugonie C 2005 *Phys.Lett.* **B623** 93–103
- [226] Ellwanger U and Hugonie C 2007 *Mod. Phys. Lett.* **A22** 1581–1590
- [227] Ellwanger U and Hugonie C 2007 *Comput. Phys. Commun.* **177** 399–407

- [228] Cavicchia L 2009 *Nucl. Phys.* **B813** 123–139
- [229] Degrassi G and Slavich P 2010 *Nucl. Phys.* **B825** 119–150
- [230] Ellis J R *et al.* 1986 *Phys. Lett.* **B176** 403
- [231] Rai B and Senjanovic G 1994 *Phys. Rev.* **D49** 2729–2733
- [232] Abel S A, Sarkar S and White P L 1995 *Nucl. Phys.* **B454** 663–684
- [233] Abel S A 1996 *Nucl. Phys.* **B480** 55–72
- [234] Panagiotakopoulos C and Tamvakis K 1999 *Phys. Lett.* **B446** 224–227
- [235] Panagiotakopoulos C and Tamvakis K 1999 *Phys. Lett.* **B469** 145–148
- [236] Franke F, Fraas H and Bartl A 1994 *Phys. Lett.* **B336** 415–422
- [237] Ananthanarayan B and Pandita P N 1995 *Phys. Lett.* **B353** 70–78
- [238] King S F and White P L 1995 *Phys. Rev.* **D52** 4183–4216
- [239] Franke F and Fraas H 1996 *Z. Phys.* **C72** 309–325
- [240] Ananthanarayan B and Pandita P N 1996 *Phys. Lett.* **B371** 245–251
- [241] Ananthanarayan B and Pandita P N 1997 *Int. J. Mod. Phys.* **A12** 2321–2342
- [242] Kim B R, Kreyerhoff G and Oh S K Prepared for Physics with $e^+ e^-$ Linear Colliders (The European Working Groups 4 Feb - 1 Sep 1995: Session 1 (Session 2: 2-3 Jun 1995 in Assergi, Italy: Session 3: 30 Aug - 1 Sep 1995 in Hamburg, Germany), Annecy, France, 4 Feb 1995
- [243] Asatrian H M and Egikian G K 1996 *Mod. Phys. Lett.* **A11** 2771–2785
- [244] Ellwanger U and Hugonie C 2000 *Eur. Phys. J.* **C13** 681–690
- [245] Ellwanger U and Hugonie C 1998 (*Preprint* hep-ph/9901309)
- [246] Demir D A 1999 (*Preprint* hep-ph/9902468)
- [247] Bastero-Gil M, Hugonie C, King S F, Roy D P and Vempati S 2000 *Phys. Lett.* **B489** 359–366
- [248] Nevzorov R B and Trusov M A 2000 *J. Exp. Theor. Phys.* **91** 1079–1097
- [249] Nevzorov R B and Trusov M A 2001 *Phys. Atom. Nucl.* **64** 1299–1314
- [250] Menon A, Morrissey D E and Wagner C E M 2004 *Phys. Rev.* **D70** 035005
- [251] Hiller G 2004 *Phys. Rev.* **D70** 034018
- [252] Cerdeno D G, Hugonie C, Lopez-Fogliani D E, Munoz C and Teixeira A M 2004 *JHEP* **12** 048
- [253] Ellwanger U, Gunion J F and Hugonie C 2005 *JHEP* **07** 041
- [254] Funakubo K, Tao S and Toyoda F 2005 *Prog. Theor. Phys.* **114** 369–389
- [255] Belanger G, Boudjema F, Hugonie C, Pukhov A and Semenov A 2005 *JCAP* **0509** 001
- [256] Kraml S and Porod W 2005 *Phys. Lett.* **B626** 175–183
- [257] Ellwanger U and Hugonie C 2006 *Comput. Phys. Commun.* **175** 290–303
- [258] Gunion J F, Hooper D and McElrath B 2006 *Phys. Rev.* **D73** 015011
- [259] Dermisek R and Gunion J F 2006 *Phys. Rev.* **D73** 111701
- [260] Schuster P C and Toro N 2005 (*Preprint* hep-ph/0512189)

- [261] Arhrib A, Cheung K, Hou T J and Song K W 2007 *JHEP* **03** 073
- [262] Huber S J, Konstandin T, Prokopec T and Schmidt M G 2006 *Nucl. Phys.* **B757** 172–196
- [263] Moretti S, Munir S and Poulou P 2007 *Phys. Lett.* **B644** 241–247
- [264] Ferrer F, Krauss L M and Profumo S 2006 *Phys. Rev.* **D74** 115007
- [265] Dermisek R and Gunion J F 2007 *Phys. Rev.* **D75** 075019
- [266] Ma E, Sahu N and Sarkar U 2007 *J. Phys.* **G34** 741–752
- [267] Dermisek R, Gunion J F and McElrath B 2007 *Phys. Rev.* **D76** 051105
- [268] Cerdeno D G, Gabrielli E, Lopez-Fogliani D E, Munoz C and Teixeira A M 2007 *JCAP* **0706** 008
- [269] Mangano M L and Nason P 2007 *Mod. Phys. Lett.* **A22** 1373–1380
- [270] Balazs C, Carena M S, Freitas A and Wagner C E M 2007 *JHEP* **06** 066
- [271] Dermisek R and Gunion J F 2007 *Phys. Rev.* **D76** 095006
- [272] Hugonie C, Belanger G and Pukhov A 2007 *JCAP* **0711** 009
- [273] Dermisek R and Gunion J F 2008 *Phys. Rev.* **D77** 015013
- [274] Domingo F and Ellwanger U 2007 *JHEP* **12** 090
- [275] Barbieri R, Hall L J, Papaioannou A Y, Pappadopulo D and Rychkov V S 2008 *JHEP* **03** 005
- [276] Forshaw J R, Gunion J F, Hodgkinson L, Papaefstathiou A and Pilkington A D 2008 *JHEP* **04** 090
- [277] Akeroyd A G, Arhrib A and Yan Q S 2008 *Eur. Phys. J.* **C55** 653–665
- [278] Heng Z, Oakes R J, Wang W, Xiong Z and Yang J M 2008 *Phys. Rev.* **D77** 095012
- [279] Djouadi A *et al.* 2008 *JHEP* **07** 002
- [280] Djouadi A, Ellwanger U and Teixeira A M 2008 *Phys. Rev. Lett.* **101** 101802
- [281] Chun E J and Roy P 2008 *JHEP* **06** 089
- [282] Ellwanger U, Jean-Louis C C and Teixeira A M 2008 *JHEP* **05** 044
- [283] He X G, Tandean J and Valencia G 2008 *JHEP* **06** 002
- [284] Belyaev A *et al.* 2008 (*Preprint* 0805.3505)
- [285] Domingo F and Ellwanger U 2008 *JHEP* **07** 079
- [286] Chang Q and Yang Y D 2009 *Phys. Lett.* **B676** 88–93
- [287] Gogoladze I, Okada N and Shafi Q 2009 *Phys. Lett.* **B672** 235–239
- [288] Cao J and Yang J M 2008 *Phys. Rev.* **D78** 115001
- [289] Domingo F, Ellwanger U, Fullana E, Hugonie C and Sanchis-Lozano M A 2009 *JHEP* **01** 061
- [290] Kraml S, Raklev A R and White M J 2009 *Phys. Lett.* **B672** 361–366
- [291] Djouadi A, Ellwanger U and Teixeira A M 2009 *JHEP* **04** 031
- [292] Belanger G, Hugonie C and Pukhov A 2009 *JCAP* **0901** 023
- [293] Dermisek R and Gunion J F 2009 *Phys. Rev.* **D79** 055014

- [294] Cao J, Logan H E and Yang J M 2009 *Phys. Rev.* **D79** 091701
- [295] Cerdeno D G and Seto O 2009 *JCAP* **0908** 032
- [296] Dermisek R and Gunion J F 2010 *Phys. Rev.* **D81** 075003
- [297] Das D and Ellwanger U 2010 *JHEP* **09** 085
- [298] Staub F, Porod W and Herrmann B 2010 *JHEP* **10** 040
- [299] Abada A, Bhattacharyya G, Das D and Weiland C 2010 (*Preprint* 1011.5037)

Chapter 3

Neutrinos

Long back in 1930, a new particle was suggested by *Pauli* to preserve the conservation of energy, conservation of momentum, and conservation of angular momentum in beta decay [1, 2]¹. The name *neutrino* was coined by *Fermi* in 1934. The much desired experimental evidence for neutrinos (actually ν_e) was finally achieved in 1956 [3]. In 1962, muon neutrino was discovered [4]. However, it took a long time till 2000 to discover ν_τ [5].

Neutrino sources are everywhere, however, they are broadly classifiable in two major classes, namely, (1) natural sources and (2) man made neutrinos. Natural neutrino sources are nuclear β decay (ν_e), solar neutrinos (ν_e), atmospheric neutrinos (ν_e, ν_μ and their anti-neutrinos) and supernovae neutrinos (all flavours) mainly. Man made neutrinos are produced by the particle accelerators and neutrinos coming out of nuclear reactors.

Neutrino physics has been seeking huge attention for the last few decades. Different aspects of neutrino physics have been discussed in references [6–32].

3.1 Neutrinos in the Standard Model

The neutrinos as discussed in chapter 1, appear to be a part of the SM. Confining our attention within the SM, it is worth listing the information about neutrinos, that “lies within the SM”

1. They are spin $\frac{1}{2}$ objects and thus follow Fermi-Dirac statistics [33, 34].
2. Neutrinos are electrically neutral fundamental particles, belonging to the lepton family. The SM contains three neutrinos, corresponding to three charged leptons.
3. They are a part of the weak isospin ($SU(2)_L$) doublet. Being charge and colour neutral neutrinos are sensitive to weak interaction only.
4. There exist two kinds of neutrino interactions in nature, (1) neutral and (2) charge current interactions (see figure 3.1).

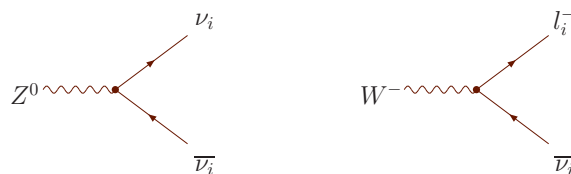


Figure 3.1: Feynman diagram for the neutral and charged current interactions. ν_i stand for different neutrino flavours like ν_e, ν_μ, ν_τ . The charged leptons (e, μ, τ) are represented by l_i s.

¹To be specific, this was an electron neutrino. ν_μ and ν_τ were hypothesized later in 1940 and 1970, respectively.

5. There are only left-chiral [35, 36] (spin anti-parallel to the momentum direction) neutrinos in nature, without any right-handed counter part. But there exists anti-neutrinos of right chirality (spin parallel to momentum).
6. Neutrinos are exactly mass less in the SM.
7. Since the neutrinos are massless within the framework of the SM, the mass basis and the weak interaction basis are same for the charged leptons. In other words, there exists no leptonic analogue of the CKM matrix (see ref. [37, 38]) with vanishing neutrino mass.

The massless neutrinos seem to work fine with the SM until the first hint of neutrino oscillation appeared in 1969 [39], which requires massive neutrinos². However, maintaining the gauge invariance, Lorentz invariance and renormalizability, there is absolutely no room for massive neutrinos in the SM (see reviews [28, 42]). It is then apparent that to explain neutrino oscillation the SM framework requires extension. We leave these modifications for time being until section 3.3. It is rather more important to know the phenomenon of neutrino oscillation. Besides, it is also important to know if neutrinos possess non-zero mass, what will be the possible experimental impressions?

3.2 Neutrino oscillation

✧ *Evidences of neutrino oscillation*

I. Atmospheric neutrino problem ► Consider the atmospheric neutrinos, which are coming from the interaction of cosmic rays with the earth's atmosphere. The charged pion (π^\pm) produced in the interaction, has the following decay chain

$$\pi^\pm \rightarrow \mu^\pm + \nu_\mu(\bar{\nu}_\mu), \quad (3.1)$$

followed by

$$\mu^\pm \rightarrow e^\pm + \nu_e(\bar{\nu}_e) + \bar{\nu}_\mu(\nu_\mu). \quad (3.2)$$

These neutrinos(anti-neutrinos) take part in charge current interaction (see figure 3.1) and produce detectable charged leptons. Looking at eqns. (3.1, 3.2) one would naively expect number wise³,

$$R_\mu = \frac{\nu_\mu(\bar{\nu}_\mu)}{\nu_e(\bar{\nu}_e)} = 2. \quad (3.3)$$

However, in reality R_μ is much smaller (~ 0.6), as observed by experiments like Kamiokande [43, 44], NUSEX [45], IMB [46, 47], Soudan-2 [48], MACRO [49, 50], Super-Kamiokande [51, 52]. The diminution in R_μ as observed by a host of experiments indicates a deficit of muon (anti)neutrino flux. This apparent discrepancy between predicted and observed neutrino flux defines the atmospheric neutrino problem.

II. Solar neutrino problem ► The Sun gets huge energy by fusing hydrogen (${}^1_1\text{H}$) to helium (${}^4_2\text{He}$) in thermonuclear reactions. There exist a few viable candidates for this reaction chain, like proton-proton (pp) cycle, carbon-nitrogen-oxygen (CNO) cycle [53, 54] etc, although the pp cycle appears to be the dominant one. The sun is a major source of electron neutrinos (see also ref. [55, 56]) following the process

$$4p \rightarrow {}^4_2\text{He} + 2e^+ + 2\nu_e, \quad (3.4)$$

where e^+ is a positron. There exist a host of literature concerning the standard solar model [9, 57–61], which account for the number of solar neutrinos expected to be detected in an earth based detector. However, only one-third of the expected solar neutrino flux has been detected by experiments

²The first idea of neutrino oscillation was given by Bruno Pontecorvo [40, 41].

³This number is actually not exactly 2, because of various uncertainties like, geometry of cosmic ray flux and neutrino flux, solar activities, uncertainty in cross section measurements, etc.

like Homestake [39, 62, 63], SAGE [64–66], GALLEX [67, 68], GNO [69], Kamiokande [70], Super-Kamiokande [71, 72], SNO [73–75] etc. The disappearance of a large fraction of solar neutrinos defines the solar neutrino problem.

There were numerous attempts to explain the discrepancy between the measured and the predicted neutrino flux for the solar and the atmospheric neutrinos. In fact, these neutrino deficits lead to the proposal of various theoretical models⁴. However, with the idea of Bruno Pontecorvo [40, 41, 77], it seems more logical to think about some sort of *conversion* among neutrino flavours while they propagate through vacuum or matter, which can lead to diminution of a specific type of flavor as reported by experiments.

✂ *Theory of neutrino oscillation*

In order to explain the Solar and atmospheric neutrino deficits, as discussed earlier it is expected that a neutrino of a specific flavour, say a , during propagation can alter its flavour to some other one, say b , at a later stage of time. Now from our knowledge of quantum mechanics it is evident that,

1. The set of linearly independent mass eigenstates form a complete basis.
2. Any arbitrary state can be expressed as a linear combination of the linearly independent mass eigenstates.

So, if neutrinos oscillate, [78–81] the flavour eigenstates, ν_e, ν_μ, ν_τ must differ from the physical or mass eigenstates and it is possible to express them as a linear combination of the neutrino mass eigenstates, ν_1, ν_2, ν_3 ⁵. Thus, we define

$$|\nu'_a\rangle = U_{ai}^* |\nu_i\rangle, \quad (3.5)$$

where ν'_a, ν_i are flavour and mass eigenstates for neutrinos, respectively and U_{ai}^* are the coefficients, carrying information of “conversion”. So if at time, $t = 0$ we have a flavour state ν_a , then the probability for transforming to another flavour state ν_b at a later time t is given by (using eqn.(3.5)),

$$P(\nu_a \rightarrow \nu_b; t) = \sum_j |U_{bj} e^{-iE_j t} U_{aj}^*|^2. \quad (3.6)$$

Eqn.(3.6) is the key equation for neutrino oscillation and the underlying physics can be explained in three pieces,

- I. U_{aj}^* is the amplitude of transformation of a flavour state ν_a into some mass eigenstate ν_j .
- II. Immediately after that, the factor $e^{-iE_j t}$ governs the evolution of mass eigenstate ν_j with time.
- III. Finally, U_{bj} is the amplitude of transformation of a time evolved mass eigenstate ν_j into some other flavor state ν_b .

A bit of algebraic trick for relativistic neutrinos of momentum p , ($E_j \simeq p + \frac{m_j^2}{2E}$) yields

$$P(\nu_a \rightarrow \nu_b; t) = \sum_{j,k} U_{bk}^* U_{ak} U_{bj} U_{aj}^* e^{-i\Delta m_{jk}^2 \frac{L}{2E}}, \quad (3.7)$$

where $\Delta m_{jk}^2 = m_j^2 - m_k^2$. m_i is the mass of ν_i state and $L \simeq t$ (L is the distance traversed by a neutrino in time t to change its flavour) using natural unit system for relativistic neutrinos. It is clear from eqn.(3.7) that oscillation probability depends on the squared mass differences rather than individual masses, thus it is impossible to probe the absolute mass scale for neutrinos with oscillation data.

It is important to note from eqn.(3.7), one can define the survival probability for a flavour ν_a as

$$P(\nu_a \rightarrow \nu_a; t) = 1 - \sum_{j,k} U_{ak}^* U_{ak} U_{aj} U_{aj}^* e^{-i\Delta m_{jk}^2 \frac{L}{2E}}. \quad (3.8)$$

⁴A discussion of these models is beyond the scope of this thesis. See ref. [76] for further discussions.

⁵Assuming three active light neutrino flavour [82]. There are controversies concerning more than three light neutrino flavours [83–86]. This may be the so-called sterile neutrino which mixes with three light neutrinos, but is phobic to weak interactions, so that invisible decay width of Z -boson remains sacred. Nevertheless, there exists literature [87–90] which deals with more than three neutrino species.

With the aid of eqn.(3.8), deficit of a particular flavour in the solar and the atmospheric neutrino flux can be explained. However, even using eqn.(3.8) it is hardly possible to account for the solar neutrino problem. This was an apparent puzzle until the matter effects in the enhancement of neutrino oscillation were understood. Eqn.(3.8) works only for oscillations in vacuum [91]. The much desired modification for explaining matter effect induced enhanced oscillations to accommodate the solar neutrino deficit was given by Mikheyev, Smirnov and Wolfenstein [92–94]. This is popularly known as the MSW effect.

✠ *What do we know about oscillations?*

It has been argued already that the theory of neutrino oscillation is sensitive to squared mass differences. It is also confirmed by this time that, it is indeed possible to explain oscillation phenomena with two massive neutrinos, consequently, two squared mass differences are enough. We define them as Δm_{solar}^2 and Δm_{atm}^2 , where the word atmospheric is abbreviated as *atm*. From the observational fact $\Delta m_{atm}^2 (\sim 10^{-3} \text{eV}^2) \gg \Delta m_{solar}^2 (\sim 10^{-5} \text{eV}^2)$. The sign of Δm_{solar}^2 has been affirmed experimentally to be positive, but Δm_{atm}^2 can be either positive or negative. With this sign ambiguity, two types of light neutrino mass spectrum are possible, namely *normal* and *inverted*. Mathematically, (i) normal hierarchy: $m_1 < m_2 \sim \sqrt{\Delta m_{solar}^2}$, $m_3 \sim \sqrt{|\Delta m_{atm}^2|}$, (ii) inverted hierarchy: $m_1 \approx m_2 \sim \sqrt{|\Delta m_{atm}^2|}$, $m_3 \ll \sqrt{|\Delta m_{atm}^2|}$, where m_1, m_2, m_3 are light neutrino masses⁶. There exists a third possibility of light neutrino mass ordering, where $m_1 \approx m_2 \approx m_3 \gg \sqrt{|\Delta m_{atm}^2|}$ with finely splitted m_i s in order to satisfy oscillation data. This is known as the quasi-degenerate spectrum. Note that, it is impossible to accommodate quasi-degenerate spectrum unless all three neutrinos are massive whereas for the normal or inverted hierarchical scheme of light neutrino mass at least two neutrinos must be massive [51, 74, 95].

Probability of flavour oscillation also contains the elements of conversion matrix, U (eqn.(3.7)). The matrix U acts as the bridge between flavour and mass eigenstates, having one index from both the basis. This matrix is the leptonic analogue of the CKM matrix (see chapter 1) and is known as the Pontecorvo-Maki-Nakagawa-Sakata or the PMNS matrix [40, 41, 77, 96]. In three flavour model this can be parametrized as [97–99]

$$U = \begin{pmatrix} c_{12}c_{13} & s_{12}c_{13} & s_{13}e^{-i\delta} \\ -s_{12}c_{23} - c_{12}s_{23}s_{13}e^{i\delta} & c_{12}c_{23} - s_{12}s_{23}s_{13}e^{i\delta} & s_{23}c_{13} \\ s_{12}s_{23} - c_{12}c_{23}s_{13}e^{i\delta} & -c_{12}s_{23} - s_{12}c_{23}s_{13}e^{-i\delta} & c_{23}c_{13} \end{pmatrix} \cdot U'(\alpha), \quad (3.9)$$

where $c_{ij} = \cos \theta_{ij}$, $s_{ij} = \sin \theta_{ij}$ and $U'(\alpha) = \text{diag}(e^{-i\alpha_1/2}, 1, e^{-i\alpha_2/2})$. Here $\alpha_1, \alpha_2, \delta$ are complex phases. The phases α_1, α_2 can be non-zero only if neutrinos are Majorana particle in nature (will be addressed later). Neutrino oscillation is insensitive to Majorana phases. The phase δ is a Dirac CP-violating phase and can appear in oscillation dynamics. We stick to Charge-Parity(CP)-preserving case (zero phases) throughout this thesis.

It is interesting to note that unlike the CKM matrix of quark sector, the PMNS matrix has a rather non-trivial structure. Present experimental evidence favours a tri-bimaximal mixing in light neutrino sector [100], though there exist other alternatives [101–106] (see also [107] and references therein)⁷. The atmospheric mixing angle (θ_{23}) is close to maximal ($\sim \pi/4$) and the solar mixing angle (θ_{12}) is also large ($\sim 35^\circ$). The third and the remaining mixing angle, the reactor angle (θ_{13}) is the most difficult one to measure. There exist a host of literature, both on theoretical prediction and experimental observation for the value and the measurement of the angle θ_{13} . (see ref. [108–113] for recent updates. Also see ref. [114]). At the zeroth-order approximation

$$\theta_{23} = \frac{\pi}{4}, \quad \theta_{12} \simeq 35^\circ, \quad \theta_{13} = 0. \quad (3.10)$$

Recently, non-zero value for the angle θ_{13} has been reported by the T2K collaboration [115] both for the normal and inverted hierarchy in the light neutrino masses. For normal (inverted) hierarchy and at 90% C.L. this value is reported to be

$$0.03(0.04) < \sin^2 2\theta_{13} < 0.28(0.34). \quad (3.11)$$

⁶It is useful to note that $m_2 > m_1$ irrespective of mass hierarchy, since $\Delta m_{solar}^2 > 0$ always. However, $\Delta m_{atm}^2 > 0$ for normal hierarchy whereas < 0 for the inverted one.

⁷Some of these proposals are now experimentally ruled out.

The oscillation parameters ($\Delta m_{sol}^2, \Delta m_{atm}^2, \theta_{23}, \theta_{12}, \theta_{13}$) are highly constrained by experiments. In table 3.1 best-fit values of these parameters for the global three-flavor neutrino oscillation data are given [111]. The experiments like Borexino [116], CHOOZ [117, 118], Double Chooz [108, 119],

Parameter	Best fit	3σ limit
$\Delta m_{sol}^2 \times 10^5 \text{ eV}^2$	$7.65^{+0.23}_{-0.20}$	$7.05 - 8.34$
$ \Delta m_{atm}^2 \times 10^3 \text{ eV}^2$	$2.40^{+0.12}_{-0.11}$	$2.07 - 2.75$
$\sin^2 \theta_{23}$	$0.50^{+0.07}_{-0.06}$	$0.25 - 0.37$
$\sin^2 \theta_{12}$	$0.304^{+0.022}_{-0.016}$	$0.36 - 0.67$
$\sin^2 \theta_{13}$	$0.01^{+0.016}_{-0.011}$	≤ 0.056

Table 3.1: Best fit values and 3σ ranges of oscillation parameters from three flavour global data [111].

KamLAND [120, 121], Kamiokande [122], Super-Kamiokande [72, 123], K2K [124], MINOS [125, 126], GNO [127, 128], SNO [129] and others are now in the era of precision measurements. More, sophisticated experiments like RENO [130], OPERA [131, 132] etc. have already been initiated and an extremely precise global fit is well anticipated in near future. One can go through ref. [133] for a recent analysis of the precision results.

✂ Searching for a neutrino mass

Theory of neutrino oscillation depends on squared mass differences, which are shown in table 3.1. It is then, natural to ask that what is the absolute scale for a neutrino mass. Is it small, \sim a few eV so that small squared mass differences (see table 3.1) seem natural or the absolute masses are much larger and have unnatural fine splittings among them.

Possible evidences of absolute neutrino mass scale can come from different experiments which are discussed below.

I. Tritium beta decay ► There are a host of experimental collaboration (Mainz [134, 135], Troitsk [136, 137], KARTIN [138, 139]) looking for the modification in the beta spectrum in the process ${}^3\text{H} \rightarrow {}^3\text{He} + e^- + \bar{\nu}_e$ in the presence of non-zero m_i . Indeed, the Kurie plot [140] shows deviation near the endpoint with $m_i \neq 0$ (see figure 3.2). The experiments, however in reality measure an effective

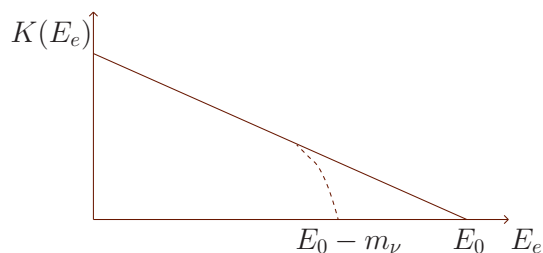


Figure 3.2: Kurie function, $K(E_e)$ versus energy (E_e) of β -particle (e^-) plot for neutrino mass, $m_\nu = 0$ (solid line) and $m_\nu \neq 0$ (dashed line). E_0 is the energy release.

neutrino mass $m_\beta = \sqrt{\sum |U_{ei}|^2 m_i^2}$ (U is the PMNS matrix). The present bound is [82]

$$m_\beta < 2.0 \text{ eV}. \quad (3.12)$$

II. Neutrinoless double beta decay ► Consider two beta decays, ($n \rightarrow p^+ + e^- + \nu_e$ or $d \rightarrow u + e^- + \nu_e$, in the quark level of proton (neutron) simultaneously, such that (anti)neutrino emitted in one decay is somehow absorbed in the other. This leads to the neutrinoless double beta decay, $0\nu\beta\beta$ (figure 3.3). However, it is clear from figure 3.3, this breaks lepton number conservation. The quantity m_L represents Majorana mass (will be addressed soon) of a left-handed neutrino, which is responsible for this lepton number violation (L). Not only the lepton number is broken in this interaction,

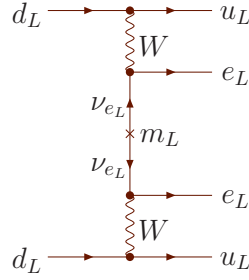


Figure 3.3: Diagram for neutrinoless double beta decay in the SM. Subscript L signifies the left handed nature of weak interaction.

but through Majorana mass term m_L process like this also breaks chirality conservation [141]. The measurable quantity is defined as $m_{\beta\beta} = \sum U_{ei}^2 m_i$. Since $m_{\beta\beta} \propto U_{ei}^2$, rather than $|U_{ei}|^2$, information about the δ -phase is not lost until one asks for CP-preservation in the lepton sector. Experimental reporting of neutrinoless double beta decay is controversial. The result obtained by Heidelberg-Moscow experiment [142–144], CUORICINO [145] suggests

$$m_{\beta\beta} < 0.2 - 0.6 \text{ eV}. \quad (3.13)$$

However, there are experiments like CUORE [145], EXO [146], GERDA [147], MAJORANA and a few others, which are expected to shed light on this claim in near future. One important point about $0\nu\beta\beta$ is that unless a neutrino possesses a Majorana mass term, $m_{\beta\beta} = 0$. This is true for different models and has been confirmed by model independent analysis [148]. It must be emphasized here

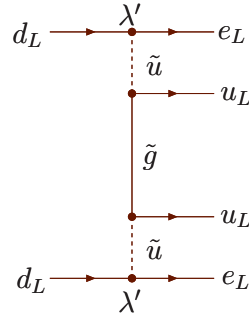


Figure 3.4: Diagram for neutrinoless double beta decay in R_p -violating supersymmetric models. See text for further details.

that, actually the presence of Majorana mass term is a sufficient condition for non-zero $m_{\beta\beta}$, but not necessary, for example $0\nu\beta\beta$ in R_p -violating (section 2.6) supersymmetric model (see figure 3.4) can occur without a neutrino Majorana mass term (see ref. [149]). In figure 3.4, \tilde{g} represents a gluino, superpartner of a gluon and \tilde{u} is a up-type squark (see figure 2.3).

III. Cosmology ► Neutrino masses are also constrained by the standard big-bang cosmology. However, in this case the bound exists on sum of neutrino masses. There were earlier works [150–152] in this connection, where, a bound on the sum of neutrino mass was obtained from the bound on the total density of the universe. However, the present bound as obtained from sophisticated experiment like WMAP [153–158] is much stringent and is given by

$$\sum_{i=1}^3 m_i \leq 0.58 \text{ eV} (95\% \text{ C.L.}). \quad (3.14)$$

Note that only for the case of quasi-degenerate light neutrino masses individual masses can be much larger compared to the squared mass differences (see table 3.1). Thus quasi-degenerate neutrinos masses are highly constrained by eqn.(3.14).

So far we have addressed the features of oscillation and non-oscillation experiments to constrain the neutrino physics. It is the time to demonstrate the origin of neutrino mass. But even before that, it is important to discuss the nature of neutrino masses, that is whether they are Dirac or Majorana particles [159, 160].

3.3 Models of neutrino mass

✂ *Nature of neutrino mass, Dirac versus Majorana*

It is well-known that the charge conjugation operator \hat{C} is defined as

$$\hat{C} : \psi \rightarrow \psi^c = C\bar{\psi}^T, \quad (3.15)$$

where C is the matrix representation for \hat{C} , T denotes transpose and ψ is a four component spinor. It is then apparent that for a charge neutral fermion

$$\psi^c = \psi. \quad (3.16)$$

Any ψ which obeys eqn.(3.16) is known as a Majorana fermion⁸. On the contrary, the so-called Dirac fermions are known to follow $\psi \neq \psi^c$. Now, since the neutrinos are the only charge neutral particle in the SM there is a possibility, that a neutrino is a Majorana particle, [161] rather than a Dirac particle [162].

I. Dirac Mass ► If there were right-handed neutrinos (ν_R) in the SM, a non-zero Dirac mass (m_D) is well expected. The mass term using eqn.(1.11) can be written as

$$y_\nu \bar{L} \tilde{\Phi} \nu_R + h.c = \frac{y_\nu \cdot v}{\sqrt{2}} \bar{\nu}_L \nu_R + h.c = m_D \bar{\nu}_L \nu_R + h.c, \quad (3.17)$$

where $\nu_{L(R)}$ is a left(right) handed neutrino field and y_ν is the neutrino Yukawa coupling. Demanding a neutrino mass ~ 1 eV one gets $y_\nu \sim 10^{-11}$. But immediately then, it is legitimate to ask why m_D is extremely small compared to other masses as shown in table 1.1 or alternatively why y_ν is much smaller, compared to say electron Yukawa coupling, $Y_e \sim 10^{-6}$. The Dirac mass terms respect the total lepton number L , but not the family lepton number, L_e, L_μ, L_τ . If $m_D \neq 0$, a neutrino is different from an anti-neutrino.

II. Majorana Mass ► A Majorana mass term not only violate the family lepton number, but also the total lepton number. In general they are given by

$$m_{ii} \bar{\nu}_i \nu_i^c, \quad (3.18)$$

where, $i = L, R$. $\nu_{L(R)}^c$ represents a CP conjugated state. A Majorana spinor has only two degrees of freedom because of eqn.(3.16), whereas a Dirac spinor has four degrees of freedom. Thus, two degenerate Majorana neutrinos of opposite CP, when maximally mixed form a Dirac neutrino. A Majorana neutrino is believed to be one of the main reasons for non-vanishing amplitude in $0\nu\beta\beta$ (see section 3.2). However, just like the Dirac case it is also important to explain how a neutrino gets a tiny Majorana mass? The answer will be given in the subsequent paragraph.

In the most general occasion, a neutrino can possess a ‘‘Dirac + Majorana’’ mass term. A term of this kind can lead to extremely interesting neutrino-anti neutrino oscillation which violates total lepton number (see ref. [14] for detailed discussion). It is also important to mention that since neutrino oscillation does not violate total lepton number, it is hardly possible to differentiate between a Dirac and a Majorana nature from the theory of neutrino oscillation. The $0\nu\beta\beta$ is definitely an evidence for Majorana nature. Besides, one can use the favour of electric and magnetic dipole moment measurement, to discriminate these scenarios [163–170].

⁸A free Majorana field is an eigenstate of charge conjugation operator.

3.3.1 Mass models I

It is apparent by now that we need to extend either the particle content of the SM or need to enlarge the gauge group to accommodate neutrino mass. In this subsection we discuss the models for neutrino mass generation without introducing supersymmetry. Some of these models generate masses at the tree level and the remaining through loop processes.

1. Renormalizable interaction with triplet Higgs.

Consider a term in the Lagrangian as

$$f_{\Delta}(\ell^T C i \sigma_2 \boldsymbol{\sigma} \ell) \Delta + h.c., \quad (3.19)$$

where C is the charge conjugation matrix, $\boldsymbol{\sigma}$'s are Pauli matrices and Δ is a *triplet* Higgs field with hypercharge, $Y = 2$. If further we assume that Δ has $L = -2$, then Lagrangian given by eqn.(3.19) conserves lepton number. The mass term for neutrinos will be then

$$m_{\nu} \approx f_{\Delta} v_{\Delta}, \quad (3.20)$$

where v_{Δ} is the VEV of Δ field. But this will also produce massless triplet Majoron [171–173] since lepton number is spontaneously broken by the VEV of $SU(2)_L$ triplet Δ field. Missing experimental evidence has ruled out this model. One alternative could be to put $L = 0$ for Δ , which breaks the lepton number explicitly. This situation, though free of triplet Majoron are highly constrained from ρ parameter measurement (eqn.(1.10)), which requires $v_{\Delta} < 8$ GeV. Once again for $m_{\nu} \sim 1$ eV, $f_{\Delta} \sim 10^{-10}$.

2. Non-renormalizable interactions.

If we want to build a model for tiny neutrino mass with the SM degrees of freedom, the immediate possibility that emerges is the so-called *dimension five* Weinberg operator [174, 175]

$$Y_{ij} \frac{(\ell_i \Phi)(\Phi \ell_j)}{M}, \quad (3.21)$$

where ℓ are the SM $SU(2)_L$ lepton doublets (eqn.(1.1)) and Φ is the SM Higgs doublet (eqn.(1.3)) with VEV $\frac{v}{\sqrt{2}}$. Y_{ij} stands for some dimensionless coupling. M is some high scale in the theory, and is the messenger of some new physics. Thus the small Majorana neutrino mass coming from this $\Delta L = 2$ operator is

$$(m_{\nu})_{ij} = \frac{Y_{ij} v^2}{2M}. \quad (3.22)$$

Note that if M is large enough ($\sim 10^{14}$ GeV) the coupling, $Y_{ij} \sim 1$ (close to perturbative cutoff), for right order of magnitude in the neutrino mass (m_{ν}) ~ 0.1 eV. However, this is a rather challenging scenario, since it is hardly possible to probe M ($\sim 10^{14}$ GeV) in a collider experiment. One viable alternative is a TeV scale M , which is possible to explore in a collider experiment. Note that for such a choice of M , Y_{ij} is much smaller.

Maintaining the gauge invariance and renormalizability, the effective operator can arise from three possible sources.

I. Fermion singlet ► The intermediate massive particle is a SM gauge singlet particle, (S). This is the example of Type-I seesaw mechanism [97, 176–181] (seesaw mechanism will be discussed later in more details). The light neutrino mass is given by

$$m_{\nu} = \frac{f_s^2 v^2}{2M_S}, \quad (3.23)$$

where M_S is the mass of the singlet fermion and f_s is the $\ell \Phi S$ coupling. (see figure 3.5 (a) and (b)). It is important to note that the $\Delta L = 2$ effect can arise either using a singlet with non-zero lepton

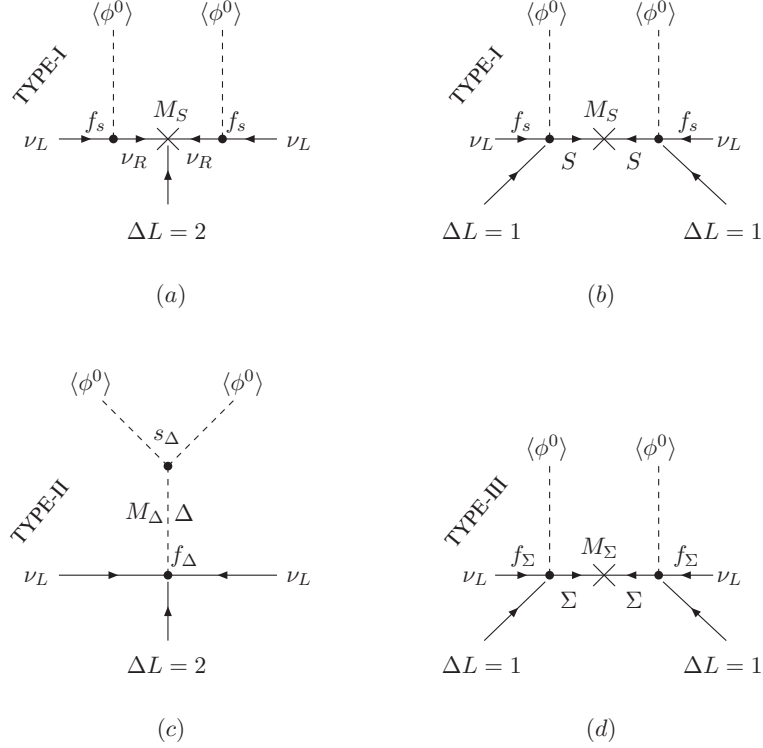


Figure 3.5: Different types of seesaw mechanism. The cross on the fermionic propagator signifies a Majorana mass term for the corresponding fermion.

number (right handed neutrino, ν_R) (figure 3.5 (a)) or through a singlet, S without lepton number (figure 3.5 (b)).

II. Scalar triplet ► The intermediate massive particle is a scalar triplet (Δ) under the group $SU(2)_L$. It is singlet under $SU(3)_C$ and has hypercharge, $Y = 2$. This is the so-called Type-II seesaw mechanism [182–186]. The light neutrino mass is given by

$$m_\nu = \frac{f_\Delta s_\Delta v^2}{2M_\Delta^2}, \quad (3.24)$$

where M_Δ is the mass of the scalar triplet. f_Δ and s_Δ are the $LL\Delta$ and $\Phi\Phi\Delta$ coupling, respectively (see figure 3.5 (c)).

III. Fermion triplet ► A triplet fermion (Σ) acts as the mediator and this is an illustration of the Type-III seesaw mechanism [187, 188]. This Σ is a triplet under $SU(2)_L$ but singlet under $SU(3)_C$. Hypercharge for Σ is zero. The light neutrino mass is given by

$$m_\nu = \frac{f_\Sigma^2 v^2}{2M_\Sigma}, \quad (3.25)$$

where M_Σ is the mass of the fermion triplet. f_Σ is the $L\Phi\Sigma$ coupling (see figure 3.5 (d)).

A very important aspect of these seesaw models and the associated Majorana nature is that they can produce same sign dilepton at a collider experiment [189] apart from a non-zero amplitude for the $0\nu\beta\beta$ process. The collider phenomenology for Type-II or III seesaw models are more attractive compared to the Type-I scenario, due to the involvement of a SM gauge singlet fermion in the latter case. Also a seesaw generated neutrino mass can have implications in flavour violating processes, [190–194] leptogenesis [195–198]. However, none of these issues are addressed here.

There exist other interesting seesaw models like (a) Inverse seesaw [199] (requires an extra SM singlet S apart from ν_R), (b) Linear seesaw [200], (c) Double seesaw [199, 201], (d) Hybrid seesaw [202–205] etc. Some of these models have definite group theoretical motivation. Also neutrino masses

can arise in the left-right symmetric model [206–209]. It is important to note that the Weinberg operator can also give rise to neutrino mass via loop effects [210–215]. Some of the very early attempts in this connection have been addressed in references [216, 217]. However, any more involved discussion of these topics are beyond the scope of this thesis. A comprehensive information about various neutrino mass models is given in ref. [76].

✦ *The seesaw mechanism*

It has been already argued that the seesaw mechanism (Type-I,II,III and others) is perhaps the most convenient way to generate small Majorana masses for neutrinos. But what is actually a seesaw mechanism and how does it lead to small Majorana mass? It is true that a Majorana mass term violates lepton number by *two units*, but this could happen either through a pair of $\Delta L = 1$ effects (see figure 3.5 (b),(d)) or by a $\Delta L = 2$ vertex (see figure 3.5 (a),(c)). We will discuss the canonical seesaw mechanism (Type-I, however this analysis is also applicable for Type-III) using a simple model containing left-handed neutrino, ν_L and some fermion f , either a SM gauge singlet (Type-I seesaw) or an $SU(2)_L$ triplet (Type-III seesaw). Further we assume that to start with Majorana mass for ν_L is absent. Majorana mass for f is given by M_f and the co-efficient of the mixing term ($\nu_L f$) is written as m_m . The mass matrix in the ν_L, f basis is given by

$$\mathcal{M} = \begin{pmatrix} 0 & m_m \\ m_m & M_f \end{pmatrix}. \quad (3.26)$$

If $M_f \gg m_m$, the eigenvalues are given as

$$m_{light} \simeq -\frac{m_m^2}{M_f}, \text{ and } m_{heavy} \simeq M_f. \quad (3.27)$$

If χ_1, χ_2 form a new basis where $\mathcal{M} \rightarrow \text{diag}(m_{light}, m_{heavy})$, then mixing between χ_1, χ_2 and ν_L, f basis is parametrized by an angle θ with

$$\tan 2\theta = \frac{2m_m}{M_f}. \quad (3.28)$$

Eqn.(3.27) is the celebrated seesaw formula for neutrino mass generation. Now the left neutrino possesses a non-zero Majorana mass term which was *zero* to start with. Also the mass m_{light} , is suppressed by a factor $\frac{m_m}{M_f}$, and thus always is small as long as $M_f \gg m_m$. Considering three generations of light neutrinos, the unitary matrix (orthogonal in the absence of complex phases) U' which rotates the off-diagonal basis (m_{light} is a 3×3 matrix for the three generation case) to the diagonal one is known as the PMNS matrix (eqn.(3.9)). Mathematically,

$$U'^T m_{light} U' = \text{diag}(m_{\nu_i}), \quad i = 1, 2, 3. \quad (3.29)$$

In the Type-I and Type-III seesaw process, the effective leptonic mixing matrix or PMNS matrix loses its unitarity [218–220] $\sim \frac{m_m}{M_f}$. The unitary nature is restored when $M_f \rightarrow \infty$. This feature is however absent in Type-II seesaw mechanism. A discussion on the phenomenological implications of this non-unitarity is beyond the scope of this thesis.

It is essential to note that when f is a right handed neutrino, ν_R , then $m_m \equiv m_D$, the Dirac mass term. Further replacing M_f by M_R , in the limit $m_D \gg M_R$, we get from eqn.(3.27)

$$m_{light} \simeq m_D - \frac{M_R}{2}, \text{ and } |m_{heavy}| \simeq m_D + \frac{M_R}{2}. \quad (3.30)$$

This pair is known to behave as Dirac neutrino in various aspects and is named as *quasi-Dirac neutrinos* [8, 221].

3.3.2 Mass models II

In this subsection we try to address the issues of neutrino mass generation in a supersymmetric theory [222], which is one of the prime themes of this thesis. \mathcal{R}_p through bilinear terms (ε_i , see eqn.(2.50))

is the simplest extension of the MSSM [223], which provides a framework for neutrino masses and mixing angles consistent with experiments. It is important to clarify that there are various sources for light neutrino mass generation in supersymmetry without \mathcal{R}_p (section 2.6), for example see refs. [224–236]. But we stick to a very special case where the origin of neutrino mass generation is entirely supersymmetric, namely through R_p -violation. An introduction to \mathcal{R}_p was given in section 2.6 and here we will concentrate only on the effect of \mathcal{R}_p in neutrino mass generation.

The effect of \mathcal{R}_p and neutrino masses in a supersymmetric theory has received immense interest for a long time and there exist a host of analyses to shed light on different phenomenological aspects of broken R_p (see section 2.6 and references therein). We quote a few of these references having connections with the theme of this thesis, namely (a) neutrino mass generation either through explicit \mathcal{R}_p [190–192, 194, 223, 237–307] or through spontaneous \mathcal{R}_p [193, 308–318] (tree and(or) loop corrections) and (b) neutrino mass generation and(or) collider phenomenology [193, 194, 238, 240, 241, 248, 251, 253, 257, 259, 265, 270, 272, 276–278, 286, 288, 291, 298, 309, 310, 314, 319–345].

We start with a brief discussion of spontaneous \mathcal{R}_p and later we will address the issues of neutrino mass generation with explicit breaking of R_p .

I. Spontaneously broken R -parity.

The idea of spontaneous \mathcal{R}_p was first implemented in ref. [346] through spontaneous violation of the lepton number. The lepton number violation occurs through the left sneutrino VEVs. It was revealed in ref. [347] that if supersymmetry breaking terms include trilinear scalar couplings and gaugino Majorana masses, only one neutrino mass would be generated at the tree level. Remaining two small masses are generated at the one-loop level [346]. Different phenomenological implications for such a model were addressed in references [251, 316, 317, 348, 349]. A consequence of spontaneous \mathcal{L} appears in the form of a massless Nambu-Goldstone boson called Majoron [171, 172]. Unfortunately, a Majoron, arising from the breaking of gauge non-singlet fields (in this case a doublet Majoron from the left sneutrino VEVs which is a member of $SU(2)_L$ family) is strongly disfavored by electroweak precision measurements (Z -boson decay width) [350–353] and astrophysical constraints [173, 354–356]. Thus this doublet-Majoron model is ruled out [309, 357, 358].

The possible shortcomings of a doublet Majoron model are removable by using the VEV of a gauge-singlet field as suggested in ref. [359]. Most of these models break the lepton number spontaneously by giving VEV to a singlet field carrying one unit of lepton number [308, 359, 360]. However, there exists model where the singlet field carries two unit of lepton number [311]. This singlet Majoron model [172] is not ruled out by LEP data. More phenomenological implications of this class of models are addressed in refs. [310, 314, 361–365].

We just briefly mentioned the basics of spontaneous \mathcal{R}_p for the sake of completeness. These issues are not a part of this thesis work and hence we do not elaborate further. A dedicated discussion on the spontaneous violation of R_p has been given in ref. [76].

II. Explicit breaking of R -parity.

The MSSM superpotential with R_p violating terms was given by eqns. (2.36) and (2.50). Since we aim to generate Majorana masses for the light neutrinos, we consider violation of the lepton number only and thus the baryon number violating terms ($\frac{1}{2}\lambda''_{ijk}\hat{u}_i^c\hat{d}_j^c\hat{d}_k^c$) are dropped for the rest of the discussions. It is perhaps, best to start with the simple most example of \mathcal{R}_p , namely bilinear R_p -violation (bR_pV) and continue the discussion with the trilinear terms (tR_pV) later.

✦ Bilinear R -parity violation

The superpotential and soft terms are given by (see eqns. (2.36), (2.37) and (2.50))

$$\begin{aligned} W^{bR_pV} &= W^{MSSM} - \epsilon_{ab}\varepsilon^i\hat{L}_i^a\hat{H}_u^b, \\ -\mathcal{L}_{\text{soft}}^{bR_pV} &= -\mathcal{L}_{\text{soft}}^{MSSM} - \epsilon_{ab}B_{\varepsilon_i}\hat{L}_i^a\hat{H}_u^b. \end{aligned} \quad (3.31)$$

Now what are the implications of eqn.(3.31)?

1. R_p is violated through lepton number violation by odd unit, $\Delta L = 1$. This is an explicit breaking and so there is no possibility for an experimentally disfavored doublet Majoron emission.

2. Similar to eqn.(2.38) one can construct the neutral scalar potential, $V_{neutral\ scalar}^{bR_p V}$. Interestingly now one get non-zero VEVs for the left sneutrino fields using the suitable minimization condition

$$\sum_j (m_{\tilde{L}}^2)^{ji} v_j' - B_{\varepsilon_i} v_2 + \gamma_g \xi_v v_i' + \varepsilon_i \eta = 0, \quad (3.32)$$

where

$$\eta = \sum_i \varepsilon^i v_i' + \mu v_1, \quad \gamma_g = \frac{1}{4}(g_1^2 + g_2^2), \quad \xi_v = \sum_i v_i'^2 + v_1^2 - v_2^2. \quad (3.33)$$

v_1, v_2 are VEVs for down and up-type Higgs fields, respectively. v_i' is the VEV acquired by ' i '-th sneutrino field. The soft masses $(m_{\tilde{L}}^2)^{ji}$ are assumed to be symmetric in ' i ' and ' j ' indices.

The masses for W, Z bosons now should be given by

$$M_W = \frac{g_2 v_{new}}{\sqrt{2}}, \quad M_Z = \frac{v_{new}}{\sqrt{2}} \sqrt{g_1^2 + g_2^2}, \quad (3.34)$$

where $v_{new}^2 = \sum v_i'^2 + v_1^2 + v_2^2$. It is apparent from eqn.(3.34) that to maintain the electroweak precision, $\sum v_i'^2 \ll v_1^2, v_2^2$, so that $\sum v_i'^2 + v_1^2 + v_2^2 \simeq v_1^2 + v_2^2$ to a very good approximation.

3. Significance of the lepton number is lost, indeed without a designated lepton number there is no difference between a lepton superfield (\hat{L}_i) and a down-type Higgs superfield, \hat{H}_d . As a consequence now the neutral sleptons (left sneutrinos ($\tilde{\nu}$) in this case) can mix with CP-odd (pseudoscalar) and even (scalar) neutral Higgs bosons. Similar mixing is allowed between charged Higgs and the charged sleptons. These enlarged scalar and pseudoscalar mass squared matrices in the basis $(\Re H_d^0, \Re H_u^0, \Re \tilde{\nu}_\alpha)$ and $(\Im H_d^0, \Im H_u^0, \Im \tilde{\nu}_\alpha)$ respectively, are given by

$$(a) (M_{scalar}^2)_{5 \times 5} = \begin{pmatrix} (\mathcal{M}_{MSSM-scalar}^2)_{2 \times 2} & (\mathcal{S}_{\tilde{\nu}_\alpha H_i^0}^2)_{2 \times 3} \\ (\mathcal{S}_{\tilde{\nu}_\alpha H_i^0}^2)^T & (\mathcal{S}_{\tilde{\nu}_\alpha \tilde{\nu}_\beta}^2)_{3 \times 3} \end{pmatrix}, \quad (3.35)$$

where $i = \begin{pmatrix} d \\ u \end{pmatrix}$ with $\alpha, \beta = 1, 2, 3$ or e, μ, τ and

$$\begin{aligned} (\mathcal{S}_{\tilde{\nu}_\alpha H_d^0}^2) &= (\mu \varepsilon_\alpha + 2\gamma_g v_\alpha' v_1), & (\mathcal{S}_{\tilde{\nu}_\alpha H_u^0}^2) &= (-B_{\varepsilon_\alpha} - 2\gamma_g v_\alpha' v_2), \\ (\mathcal{S}_{\tilde{\nu}_\alpha \tilde{\nu}_\beta}^2) &= \varepsilon_\alpha \varepsilon_\beta + \gamma_g \xi_v \delta_{\alpha\beta} + 2\gamma_g v_\alpha' v_\beta' + (m_{\tilde{L}}^2)_{\alpha\beta}, \end{aligned} \quad (3.36)$$

and (b)

$$(M_{pseudoscalar}^2)_{5 \times 5} = \begin{pmatrix} (\mathcal{M}_{MSSM-pseudoscalar}^2)_{2 \times 2} & (\mathcal{P}_{\tilde{\nu}_\alpha H_i^0}^2)_{2 \times 3} \\ (\mathcal{P}_{\tilde{\nu}_\alpha H_i^0}^2)^T & (\mathcal{P}_{\tilde{\nu}_\alpha \tilde{\nu}_\beta}^2)_{3 \times 3} \end{pmatrix}, \quad (3.37)$$

with

$$\begin{aligned} (\mathcal{P}_{\tilde{\nu}_\alpha H_d^0}^2) &= (-\mu \varepsilon_\alpha), & (\mathcal{P}_{\tilde{\nu}_\alpha H_u^0}^2) &= (B_{\varepsilon_\alpha}), \\ (\mathcal{P}_{\tilde{\nu}_\alpha \tilde{\nu}_\beta}^2) &= \varepsilon_\alpha \varepsilon_\beta + \gamma_g \xi_v \delta_{\alpha\beta} + (m_{\tilde{L}}^2)_{\alpha\beta}. \end{aligned} \quad (3.38)$$

Here ' \Re ' and ' \Im ' correspond to the real and imaginary part of a neutral scalar field.

The charged scalar mass squared matrix with the basis choice $(H_d^+, H_u^+, \tilde{\ell}_{\alpha R}^+, \tilde{\ell}_{\alpha L}^+)$ looks like

$$(M_{charged\ scalar}^2)_{8 \times 8} = \begin{pmatrix} (\mathcal{M}_{MSSM-charged}^2)_{2 \times 2} & (\mathcal{C}_{\tilde{\ell}_{\alpha X} H_i}^2)_{2 \times 6} \\ (\mathcal{C}_{\tilde{\ell}_{\alpha X} H_i}^2)^T & (\mathcal{C}_{\tilde{\ell}_{\alpha X} \tilde{\ell}_{\beta Y}}^2)_{6 \times 6} \end{pmatrix}, \quad (3.39)$$

where $X, Y = L, R$ and

$$\begin{aligned}
(\mathcal{C}_{\tilde{\ell}_{\alpha R} H_d}^2)_{1 \times 3} &= (Y_e^{\alpha\beta} \varepsilon_\beta v_2 - (A_e Y_e)^{\alpha\beta} v'_\beta), \\
(\mathcal{C}_{\tilde{\ell}_{\alpha L} H_d}^2)_{1 \times 3} &= (\mu \varepsilon_\alpha - Y_e^{\alpha\alpha} Y_e^{\beta\alpha} v'_\beta v_1 + \frac{g_2^2}{2} v'_\alpha v_1), \\
(\mathcal{C}_{\tilde{\ell}_{\alpha R} H_u}^2)_{1 \times 3} &= (-\mu Y_e^{\beta\alpha} v'_\beta + Y_e^{\beta\alpha} \varepsilon_\beta v_1), \quad (\mathcal{C}_{\tilde{\ell}_{\alpha L} H_u}^2)_{1 \times 3} = (\frac{g_2^2}{2} v'_\alpha v_2 + B_{\varepsilon_\alpha}), \\
(\mathcal{C}_{\tilde{\ell}_{\alpha L} \tilde{\ell}_{\beta L}}^2)_{3 \times 3} &= (\varepsilon_\alpha \varepsilon_\beta + Y_e^{\alpha\rho} Y_e^{\beta\rho} v_1^2 + \gamma_g \xi_v \delta_{\alpha\beta} - \frac{g_2^2}{2} \mathcal{D}_{\alpha\beta} + (m_L^2)^{\alpha\beta}), \\
(\mathcal{C}_{\tilde{\ell}_{\alpha R} \tilde{\ell}_{\beta R}}^2)_{3 \times 3} &= (Y_e^{\rho\alpha} Y_e^{\sigma\beta} v'_\rho v'_\sigma + Y_e^{\rho\alpha} Y_e^{\rho\beta} v_1^2 + (m_{\tilde{e}^c}^2)^{\alpha\beta} - \frac{g_1^2}{2} \xi_v \delta_{\alpha\beta}), \\
(\mathcal{C}_{\tilde{\ell}_{\alpha L} \tilde{\ell}_{\beta R}}^2)_{3 \times 3} &= (-\mu Y_e^{\alpha\beta} v_2 + (A_e Y_e)^{\alpha\beta} v_1),
\end{aligned} \tag{3.40}$$

where $\mathcal{D}_{\alpha\beta} = \{\xi_v \delta_{\alpha\beta} - v'_\alpha v'_\beta\}$. The soft-terms are assumed to be symmetric. The 2×2 MSSM scalar, pseudoscalar and charged scalar mass squared matrices are given in appendix A.

4. In a similar fashion charged leptons ($\ell_\alpha \equiv e, \mu, \tau$) mix with charged gauginos as well as with charged higgsinos and yield an enhanced chargino mass matrix. In the basis, $-i\tilde{\lambda}_2^+, \tilde{H}_u^+, \ell_{\alpha R}^+$ (column) and $-i\tilde{\lambda}_2^-, \tilde{H}_d^-, \ell_{\beta L}^-$ (row)

$$(M_{chargino})_{5 \times 5} = \begin{pmatrix} (M_{MSSM}^{chargino})_{2 \times 2} & \begin{pmatrix} 0 \\ Y^{\rho\alpha} v'_\rho \end{pmatrix}_{2 \times 3} \\ \begin{pmatrix} g_2 v'_\alpha & \varepsilon_\alpha \end{pmatrix}_{3 \times 2} & (Y^{\beta\alpha} v_1)_{3 \times 3} \end{pmatrix}. \tag{3.41}$$

With this enhancement eqn.(2.43) looks like

$$\begin{aligned}
\chi_i^+ &= V_{i1} \tilde{W}^+ + V_{i2} \tilde{H}_u^+ + V_{i,\alpha+2} \ell_{\alpha R}^+, \\
\chi_i^- &= U_{i1} \tilde{W}^- + U_{i2} \tilde{H}_d^- + U_{i,\alpha+2} \ell_{\alpha L}^-.
\end{aligned} \tag{3.42}$$

The neutral fermions also behave in a similar manner. The neutralino mass matrix now can accommodate three light neutrinos ($\nu \equiv \nu_L$) apart from the four MSSM neutralinos. The extended neutralino mass matrix in the basis $\tilde{B}^0, \tilde{W}_3^0, \tilde{H}_d^0, \tilde{H}_u^0, \nu_\alpha$ is written as

$$(M_{neutralino})_{7 \times 7} = \begin{pmatrix} (M_{MSSM}^{neutralino})_{4 \times 4} & ((m)_{3 \times 4})^T \\ (m)_{3 \times 4} & (0)_{3 \times 3} \end{pmatrix}, \tag{3.43}$$

with

$$(m)_{3 \times 4} = \begin{pmatrix} -\frac{g_1}{\sqrt{2}} v'_\alpha & \frac{g_2}{\sqrt{2}} v'_\alpha & 0 & -\varepsilon_\alpha \end{pmatrix}. \tag{3.44}$$

Just like the charginos, for the neutralinos one can rewrite eqn.(2.41) in modified form as

$$\chi_i^0 = N_{i1} \tilde{B}^0 + N_{i2} \tilde{W}_3^0 + N_{i3} \tilde{H}_d^0 + N_{i4} \tilde{H}_u^0 + N_{i,\alpha+4} \nu_\alpha. \tag{3.45}$$

Chargino and neutralino mass matrices for MSSM are given in appendix A.

5. In eqn.(3.43) entries of the 4×4 MSSM block are \sim TeV scale, which are \gg entries of $(m)_{3 \times 4}$. Besides, the 3×3 null matrix $(0)_{3 \times 3}$ signifies the absence of Majorana mass terms for the left-handed neutrinos. This matrix has a form similar to that of eqn.(3.26), thus the effective light neutrino mass matrix is given by (using eqn.(3.27))

$$m_{seesaw} = -(m)_{3 \times 4} \{ (M_{MSSM}^{neutralino})_{4 \times 4} \}^{-1} \{ (m)_{3 \times 4} \}^T, \tag{3.46}$$

or in component form

$$(m_{seesaw})_{\alpha\beta} = \frac{g_1^2 M_2 + g_2^2 M_1}{2 \text{Det}[(M_{MSSM}^{neutralino})_{4 \times 4}]} (\mu v'_\alpha - \varepsilon_\alpha v_1) (\mu v'_\beta - \varepsilon_\beta v_1). \tag{3.47}$$

Assuming M_1, M_2, μ, v_1, v_2 are $\sim \tilde{m}$, a generic mass scale (say EWSB scale or the scale of the soft supersymmetry breaking terms) and $g_1, g_2 \sim \mathcal{O}(1)$ we get from eqn.(3.47)

$$(m_{seesaw})_{\alpha\beta} \approx \underbrace{\frac{v'_\alpha v'_\beta}{\tilde{m}}}_I + \underbrace{\frac{\varepsilon_\alpha \varepsilon_\beta}{\tilde{m}}}_{II} - \underbrace{\frac{(\varepsilon_\alpha v'_\beta + \alpha \leftrightarrow \beta)}{\tilde{m}}}_{III}. \quad (3.48)$$

The first term of eqn.(3.48) is coming from the *gaugino seesaw* effect, which is originating though the mixing of light neutrinos with either a bino (\tilde{B}^0) or a neutral wino (\tilde{W}_3^0). This is also another example for a Type-I (bino) + Type-III (wino) seesaw (see figure 3.6 (a),(b)). The second and third

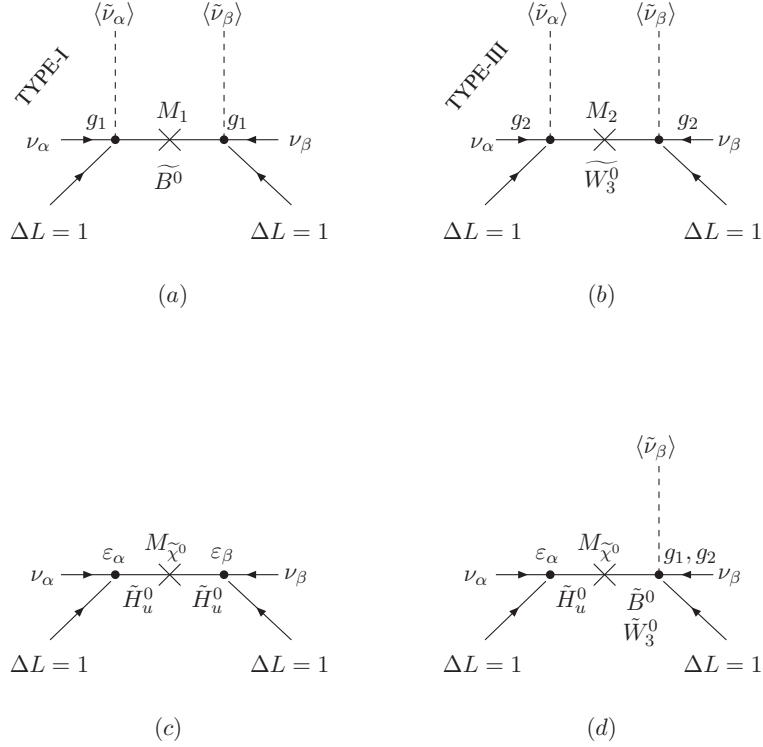


Figure 3.6: Different types of tree level contributions to the neutrino mass in a $bR_p V$ supersymmetric model. The cross on the neutralino propagator signifies a Majorana mass term for the neutralino.

contributions are represented by (c) and (d) of figure 3.6. There is one extremely important point to note about this analysis, that is if $\varepsilon_\alpha = 0$ but B_{ε_α} are not, even then $v'_\alpha \neq 0$ (see eqn.(3.32)). Thus even if R_p violation is rotated away from the superpotential, effect of \tilde{R}_p in the soft terms can still trigger non-zero neutrino mass as shown by (a), (b) of figure 3.6. However, this analysis is strictly valid if $B_{\varepsilon_\alpha} \not\propto \varepsilon_\alpha$.

If we define $\mu'_\alpha = (\mu v'_\alpha - \varepsilon_\alpha v_1)$, then using the following set of relations, namely, $g_1^2/(g_1^2 + g_2^2) = \sin^2 \theta_W$, $g_2^2/(g_1^2 + g_2^2) = \cos^2 \theta_W$, $M_2^2 = (1/2)(g_1^2 + g_2^2)(v_1^2 + v_2^2)$ and the fact $\text{Det}[(M_{MSSM}^{neutralino})_{4 \times 4}] = (g_1^2 M_2 + g_2^2 M_1)v_1 v_2 \mu - M_1 M_2 \mu^2$, we get an alternative expression of eqn.(3.48)

$$(m_{seesaw})_{\alpha\beta} \approx \frac{\mu'_\alpha \mu'_\beta}{\tilde{m}} \cos^2 \beta, \quad (3.49)$$

where $\tan \beta = v_2/v_1$ holds good with $v'_\alpha \ll v_1, v_2$. The problem with this tree level effective light neutrino mass matrix is that, it gives only one *non-zero* eigenvalue, given by

$$m_{neut} = \frac{|\mu'_\alpha|^2}{\tilde{m}} \cos^2 \beta. \quad (3.50)$$

The *only non-zero* neutrino mass at the tree level of a bR_pV model is suppressed by squared R_p -violating parameter and also by $\tan^{-2}\beta$ for $\tan\beta \gg 1$. With $\varepsilon_\alpha \sim 10^{-4}$ GeV and $\tilde{m} \sim 1$ TeV one gets $m_{neut} \sim 10^{-11}$ GeV, which is the scale for the atmospheric neutrinos⁹. But to accommodate three flavour global data [111, 113] one requires at least two massive neutrinos!

◆ *Loop corrections in bilinear R -parity violation*

The remedy to this problem can come from the one-loop contributions to the light neutrino masses. The dominant diagrams are shown in figure 3.7. Before discussing these diagrams and their contributions further it is worthy to explain the meaning of symbols used in figure 3.7. The quantity B'_α denotes mixing between a left handed sneutrino $\tilde{\nu}_\alpha$ (see eqns.(3.36), (3.38)) and physical MSSM Higgs bosons (eqn.(2.46)). $\tilde{\mu}_\alpha$ is either ε_α ($\nu_\alpha \tilde{H}_u$ mixing, see eqn.(3.44)) or $g_1 v'_\alpha, g_2 v'_\alpha$ ($\nu_\alpha \tilde{B}^0, \nu_\alpha \tilde{W}_3^0$ mixing, see eqn.(3.44)) (figure (a) and (b)). In figure (c) a *blob* on the scalar line indicates a mixing between left and right handed up-type squarks, which exists if one has either gauginos ($\tilde{B}^0, \tilde{W}_3^0$) or up-type higgsino (\tilde{H}_u^0) on both the sides. However, if one puts gauginos on one side and higgsino on the other, then this left-right mixing is absent. This situation is represented by a void circle on the scalar line around the blob. In figure (d) g_α, g_β represents neutrino-gaugino mixing (eqn.(3.44)). f denotes a *down-type* fermion, that is either a charged lepton, ($\ell_k = e, \mu, \tau$) or a down quark, ($d_k = d, s, b$). There also exist more complicated diagrams for down-type fermion loops as shown in figure (e, f). η_χ represents mixing of a down-type higgsino with neutral gauginos and up-type higgsino (see eqn.(A.7)). The last two diagrams (g, h) arise from chargino-charged scalar contribution to neutrino mass. A *cross* on the fermion line represents a mass insertion, responsible for a chirality flip. In all of these diagrams $\Delta L = 2$ effect is coming from a pair of $\Delta L = 1$ contributions. For diagrams (g, h) the blobs and the cross represent mixing only without any chirality flip (see eqns.(3.40), (3.41)).

These diagrams are shown for a general basis where both of the bilinear R_p -violating parameters (ε_α) and sneutrino VEVs (v'_α) are non-vanishing. When $v'_\alpha = 0$, using the minimization condition for left sneutrinos (eqn. (3.32)), diagram (a) of figure 3.7 reduces to the well-known BB -loop [228, 281, 285, 296].

This BB loop can either give mass to one more neutrino state (not to that one which was already massive at the tree level so long $B_{\varepsilon_\alpha} \not\propto \varepsilon_\alpha$) when sneutrino masses are degenerate or can contribute to all three light neutrino masses with non-degenerate sneutrinos. Assuming all the scalar and neutralino masses $\sim \tilde{m}$, an approximate expression for this loop contribution to light neutrino masses with degenerate sneutrinos is given by [296, 297].

$$m_{\alpha\beta}^{BB} \simeq \frac{g_2^2}{64\pi^2 \cos^2 \beta} \frac{B'_\alpha B'_\beta}{\tilde{m}^3}. \quad (3.51)$$

It is important to mention that in order to generate solar neutrino mass square difference using loop corrections one should naively expect $B' \sim (0.1 - 1)$ GeV², with the assumption of normal hierarchical structure in light neutrino masses.

In a similar fashion the loop shown by diagram (b) of figure 3.7 is an example of the μB -type loop at $v'_\alpha = 0$ [281, 285, 296, 297]. This loop involves neutrino-gaugino or neutrino-higgsino mixing (collectively labeled as $\tilde{\mu}_\alpha$, see eqn.(3.44)) together with sneutrino-Higgs mixing (B'_β , see eqns.(3.36), (3.38), (2.46)). Assuming all the masses (Higgs, sneutrino, neutralino) are at the weak scale \tilde{m} , an approximate contribution is given by [281, 285, 296, 297]

$$m_{\alpha\beta}^{\mu B} \simeq \frac{g_2^2}{64\pi^2 \cos \beta} \frac{\tilde{\mu}_\alpha B'_\beta + \tilde{\mu}_\beta B'_\alpha}{\tilde{m}^2}. \quad (3.52)$$

It is evident from the structure of right hand side of eqn.(3.52) that the μB loop contributes to more than one neutrino masses. However, presence of $\tilde{\mu}_\alpha$ makes this loop contribution sub-leading to neutrino masses compared to the BB loop [294, 296, 297]. For large values of $\tan \beta$ ($\tan \beta \gg 1$) the BB -loop and the μB -loop are enhanced by $\tan^2 \beta$ and $\tan \beta$, respectively.

Contributions to neutrino masses from quark-squark loops are given by diagrams (c, d, e, f) of figure 3.7. Diagram (c) represents an up-type quark-squark loops. This diagram can yield large contribution

⁹Assuming normal hierarchy in light neutrino masses.

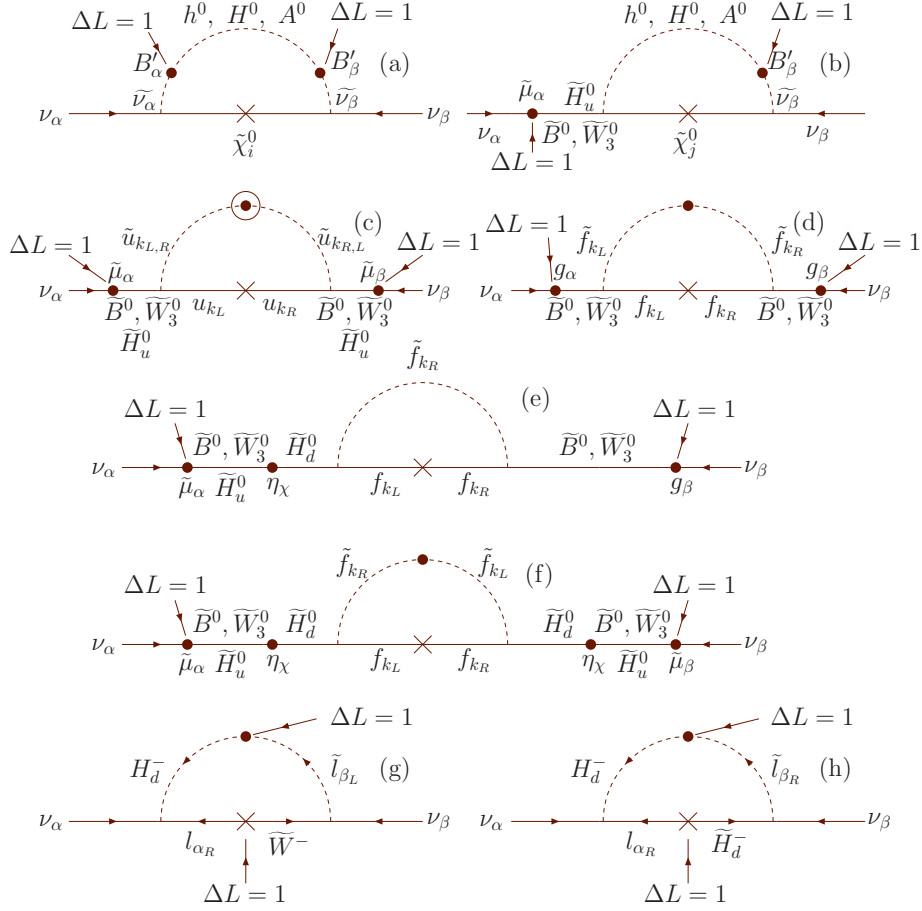


Figure 3.7: Neutrino mass generation through loops in a model with bR_pV . For details of used symbols see text.

to neutrino mass particularly when it is a top-stop ($t - \tilde{t}$) loop, because of the large top Yukawa coupling, Y_t . This loop contribution is proportional to $\tilde{\mu}_\alpha \tilde{\mu}_\beta$, which is exactly same as the tree level one (see eqn.(3.49)), thus this entire effect eventually gives a correction to a neutrino mass which is already massive at the tree level [302]. An approximate expression for this loop is given by

$$m_{\alpha\beta}^{u_k \tilde{u}_k} (\text{no blob}) \simeq \frac{N_c f_{u\tilde{u}}^2}{16\pi^2} \frac{m_{u_k} \tilde{\mu}_\alpha \tilde{\mu}_\beta}{\tilde{m}^2}, \quad m_{\alpha\beta}^{u_k \tilde{u}_k} (\text{blob}) \simeq \frac{N_c f_{u\tilde{u}}^2}{16\pi^2} \frac{m_{u_k}^2 \tilde{\mu}_\alpha \tilde{\mu}_\beta}{\tilde{m}^3}, \quad (3.53)$$

where m_{u_k} is the mass of up-quark of type k . The coupling factor $f_{u\tilde{u}}^2$ is either $g_i g_j$ or $g_i Y_{u_k}$ ¹⁰ with $i = 1, 2$. N_c is the colour factor which is 3 for quarks. For the case of left right sfermion mixing we use the relation

$$m_{f_k}^{2LR} \approx m_{f_k} \tilde{m}. \quad (3.54)$$

In a similar fashion for a down type fermion-sfermion, $f_k - \tilde{f}_k$ (charged lepton-slepton or down quark-squark) (see diagram (d) of figure 3.7) an approximate expression is given by (using eqn.(3.54))

$$m_{\alpha\beta}^{f_k \tilde{f}_k} \simeq \frac{N_c f_{f\tilde{f}}^2}{16\pi^2} \frac{m_{f_k}^2 g_\alpha g_\beta}{\tilde{m}^3}, \quad (3.55)$$

where m_{f_k} is the mass of down-type fermion of type k ¹¹. $N_c = 3$ for quarks but = 1 for leptons. The coupling factor $f_{f\tilde{f}}^2$ is $g_i g_j$ with $i = 1, 2$. The quantity g_α denotes mixing between a neutrino and a

¹⁰ $u_k \equiv u, c, t$.

¹¹ $f = d_k \equiv d, s, b$ or $f = \ell_k \equiv e, \mu, \tau$.

gaugino. However, for down-type fermion-sfermion there exist other complicated loop diagrams like (e, f) [302] of figure 3.7. These loops give contribution of the approximate form

$$m_{\alpha\beta}^{\prime f_k \tilde{f}_k} \simeq \frac{N_c f_{f\tilde{f}}^{\prime 2} \eta_\chi}{16\pi^2} \frac{m_{f_k} (\tilde{\mu}_\alpha g_\beta + \alpha \leftrightarrow \beta)}{\tilde{m}^3}, \quad (3.56)$$

for diagram (e) and

$$m_{\alpha\beta}^{\prime\prime f_k \tilde{f}_k} \simeq \frac{N_c f_{f\tilde{f}}^{\prime\prime 2} \eta_\chi^2}{16\pi^2} \frac{m_{f_k}^2 \tilde{\mu}_\alpha \tilde{\mu}_\beta}{\tilde{m}^5}, \quad (3.57)$$

for diagram (f) , respectively. The quantity $f_{f\tilde{f}}^{\prime 2}$ is $g_i Y_{f_k}$ whereas $f_{f\tilde{f}}^{\prime\prime 2}$ represents $Y_{f_k}^2$ with $i = 1, 2$ and Y_{f_k} being either charged lepton or down quark Yukawa couplings. It is apparent that eqns.(3.55), (3.57) once again contribute to the “same neutrino” which is already massive at the tree level. However, eqn.(3.56) will contribute to more than one neutrino masses. Note that since contributions of these set of diagrams are proportional to the fermion mass, m_{f_k} , they are important only for bottom quark and tau-lepton along with the corresponding scalar states running in the loop.

Diagrams (g, h) are the chargino-charged scalar loop contributions to light neutrino mass [301]. An approximate form for these loops are given by

$$m_{\alpha\beta}^{(g)} \simeq \frac{g_2^2 Y_{\ell_k} v'_\alpha B''_\beta}{16\pi^2 \tilde{m}}, \quad m_{\alpha\beta}^{(h)} \simeq \frac{Y_{\ell_k}^3 v'_\alpha B''_\beta}{16\pi^2 \tilde{m}}, \quad (3.58)$$

where Y_{ℓ_k} are the charged lepton Yukawa couplings and B''_β ($\sim B'$) represents a generic charged slepton-charged Higgs mixing (see eqn.(3.40)). These contributions vanishes identically when $v'_\alpha = 0$. These contributions being proportional to small parameters like v' , Y_{ℓ} , are *much smaller* compared to the other types of loops. Various couplings needed here can be found in references like [254, 280, 295, 366–369].

◆ *Trilinear R -parity violation and loop corrections*

The so-called trilinear couplings, contribute to light neutrino mass through loops only [228, 264, 281, 296]. Possible diagrams are shown in figure 3.8.

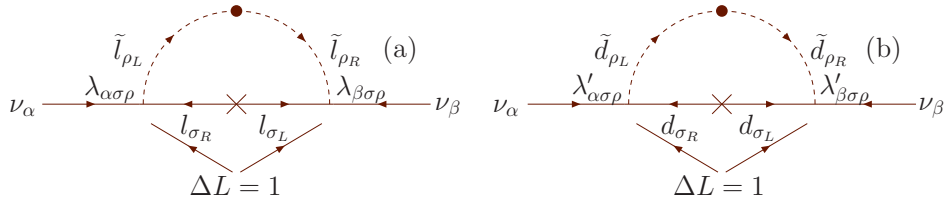


Figure 3.8: Neutrino mass generation through loops in a model with $tR_p V$.

Using eqn.(3.54) these contributions can be written as

$$m_{\alpha\beta}^{\lambda\lambda} \simeq \frac{N_c \lambda_{\alpha\sigma\rho} \lambda_{\beta\sigma\rho}}{8\pi^2} \frac{m_{\ell_\sigma} m_{\ell_\rho}}{\tilde{m}}, \quad m_{\alpha\beta}^{\lambda'\lambda'} \simeq \frac{N_c \lambda'_{\alpha\sigma\rho} \lambda'_{\beta\sigma\rho}}{8\pi^2} \frac{m_{d_\sigma} m_{d_\rho}}{\tilde{m}}, \quad (3.59)$$

where N_c is 1(3) for $\lambda\lambda(\lambda'\lambda')$ loop. Contributions of these diagrams are suppressed by squared R_p violating couplings λ^2, λ'^2 and squared charged lepton, down-type quark masses apart from usual loop suppression factor. Thus usually these loop contributions are quiet small [264].

◆ *Loop corrections in $bR_p V + tR_p V$*

There also exist a class of one-loop diagrams which involve both bilinear and trilinear R_p violating couplings, as shown figure 3.9 [281, 285, 296, 297]. One can write down these loop contributions approximately as

$$(i) \quad m_{\alpha\beta}^{\mu f} \simeq \frac{N_c \tilde{\mu}_\alpha \eta_\chi Y_{f\sigma} f_{\beta\sigma\sigma}}{16\pi^2} \frac{m_{f_\sigma}^2}{\tilde{m}^3} + \alpha \leftrightarrow \beta, \quad (3.60)$$

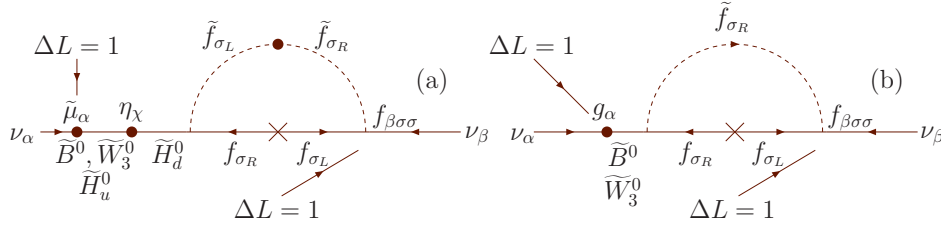


Figure 3.9: Neutrino mass generation through loops in a model with both bR_pV and tR_pV . \tilde{f}_σ is either a charged slepton with $f_{\beta\sigma\sigma} = \lambda_{\beta\sigma\sigma}$ or a down-type squark with $f_{\beta\sigma\sigma} = \lambda'_{\beta\sigma\sigma}$. $\tilde{\mu}_\alpha, \eta_\chi, g_\alpha$ are same as explained in figure 3.8. The cross have similar explanation as discussed in figure 3.7.

for diagram (a) where $N_c = 1(3)$ for charged lepton (down-type quark), Y_{f_σ} is either a charged lepton or a down-type Yukawa coupling and

$$(ii) \quad m_{\alpha\beta}^{\mu f} \simeq \frac{N_c g_\alpha g_i f_{\beta\sigma\sigma} m_{f_\sigma}}{16\pi^2 \tilde{m}} + \alpha \leftrightarrow \beta, \quad (3.61)$$

for diagram (b). The quantity $f_{\alpha\sigma\sigma}$ represents either $\lambda_{\alpha\sigma\sigma}$ or $\lambda'_{\alpha\sigma\sigma}$ couplings. g_α represents a neutrino-gaugino mixing (see eqn.(3.44)). $i = 1, 2$. These contributions are suppressed by a pair of R_p -violating couplings ($\mu\lambda/\mu\lambda'$) or product of sneutrino VEVs and trilinear R_p -violating couplings ($v'\lambda/v'\lambda'$), a loop factor and at least by a fermion mass (\propto Yukawa coupling) [296, 297]. Also contributions of diagram (a) is negligible compared to that of (b) by a factor of squared Yukawa coupling. Contributions of these loops are second order in the above mentioned suppression factors (similar to that of μB loop) once the tree level effect is taken into account.

There are literature where these loop contributions are analysed in a basis independent formalism [281, 285, 297] (also see refs. [263, 282, 370–372] for basis independent parameterizations of R_p). For this discussion we stick to the “mass insertion approximation” but alternatively it is also possible to perform these entire analysis in physical or mass basis [254, 280, 301]. The mass insertion approximation works well since the effect of R_p -violating parameters are expected to be small in order to account for neutrino data. All of these calculations are performed assuming no flavour mixing for the sfermions.

◆ A comparative study of different loop contribution

Usually the trilinear loops ($\lambda\lambda, \lambda'\lambda'$) are doubly Yukawa suppressed (through fermion masses) and they yield rather small contributions. The μB -type, $\mu\lambda, \mu\lambda'$ loop contributions to the light neutrino masses are second order in suppression factors. The $\mu\lambda, \mu\lambda'$ loop contributions are also suppressed by single Yukawa coupling. The Yukawa couplings (either double or single) are also present in the quark-squark or charged lepton-slepton loops. However, in most of the occasions they give corrections to the tree level neutrino mass, though other contributions can also exist (see eqn.(3.56)). These loops are sometimes dominant [267, 280, 295] provided the BB -type loop suffers large cancellation among different Higgs contributions. In general the second neutrino receives major contribution from the BB loop.

In the situation when $\tan\beta$ is large, the tree level contribution (see eqn.(3.49)) can be smaller compared to the loop contributions. In this situation, the tree level result usually account for the solar neutrino mass scale whereas the loop corrections generate the atmospheric mass scale. In conventional scenario when tree level effect is leading, it is easy to fit the normal hierarchical spectrum of neutrino mass in an R_p -violating theory.

3.4 Testing neutrino oscillation at Collider

We have already spent enough time to discuss the issue of light neutrino mass generation. It is then legitimate to ask what are the possible experimental implications of a massive neutrino? It was first advocated in ref. [331] that in a simple supersymmetric model with only bR_pV it is possible to get some kind of relation between the neutrino sector and the decays of the LSP. This kind of model predicts

comparable numbers of muons and taus, produced together with the W -boson, in decays of the lightest neutralino. Usually for an appreciable region of parameter space the lightest neutralino is the LSP. Additionally, the appearance of a measurable “displaced vertex” was also addressed in ref. [331] which is extremely useful for a collider related study to efface undesired backgrounds. This novel feature also has been addressed in refs. [265, 270, 286, 345]. See also refs. [248, 339, 373–376] for tests of neutrino properties at accelerator experiments.

The correlation between a LSP decay and neutrino physics is apparent for supersymmetric models with bilinear R_p , since the same parameter ε_α is involved in both the analysis. For example, if the neutralino LSP, $\tilde{\chi}_1^0$ decays into a charged lepton and W -boson [331] then following [272, 286] one can get approximately

$$\frac{(\tilde{\chi}_1^0 \rightarrow \mu^\pm W^\mp)}{(\tilde{\chi}_1^0 \rightarrow \tau^\pm W^\mp)} \simeq \left(\frac{\mu'_\mu}{\mu'_\tau} \right)^2 = \tan^2 \theta_{23}, \quad (3.62)$$

where $\mu_\alpha = \mu v'_\alpha - \varepsilon_\alpha v_1$ with $\alpha = e, \mu, \tau$ and $\tan^2 \theta_{23}$ is the atmospheric mixing angle. Similar correlations with trilinear R_p parameters are lost [270] since the model became less predictive with a larger set of parameters. A rigorous discussion of these correlations has been given in ref. [344].

We note in passing that when the LSP is no longer stable (due to R_p) it is not necessary for them to be charge or colour neutral [377–379]. With broken R_p any sparticle (charginos [380], squarks, gluinos [381–383], sneutrinos [384], (see also ref. [379])) can be the LSP. It was pointed out in ref. [339] that whatever be the LSP, measurements of branching ratios at future accelerators will provide a definite test of bilinear R_p breaking as the model of neutrino mass.

Bibliography

- [1] Fermi E 1934 *Nuovo Cim.* **11** 1–19
- [2] Fermi E 1934 *Z. Phys.* **88** 161–177
- [3] Cowan C L, Reines F, Harrison F B, Kruse H W and McGuire A D 1956 *Science* **124** 103–104
- [4] Danby G *et al.* 1962 *Phys. Rev. Lett.* **9** 36–44
- [5] Kodama K *et al.* (DONUT) 2001 *Phys. Lett.* **B504** 218–224
- [6] Frampton P H and Vogel P 1982 *Phys. Rept.* **82** 339–388
- [7] Boehm F and Vogel P Cambridge, UK: Univ. PR. (1987) 211p
- [8] Bilenky S M and Petcov S T 1987 *Rev. Mod. Phys.* **59** 671
- [9] Bahcall J N Cambridge, UK: Univ. PR. (1989) 567p
- [10] Kayser B, Gibrat-Debu F and Perrier F 1989 *World Sci. Lect. Notes Phys.* **25** 1–117
- [11] Mohapatra R N and Pal P B 1991 *World Sci. Lect. Notes Phys.* **41** 1–318
- [12] Gelmini G and Roulet E 1995 *Rept. Prog. Phys.* **58** 1207–1266
- [13] Barbieri R, Hall L J, Tucker-Smith D, Strumia A and Weiner N 1998 *JHEP* **12** 017
- [14] Bilenky S M, Giunti C and Grimus W 1999 *Prog. Part. Nucl. Phys.* **43** 1–86
- [15] Fisher P, Kayser B and McFarland K S 1999 *Ann. Rev. Nucl. Part. Sci.* **49** 481–528
- [16] Kayser B and Mohapatra R N In *Caldwell, D.O. (ed.): Current aspects of neutrino physics* 17-38
- [17] Langacker (ed) P Singapore, Singapore: World Scientific (2000) 649 p
- [18] Caldwell (Ed) D O Berlin, Germany: Springer (2001) 338 p
- [19] Gonzalez-Garcia M C and Nir Y 2003 *Rev. Mod. Phys.* **75** 345–402
- [20] Pakvasa S and Valle J W F 2004 *Proc. Indian Natl. Sci. Acad.* **70A** 189–222
- [21] Barger V, Marfatia D and Whisnant K 2003 *Int. J. Mod. Phys.* **E12** 569–647
- [22] Grossman Y 2003 (*Preprint hep-ph/0305245*)
- [23] King S F 2004 *Rept. Prog. Phys.* **67** 107–158
- [24] Altarelli (ed) G and Winter (ed) K 2003 *Springer Tracts Mod. Phys.* **190** 1–248
- [25] Altarelli G and Feruglio F 2004 *New J. Phys.* **6** 106
- [26] Giunti C 2004 (*Preprint hep-ph/0409230*)

- [27] Kayser B 2005 (*Preprint* hep-ph/0506165)
- [28] Mohapatra R N *et al.* 2007 *Rept. Prog. Phys.* **70** 1757–1867
- [29] Mohapatra R N and Smirnov A Y 2006 *Ann. Rev. Nucl. Part. Sci.* **56** 569–628
- [30] Strumia A and Vissani F 2006 (*Preprint* hep-ph/0606054)
- [31] Valle J W F 2006 *J. Phys. Conf. Ser.* **53** 473–505
- [32] Gonzalez-Garcia M C and Maltoni M 2008 *Phys. Rept.* **460** 1–129
- [33] Fermi E 1926 *Rend. Lincei.* **3** 145–149
- [34] Dirac P A M 1926 *Proc. Roy. Soc. Lond.* **A112** 661–677
- [35] Lee T D and Yang C N 1956 *Phys. Rev.* **104** 254–258
- [36] Wu C S, Ambler E, Hayward R W, Hoppes D D and Hudson R P 1957 *Phys. Rev.* **105** 1413–1414
- [37] Cabibbo N 1963 *Phys. Rev. Lett.* **10** 531–533
- [38] Kobayashi M and Maskawa T 1973 *Prog. Theor. Phys.* **49** 652–657
- [39] Davis Jr R, Harmer D S and Hoffman K C 1968 *Phys. Rev. Lett.* **20** 1205–1209
- [40] Pontecorvo B 1957 *Sov. Phys. JETP* **6** 429
- [41] Pontecorvo B 1958 *Sov. Phys. JETP* **7** 172–173
- [42] Akhmedov E K 1999 (*Preprint* hep-ph/0001264)
- [43] Hirata K S *et al.* (Kamiokande-II) 1992 *Phys. Lett.* **B280** 146–152
- [44] Fukuda Y *et al.* (Kamiokande) 1994 *Phys. Lett.* **B335** 237–245
- [45] Aglietta M *et al.* (The NUSEX) 1989 *Europhys. Lett.* **8** 611–614
- [46] Casper D *et al.* 1991 *Phys. Rev. Lett.* **66** 2561–2564
- [47] Becker-Szendy R *et al.* 1992 *Phys. Rev.* **D46** 3720–3724
- [48] Allison W W M *et al.* 1997 *Phys. Lett.* **B391** 491–500
- [49] Ambrosio M *et al.* (MACRO) 1998 *Phys. Lett.* **B434** 451–457
- [50] Ronga F *et al.* (MACRO) 1999 *Nucl. Phys. Proc. Suppl.* **77** 117–122
- [51] Fukuda Y *et al.* (Super-Kamiokande) 1998 *Phys. Rev. Lett.* **81** 1562–1567
- [52] Fukuda Y *et al.* (Super-Kamiokande) 1999 *Phys. Rev. Lett.* **82** 2644–2648
- [53] Bethe H A 1939 *Phys. Rev.* **55** 434–456
- [54] Bahcall J N 2001 *SLAC Beam Line* **31N1** 2–12
- [55] Bahcall (Ed) J N, Davis (Ed) R, Parker (Ed) P, Smirnov (Ed) A and Ulrich (Ed) R Reading, USA: Addison-Wesley (1995) 440 p. (Frontiers in physics. 92)
- [56] Bahcall J N 2000 *Phys. Rept.* **333** 47–62
- [57] Bahcall J N and Ulrich R K 1988 *Rev. Mod. Phys.* **60** 297–372
- [58] Turck-Chieze S, Cahen S, Casse M and Doom C 1988 *Astrophys. J.* **335** 415–424
- [59] Turck-Chieze S and Lopes I 1993 *Astrophys. J.* **408** 347–367

- [60] Bahcall J N and Pinsonneault M H 1992 *Rev. Mod. Phys.* **64** 885–926
- [61] Bahcall J N, Basu S and Pinsonneault M H 1998 *Phys. Lett.* **B433** 1–8
- [62] Davis R 1994 *Prog. Part. Nucl. Phys.* **32** 13–32
- [63] Cleveland B T *et al.* 1998 *Astrophys. J.* **496** 505–526
- [64] Abdurashitov D N *et al.* 1996 *Phys. Rev. Lett.* **77** 4708–4711
- [65] Abdurashitov J N *et al.* (SAGE) 1999 *Phys. Rev.* **C60** 055801
- [66] Abdurashitov J N *et al.* (SAGE) 2009 *Phys. Rev.* **C80** 015807
- [67] Anselmann P *et al.* (GALLEX) 1992 *Phys. Lett.* **B285** 376–389
- [68] Hampel W *et al.* (GALLEX) 1999 *Phys. Lett.* **B447** 127–133
- [69] Altmann M *et al.* (GNO) 2000 *Phys. Lett.* **B490** 16–26
- [70] Hirata K S *et al.* (KAMIOKANDE-II) 1990 *Phys. Rev. Lett.* **65** 1297–1300
- [71] Fukuda S *et al.* (Super-Kamiokande) 2001 *Phys. Rev. Lett.* **86** 5651–5655
- [72] Cravens J P *et al.* (Super-Kamiokande) 2008 *Phys. Rev.* **D78** 032002
- [73] Boger J *et al.* (SNO) 2000 *Nucl. Instrum. Meth.* **A449** 172–207
- [74] Ahmad Q R *et al.* (SNO) 2002 *Phys. Rev. Lett.* **89** 011301
- [75] Aharmim B *et al.* (SNO) 2005 *Phys. Rev.* **C72** 055502
- [76] Vicente A 2011 (*Preprint* 1104.0831)
- [77] Pontecorvo B 1968 *Sov. Phys. JETP* **26** 984–988
- [78] Kayser B 1981 *Phys. Rev.* **D24** 110
- [79] Giunti C, Kim C W and Lee U W 1991 *Phys. Rev.* **D44** 3635–3640
- [80] Rich J 1993 *Phys. Rev.* **D48** 4318–4325
- [81] Grossman Y and Lipkin H J 1997 *Phys. Rev.* **D55** 2760–2767
- [82] Nakamura K *et al.* (Particle Data Group) 2010 *J. Phys.* **G37** 075021
- [83] Athanassopoulos C *et al.* (LSND) 1996 *Phys. Rev. Lett.* **77** 3082–3085
- [84] Athanassopoulos C *et al.* (LSND) 1998 *Phys. Rev. Lett.* **81** 1774–1777
- [85] Aguilar-Arevalo A A *et al.* (The MiniBooNE) 2007 *Phys. Rev. Lett.* **98** 231801
- [86] Aguilar-Arevalo A A *et al.* (The MiniBooNE) 2010 *Phys. Rev. Lett.* **105** 181801
- [87] Ma E and Roy P 1995 *Phys. Rev.* **D52** 4780–4783
- [88] Goswami S 1997 *Phys. Rev.* **D55** 2931–2949
- [89] Sarkar S 1996 *Rept. Prog. Phys.* **59** 1493–1610
- [90] Gaur N, Ghosal A, Ma E and Roy P 1998 *Phys. Rev.* **D58** 071301
- [91] Gribov V N and Pontecorvo B 1969 *Phys. Lett.* **B28** 493
- [92] Wolfenstein L 1978 *Phys. Rev.* **D17** 2369–2374
- [93] Mikheev S P and Smirnov A Y 1985 *Sov. J. Nucl. Phys.* **42** 913–917

- [94] Mikheev S P and Smirnov A Y 1986 *Nuovo Cim.* **C9** 17–26
- [95] Eguchi K *et al.* (KamLAND) 2003 *Phys. Rev. Lett.* **90** 021802
- [96] Maki Z, Nakagawa M and Sakata S 1962 *Prog. Theor. Phys.* **28** 870–880
- [97] Schechter J and Valle J W F 1980 *Phys. Rev.* **D22** 2227
- [98] Chau L L and Keung W Y 1984 *Phys. Rev. Lett.* **53** 1802
- [99] Eidelman S *et al.* (Particle Data Group) 2004 *Phys. Lett.* **B592** 1
- [100] Harrison P F, Perkins D H and Scott W G 2002 *Phys. Lett.* **B530** 167
- [101] Harrison P F, Perkins D H and Scott W G 1995 *Phys. Lett.* **B349** 137–144
- [102] Altarelli G and Feruglio F 1998 *JHEP* **11** 021
- [103] Barger V D, Pakvasa S, Weiler T J and Whisnant K 1998 *Phys. Lett.* **B437** 107–116
- [104] Baltz A J, Goldhaber A S and Goldhaber M 1998 *Phys. Rev. Lett.* **81** 5730–5733
- [105] Barger V D, Weiler T J and Whisnant K 1998 *Phys. Lett.* **B440** 1–6
- [106] Bjorken J D, Harrison P F and Scott W G 2006 *Phys. Rev.* **D74** 073012
- [107] Mohapatra R N and Nussinov S 1999 *Phys. Rev.* **D60** 013002
- [108] Ardellier F *et al.* (Double Chooz) 2006 (*Preprint* hep-ex/0606025)
- [109] Guo X *et al.* (Daya-Bay) 2007 (*Preprint* hep-ex/0701029)
- [110] Fogli G L, Lisi E, Marrone A, Palazzo A and Rotunno A M 2008 *Phys. Rev. Lett.* **101** 141801
- [111] Schwetz T, Tortola M A and Valle J W F 2008 *New J. Phys.* **10** 113011
- [112] Maltoni M and Schwetz T 2008 *PoS IDM2008* 072
- [113] Gonzalez-Garcia M C, Maltoni M and Salvado J 2010 *JHEP* **04** 056
- [114] Mezzetto M 2009 (*Preprint* 0905.2842)
- [115] Abe K *et al.* (T2K) 2011 *Phys. Rev. Lett.* **107** 041801
- [116] Arpesella C *et al.* (The Borexino) 2008 *Phys. Rev. Lett.* **101** 091302
- [117] Apollonio M *et al.* (CHOOZ) 1999 *Phys. Lett.* **B466** 415–430
- [118] Apollonio M *et al.* (CHOOZ) 2003 *Eur. Phys. J.* **C27** 331–374
- [119] Ardellier F *et al.* 2004 (*Preprint* hep-ex/0405032)
- [120] Abe S *et al.* (KamLAND) 2008 *Phys. Rev. Lett.* **100** 221803
- [121] Gando A *et al.* (The KamLAND) 2011 *Phys. Rev.* **D83** 052002
- [122] Wendell R *et al.* (Kamiokande) 2010 *Phys. Rev.* **D81** 092004
- [123] Abe K *et al.* (Super-Kamiokande) 2011 *Phys. Rev.* **D83** 052010
- [124] Ahn M H *et al.* (K2K) 2006 *Phys. Rev.* **D74** 072003
- [125] Adamson P *et al.* (MINOS) 2008 *Phys. Rev. Lett.* **101** 131802
- [126] Adamson P *et al.* (The MINOS) 2011 *Phys. Rev. Lett.* **106** 181801
- [127] Kirsten T A (GNO) 2003 *Nucl. Phys. Proc. Suppl.* **118** 33–38

- [128] Altmann M *et al.* (GNO) 2005 *Phys. Lett.* **B616** 174–190
- [129] Aharmim B *et al.* (SNO) 2010 *Phys. Rev.* **C81** 055504
- [130] Ahn J K *et al.* (RENO) 2010 (*Preprint* 1003.1391)
- [131] Acquafredda R *et al.* (OPERA) 2006 *New J. Phys.* **8** 303
- [132] Acquafredda R *et al.* 2009 *JINST* **4** P04018
- [133] Schwetz T, Tortola M and Valle J W F 2011 *New J. Phys.* **13** 063004
- [134] Bonn J *et al.* 2001 *Nucl. Phys. Proc. Suppl.* **91** 273–279
- [135] Kraus C *et al.* 2005 *Eur. Phys. J.* **C40** 447–468
- [136] Belesev A I *et al.* 1995 *Phys. Lett.* **B350** 263–272
- [137] Lobashev V M *et al.* 2001 *Nucl. Phys. Proc. Suppl.* **91** 280–286
- [138] Osipowicz A *et al.* (KATRIN) 2001 (*Preprint* hep-ex/0109033)
- [139] Lobashev V M 2003 *Nucl. Phys.* **A719** 153–160
- [140] Kurie F N D, Richardson J R and Paxton H C 1936 *Phys. Rev.* **49** 368–381
- [141] Beshtoev K M 2009 *Phys. Part. Nucl. Lett.* **6** 397–402
- [142] Baudis L *et al.* 1999 *Phys. Rev. Lett.* **83** 41–44
- [143] Klapdor-Kleingrothaus H V, Krivosheina I V, Dietz A and Chkvorets O 2004 *Phys. Lett.* **B586** 198–212
- [144] Klapdor-Kleingrothaus H V and Krivosheina I V 2006 *Mod. Phys. Lett.* **A21** 1547–1566
- [145] Arnaboldi C *et al.* (CUORICINO) 2008 *Phys. Rev.* **C78** 035502
- [146] Gornea R (EXO) 2010 *J. Phys. Conf. Ser.* **259** 012039
- [147] Smolnikov A A (GERDA) 2008 (*Preprint* 0812.4194)
- [148] Schechter J and Valle J W F 1982 *Phys. Rev.* **D25** 2951
- [149] Hirsch M, Klapdor-Kleingrothaus H V and Kovalenko S G 1996 *Phys. Rev.* **D53** 1329–1348
- [150] Gershtein S S and Zeldovich Y B 1966 *JETP Lett.* **4** 120–122
- [151] Cowsik R and McClelland J 1972 *Phys. Rev. Lett.* **29** 669–670
- [152] Szalay A S and Marx G 1976 *Astron. Astrophys.* **49** 437–441
- [153] Komatsu E *et al.* (WMAP) 2009 *Astrophys. J. Suppl.* **180** 330–376
- [154] Dunkley J *et al.* (WMAP) 2009 *Astrophys. J. Suppl.* **180** 306–329
- [155] Hinshaw G *et al.* (WMAP) 2009 *Astrophys. J. Suppl.* **180** 225–245
- [156] Komatsu E *et al.* (WMAP) 2011 *Astrophys. J. Suppl.* **192** 18
- [157] Larson D *et al.* 2011 *Astrophys. J. Suppl.* **192** 16
- [158] Jarosik N *et al.* 2011 *Astrophys. J. Suppl.* **192** 14
- [159] Fiorini E Prepared for 3rd International Workshop on NO-VE: Neutrino Oscillations in Venice: 50 Years after the Neutrino Experimental Discovery, Venice, Italy, 7-10 Feb 2006
- [160] Kayser B 2009 *J. Phys. Conf. Ser.* **173** 012013

- [161] Majorana E 1937 *Nuovo Cim.* **14** 171–184
- [162] Dirac P A M 1928 *Proc. Roy. Soc. Lond.* **A117** 610–624
- [163] Bernstein J, Ruderman M and Feinberg G 1963 *Phys. Rev.* **132** 1227–1233
- [164] Okun L B, Voloshin M B and Vysotsky M I 1986 *Sov. J. Nucl. Phys.* **44** 440
- [165] Schechter J and Valle J W F 1981 *Phys. Rev.* **D24** 1883–1889
- [166] Nieves J F 1982 *Phys. Rev.* **D26** 3152
- [167] Kayser B 1982 *Phys. Rev.* **D26** 1662
- [168] Shrock R E 1982 *Nucl. Phys.* **B206** 359
- [169] Babu K S and Mathur V S 1987 *Phys. Lett.* **B196** 218
- [170] Raffelt G G 1999 *Phys. Rept.* **320** 319–327
- [171] Gelmini G B and Roncadelli M 1981 *Phys. Lett.* **B99** 411
- [172] Chikashige Y, Mohapatra R N and Peccei R D 1981 *Phys. Lett.* **B98** 265
- [173] Georgi H M, Glashow S L and Nussinov S 1981 *Nucl. Phys.* **B193** 297
- [174] Weinberg S 1979 *Phys. Rev. Lett.* **43** 1566–1570
- [175] Weinberg S 1980 *Phys. Rev.* **D22** 1694
- [176] Minkowski P 1977 *Phys. Lett.* **B67** 421
- [177] Yanagida T In Proceedings of the Workshop on the Baryon Number of the Universe and Unified Theories, Tsukuba, Japan, 13-14 Feb 1979
- [178] Glashow S L 1980 *NATO Adv. Study Inst. Ser. B Phys.* **59** 687
- [179] Mohapatra R N and Senjanovic G 1980 *Phys. Rev. Lett.* **44** 912
- [180] Gell-Mann M, Ramond P and Slansky R Print-80-0576 (CERN)
- [181] Schechter J and Valle J W F 1982 *Phys. Rev.* **D25** 774
- [182] Konetschny W and Kummer W 1977 *Phys. Lett.* **B70** 433
- [183] Magg M and Wetterich C 1980 *Phys. Lett.* **B94** 61
- [184] Lazarides G, Shafi Q and Wetterich C 1981 *Nucl. Phys.* **B181** 287
- [185] Cheng T P and Li L F 1980 *Phys. Rev.* **D22** 2860
- [186] Mohapatra R N and Senjanovic G 1981 *Phys. Rev.* **D23** 165
- [187] Foot R, Lew H, He X G and Joshi G C 1989 *Z. Phys.* **C44** 441
- [188] Ma E 1998 *Phys. Rev. Lett.* **81** 1171–1174
- [189] Keung W Y and Senjanovic G 1983 *Phys. Rev. Lett.* **50** 1427
- [190] Hall L J and Suzuki M 1984 *Nucl. Phys.* **B231** 419
- [191] Lee I H 1984 *Phys. Lett.* **B138** 121
- [192] Lee I H 1984 *Nucl. Phys.* **B246** 120
- [193] Dawson S 1985 *Nucl. Phys.* **B261** 297

- [194] Dimopoulos S and Hall L J 1988 *Phys. Lett.* **B207** 210
- [195] Fukugita M and Yanagida T 1986 *Phys. Lett.* **B174** 45
- [196] Luty M A 1992 *Phys. Rev.* **D45** 455–465
- [197] Buchmuller W, Di Bari P and Plumacher M 2005 *Ann. Phys.* **315** 305–351
- [198] Davidson S, Nardi E and Nir Y 2008 *Phys. Rept.* **466** 105–177
- [199] Mohapatra R N and Valle J W F 1986 *Phys. Rev.* **D34** 1642
- [200] Malinsky M, Romao J C and Valle J W F 2005 *Phys. Rev. Lett.* **95** 161801
- [201] Mohapatra R N 1986 *Phys. Rev. Lett.* **56** 561–563
- [202] Wetterich C 1981 *Nucl. Phys.* **B187** 343
- [203] Wetterich C 1999 *Phys. Lett.* **B451** 397–405
- [204] Antusch S and King S F 2005 *Nucl. Phys.* **B705** 239–268
- [205] Chen S L, Frigerio M and Ma E 2005 *Nucl. Phys.* **B724** 423–431
- [206] Pati J C and Salam A 1974 *Phys. Rev.* **D10** 275–289
- [207] Mohapatra R N and Pati J C 1975 *Phys. Rev.* **D11** 2558
- [208] Senjanovic G and Mohapatra R N 1975 *Phys. Rev.* **D12** 1502
- [209] Senjanovic G 1979 *Nucl. Phys.* **B153** 334
- [210] Zee A 1980 *Phys. Lett.* **B93** 389
- [211] Zee A 1986 *Nucl. Phys.* **B264** 99
- [212] Babu K S 1988 *Phys. Lett.* **B203** 132
- [213] Branco G C, Grimus W and Lavoura L 1989 *Nucl. Phys.* **B312** 492
- [214] Ma E 2006 *Phys. Rev.* **D73** 077301
- [215] Ma E 2008 *Mod. Phys. Lett.* **A23** 647–652
- [216] Georgi H and Glashow S L 1973 *Phys. Rev.* **D7** 2457–2463
- [217] Cheng T P and Li L F 1978 *Phys. Rev.* **D17** 2375
- [218] Langacker P and London D 1988 *Phys. Rev.* **D38** 907
- [219] Antusch S, Biggio C, Fernandez-Martinez E, Gavela M B and Lopez-Pavon J 2006 *JHEP* **10** 084
- [220] Ma E 2009 *Mod. Phys. Lett.* **A24** 2161–2165
- [221] Wolfenstein L 1981 *Nucl. Phys.* **B186** 147
- [222] Hirsch M and Valle J W F 2004 *New J. Phys.* **6** 76
- [223] Diaz M A, Romao J C and Valle J W F 1998 *Nucl. Phys.* **B524** 23–40
- [224] Borzumati F and Masiero A 1986 *Phys. Rev. Lett.* **57** 961
- [225] Hisano J, Moroi T, Tobe K and Yamaguchi M 1996 *Phys. Rev.* **D53** 2442–2459
- [226] Hisano J, Moroi T, Tobe K, Yamaguchi M and Yanagida T 1995 *Phys. Lett.* **B357** 579–587
- [227] Hirsch M, Klapdor-Kleingrothaus H V and Kovalenko S G 1997 *Phys. Lett.* **B398** 311–314

- [228] Grossman Y and Haber H E 1997 *Phys. Rev. Lett.* **78** 3438–3441
- [229] Hirsch M, Klapdor-Kleingrothaus H V and Kovalenko S G 1998 *Phys. Rev.* **D57** 1947–1961
- [230] Davidson S and King S F 1998 *Phys. Lett.* **B445** 191–198
- [231] Aulakh C S, Melfo A, Rasin A and Senjanovic G 1999 *Phys. Lett.* **B459** 557–562
- [232] Casas J A, Espinosa J R, Ibarra A and Navarro I 2000 *Nucl. Phys.* **B569** 82–106
- [233] Arkani-Hamed N, Hall L J, Murayama H, Tucker-Smith D and Weiner N 2001 *Phys. Rev.* **D64** 115011
- [234] Das D and Roy S 2010 *Phys. Rev.* **D82** 035002
- [235] Aoki M, Kanemura S, Shindou T and Yagyu K 2010 *JHEP* **07** 084
- [236] Abada A, Bhattacharyya G, Das D and Weiland C 2010 (*Preprint* 1011.5037)
- [237] Joshipura A S and Nowakowski M 1995 *Phys. Rev.* **D51** 2421–2427
- [238] de Campos F, Garcia-Jareno M A, Joshipura A S, Rosiek J and Valle J W F 1995 *Nucl. Phys.* **B451** 3–15
- [239] Banks T, Grossman Y, Nardi E and Nir Y 1995 *Phys. Rev.* **D52** 5319–5325
- [240] Nowakowski M and Pilaftsis A 1996 *Nucl. Phys.* **B461** 19–49
- [241] Akeroyd A G, Diaz M A, Ferrandis J, Garcia-Jareno M A and Valle J W F 1998 *Nucl. Phys.* **B529** 3–22
- [242] Faessler A, Kovalenko S and Simkovic F 1998 *Phys. Rev.* **D58** 055004
- [243] Hirsch M and Valle J W F 1999 *Nucl. Phys.* **B557** 60–78
- [244] Chang C H and Feng T F 2000 *Eur. Phys. J.* **C12** 137–160
- [245] Datta A, Mukhopadhyaya B and Roy S 2000 *Phys. Rev.* **D61** 055006
- [246] Diaz M A, Ferrandis J, Romao J C and Valle J W F 2000 *Nucl. Phys.* **B590** 3–18
- [247] Aulakh C S, Bajc B, Melfo A, Rasin A and Senjanovic G 2001 *Nucl. Phys.* **B597** 89–109
- [248] Restrepo D, Porod W and Valle J W F 2001 *Phys. Rev.* **D64** 055011
- [249] Abada A and Moreau G 2006 *JHEP* **08** 044
- [250] Abada A, Bhattacharyya G and Moreau G 2006 *Phys. Lett.* **B642** 503–509
- [251] Ellis J R, Gelmini G, Jarlskog C, Ross G G and Valle J W F 1985 *Phys. Lett.* **B150** 142
- [252] Barbieri R, Guzzo M M, Masiero A and Tommasini D 1990 *Phys. Lett.* **B252** 251–255
- [253] Enqvist K, Masiero A and Riotto A 1992 *Nucl. Phys.* **B373** 95–116
- [254] Hempfling R 1996 *Nucl. Phys.* **B478** 3–30
- [255] de Carlos B and White P L 1996 *Phys. Rev.* **D54** 3427–3446
- [256] Borzumati F, Grossman Y, Nardi E and Nir Y 1996 *Phys. Lett.* **B384** 123–130
- [257] Nilles H P and Polonsky N 1997 *Nucl. Phys.* **B484** 33–62
- [258] Nardi E 1997 *Phys. Rev.* **D55** 5772–5779
- [259] Roy S and Mukhopadhyaya B 1997 *Phys. Rev.* **D55** 7020–7029

- [260] Drees M, Pakvasa S, Tata X and ter Veldhuis T 1998 *Phys. Rev.* **D57** 5335–5339
- [261] Chun E J, Kang S K, Kim C W and Lee U W 1999 *Nucl. Phys.* **B544** 89–103
- [262] Bednyakov V, Faessler A and Kovalenko S 1998 *Phys. Lett.* **B442** 203–208
- [263] Ferrandis J 1999 *Phys. Rev.* **D60** 095012
- [264] Grossman Y and Haber H E 1999 *Phys. Rev.* **D59** 093008
- [265] Chun E J and Lee J S 1999 *Phys. Rev.* **D60** 075006
- [266] Rakshit S, Bhattacharyya G and Raychaudhuri A 1999 *Phys. Rev.* **D59** 091701
- [267] Kaplan D E and Nelson A E 2000 *JHEP* **01** 033
- [268] Ma E, Raidal M and Sarkar U 1999 *Phys. Lett.* **B460** 359–364
- [269] Joshipura A S and Vempati S K 1999 *Phys. Rev.* **D60** 111303
- [270] Choi S Y, Chun E J, Kang S K and Lee J S 1999 *Phys. Rev.* **D60** 075002
- [271] Grossman Y and Haber H E 1999 (*Preprint hep-ph/9906310*)
- [272] Romao J C, Diaz M A, Hirsch M, Porod W and Valle J W F 2000 *Phys. Rev.* **D61** 071703
- [273] Abada A and Losada M 2000 *Nucl. Phys.* **B585** 45–78
- [274] Haug O, Vergados J D, Faessler A and Kovalenko S 2000 *Nucl. Phys.* **B565** 38–48
- [275] Chun E J and Kang S K 2000 *Phys. Rev.* **D61** 075012
- [276] Takayama F and Yamaguchi M 2000 *Phys. Lett.* **B476** 116–123
- [277] Davidson S, Losada M and Rius N 2000 *Nucl. Phys.* **B587** 118–146
- [278] Adhikari R and Omanovic G 1999 *Phys. Rev.* **D59** 073003
- [279] Hirsch M, Romao J C and Valle J W F 2000 *Phys. Lett.* **B486** 255–262
- [280] Hirsch M, Diaz M A, Porod W, Romao J C and Valle J W F 2000 *Phys. Rev.* **D62** 113008
- [281] Davidson S and Losada M 2000 *JHEP* **05** 021
- [282] Grossman Y and Haber H E 2001 *Phys. Rev.* **D63** 075011
- [283] Abada A and Losada M 2000 *Phys. Lett.* **B492** 310–320
- [284] Mira J M, Nardi E, Restrepo D A and Valle J W F 2000 *Phys. Lett.* **B492** 81–90
- [285] Davidson S and Losada M 2002 *Phys. Rev.* **D65** 075025
- [286] Porod W, Hirsch M, Romao J and Valle J W F 2001 *Phys. Rev.* **D63** 115004
- [287] Joshipura A S, Vaidya R D and Vempati S K 2002 *Phys. Rev.* **D65** 053018
- [288] Barger V D, Han T, Hesselbach S and Marfatia D 2002 *Phys. Lett.* **B538** 346–352
- [289] Abada A, Davidson S and Losada M 2002 *Phys. Rev.* **D65** 075010
- [290] Joshipura A S, Vaidya R D and Vempati S K 2002 *Nucl. Phys.* **B639** 290–306
- [291] Chun E J, Jung D W, Kang S K and Park J D 2002 *Phys. Rev.* **D66** 073003
- [292] Borzumati F and Lee J S 2002 *Phys. Rev.* **D66** 115012
- [293] Abada A, Bhattacharyya G and Losada M 2002 *Phys. Rev.* **D66** 071701

- [294] Chun E J, Jung D W and Park J D 2003 *Phys. Lett.* **B557** 233–239
- [295] Diaz M A, Hirsch M, Porod W, Romao J C and Valle J W F 2003 *Phys. Rev.* **D68** 013009
- [296] Grossman Y and Rakshit S 2004 *Phys. Rev.* **D69** 093002
- [297] Rakshit S 2004 *Mod. Phys. Lett.* **A19** 2239–2258
- [298] Jung D W, Kang S K, Park J D and Chun E J 2004 *JHEP* **08** 017
- [299] Chun E J and Park S C 2005 *JHEP* **01** 009
- [300] Chemtob M and Pandita P N 2006 *Phys. Rev.* **D73** 055012
- [301] Dedes A, Rimmer S and Rosiek J 2006 *JHEP* **08** 005
- [302] Mukhopadhyaya B and Srikanth R 2006 *Phys. Rev.* **D74** 075001
- [303] Chun E J and Kim H B 2006 *JHEP* **10** 082
- [304] Dedes A, Haber H E and Rosiek J 2007 *JHEP* **11** 059
- [305] Dey P, Kundu A, Mukhopadhyaya B and Nandi S 2008 *JHEP* **12** 100
- [306] Hundi R S, Pakvasa S and Tata X 2009 *Phys. Rev.* **D79** 095011
- [307] Jean-Louis C C and Moreau G 2010 *J. Phys.* **G37** 105015
- [308] Romao J C and Valle J W F 1992 *Nucl. Phys.* **B381** 87–108
- [309] Nogueira P, Romao J C and Valle J W F 1990 *Phys. Lett.* **B251** 142–149
- [310] Romao J C, Rius N and Valle J W F 1991 *Nucl. Phys.* **B363** 369–384
- [311] Giudice G F, Masiero A, Pietroni M and Riotto A 1993 *Nucl. Phys.* **B396** 243–260
- [312] Kitano R and Oda K y 2000 *Phys. Rev.* **D61** 113001
- [313] Frank M, Huitu K and Ruppell T 2007 *Eur. Phys. J.* **C52** 413–423
- [314] Hirsch M, Vicente A and Porod W 2008 *Phys. Rev.* **D77** 075005
- [315] Mitra M 2010 *JHEP* **11** 026
- [316] Ross G G and Valle J W F 1985 *Phys. Lett.* **B151** 375
- [317] Santamaria A and Valle J W F 1987 *Phys. Lett.* **B195** 423
- [318] Umemura I and Yamamoto K 1994 *Nucl. Phys.* **B423** 405–436
- [319] Barger V D, Giudice G F and Han T 1989 *Phys. Rev.* **D40** 2987
- [320] Barbieri R, Brahm D E, Hall L J and Hsu S D H 1990 *Phys. Lett.* **B238** 86
- [321] Gonzalez-Garcia M C, Romao J C and Valle J W F 1993 *Nucl. Phys.* **B391** 100–126
- [322] Dreiner H K and Ross G G 1991 *Nucl. Phys.* **B365** 597–613
- [323] Godbole R M, Roy P and Tata X 1993 *Nucl. Phys.* **B401** 67–92
- [324] Butterworth J and Dreiner H K 1993 *Nucl. Phys.* **B397** 3–34
- [325] Bhattacharyya G, Ellis J R and Sridhar K 1995 *Mod. Phys. Lett.* **A10** 1583–1592
- [326] Bhattacharyya G, Choudhury D and Sridhar K 1995 *Phys. Lett.* **B355** 193–198
- [327] Adhikari R and Mukhopadhyaya B 1996 *Phys. Lett.* **B378** 342–346

- [328] Choudhury D and Roy P 1996 *Phys. Lett.* **B378** 153–158
- [329] Kim J E, Ko P and Lee D G 1997 *Phys. Rev.* **D56** 100–106
- [330] Choudhury D and Raychaudhuri S 1997 *Phys. Lett.* **B401** 54–61
- [331] Mukhopadhyaya B, Roy S and Vissani F 1998 *Phys. Lett.* **B443** 191–195
- [332] Diaz M A, Torrente-Lujan E and Valle J W F 1999 *Nucl. Phys.* **B551** 78–92
- [333] Bisset M, Kong O C W, Macesanu C and Orr L H 2000 *Phys. Rev.* **D62** 035001
- [334] Mukhopadhyaya B and Roy S 1999 *Phys. Rev.* **D60** 115012
- [335] Ghosh D K, Godbole R M and Raychaudhuri S 1999 (*Preprint hep-ph/9904233*)
- [336] Allanach B *et al.* (R parity Working Group) 1999
- [337] Datta A, Gandhi R, Mukhopadhyaya B and Mehta P 2001 *Phys. Rev.* **D64** 015011
- [338] Saha J P and Kundu A 2002 *Phys. Rev.* **D66** 054021
- [339] Hirsch M and Porod W 2003 *Phys. Rev.* **D68** 115007
- [340] Datta A and Poddar S 2007 *Phys. Rev.* **D75** 075013
- [341] Arhrib A *et al.* 2010 *Phys. Rev.* **D82** 053004
- [342] Bandyopadhyay P, Choubey S and Mitra M 2009 *JHEP* **10** 012
- [343] Fileviez Perez P, Han T and Li T 2009 *Phys. Rev.* **D80** 073015
- [344] Nath P *et al.* 2010 *Nucl. Phys. Proc. Suppl.* **200-202** 185–417
- [345] De Campos F *et al.* 2010 *Phys. Rev.* **D82** 075002
- [346] Aulakh C S and Mohapatra R N 1982 *Phys. Lett.* **B119** 136
- [347] Nieves J F 1984 *Phys. Lett.* **B137** 67
- [348] Santamaria A and Valle J W F 1989 *Phys. Rev.* **D39** 1780–1783
- [349] Santamaria A and Valle J W F 1988 *Phys. Rev. Lett.* **60** 397–400
- [350] Adeva B *et al.* (L3) 1989 *Phys. Lett.* **B231** 509
- [351] Decamp D *et al.* (ALEPH) 1989 *Phys. Lett.* **B231** 519
- [352] Akrawy M Z *et al.* (OPAL) 1989 *Phys. Lett.* **B231** 530
- [353] Aarnio P A *et al.* (Delphi) 1989 *Phys. Lett.* **B231** 539
- [354] Fukugita M, Watamura S and Yoshimura M 1982 *Phys. Rev. Lett.* **48** 1522
- [355] Raffelt G G Chicago, USA: Univ. Pr. (1996) 664 p
- [356] Kachelriess M, Tomas R and Valle J W F 2000 *Phys. Rev.* **D62** 023004
- [357] Gonzalez-Garcia M C and Nir Y 1989 *Phys. Lett.* **B232** 383
- [358] Romao J C and Nogueira P 1990 *Phys. Lett.* **B234** 371
- [359] Masiero A and Valle J W F 1990 *Phys. Lett.* **B251** 273–278
- [360] Romao J C, Santos C A and Valle J W F 1992 *Phys. Lett.* **B288** 311–320
- [361] Hirsch M, Romao J C, Valle J W F and Villanova del Moral A 2004 *Phys. Rev.* **D70** 073012

- [362] Hirsch M, Romao J C, Valle J W F and Villanova del Moral A 2006 *Phys. Rev.* **D73** 055007
- [363] Hirsch M and Porod W 2006 *Phys. Rev.* **D74** 055003
- [364] Hirsch M, Vicente A, Meyer J and Porod W 2009 *Phys. Rev.* **D79** 055023
- [365] Bhattacharyya G and Pal P B 2010 *Phys. Rev.* **D82** 055013
- [366] Haber H E and Kane G L 1985 *Phys. Rept.* **117** 75–263
- [367] Gunion J F and Haber H E 1986 *Nucl. Phys.* **B272** 1
- [368] Rosiek J 1990 *Phys. Rev.* **D41** 3464
- [369] Rosiek J 1995 (*Preprint* hep-ph/9511250)
- [370] Davidson S and Ellis J R 1997 *Phys. Lett.* **B390** 210–220
- [371] Davidson S and Ellis J R 1997 *Phys. Rev.* **D56** 4182–4193
- [372] Davidson S 1998 *Phys. Lett.* **B439** 63–70
- [373] Bartl A, Porod W, Restrepo D, Romao J and Valle J W F 2001 *Nucl. Phys.* **B600** 39–61
- [374] Hirsch M, Porod W, Romao J C and Valle J W F 2002 *Phys. Rev.* **D66** 095006
- [375] Bartl A, Hirsch M, Kernreiter T, Porod W and Valle J W F 2003 *JHEP* **11** 005
- [376] Bartl A, Hirsch M, Kernreiter T, Porod W and Valle J W F LC-TH-2003-047
- [377] Wolfram S 1979 *Phys. Lett.* **B82** 65
- [378] Dover C B, Gaisser T K and Steigman G 1979 *Phys. Rev. Lett.* **42** 1117
- [379] Ellis J R, Hagelin J S, Nanopoulos D V, Olive K A and Srednicki M 1984 *Nucl. Phys.* **B238** 453–476
- [380] Feng J L, Moroi T, Randall L, Strassler M and Su S f 1999 *Phys. Rev. Lett.* **83** 1731–1734
- [381] Raby S 1998 *Phys. Lett.* **B422** 158–162
- [382] Baer H, Cheung K m and Gunion J F 1999 *Phys. Rev.* **D59** 075002
- [383] Raby S and Tobe K 1999 *Nucl. Phys.* **B539** 3–22
- [384] Hagelin J S, Kane G L and Raby S 1984 *Nucl. Phys.* **B241** 638

Chapter 4

$\mu\nu$ SSM: neutrino masses and mixing

4.1 Introducing $\mu\nu$ SSM

As discussed earlier, the minimal supersymmetric standard model (MSSM) is not free from drawbacks. We have addressed these issues in the context of the μ -problem [1] and light neutrino mass generation. Supersymmetric theories can accommodate massive neutrinos either through \mathcal{R}_p or using seesaw mechanism. Regarding the μ -problem, as discussed in section 2.9, a simple solution is given by the NMSSM. There exist a host of NMSSM models where the superpotential contains either explicit R_p -violating couplings [2–8] or use spontaneous violation of R_p [9] to accommodate light neutrino masses apart from offering a solution to the μ -problem. Unfortunately, NMSSM models of neutrino mass generation with bR_pV suffer from the ϵ -problem [10]. Besides, with bilinear \mathcal{R}_p not all the neutrino masses are generated at the tree level. Thus loop corrections are unavoidable to account for the three flavour oscillation data. Loop effects are compulsory for models with tR_pV where all of the neutrino masses appear at loop level. Certainly, larger number of trilinear couplings reduce the predictability of these models. An elegant alternative is given by NMSSM models with spontaneous \mathcal{R}_p where apart from a singlet superfield, \hat{S} (to solve the μ -problem) one requires a right-handed neutrino superfield, $\hat{\nu}^c$ to accommodate massive neutrinos. The issues of light neutrino mass generation together with a solution to the μ -problem in R_p -conserving NMSSM models have been addressed in references [11–13].

So, in a nutshell, the well-known NMSSM models of neutrino mass generation either suffer from the naturalness problem or are less predictive due to the presence of either large number of couplings or additional superfields. Now following the structure of the SM it seems rather natural to add right-handed neutrino superfields with the MSSM superfields in order to generate neutrino masses. Also being a SM gauge singlet, a right-handed neutrino superfield, $\hat{\nu}^c$ can act as a viable alternative for the singlet field (\hat{S}) of NMSSM used to solve the μ -problem.

The novel idea of solving the μ -problem and light neutrino mass generation simultaneously in a supersymmetric model using *only* right-handed neutrino superfields, $\hat{\nu}_i^c$ was advocated in ref. [14]. This model is popularly known as the “ μ from ν ” *supersymmetric standard model* or $\mu\nu$ SSM [14]. Details of this model will be provided in the next sub-section.

In this chapter we plan to discuss the $\mu\nu$ SSM model first with necessary details like neutral scalar potential, minimization conditions, scalar sector, fermionic sector etc. and later we aim to discuss the issues of light neutrino masses and mixing in the $\mu\nu$ SSM at the tree level as well as with one-loop radiative corrections.

4.2 The model

In this section we introduce the model along the lines of ref. [14], discuss its basic features and set our notations. Throughout this thesis we consider three generations of right-handed neutrino superfield ($\hat{\nu}_i^c$) apart from the MSSM superfields as proposed in ref. [14]. We start with the model superpotential and the soft terms and continue our discussion with the minimization conditions later.

✦ *Superpotential*

The $\mu\nu$ SSM superpotential is given by

$$W^{\mu\nu SSM} = W'^{MSSM} + \epsilon_{ab} Y_\nu^{ij} \hat{H}_u^b \hat{L}_i^a \hat{\nu}_j^c - \underbrace{\epsilon_{ab} \lambda^i \hat{\nu}_i^c \hat{H}_d^a \hat{H}_u^b}_{\Delta L=1} + \overbrace{\frac{1}{3} \kappa^{ijk} \hat{\nu}_i^c \hat{\nu}_j^c \hat{\nu}_k^c}_{\Delta L=3}, \quad (4.1)$$

where W'^{MSSM} is the MSSM superpotential (see eqns.(2.36), (2.55)) but without the $\epsilon_{ab} \mu \hat{H}_d^a \hat{H}_u^b$ -term. The superfields $\hat{H}_d, \hat{H}_u, \hat{L}_i$ are usual MSSM down-type Higgs, up-type Higgs and $SU(2)_L$ doublet lepton superfields. Since right-handed neutrinos carry a non-zero lepton number, the third and fourth terms of eqn.(4.1) violate lepton number by odd unit(s) (*one* and *three*, respectively). Violation of lepton number by odd units is the source of \mathcal{R}_p (eqn.(2.52)) is $\mu\nu$ SSM.

It is important to mention the implications of different terms of eqn.(4.1) at this stage.

- The second term $\epsilon_{ab} Y_\nu^{ij} \hat{H}_u^b \hat{L}_i^a \hat{\nu}_j^c$ respects lepton number conservation to start with. However, after EWSB these terms give rise to effective bilinear R_p -violating terms as $\epsilon^i L_i H_u$ with $\epsilon^i = Y_\nu^{ij} v_j^c$. v_j^c denotes the VEV acquired by j -th right-handed sneutrino. Besides, a term of this kind also give rise to Dirac neutrino mass matrix with entries as $m_{D_{ij}} = Y_\nu^{ij} v_2$.
- The third term $\epsilon_{ab} \lambda^i \hat{\nu}_i^c \hat{H}_d^a \hat{H}_u^b$ after EWSB generates an effective μ -term as $\mu = \sum \lambda_i v_i^c$. This term violates lepton number by one unit.
- The last term $\frac{1}{3} \kappa^{ijk} \hat{\nu}_i^c \hat{\nu}_j^c \hat{\nu}_k^c$ violates lepton number by three units. Note that this term is allowed by all possible symmetry arguments. Now if $\kappa^{ijk} = 0$ to start with then the Lagrangian has a global $U(1)$ symmetry which is broken spontaneously by the VEVs of the scalar fields and leads to unacceptable massless axion. In order to avoid axions non-zero values for κ^{ijk} are essential [15]. Besides, after EWSB the last term of eqn.(4.1) produces entries for the right-handed neutrino Majorana mass matrix as $m_{\nu_{ij}^c} = 2\kappa^{ijk} v_k^c$.
- As already mentioned, a Z_3 symmetry is imposed on the $\mu\nu$ SSM superpotential (eqn.(4.1)) to forbid appearance of any bilinear term. This feature is similar to the NMSSM models as stated in section 2.9. Thus similar to the NMSSM, the $\mu\nu$ SSM also suffers from the problem of cosmological domain wall formation [16–18]. However, the problem can be ameliorated through well known methods [19–21].
- The conventional trilinear couplings $\lambda^{ijk}, \lambda^{ijk}$ (see eqn.(2.50)) can be generated in $\mu\nu$ SSM at one-loop level as shown in figure 4.1 [22].

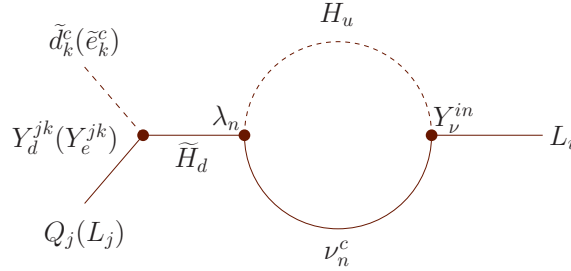


Figure 4.1: One-loop generation of the $\lambda^{ijk}, \lambda^{ijk}$ terms in the superpotential. These terms are proportional to product of two Yukawa couplings and λ . Product of two Yukawa couplings assures smallness of the $\lambda^{ijk}, \lambda^{ijk}$ couplings.

A term of the type $Y_\nu L H_u \nu^c$ has been considered also in ref. [23] in the context of light neutrino mass generation, but without offering any attempts to solve the μ -problem. In ref. [24] couplings of the form $Y_\nu L H_u \nu^c$ and $\lambda H_d H_u \nu^c$ were considered along with Majorana mass terms $\frac{1}{2} M^{ij} \nu_i^c \nu_j^c$ for right-handed neutrinos. However, in this case the contribution of $\lambda H_d H_u \nu^c$ for generating the μ -term is negligible because the right-handed sneutrinos ($\tilde{\nu}_i^c$), being super heavy, do not acquire sizable vacuum expectation values. In reference [24] the term $\lambda H_d H_u \nu^c$ has been utilized for the purpose of thermal seesaw leptogenesis.

✦ *Soft terms*

Confining ourselves in the framework of supergravity mediated supersymmetry breaking, the Lagrangian $\mathcal{L}_{soft}^{\mu\nu SSM}$, containing the soft-supersymmetry-breaking terms is given by

$$\begin{aligned} -\mathcal{L}_{soft}^{\mu\nu SSM} &= -\mathcal{L}'_{soft}{}^{MSSM} + (m_{\tilde{\nu}^c}^2)^{ij} \tilde{\nu}_i^{c*} \tilde{\nu}_j^c \\ &+ \{\epsilon_{ab} (A_\nu Y_\nu)^{ij} H_u^b \tilde{L}_i^a \tilde{\nu}_j^c - \epsilon_{ab} (A_\lambda \lambda)^i \tilde{\nu}_i^c H_d^a H_u^b \\ &+ \frac{1}{3} (A_\kappa \kappa)^{ijk} \tilde{\nu}_i^c \tilde{\nu}_j^c \tilde{\nu}_k^c + h.c.\}, \end{aligned} \quad (4.2)$$

where $\mathcal{L}'_{soft}{}^{MSSM}$ denotes $\mathcal{L}_{soft}^{MSSM}$ without the B_μ term (see eqn.(2.37)). $(m_{\tilde{\nu}^c}^2)^{ij}$ denote soft square masses for right-handed sneutrinos.

✂ Scalar potential and minimization

The tree-level scalar potential receives the usual D and F term (see eqn.(2.38), where $\left| \frac{\partial W^{\mu\nu SSM}}{\partial \phi^{\mu\nu SSM}} \right|^2 \equiv F^*F$ with ϕ as any superfields of the $\mu\nu SSM$) contributions, in addition to the terms from $\mathcal{L}_{soft}^{\mu\nu SSM}$. We adhere to the CP -preserving case, so that only the real parts of the neutral scalar fields develop, in general, the following VEVs,

$$\langle H_d^0 \rangle = v_1, \quad \langle H_u^0 \rangle = v_2, \quad \langle \tilde{\nu}_i \rangle = v'_i, \quad \langle \tilde{\nu}_i^c \rangle = v_i^c. \quad (4.3)$$

In eqn.(4.3) $i = 1, 2, 3 \equiv e, \mu, \tau$. The tree level neutral scalar potential looks like [14, 22, 25–27]

$$\begin{aligned} \langle V_{\text{neutral}} \rangle &= \left| \sum_{i,j} Y_\nu^{ij} v'_i v_j^c - \sum_i \lambda^i v_i^c v_1 \right|^2 \\ &+ \sum_j \left| \sum_i Y_\nu^{ij} v'_i v_2 - \lambda^j v_1 v_2 + \sum_{i,k} \kappa^{ijk} v_i^c v_k^c \right|^2 + \left| \sum_i \lambda^i v_i^c v_2 \right|^2 \\ &+ \sum_i \left| \sum_j Y_\nu^{ij} v_2 v_j^c \right|^2 + \left(\frac{g_1^2 + g_2^2}{8} \right) \left[\sum_i |v_i^c|^2 + |v_1|^2 - |v_2|^2 \right]^2 \\ &+ \left[\sum_{i,j} (A_\nu Y_\nu)^{ij} v'_i v_j^c v_2 - \sum_i (A_\lambda \lambda)^i v_i^c v_1 v_2 + \text{H.c.} \right] \\ &+ \left[\sum_{i,j,k} \frac{1}{3} (A_\kappa \kappa)^{ijk} v_i^c v_j^c v_k^c + \text{H.c.} \right] + \sum_{i,j} (m_{\tilde{L}}^2)^{ij} v_i^{c*} v_j^c \\ &+ \sum_{i,j} (m_{\tilde{\nu}^c}^2)^{ij} v_i^{c*} v_j^c + m_{H_u}^2 |v_2|^2 + m_{H_d}^2 |v_1|^2. \end{aligned} \quad (4.4)$$

One important thing is to notice that the potential is bounded from below because the coefficient of the fourth power of all the eight superfields are positive (see eqn.(4.4)). We shall further assume that all the parameters present in the scalar potential are real. From eqn.(4.4), the minimization conditions with respect to v_i^c, v'_i, v_2, v_1 are

$$\begin{aligned} 2 \sum_j u_c^{ij} \zeta^j + \sum_k Y_\nu^{ki} r_c^k v_2^2 + \sum_j (m_{\tilde{\nu}^c}^2)^{ji} v_j^c + \rho^i \eta + \mu \lambda^i v_2^2 + (A_x x)^i &= 0, \\ \sum_j Y_\nu^{ij} v_2 \zeta^j + \sum_j (m_{\tilde{L}}^2)^{ji} v'_j + \sum_j (A_\nu Y_\nu)^{ij} v_j^c v_2 + \gamma_g \xi_v v'_i + r_c^i \eta &= 0, \\ \sum_j \rho^j \zeta^j + \sum_i r_c^{i2} v_2 + \sum_i (A_\nu Y_\nu)^{ij} v'_i v_j^c - \sum_i (A_\lambda \lambda)^i v_i^c v_1 + X^u v_2 &= 0, \\ -\sum_j \lambda^j v_2 \zeta^j - \mu \sum_j r_c^j v'_j - \sum_i (A_\lambda \lambda)^i v_i^c v_2 + X^d v_1 &= 0, \end{aligned} \quad (4.5)$$

with $X^u = m_{H_u}^2 + \mu^2 - \gamma_g \xi_v$, $X^d = m_{H_d}^2 + \mu^2 + \gamma_g \xi_v$ and

$$\begin{aligned}
(A_x x)^i &= \sum_j (A_\nu Y_\nu)^{ji} v'_j v_2 + \sum_{j,k} (A_\kappa \kappa)^{ijk} v_j^c v_k^c - (A_\lambda \lambda)^i v_1 v_2, \\
r_c^i &= \varepsilon^i = \sum_j Y_\nu^{ij} v_j^c, \quad r^i = \sum_j Y_\nu^{ij} v'_j, \quad u_c^{ij} = \sum_k \kappa^{ijk} v_k^c, \\
\zeta^j &= \sum_i u_c^{ij} v_i^c + r^j v_2 - \lambda^j v_1 v_2, \quad \mu = \sum_i \lambda^i v_i^c, \quad \rho^i = r^i - \lambda^i v_1, \\
\eta &= \sum_i r_c^i v'_i - \mu v_1, \quad \gamma_g = \frac{1}{4}(g_1^2 + g_2^2), \quad \xi_v = \sum_i v_i'^2 + v_1^2 - v_2^2.
\end{aligned} \tag{4.6}$$

In deriving the above equations, it has been assumed that κ^{ijk} , $(A_\kappa \kappa)^{ijk}$, Y_ν^{ij} , $(A_\nu Y_\nu)^{ij}$, $(m_{\bar{\nu}c}^2)^{ij}$, $(m_L^2)^{ij}$ are all symmetric in their indices.

It is important to know that now the Majorana masses for right-handed neutrinos ($2\kappa^{ijk} v_k^c$) are at the TeV scale with $\kappa \sim \mathcal{O}(1)$ and TeV scale v_i^c (see first one of eqn.(4.5)). For neutrino Dirac masses ($Y_\nu^{ij} v_2$) $\sim 10^{-4}$ GeV the neutrino Yukawa couplings (Y_ν^{ij}) must also be very small $\sim \mathcal{O}(10^{-7})$, in order to get correct neutrino mass scale using a seesaw mechanism involving TeV scale right-handed neutrino. This immediately tells us that in the limit $Y_\nu^{ij} \rightarrow 0$, (see second one of eqn.(4.5)) $v'_i \rightarrow 0$. So in order to get appropriate neutrino mass scale both Y_ν^{ij} and v'_i have to be small.

Ignoring the terms of the second order in Y_ν^{ij} and considering $(v_1'^2 + v_2^2 - v_2'^2) \approx (v_1^2 - v_2^2)$ (which is a good approximation), and $(m_L^2)^{ij} = (m_L^2) \delta^{ij}$, we can easily solve second one of eqn.(4.5) as (using eqn. (4.6))

$$v'_i \approx - \left\{ \frac{Y_\nu^{ik} u_c^{kj} v_2 - \mu v_1 Y_\nu^{ij} + (A_\nu Y_\nu)^{ij} v_2}{\gamma_g (v_1^2 - v_2^2) + (m_L^2)} \right\} v_j^c + \left\{ \frac{Y_\nu^{ij} \lambda^j v_1 v_2^2}{\gamma_g (v_1^2 - v_2^2) + (m_L^2)} \right\}. \tag{4.7}$$

Note from eqn.(4.7), that the left-handed sneutrinos can acquire, in general, non-vanishing, non-degenerate VEVs even in the limit of zero vacuum expectation values of the gauge singlet sneutrinos [25]. However, zero VEVs of all the three gauge singlet sneutrinos is not an acceptable solution since in that case no μ -term ($\sum \lambda_i v_i^c$) will be generated. It is essential to ensure that the extremum value of the potential corresponds to the minimum of the potential, by studying the second derivatives.

The neutral scalar potential and the minimization conditions in $\mu\nu$ SSM but for complex VEVs, have been discussed in ref. [28] in the context of spontaneous CP violation and its implications in neutrino physics.

4.3 Scalar sector of $\mu\nu$ SSM

It is evident from eqns.(4.1) and (4.2) that lepton number (L) is no longer conserved in $\mu\nu$ SSM. In this situation states having zero lepton number can mix with states having $L \neq 0$. These lepton number violating mixings in turn result in larger (8×8) mass squared matrices for CP -even neutral scalar, CP -odd neutral pseudoscalar and charged scalar states. This is a consequence of the fact that in $\mu\nu$ SSM three generations of left and right-handed sneutrinos can mix with neutral Higgs bosons. In a similar fashion charged sleptons mix with the charged Higgs bosons. The enhancement over the 2×2 MSSM structure (see appendix A) is phenomenologically very rich. Detailed structures for neutral scalar, pseudoscalar and the charged scalar mass squared matrices are given in appendix B. In our numerical analysis we confirm the existence of two charged and one neutral Goldstone boson(s) in the charged scalar and pseudoscalar sector. In addition, we have checked that all the eigenvalues of the scalar, pseudoscalar, and charged scalar mass-squared matrices (apart from the Goldstone bosons) appear to be positive (*non-tachyonic*) for a minima. These matrices are addressed in refs. [22, 25, 26]. In appendix B squark mass squared matrices are also addressed [22, 25].

Before discussing the scalar sector of this model further, it is important to point out the approximation and simplification used for involved numerical analysis. For numerical calculations we assume all

soft-masses, λ^i, κ^{ijk} and the corresponding soft parameters $(A_\lambda \lambda)^i, (A_\kappa \kappa)^{ijk}$ to be flavour diagonal as well as flavour blind. However the neutrino Yukawa couplings (Y_ν^{ij}) and the respective soft parameters $(A_\nu Y_\nu)^{ij}$ are chosen to be flavour diagonal. For simplicity all three right sneutrino VEVs are assumed to be degenerate (v^c). Mathematically,

$$\begin{aligned} \kappa^{ijk} &= \kappa \delta^{ij} \delta^{jk}, & (A_\kappa \kappa)^{ijk} &= (A_\kappa \kappa) \delta^{ij} \delta^{jk}, \\ Y_\nu^{ij} &= Y_\nu^{ii} \delta^{ij}, & (A_\nu Y_\nu)^{ij} &= (A_\nu Y_\nu)^{ii} \delta^{ij}, \\ \lambda^i &= \lambda, & (A_\lambda \lambda)^i &= (A_\lambda \lambda), & v_i^c &= v^c, \\ (m_L^2)^{ij} &= (m_L^2) \delta^{ij}, & (m_{\nu^c}^2)^{ij} &= (m_{\nu^c}^2) \delta^{ij}. \end{aligned} \quad (4.8)$$

Coming back to the scalar sector of the $\mu\nu$ SSM, apart from excluding the corner of parameter space responsible for tachyons, additional constraints on the parameter space can come from the existence of false minima as well as from the perturbativity of the model parameters (free from Landau pole). A detailed discussion on this issue has been presented in ref. [22] and the regions excluded by the existence of false minima have been shown. One can check from these figures that mostly the lower part of the region allowed by the absence of tachyons, are excluded by the existence of false minima. In our analysis, we have chosen the parameter points in such a way that they should be well above the regions disallowed by the existence of false minima. Nevertheless, in the case of gauge-singlet neutrino (ν^c) dominated lightest neutralino (to be discussed in the next chapter), the value of κ that we have chosen is 0.07 with two different values of λ , namely, 0.1 and 0.29. In this case, there is a possibility that these points might fall into the regions disallowed by the existence of false minima. However, we have checked that even if we take the value of κ to be higher (0.2 or so), with appropriately chosen λ , our conclusions do not change much. For such a point in the parameter space, it is likely that the existence of false minima can be avoided.

Let us also mention here that the sign of the μ -term is controlled by the sign of the VEV v^c (assuming a positive λ), which is controlled by the signs of $A_\lambda \lambda$ and $A_\kappa \kappa$. If $A_\lambda \lambda$ is negative and $A_\kappa \kappa$ is positive then the sign of the μ parameter is negative whereas for opposite signs of the above quantities, we get a positive sign for the μ parameter.

The eigenvalues of the scalar mass-squared matrices and the right-handed sneutrino VEVs (v^c) are not very sensitive to the change in neutrino Yukawa couplings ($Y_\nu \sim \mathcal{O}(10^{-7})$) and the corresponding soft parameter $A_\nu Y_\nu$ ($\sim \mathcal{O}(10^{-4})$ GeV). On the other hand, the values of $\tan\beta$ and the coefficients λ and κ are very important in order to satisfy various constraints on the scalar sector mentioned earlier. In figure 4.2, we have plotted the allowed regions in the $(\lambda-\kappa)$ plane for $\tan\beta = 10$ [25]. Relevant parameters are given in table 4.1.

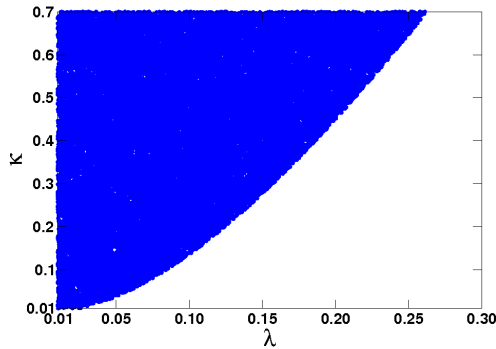


Figure 4.2: Allowed regions in $(\lambda-\kappa)$ plane which satisfy various constraints on the scalar sector, for $\tan\beta = 10$. λ and κ were allowed to vary from 0.005 to 0.50 and 0.005 to 0.70, respectively. Corresponding set of other parameters are given in table 4.1.

The upper limit of the value of κ is taken to be ~ 0.7 because of the constraints coming from the existence of Landau pole [22]. With the values of different parameters satisfying the constraints in the scalar sector (see figure 4.2), we will go on to calculate the neutrino masses and the mixing patterns in the next few sections.

Parameter	Chosen Value	Parameter	Chosen Value
$(A_\lambda\lambda)$	$1000 \times \lambda$ GeV	$(A_\kappa\kappa)$	$1000 \times \kappa$ GeV
Y_ν^{11}	5.0×10^{-7}	$(A_\nu Y_\nu)^{11}$	5.0×10^{-4} GeV
Y_ν^{22}	4.0×10^{-7}	$(A_\nu Y_\nu)^{22}$	4.0×10^{-4} GeV
Y_ν^{33}	3.0×10^{-7}	$(A_\nu Y_\nu)^{33}$	3.0×10^{-4} GeV
$m_{\tilde{L}}^2$	400^2 GeV ²	$m_{\tilde{\nu}^c}^2$	300^2 GeV ²

Table 4.1: Relevant parameter choices for figure 4.2 consistent with the EWSB conditions and non-tachyonic nature for squared scalar masses. Eqn.(4.8) has been used and we choose $\tan\beta = 10$.

It is also important to discuss the bounds on the lightest Higgs boson mass in $\mu\nu$ SSM. Neglecting small neutrino Yukawa couplings Y_ν^{ij} , the tree level upper bound on the lightest neutral Higgs mass [15, 29–32] is given by (see eqn.(2.57))

$$m_{h^0}^2 \lesssim M_Z^2 [\cos^2 2\beta + 3.62 \lambda^i \lambda_i \sin^2 2\beta]. \quad (4.9)$$

Apparently, one can optimize this bound by choosing small $\tan\beta$ and large $\lambda^i \lambda_i$ values simultaneously. Similar to the NMSSM [33–35] the upper bound for the lightest $SU(2)_L$ doublet-like Higgs boson mass in the $\mu\nu$ SSM is ~ 140 GeV for $\tan\beta \sim 2$ [22]. Such a conclusion strictly demands small mixing among the MSSM Higgs and the right-handed sneutrinos $\tilde{\nu}_i^c$ (see eqns. (B.13), (B.14)).

It should be mentioned at this point that the radiative corrections to the lightest Higgs boson mass, can be significant in some regions of the parameter space as discussed in ref. [22]. It has been shown that the light Higgs mass larger than the LEP lower limit of 114 GeV can be obtained with the value of A_t (trilinear coupling in the scalar sector for the stop) within 1-2.4 TeV and when the mixing of the light Higgs with the right-handed sneutrino is small. The latter requirement is fulfilled in most of the cases that we have considered and in some cases the mixing is slightly larger. However, there is always the freedom of choosing the value of A_t appropriately. Hence, it would be fair to say that the experimental limits on the light Higgs boson mass can be satisfied in our analysis.

Before starting the next section we want to emphasize that the parameters chosen for our numerical analysis are just for illustrative purpose. These are not some particular and specific choices in some sacred corner of the model space. Since we have a large parameter space, it is always possible to choose a different parameter point with the same characteristic features satisfying all the experimental constraints.

4.4 Fermions in $\mu\nu$ SSM

Effect of \mathcal{R}_p in the superpotential and in the soft terms (eqns.(4.1), (4.2)) is responsible for enrichment in the scalar sector. In an identical fashion, the neutral and the charged fermion mass matrices also receive enhancement through lepton number violating couplings.

✦ *Neutralino mass matrix*

The neutral fermions of the MSSM ($\tilde{B}^0, \tilde{W}_3^0, \tilde{H}_d^0, \tilde{H}_u^0$), through second, third and fourth terms of $\mu\nu$ SSM superpotential (eqn.(4.1)), can mix with three generations of left and right-handed neutrinos, ν_i and ν_i^c respectively. The neutralino mass matrix for $\mu\nu$ SSM is thus a 10×10 symmetric matrix [14, 22, 25–27].

In the weak interaction basis defined by

$$\Psi^{0T} = \left(\tilde{B}^0, \tilde{W}_3^0, \tilde{H}_d^0, \tilde{H}_u^0, \nu_\alpha^c, \nu_\alpha \right), \quad (4.10)$$

where $\alpha = 1, 2, 3 \equiv e, \mu, \tau$. The neutral fermion mass term in the Lagrangian is of the form

$$\mathcal{L}_{neutral}^{mass} = -\frac{1}{2} \Psi^{0T} \mathcal{M}_n \Psi^0 + \text{H.c.}, \quad (4.11)$$

The massless neutrinos now can acquire masses due to their mixing with the MSSM neutralinos and the gauge singlet right-handed neutrinos. The three lightest eigenvalues of this 10×10 neutralino mass matrix correspond to the three light physical neutrinos, which are expected to be very small in order to satisfy the experimental data on massive neutrinos (see table 3.1). The matrix \mathcal{M}_n can be written in the following fashion

$$\mathcal{M}_n = \begin{pmatrix} M_{7 \times 7} & m_{3 \times 7}^T \\ m_{3 \times 7} & 0_{3 \times 3} \end{pmatrix}, \quad (4.12)$$

where using eqn.(4.6)

$$M_{7 \times 7} = \begin{pmatrix} M_1 & 0 & -\frac{g_1}{\sqrt{2}}v_1 & \frac{g_1}{\sqrt{2}}v_2 & 0 & 0 & 0 \\ 0 & M_2 & \frac{g_2}{\sqrt{2}}v_1 & -\frac{g_2}{\sqrt{2}}v_2 & 0 & 0 & 0 \\ -\frac{g_1}{\sqrt{2}}v_1 & \frac{g_2}{\sqrt{2}}v_1 & 0 & -\mu & -\lambda^e v_2 & -\lambda^\mu v_2 & -\lambda^\tau v_2 \\ \frac{g_1}{\sqrt{2}}v_2 & -\frac{g_2}{\sqrt{2}}v_2 & -\mu & 0 & \rho^e & \rho^\mu & \rho^\tau \\ 0 & 0 & -\lambda^e v_2 & \rho^e & 2u_c^{ee} & 2u_c^{e\mu} & 2u_c^{e\tau} \\ 0 & 0 & -\lambda^\mu v_2 & \rho^\mu & 2u_c^{\mu e} & 2u_c^{\mu\mu} & 2u_c^{\mu\tau} \\ 0 & 0 & -\lambda^\tau v_2 & \rho^\tau & 2u_c^{\tau e} & 2u_c^{\tau\mu} & 2u_c^{\tau\tau} \end{pmatrix}, \quad (4.13)$$

and

$$m_{3 \times 7} = \begin{pmatrix} -\frac{g_1}{\sqrt{2}}v'_e & \frac{g_2}{\sqrt{2}}v'_e & 0 & r_c^e & Y_\nu^{ee}v_2 & Y_\nu^{e\mu}v_2 & Y_\nu^{e\tau}v_2 \\ -\frac{g_1}{\sqrt{2}}v'_\mu & \frac{g_2}{\sqrt{2}}v'_\mu & 0 & r_c^\mu & Y_\nu^{\mu e}v_2 & Y_\nu^{\mu\mu}v_2 & Y_\nu^{\mu\tau}v_2 \\ -\frac{g_1}{\sqrt{2}}v'_\tau & \frac{g_2}{\sqrt{2}}v'_\tau & 0 & r_c^\tau & Y_\nu^{\tau e}v_2 & Y_\nu^{\tau\mu}v_2 & Y_\nu^{\tau\tau}v_2 \end{pmatrix}. \quad (4.14)$$

Note that the top-left 4×4 block of the matrix $M_{7 \times 7}$ is the usual neutralino mass matrix of the MSSM (see eqn.(A.7)). The bottom right 3×3 block represents the Majorana mass matrix for gauge singlet neutrinos, which will be taken as diagonal (see eqn.(4.8)) in the subsequent analysis. The entries of $M_{7 \times 7}$ are in general of the order of the electroweak scale whereas the entries of $m_{3 \times 7}$ are much smaller $\sim \mathcal{O}(10^{-5})$ GeV. Hence, the matrix (4.12) has a seesaw structure, which will give rise to three very light eigenvalues corresponding to three light neutrinos. The correct neutrino mass scale of $\sim 10^{-2}$ eV can easily be obtained with such a structure of the 10×10 neutralino mass matrix. It has been shown in ref. [25] that one can obtain the correct mass-squared differences and the mixing pattern for the light neutrinos even with the choice of flavour diagonal neutrino Yukawa couplings in eqn.(4.14). Besides, the choice of flavour diagonal neutrino Yukawa couplings (eqn.(4.8)) makes the analysis simpler with a reduced number of parameters and makes the model more predictive. As we will show later, it is possible to find out the correct mixing pattern and the mass hierarchies (both normal and inverted) among the light neutrinos in such a situation, even at the tree level [25].

In order to obtain the physical neutralino states, one needs to diagonalize the 10×10 matrix \mathcal{M}_n . As in the case of MSSM, the symmetric mass matrix \mathcal{M}_n can be diagonalized with one unitary matrix \mathbf{N} . The mass eigenstates χ_i^0 are related to flavour eigenstates Ψ_j^0 (eqn.(4.10)) as

$$\chi_i^0 = \mathbf{N}_{i1}\tilde{B}^0 + \mathbf{N}_{i2}\tilde{W}_3^0 + \mathbf{N}_{i3}\tilde{H}_d^0 + \mathbf{N}_{i4}\tilde{H}_u^0 + \mathbf{N}_{i,\alpha+4}\nu_\alpha^c + \mathbf{N}_{i,\alpha+7}\nu_\alpha. \quad (4.15)$$

where the 10×10 unitary matrix \mathbf{N} satisfies

$$\mathbf{N}^* \mathcal{M}_n \mathbf{N}^{-1} = \mathcal{M}_D^0 = \text{diag}(m_{\tilde{\chi}_i^0}, m_{\nu_j}), \quad (4.16)$$

with the diagonal neutralino mass matrix denoted as \mathcal{M}_D^0 . i and j runs from 1 to 7 and 1 to 3, respectively. The quantity $m_{\tilde{\chi}_i^0}$ represent neutralino masses. Physical neutrino masses are being represented by m_{ν_j} . It is, in general, very difficult to predict the nature of the lightest neutralino (out

of seven χ_i^0) state since that depends on several unknown parameters. Neutralino mass matrix for $\mu\nu$ SSM with complex VEVs is given in ref. [28].

✦ *Chargino mass matrix*

Similar augmentation in the charged lepton sector result in a 5×5 chargino mass matrix where the charged electroweak gauginos ($-i\tilde{\lambda}_2^\pm$) and higgsinos ($\tilde{H}_u^+, \tilde{H}_d^-$) mix with charged leptons through R_p violating couplings. These mixings are coming from the second term of eqn.(4.1) and as well as from non-zero left-handed sneutrino VEVs.

In the weak interaction basis defined by

$$\Psi^{+T} = (-i\tilde{\lambda}_2^+, \tilde{H}_u^+, \ell_R^+), \quad \Psi^{-T} = (-i\tilde{\lambda}_2^-, \tilde{H}_d^-, \ell_L^-),$$

where $\ell = e, \mu, \tau$. The charged fermion mass term in the Lagrangian is of the form

$$\mathcal{L}_{charged}^{mass} = -\frac{1}{2} \begin{pmatrix} \Psi^{+T} & \Psi^{-T} \end{pmatrix} \begin{pmatrix} 0_{5 \times 5} & m_{5 \times 5}^T \\ m_{5 \times 5} & 0_{5 \times 5} \end{pmatrix} \begin{pmatrix} \Psi^+ \\ \Psi^- \end{pmatrix}. \quad (4.17)$$

Here we have included all three generations of charged leptons and assumed that the charged lepton Yukawa couplings are in the diagonal form. The matrix $m_{5 \times 5}$ using eqn.(4.6) is given by [22, 25, 27]

$$m_{5 \times 5} = \begin{pmatrix} M_2 & g_2 v_2 & 0 & 0 & 0 \\ g_2 v_1 & \mu & -Y_e^{ee} v'_e & -Y_e^{\mu\mu} v'_\mu & -Y_e^{\tau\tau} v'_\tau \\ g_2 v'_e & -r_c^e & Y_e^{ee} v_1 & 0 & 0 \\ g_2 v'_\mu & -r_c^\mu & 0 & Y_e^{\mu\mu} v_1 & 0 \\ g_2 v'_\tau & -r_c^\tau & 0 & 0 & Y_e^{\tau\tau} v_1 \end{pmatrix}. \quad (4.18)$$

The charged fermion masses are obtained by applying a bi-unitary transformation like

$$\mathbf{U}^* m_{5 \times 5} \mathbf{V}^{-1} = \mathcal{M}_D^\pm, \quad (4.19)$$

where \mathbf{U} and \mathbf{V} are two unitary matrices and \mathcal{M}_D^\pm is the diagonal matrix. Relations between the mass χ_i^\pm and flavour eigenstates for charginos are same as eqn.(3.42), namely

$$\begin{aligned} \chi_i^+ &= \mathbf{V}_{i1} \tilde{W}^+ + \mathbf{V}_{i2} \tilde{H}_u^+ + \mathbf{V}_{i,\alpha+2} \ell_{\alpha R}^+, \\ \chi_i^- &= \mathbf{U}_{i1} \tilde{W}^- + \mathbf{U}_{i2} \tilde{H}_d^- + \mathbf{U}_{i,\alpha+2} \ell_{\alpha L}^-, \end{aligned} \quad (4.20)$$

where $\tilde{W}^\pm \equiv -i\tilde{\lambda}_2^\pm$.

It is important to note that the off-diagonal elements (except for 12 and 21 elements) of the chargino mass matrix (eqn. (4.18)) either contain Y_ν^{ij} ($r_c^i = \sum Y_\nu^{ij} v_j^c$) or left-handed sneutrino VEVs v'_i , both of which are very small $\sim \mathcal{O}(10^{-4} \text{ GeV})$. This indicates that the physical charged lepton eigenstates will have very small admixture of charged higgsino and charged gaugino states. So it is safe to assume (also verified numerically) that these lepton number violating mixing have very little effect on the mass eigenstates of the charged leptons. Thus, while writing down the PMNS matrix [36–39] (eqn.(3.9)), it is justified to assume that one is working in the basis where the charged lepton mass matrix is already in the diagonal form [25].

So far all of the neutralinos and charginos are considered in two-component form. Corresponding four component neutralino, chargino and charge conjugated chargino spinors are respectively defined as

$$\tilde{\chi}_i^0 = \begin{pmatrix} \chi_i^0 \\ \chi_i^0 \end{pmatrix}, \quad \tilde{\chi}_i = \begin{pmatrix} \chi_i^+ \\ \chi_i^- \end{pmatrix}, \quad \tilde{\chi}_i^c = \begin{pmatrix} \chi_i^- \\ \chi_i^+ \end{pmatrix}, \quad (4.21)$$

where χ_i^0 and χ_i^\pm are two component neutral and charged spinors, respectively. In our analysis the charged leptons are represented by their charged conjugate fields [40], which are positively charged.

Unlike the scalar mass squared matrices, eigenvalues of the neutralino or chargino mass matrix can be either positive or negative. It is always possible to remove the wrong signs via appropriate rotations. However, then one should be very careful about the corresponding Feynman rules. A viable alternative is to live with the signs of fermion masses (η_i for neutralinos and ϵ_i for charginos) and incorporate them properly in the respective Feynman rules [41].

For the sake of completeness we also write down the quark mass matrices in $\mu\nu$ SSM in appendix B.

4.5 Neutrinos at the tree level

It has been already emphasized that the 10×10 neutralino mass matrix \mathcal{M}_n possesses a seesaw like structure. The effective light neutrino mass matrix M_ν^{seesaw} , arising via the seesaw mechanism in the presence of explicit lepton number violation, is in general given by

$$M_\nu^{seesaw} = -m_{3 \times 7} M_{7 \times 7}^{-1} m_{3 \times 7}^T. \quad (4.22)$$

With small R_p , it is possible to carry out a perturbative diagonalization of the 10×10 neutralino mass matrix (see [42]), by defining [43, 44] a matrix ξ as

$$\xi = m_{3 \times 7} M_{7 \times 7}^{-1}. \quad (4.23)$$

If the elements of ξ satisfy $\xi_{ij} \ll 1$, then this can be used as an expansion parameter to get an approximate analytical solution for the matrix \mathbf{N} (see eqn.(4.16)). A general expression for the elements of ξ with simplified assumptions can be written in the form $\mathcal{A}'a_i + \mathcal{B}'b_i + \mathcal{C}'c_i$, where

$$a_i = Y_\nu^{ii} v_2, \quad c_i = v'_i, \quad b_i = (Y_\nu^{ii} v_1 + 3\lambda v'_i) = (a_i \cot \beta + 3\lambda c_i), \quad (4.24)$$

with $i = e, \mu, \tau \equiv 1, 2, 3$, $\tan \beta = \frac{v_2}{v_1}$ and $\mathcal{A}', \mathcal{B}', \mathcal{C}'$ are complicated functions of various parameters of the model [27]. The complete expressions for the elements of ξ [27] are given in appendix C. In deriving detailed expression for ξ 's we neglect the sub-dominant terms $\sim \mathcal{O}(\frac{v'^3}{\tilde{m}^3}, \frac{Y_\nu v'^2}{\tilde{m}^2}, \frac{Y_\nu^2 v'}{\tilde{m}})$, where \tilde{m} is the electroweak (or supersymmetry breaking) scale.

With the help of eqn.(4.23), eqn.(4.22) reduces to

$$M_\nu^{seesaw} = -\xi m_{3 \times 7}^T. \quad (4.25)$$

Using the favour of eqn.(4.8) in eqn.(4.25), together with the expressions for ξ^{ij} given in appendix C, entries for the 3×3 matrix M_ν^{seesaw} are approximately given as (neglecting terms \propto fourth power in Y_ν^{ij}, v'_i (separately or in a product) [25, 28])

$$\begin{aligned} (M_\nu^{seesaw})_{ij} &\approx \frac{v_2^2}{6\kappa v^c} Y_\nu^{ii} Y_\nu^{jj} (1 - 3\delta_{ij}) \\ &- \frac{1}{2M_{eff}} \left[v'_i v'_j + \frac{v_1 v^c (Y_\nu^{ii} v'_j + Y_\nu^{jj} v'_i)}{\mu} + \frac{Y_\nu^{ii} Y_\nu^{jj} v_1^2 v^c}{\mu^2} \right]. \end{aligned} \quad (4.26)$$

Here we have used

$$\begin{aligned} M_{eff} &= M \left[1 - \frac{v^2}{2MA\mu} \left(\kappa v^c \sin 2\beta + \frac{\lambda v^2}{2} \right) \right], \\ v_2 &= v \sin \beta, \quad v_1 = v \cos \beta, \quad \mu = 3\lambda v^c, \\ A &= (\kappa v^c + \lambda v_1 v_2), \quad \frac{1}{M} = \frac{g_1^2}{M_1} + \frac{g_2^2}{M_2}. \end{aligned} \quad (4.27)$$

Before proceeding further it is important to discuss eqn.(4.26) in more details [25,27].

I. First consider the limit $v^c \rightarrow \infty$ and $v \rightarrow 0$ ($\Rightarrow v_1, v_2 \rightarrow 0$). Immediately eqn. (4.26) reduces to

$$(M_\nu^{seesaw})_{ij} \approx -\frac{v'_i v'_j}{2M} \Rightarrow m_\nu \sim \frac{(g_1 c_i)^2}{M_1} + \frac{(g_2 c_i)^2}{M_2}, \quad (4.28)$$

which is the first part of the second term of eqn.(4.26). In this case the elements of the neutrino mass matrix are bilinear in the left-handed sneutrino VEVs and they appear due to a seesaw effect involving the gauginos. This is known as the ‘‘gaugino seesaw’’ effect and neutrino mass generation through this effect is a characteristic feature of the bilinear R_p violating model. This effect is present in this model because we have seen earlier that the effective bilinear R_p violating terms are generated in the scalar potential as well as in the superpotential through the vacuum expectation values of the gauge singlet sneutrinos ($\varepsilon^i = Y^{ij} v_j^c$). In gaugino seesaw the role of the *Dirac* mass terms are played by $g_1 v'_i$ and $g_2 v'_i$, where g_1, g_2 are the $U(1)$ and the $SU(2)$ gauge couplings respectively and v'_i ($\equiv c_i$ (eqn.(4.24))) stand for the left-handed sneutrino VEVs. The role of the *Majorana* masses are played by the gaugino soft masses M_1, M_2 . The gaugino seesaw effect is closely analogous to the TYPE-I [42,45–50] + Type-III seesaw mechanism [51,52] due to simultaneous involvement of a singlet (\tilde{B}^0) and triplet fermion (\tilde{W}_3^0) (see section 3.3.2, figure 3.6, diagrams (a, b)). This analogy has been pointed out in ref. [27]. Note that the gaugino seesaw effect can generate mass for only one doublet neutrino, as shown in eqn.(4.28).

II. In the limit $M \rightarrow \infty$, eqn.(4.26) reduces to

$$(M_\nu^{seesaw})_{ij} \approx \frac{v_2^2}{6\kappa v^c} Y_\nu^{ii} Y_\nu^{jj} (1 - 3\delta_{ij}) \equiv \frac{a_i a_j}{3m_{\nu^c}} (1 - 3\delta_{ij}), \quad (4.29)$$

which corresponds to the ‘‘ordinary seesaw’’ effect between the left-handed and gauge singlet right-handed neutrinos. Remember that the effective Majorana masses for the gauge singlet neutrinos are given by $m_\nu^c = 2\kappa v^c$ and the usual Dirac masses are given by $a_i = Y_\nu^{ii} v_2$. The ordinary seesaw effect can generate, in general, masses for more than one neutrinos. Thus depending on the magnitudes and the hierarchies of various diagonal neutrino Yukawa couplings Y_ν^{ii} , one can generate normal or inverted hierarchy of neutrino masses (combining with the ‘‘gaugino seesaw’’ effect) corresponding to atmospheric and solar mass squared differences [25].

It is also interesting to note that a conventional ordinary seesaw (generated only through the mixing between left-handed and right-handed neutrinos) in contrast to eqn.(4.29) would give rise to a mass matrix of the form [28]

$$(M_\nu^{seesaw})_{ij} \approx -\frac{v_2^2}{2\kappa v^c} Y_\nu^{ii^2}. \quad (4.30)$$

The off-diagonal contributions as shown in eqn.(4.29) are arising from an effective mixing between the right-handed neutrinos and Higgsinos. Hence, when right-handed neutrinos are also decoupled ($v^c \rightarrow \infty$), the neutrino masses are zero as corresponds to the case of a seesaw with only Higgsinos [28].

4.5.1 Neutrino masses at the tree level

Eqn.(4.26) can be re-casted in a compact form using eqns.(4.24) (4.27) as

$$(M_\nu^{seesaw})_{ij} = \frac{1}{6\kappa v^c} a_i a_j (1 - 3\delta_{ij}) + \frac{2Av^c}{3\Delta} b_i b_j, \quad (4.31)$$

or alternatively using eqn.(4.24) in a more elucidate form as

$$(M_\nu^{seesaw})_{ij} = f_1 a_i a_j + f_2 c_i c_j + f_3 (a_i c_j + a_j c_i), \quad (4.32)$$

with

$$f_1 = \frac{1}{6\kappa v^c} (1 - 3\delta_{ij}) + \frac{2Av^c \cot^2 \beta}{3\Delta}, \quad f_2 = \frac{2A\lambda\mu}{\Delta}, \quad f_3 = \frac{2A\mu \cot \beta}{3\Delta}, \quad (4.33)$$

and $\Delta = \lambda^2 (v_1^2 + v_2^2)^2 + 4\lambda\kappa v_1 v_2 v^c - 4\lambda A\mu M$. It is apparent from eqn.(4.31) that the second term ($\propto b_i b_j$) can contribute to only one neutrino mass, $\propto b_i^2$. However, presence of $(1 - 3\delta^{ij})$ factor in the

first term assures non-zero masses for other neutrinos. If we concentrate on the normal hierarchical scheme of light neutrino masses, then with suitable choice of model ingredients it is possible to generate the atmospheric neutrino mass scale ($\sim \mathcal{O}(10^{-11})$ GeV) from the second term, whereas relatively small solar scale ($\sim \mathcal{O}(10^{-12})$ GeV) emerges from the first term of eqn.(4.31). The imposed order of magnitude difference between the first and the second term of eqn.(4.31) through certain choices of model parameters can be used to extract the eigenvalues of eqn.(4.31) analytically. Choosing the dominant terms to be $\propto b_i b_j$, which contribute to only one neutrino mass, it is possible to apply the techniques of degenerate perturbation theory to extract the effect of the perturbed term ($\propto a_i a_j$) over the unperturbed one ($\propto b_i b_j$) [25]. It has to be clarified here that actually in $\mu\nu$ SSM for a novel region of the parameter space $b_i \sim a_i$ [25], however, with a clever choice of the λ and κ parameter it is possible to vary the order of magnitude of the co-efficients in front ($\frac{1}{6\kappa v^c}, \frac{2Av^c}{3\Delta}$, see eqn.(4.31)). For the chosen set of parameters (see table 4.2) co-efficients of the $a_i a_j$ term is an order of magnitude smaller compared to that of $b_i b_j$ [25]. So the perturbative approach is well justified. As shown in ref. [25] it is possible to extract simple analytical form for light neutrino masses in this approach. Detailed expressions for the eigenvectors and eigenvalues of eqn.(4.31) obtained through perturbative calculations are given in appendix C. It is interesting to see from eqn.(C.6) that the correction to unperturbed eigenvalues are proportional to the effect of ordinary seesaw [25].

The numerical values of the solar and atmospheric mass squared differences Δm_{solar}^2 ($\equiv \Delta m_{21}^2$) and Δm_{atm}^2 ($\equiv \Delta m_{31}^2$) as obtained from full numerical calculations (Using eqn.(4.22)) and from appropriate analytical formulae (Using eqn.(C.6)) have been shown in table 4.3¹ and the results show good agreement [25]. The numerical calculations have been performed with the help of a code developed by us using Mathematica [53]. In our numerical analysis for the normal hierarchical pattern in light neutrino masses, we choose $m_2|_{max} < 1.0 \times 10^{-11}$ GeV [25]. Results of table 4.3 are consistent with the three flavour global neutrino data [54, 55] as shown in table 3.1 in the 3σ limit. It is interesting to observe that unlike conventional bilinear R_p violating models, in $\mu\nu$ SSM all three neutrinos are massive itself at the tree level. Consequently, it is possible to accommodate the three flavour global neutrino data (table 3.1) at the tree level even with the choice of diagonal neutrino Yukawa couplings (see table 4.2) [25].

Parameter	Chosen Value	Parameter	Chosen Value
λ	0.06	$(A_\lambda \lambda)$	-60 GeV
κ	0.65	$(A_\kappa \kappa)$	650 GeV
Y_ν^{11}	4.57×10^{-7}	$(A_\nu Y_\nu)^{11}$	1.57×10^{-4} GeV
Y_ν^{22}	6.37×10^{-7}	$(A_\nu Y_\nu)^{22}$	4.70×10^{-4} GeV
Y_ν^{33}	1.80×10^{-7}	$(A_\nu Y_\nu)^{33}$	3.95×10^{-4} GeV
M_1	325 GeV	M_2	650 GeV
$m_{\tilde{L}}^2$	400^2 GeV ²	$m_{\tilde{\nu}^c}^2$	300^2 GeV ²

Table 4.2: Parameter choices (consistent with figure 4.2) for result presented in table 4.3. Eqn.(4.8) has been used here and we choose $\tan \beta = 10$.

Both left and right sneutrino VEVs (v'_i, v_i^c , respectively) are derived using the set of parameters given in table 4.2. The relation between the gaugino soft masses M_1 and M_2 are assumed to be GUT (grand unified theory) motivated, so that, at the electroweak scale, we have $M_1 : M_2 = 1 : 2$.

4.5.2 Neutrino mixing at the tree level

The expansion parameter ξ (see eqns.(C.1)) has been introduced in eqn.(4.23) to perform perturbative diagonalization of the 10×10 neutralino mass matrix \mathcal{M}_n . It is possible to express the neutralino mixing matrix \mathbf{N} (see eqn.(4.16)) in leading order in ξ as

$$\mathbf{N}^* = \begin{pmatrix} \mathcal{N}^* & 0 \\ 0 & U^T \end{pmatrix} \begin{pmatrix} 1 - \frac{1}{2}\xi^\dagger \xi & \xi^\dagger \\ -\xi & 1 - \frac{1}{2}\xi \xi^\dagger \end{pmatrix}. \quad (4.34)$$

¹A typo has been corrected compared to ref. [25]. Also to denote individual neutrino masses, m_{ν_i} are used instead of m_i (ref. [25]).

	m_ν (eV) ($\times 10^3$)			Δm_{21}^2 (eV 2)	Δm_{31}^2 (eV 2)
	m_{ν_1}	m_{ν_2}	m_{ν_3}	($\times 10^5$)	($\times 10^3$)
Using eqn.(4.22)	4.169	9.970	48.23	8.203	2.307
Using eqn.(C.6)	4.168	9.468	47.71	7.228	2.187

Table 4.3: Absolute values of the neutrino masses and the mass-squared differences for a sample point of the parameter space [25]. Results for full numerical analysis have been obtained using eqn.(4.22). Approximate analytical expressions of eqn.(C.6) have been used for comparison. Parameter choices are given in table 4.2.

The 10×10 neutralino mass matrix \mathcal{M}_n can approximately be block diagonalized to the form $\text{diag}(M_{7 \times 7}, M_\nu^{\text{seesaw}})$, by the matrix defined in eqn.(4.34). The matrices \mathcal{N} and U , defined in eqn.(4.34), are used to diagonalize $M_{7 \times 7}$ and M_ν^{seesaw} in the following manner (using eqn.(4.16)),

$$\begin{aligned} \mathcal{N}^* M_{7 \times 7} \mathcal{N}^\dagger &= \text{diag}(m_{\tilde{\chi}_i^0}), \\ U^T M_\nu^{\text{seesaw}} U &= \text{diag}(m_{\nu_1}, m_{\nu_2}, m_{\nu_3}). \end{aligned} \quad (4.35)$$

Where U is the non-trivial leptonic mixing matrix, known as PMNS matrix [36–39]. As already stated in section 3.2, a non-trivial neutrino mixing is a consequence of massive neutrinos. If we adhere to a scenario where CP is preserved, the PMNS matrix following eqn.(3.9) can be written as

$$U = \begin{pmatrix} c_{12}c_{13} & s_{12}c_{13} & s_{13} \\ -s_{12}c_{23} - c_{12}s_{23}s_{13} & c_{12}c_{23} - s_{12}s_{23}s_{13} & s_{23}c_{13} \\ s_{12}s_{23} - c_{12}c_{23}s_{13} & -c_{12}s_{23} - s_{12}c_{23}s_{13} & c_{23}c_{13} \end{pmatrix}, \quad (4.36)$$

where $c_{ij} = \cos \theta_{ij}$, $s_{ij} = \sin \theta_{ij}$.

It is definitely possible to extract the mixing angles from U in a full numerical analysis. However, it is always useful to do the same with a simplified approximate analytical analysis (if at all possible) to get an idea about the relative importance of the different parameters. An analysis of this kind for light neutrino mixing angles using degenerate perturbation theory has been addressed in ref. [25]. We showed that it is possible to write down the PMNS matrix U as (eqn.(C.12))

$$U = \begin{pmatrix} \mathcal{Y}_1 & \mathcal{Y}_2 & \mathcal{Y}_3 \end{pmatrix}_{3 \times 3}, \quad (4.37)$$

where \mathcal{Y}_i 's are defined in appendix C.2. Using eqn.(4.37) it is possible to derive appropriate expressions for the light neutrino mixing angles $\theta_{13}, \theta_{23}, \theta_{12}$ as [25]

$$\sin^2 \theta_{13} = \frac{b_e^2}{b_e^2 + b_\mu^2 + b_\tau^2}. \quad (4.38)$$

$$\sin^2 \theta_{23} = \frac{b_\mu^2}{b_\mu^2 + b_\tau^2}. \quad (4.39)$$

$$\sin^2 \theta_{12} \approx 1 - \left(\alpha'_1 + \alpha'_2 \frac{b_e}{b_\tau} \right)^2, \quad (4.40)$$

where b_i 's are given by eqn.(4.24). The quantities α'_1, α'_2 are given by eqn.(C.9).

It is apparent from eqn.(4.38) that if we want the (13) mixing angle to be small (which is supported by data, see table 3.1) then one must have $b_e^2 \ll (b_\mu^2 + b_\tau^2)$. On the other hand, since the (23) mixing angle θ_{23} is maximal by nature ($\sim 45^\circ$, see table 3.1), it is natural to expect $b_\mu^2 = b_\tau^2$. The formula for solar mixing angle θ_{12} is a bit complicated. Nevertheless, in order to have $\theta_{12} \sim 35^\circ$, the square root of the second term on the right hand side of eqn.(4.40) should be approximately 0.8. So these approximate analytical formulae clearly help us to choose suitable corner of parameter space rather than performing a blind search, which is the power of the analytical approach.

mixing angles in degree	Using (4.22)	Using (C.12)
θ_{12}	36.438	37.287
θ_{13}	9.424	6.428
θ_{23}	38.217	42.675

Table 4.4: Neutrino mixing angles using eqn.(4.22) and eqn.(C.12) Parameter choices are given in table 4.2. These values are consistent with entries of table 3.1 in the 3σ limit [54].

We compare three light neutrino mixing angles as obtained from eqn.(4.37) to that obtained in full numerical analysis using eqn.(4.22) in table 4.4. Neutrino masses are taken to be normal hierarchical.

We can see that for this set of chosen parameters (table 4.2), numerical and approximate analytical results give quite good agreement. Naturally, one would be interested to check the predictions made in eqns. (4.38), (4.39), and (4.40) over a wide region in the parameter space and see the deviations from the full numerical calculations. These are shown in figures.4.3, 4.4 [25].

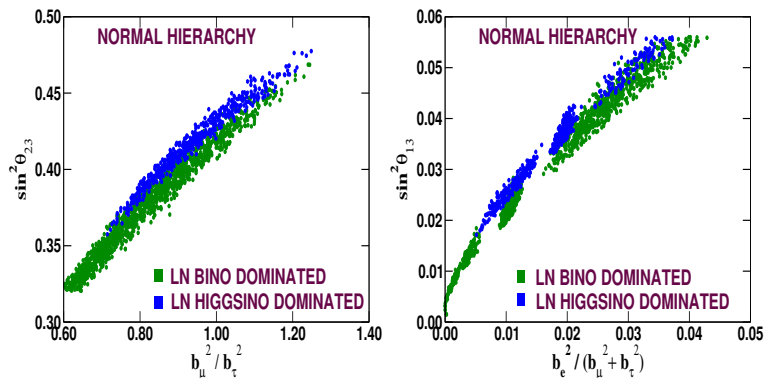


Figure 4.3: Scatter plot of the neutrino mixing angle $\sin^2 \theta_{23}$ (left) and $\sin^2 \theta_{13}$ (right) as a function of the ratio $\frac{b_\mu^2}{b_\tau^2}$ and $\frac{b_e^2}{b_\mu^2 + b_\tau^2}$. Values of model parameters are given in table 4.5. The lightest neutralino (LN) is either a bino (\tilde{B}^0) or a higgsino ($\tilde{H}_u^0, \tilde{H}_d^0$) dominated. Light neutrino mass ordering is normal hierarchical.

It is apparent from the left diagram of figure 4.3 that for $b_\mu^2 = b_\tau^2$, the value of $\sin^2 \theta_{23}$ varies in the range 0.41 – 0.44, which corresponds to θ_{23} between 40° and 42° . On the other hand, eqn.(4.39) tells that for $b_\mu^2 = b_\tau^2$, $\sin^2 \theta_{23} = 0.5$. So for a wide region of parameter space result from the numerical calculation is reasonably close to the prediction from the approximate analytical formula.

Also from figure 4.4 as $(\alpha'_1 + \alpha'_2 \frac{b_e}{b_\tau})^2 \rightarrow 0.50$, $\sin^2 \theta_{12}$ tends to be maximal, that is $\theta_{12} = 45^\circ$, which is well expected.

Concerning table 4.5 it has to be emphasized here that the allowed regions in the $\lambda - \kappa$ plane (see figure 4.2) are not very sensitive to the values of Y_ν and $A_\nu Y_\nu$ due to their smallness. Hence we choose to vary them randomly (see table 4.5), in order to accommodate the three flavour global neutrino data.

So far we considered eqn.(4.31) in the limit when with suitable choice of model parameters the terms $\propto a_i a_j$ can act as perturbation over the second term. However, the huge parameter space for $\mu\nu$ SSM always leaves room for the inverse situation. In other words there exists suitable corner of parameter space where the first term of eqn.(4.31) is the dominant one and then eqn.(4.39) can be expressed as

$$\sin^2 \theta_{23} = \frac{a_\mu^2}{a_\mu^2 + a_\tau^2}. \quad (4.41)$$

This is exactly what is shown by figure 4.5. Note that for $a_\mu^2 = a_\tau^2$, the atmospheric mixing angle becomes maximal.

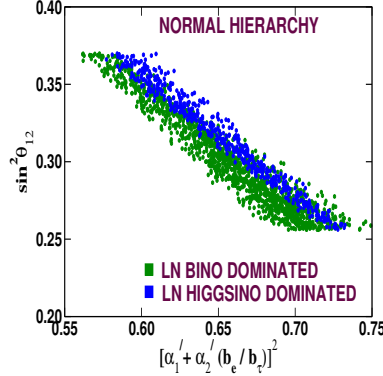


Figure 4.4: $\sin^2 \theta_{12}$ versus $(\alpha'_1 + \alpha'_2 \frac{b_e}{b_\tau})^2$ scatter plot. Parameter choice and mass hierarchy is same as figure 4.3.

Parameter	Chosen Value	Parameter	Chosen Value
Y_ν^{11}	$3.55 - 5.45 \times 10^{-7}$	$(A_\nu Y_\nu)^{11}$	$1.25 - 1.95 \times 10^{-4}$ GeV
Y_ν^{22}	$5.55 - 6.65 \times 10^{-7}$	$(A_\nu Y_\nu)^{22}$	$3.45 - 4.95 \times 10^{-4}$ GeV
Y_ν^{33}	$1.45 - 3.35 \times 10^{-7}$	$(A_\nu Y_\nu)^{33}$	$2.35 - 4.20 \times 10^{-4}$ GeV
$m_{\tilde{L}}^2$	400^2 GeV ²	$m_{\tilde{\nu}^c}^2$	300^2 GeV ²
λ	0.06(0.13)	$(A_\lambda \lambda)$	$-1000 \times \lambda$ GeV
κ	0.65	$(A_\kappa \kappa)$	$1000 \times \kappa$ GeV
M_1	110(325) GeV	M_2	$2 \times M_1$ GeV

Table 4.5: Parameter choices (consistent with figure 4.2) for figures 4.3, 4.4. $\lambda = 0.06(0.13)$ for a bino(higgsino) dominated lightest neutralino. Similarly, $M_1 = 110$ (325) GeV for a bino (higgsino) dominated lightest neutralino. Eqn.(4.8) has been used here and we choose $\tan \beta = 10$. The set of chosen parameters are consistent with the constraints of the scalar sector.

In figure 4.6, we have shown the regions in the various Y_ν planes satisfying the three flavour global neutrino data. The values of other parameters are as shown in table 4.5 for the case where the lightest neutralino ($\tilde{\chi}_1^0$) is bino dominated. We can see from these figures that the allowed values of Y_ν 's show a mild hierarchy such that $Y_\nu^{22} > Y_\nu^{11} > Y_\nu^{33}$ [25].

Similar studies have been performed for the inverted hierarchical case and the allowed region shows that the magnitudes of the neutrino Yukawa couplings are larger compared to the case of normal hierarchical scheme of the neutrino masses with a different hierarchy among the Y_ν 's themselves ($Y_\nu^{11} > Y_\nu^{22} > Y_\nu^{33}$). In this case $\sin^2 \theta_{12}$ shows an increasing behaviour with the ratio b_e^2/b_μ^2 , similar to the one shown by $\sin^2 \theta_{23}$ with b_μ^2/b_τ^2 in the normal hierarchical scenario (see figure 4.3). On the other hand, $\sin^2 \theta_{23}$ shows a decreasing behaviour with b_μ^2/b_τ^2 . In all these cases, the solar and atmospheric mass-squared differences are within the 3σ limits (table 3.1).

4.6 Neutrinos at the loop level

It is legitimate to ask that what is the motivation for performing loop calculations in $\mu\nu$ SSM when all three neutrinos can acquire masses at the tree level [25]? In fact this is a feature where the $\mu\nu$ SSM model is apparently successful over most of the other models of light neutrino mass generation where loop corrections are unavoidable in order to account for oscillation data. However, in the regime of renormalizable quantum field theories, stability of any tree level analysis must be re-examined in the light of radiative corrections. Following this prescription, the results of neutrino masses and mixing will be more robust, once tree level analysis is further improved by incorporating radiative corrections. The radiative corrections may have sizable effect on the neutrino data at one-loop level. Thus, although all

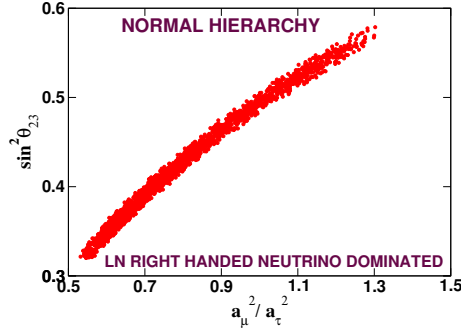


Figure 4.5: Scatter plot of the neutrino mixing angle $\sin^2 \theta_{23}$ as a function of the ratio $\frac{a_\mu^2}{a_\tau^2}$. The lightest neutralino (LN) is right-handed neutrino (ν^c) dominated.

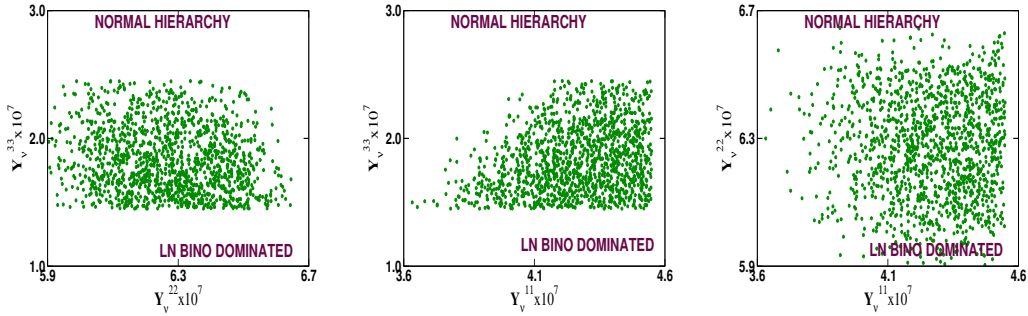


Figure 4.6: Plots for normal hierarchical scheme of neutrino mass in $Y_\nu^{22} - Y_\nu^{33}$, $Y_\nu^{11} - Y_\nu^{33}$ and $Y_\nu^{11} - Y_\nu^{22}$ plane when the lightest neutralino (LN) is bino dominated.

three SM neutrinos acquire non-zero masses in the $\mu\nu$ SSM even at the tree level [25], it is interesting to investigate the fate of those tree level masses and mixing when exposed to one-loop corrections. With this in view, in the following subsections we perform a systematic study of the neutrino masses and mixing with all possible one-loop corrections both analytically and numerically. In the subsequent subsections, while showing the results of one-loop corrections, we try to explain the deviations (which may or may not be prominent) from the tree level analysis. The complete set of one-loop diagrams are shown in figure 4.7. Before going into the details, let us discuss certain relevant issues of one-loop correction and renormalization for the neutralino-neutrino sector. The most general one-loop contribution to the unrenormalized neutralino-neutrino two-point function can be expressed as

$$i\Sigma_{\tilde{\chi}^0\tilde{\chi}^0}^{ij}(p) = i\{\not{p}[P_L\Sigma_{ij}^L(p^2) + P_R\Sigma_{ij}^R(p^2)] - [P_L\Pi_{ij}^L(p^2) + P_R\Pi_{ij}^R(p^2)]\}, \quad (4.42)$$

where P_L and P_R are defined as $\frac{1-\gamma_5}{2}$ and $\frac{1+\gamma_5}{2}$, respectively. $i, j = 1, \dots, 10$ and p is the external momentum. The unrenormalized self-energies $\Sigma^{L,R}$ and $\Pi^{L,R}$ depend on the squared external momentum (p^2). The generic self energies $\Sigma_{ij}^{L(R)}$, $\Pi_{ij}^{L(R)}$ of the Majorana neutralinos and neutrinos must be symmetric in its indices, i and j . \overline{DR} scheme [56–60] has been used to regularize one-loop contributions. In the \overline{DR} scheme², the counter-terms cancel only the divergent pieces of the self-energies. Thus the self energies become finite but depend on the arbitrary scale of renormalization. To resolve this scale dependency, the tree level masses are promoted to running masses in which they cancel the explicit scale dependence of the self energies Σ, Π [62]. The resulting one-loop corrected mass matrix

²In \overline{DR} scheme the subtraction procedure is same as \overline{MS} [61] scheme and the momentum integrals are also evaluated with D dimensions. However, the *Dirac algebras* are done strictly in four dimensions since only in four dimensions the numbers of fermions and bosons match in the case of a supersymmetric system.

using dimensional reduction (\overline{DR}) scheme is given by

$$\begin{aligned}
(\mathcal{M}_{\tilde{\chi}^0}^{\text{tree}+1\text{-loop}})_{ij} &= m_{\tilde{\chi}^0}(\mu_R)\delta^{ij} + \frac{1}{2} \left(\tilde{\Pi}_{ij}^V(m_i^2) + \tilde{\Pi}_{ij}^V(m_j^2) \right) \\
&- m_{\tilde{\chi}_i^0} \tilde{\Sigma}_{ij}^V(m_i^2) - m_{\tilde{\chi}_j^0} \tilde{\Sigma}_{ij}^V(m_j^2),
\end{aligned}
\tag{4.43}$$

with

$$\tilde{\Sigma}_{ij}^V = \frac{1}{2}(\tilde{\Sigma}_{ij}^L + \tilde{\Sigma}_{ij}^R), \quad \tilde{\Pi}_{ij}^V = \frac{1}{2}(\tilde{\Pi}_{ij}^L + \tilde{\Pi}_{ij}^R),
\tag{4.44}$$

where the tree level neutralino mass ($m_{\tilde{\chi}^0}$) is defined at the renormalization scale μ_R , set at the electroweak scale. Here, the word *neutralino mass* stands for all the *ten* eigenvalues of the 10×10 neutralino mass matrix. The self-energies Σ , Π are also renormalized in the \overline{DR} scheme and denoted by $\tilde{\Sigma}$ and $\tilde{\Pi}$ respectively. The detailed expressions of $\tilde{\Sigma}_{ij}^V$ and $\tilde{\Pi}_{ij}^V$ depend on corresponding Feynman rules and the Passarino-Veltman functions [61,63]. In the next section we will describe our calculational

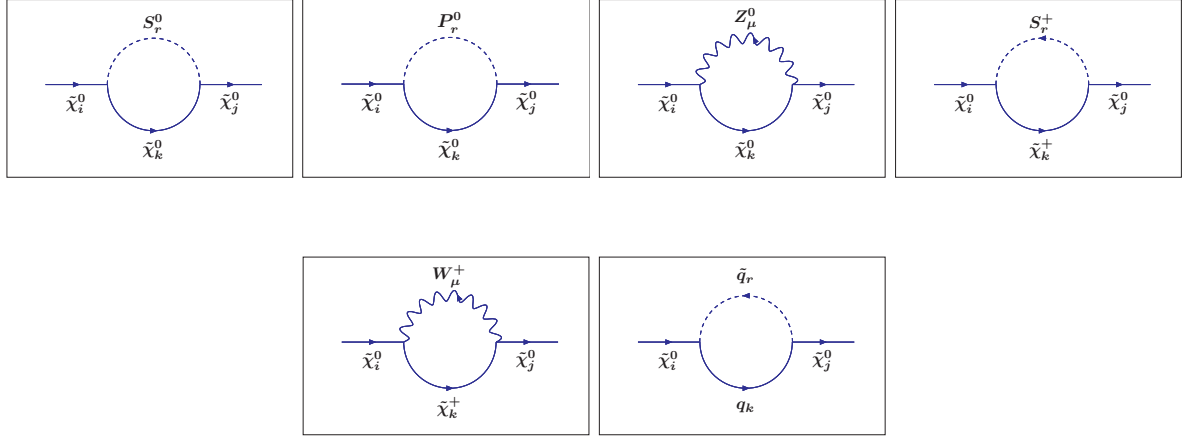


Figure 4.7: One-loop diagrams contributing to the neutralino masses. The various contributions are arising from (clockwise from top left) (a) neutralino-neutralino-neutral scalar loop, (b) neutralino-neutralino-neutral pseudoscalar loop, (c) neutralino-neutralino- Z_μ^0 loop, (d) neutralino-chargino-charged scalar loop, (e) neutralino-chargino- W_μ^\pm loop, (f) neutralino-quark-squark loop.

approach.

4.7 Analysis of neutrino masses and mixing at one-loop

In this section we consider the effect of radiative corrections to the light neutrino masses and mixing. Just for the sake of completeness it is always better to recapitulate some of the earlier works regarding one-loop corrections to the neutralino-neutrino sector. The complete set of radiative corrections to the neutralino mass matrix in the R_p conserving MSSM was discussed in ref. [64,65], and the leading order neutrino masses has been derived in ref. [66]. One-loop radiative corrections to the neutrino-neutralino mass matrix in the context of a R_p -violating model were calculated in ref. [67] using 't-Hooft-Feynman gauge. In ref. [62], R_ξ gauge has been used to compute the corrections to the neutrino-neutralino mass matrix at one-loop level in an R_p -violating scenario. For our one-loop calculations we choose to work with 't-Hooft-Feynman gauge, i.e. $\xi = 1$. Neutrino mass generation at the one-loop level in other variants of R_p -violating MSSM has been widely addressed in literature, which are already given in the beginning of subsection 3.3.2. We note in passing that in a recent reference [68] on-shell renormalization of neutralino and chargino mass matrices in R_p violating models has been addressed, which also includes the $\mu\nu$ SSM.

We begin by outlining the strategy of our analysis. We start with a general 10×10 neutralino matrix, with off-diagonal entries as well, which has a seesaw structure in the flavour-basis (see eqn.(4.12)). Schematically, we can rewrite eqn.(4.12) as,

$$\mathcal{M}_n = \begin{pmatrix} M_f & m_{D_f}^T \\ m_{D_f} & 0 \end{pmatrix}, \quad (4.45)$$

where the orders of the block matrices are same as those indicated in eqn. (4.12), and the subscript ‘ f ’ denotes the flavour basis. Here M_f stands for the 7×7 Majorana mass matrix of the heavy states, while m_{D_f} contains the 3×7 Dirac type masses for the left-handed neutrinos. In the next step, instead of utilizing the seesaw structure of this matrix to generate the effective light neutrino mass matrix for the three active light neutrino species, we *diagonalize* the entire 10×10 matrix \mathcal{M}_n . The diagonal 10×10 matrix \mathcal{M}_D^0 (eqn.(4.16)) thus contains tree level neutralino masses, which we symbolically write as [27]

$$\mathcal{M}_D^0 = \begin{pmatrix} M_m & 0 \\ 0 & m_m \end{pmatrix}, \quad (4.46)$$

where M_m (m_m) are the masses of the heavy states (left-handed neutrinos). Following eqn.(4.35) one can write

$$\begin{aligned} M_m &= \text{diag}(m_{\tilde{\chi}_1^0}, m_{\tilde{\chi}_2^0}, m_{\tilde{\chi}_3^0}, m_{\tilde{\chi}_4^0}, m_{\tilde{\chi}_5^0}, m_{\tilde{\chi}_6^0}, m_{\tilde{\chi}_7^0}), \\ m_m &= \text{diag}(m_{\nu_1}, m_{\nu_2}, m_{\nu_3}). \end{aligned} \quad (4.47)$$

At this stage we turn on all possible one-loop interactions as shown in figure 4.7, so that the 10×10 matrix \mathcal{M}_D^0 picks up radiatively generated entries, both diagonal and off-diagonal. The resulting one-loop corrected Lagrangian for the neutralino mass terms in the $\tilde{\chi}^0$ basis, following eqn.(4.11), can be written as

$$\mathcal{L}' = -\frac{1}{2} \chi^{0T} (\mathcal{M}_D^0 + \mathcal{M}^1) \chi^0 + \text{H.c.}, \quad (4.48)$$

where \mathcal{M}^1 contains the effect of one-loop corrections. The 10×10 matrix \mathcal{M}_D^0 is diagonal, but the matrix \mathcal{M}^1 is a general symmetric matrix with off diagonal entries.

One can rewrite the above equation, using eqns.(4.15) and (4.16), as

$$\mathcal{L}' = -\frac{1}{2} \Psi^{0T} (\mathcal{M}_n + \mathbf{N}^T \mathcal{M}^1 \mathbf{N}) \Psi^0 + \text{H.c.} \quad (4.49)$$

This is nothing but the *one-loop corrected* neutralino mass term in the Lagrangian in the flavour basis. Symbolically [27],

$$\mathcal{L}' = -\frac{1}{2} \Psi^{0T} \mathcal{M}' \Psi^0 + \text{H.c.}, \quad (4.50)$$

with the 10×10 matrix \mathcal{M}' having the form [27]

$$\mathcal{M}' = \begin{pmatrix} M_f + \Delta M_f & (m_{D_f} + \Delta m_{D_f})^T \\ m_{D_f} + \Delta m_{D_f} & \Delta m_f \end{pmatrix}. \quad (4.51)$$

The quantities ΔM_f and Δm_f stand for one-loop corrections to the heavy neutralino states and light neutrino states respectively, in the flavour basis Ψ^0 . The entity Δm_{D_f} arises because of the off diagonal interactions, i.e. between the heavy neutralinos and the light neutrinos, in the same basis (Ψ^0). Note that all of ΔM_f , Δm_{D_f} , Δm_f in the χ_0 basis are given by the second term on the right hand side of eqn.(4.43). We suitably transform them into the basis Ψ^0 with the help of neutralino mixing matrix \mathbf{N} . From the order of magnitude approximations³ the matrix \mathcal{M}' once again possesses a seesaw structure, and one can therefore write down the one-loop corrected effective light neutrino mass matrix as

$$(M^{\nu'})_{\text{eff}} \approx \Delta m_f - (m_{D_f} + \Delta m_{D_f})(M_f + \Delta M_f)^{-1}((m_{D_f} + \Delta m_{D_f})^T). \quad (4.52)$$

³The loop corrections are at least suppressed by a loop factor $\frac{1}{16\pi^2}$ and thus tree level order of magnitude approximations are still valid.

Let us now present an approximate form of eqn.(4.52). For simplicity, let us begin by assuming the quantities present in eqn.(4.52) to be c-numbers (not matrices). In addition, assume $M_f \gg \Delta M_f$ (justified later), so that eqn.(4.52) may be written as,

$$(M^{\nu'})_{\text{eff}} \approx \Delta m_f - \delta \times M_f \left\{ \left(\frac{m_{D_f}}{M_f} \right)^2 + 2 \left(\frac{m_{D_f}}{M_f} \right) \left(\frac{\Delta m_{D_f}}{M_f} \right) + \left(\frac{\Delta m_{D_f}}{M_f} \right)^2 \right\}, \quad (4.53)$$

with $\delta = \left(1 - \frac{\Delta M_f}{M_f}\right)$. Now, even when $\Delta m_{D_f} \sim \frac{1}{16\pi^2} m_{D_f}$ and $\Delta M_f \sim \frac{1}{16\pi^2} M_f$, eqn.(4.53) looks like

$$(M^{\nu'})_{\text{eff}} \approx \Delta m_f - M_f \left(1 - \frac{1}{16\pi^2}\right) \left\{ \left(\frac{m_{D_f}}{M_f} \right)^2 + \frac{2}{16\pi^2} \left(\frac{m_{D_f}}{M_f} \right) + \frac{1}{256\pi^4} \left(\frac{m_{D_f}}{M_f} \right)^2 \right\}. \quad (4.54)$$

Thus, up to a very good approximation one can rewrite eqn.(4.54) as

$$(M^{\nu'})_{\text{eff}} \approx \Delta m_f - M_f \left(\frac{m_{D_f}}{M_f} \right)^2. \quad (4.55)$$

Reimposing the matrix structure and using eqn.(4.22), eqn.(4.55) can be modified as,

$$(M^{\nu'})_{\text{eff}} \approx \Delta m_f + M_\nu^{\text{seesaw}}. \quad (4.56)$$

The eigenvalues of the 3×3 one-loop corrected neutrino mass matrix $(M^{\nu'})_{\text{eff}}$ thus correspond to one-loop corrected light neutrino masses. In conclusion, it is legitimate to calculate one-loop corrections to the 3×3 light neutrino mass matrix only (see eqn.(4.56)), and diagonalize it to get the corresponding one-loop corrected mass eigenvalues [27].

Let us denote the one-loop corrections to the masses of heavy neutralinos and light neutrinos in the basis χ^0 by ΔM and Δm respectively. The one-loop corrections arising from neutralino-neutrino interactions is denoted by Δm_D in the same basis. The tree level neutralino mixing matrix \mathbf{N} , in the leading power of expansion matrix ξ (eqn.(4.23)), using eqn.(4.34) can be written as,

$$\mathbf{N} = \begin{pmatrix} \mathcal{N} & \mathcal{N}\xi^T \\ -U^\dagger\xi^* & U^\dagger \end{pmatrix} = \begin{pmatrix} \tilde{N}_{7 \times 7} & \tilde{N}_{7 \times 3} \\ \tilde{N}_{3 \times 7} & \tilde{N}_{3 \times 3} \end{pmatrix}. \quad (4.57)$$

Now from the order of magnitude approximation of ξ (eqn.(4.23)) we get approximately $\xi \sim (m_D^\nu/M_{\tilde{\chi}^0})$, where m_D^ν represents a generic entry of $m_{3 \times 7}$ matrix and $M_{\tilde{\chi}^0}$ that of $M_{7 \times 7}$ (see eqn.(4.12)). So apparently the entries of the matrices $\tilde{N}_{7 \times 3}$, $\tilde{N}_{3 \times 7}$ suffers a suppression $\sim \mathcal{O}(m_D^\nu/M_{\tilde{\chi}^0})$, due to very small neutrino-neutralino mixing [69]. The quantities $m_D^\nu \sim \mathcal{O}(10^{-4} \text{ GeV})$ and $M_{\tilde{\chi}^0} \sim \mathcal{O}(10^2 \text{ GeV})$ represent the Dirac mass of a left-handed neutrino (ν_i) and the Majorana mass of a neutralino (χ_i^0), respectively. From eqns.(4.49), (4.57) it is easy to figure out the relation between Δm and Δm_f as,

$$\Delta m_f = \tilde{N}_{7 \times 3}^T \Delta M \tilde{N}_{7 \times 3} + \tilde{N}_{7 \times 3}^T \Delta m_D^T \tilde{N}_{3 \times 3} + \tilde{N}_{3 \times 3}^T \Delta m_D \tilde{N}_{7 \times 3} + \tilde{N}_{3 \times 3}^T \Delta m \tilde{N}_{3 \times 3}. \quad (4.58)$$

Now as argued earlier, for a Dirac neutrino, the mass is $\lesssim \mathcal{O}(10^{-4} \text{ GeV})$, while for a neutralino, the mass is $\sim \mathcal{O}(10^2 \text{ GeV})$. This means that the entries of the off-diagonal blocks in eqn.(4.57) are $\lesssim \mathcal{O}(10^{-6})$. Therefore, for all practical purpose, one can neglect the first three terms in comparison to the fourth term on the right hand side of eqn.(4.58). Thus,

$$\Delta m_f \approx \tilde{N}_{3 \times 3}^T \Delta m \tilde{N}_{3 \times 3}. \quad (4.59)$$

up to a very good approximation. With this in view, our strategy is to compute the one-loop corrections in the χ^0 basis first, and then use eqn.(4.59) to obtain the corresponding corrections in the flavour basis. Finally, adding tree level contribution M_ν^{seesaw} (eqn.(4.22)) to Δm_f (eqn.(4.59)), we diagonalize

eqn.(4.56) to obtain the one-loop corrected neutrino masses. We have performed all calculations in the 't-Hooft-Feynman gauge. Let us also note in passing that the form of eqn.(4.43) predicts off-diagonal entries ($i \neq j$). The off-diagonal elements are responsible for the admixtures between diagonal entries, which become dominant only when $(m_{\tilde{\chi}_i^0} - m_{\tilde{\chi}_j^0}) \lesssim (\frac{\alpha}{4\pi}) \times$ some electroweak scale mass, (using the essence of eqn.(3.28)) and then, one can choose $p^2 = \overline{m^2} = (m_{\tilde{\chi}_i^0}^2 + m_{\tilde{\chi}_j^0}^2)/2$ for external momentum [67]. Thus, one can conclude that unless the tree level masses are highly degenerate, the off-diagonal radiative corrections can be neglected for all practical purposes, when at least one indices i or j refers to a heavy states.

The self-energy corrections contain entries of the neutralino mixing matrix \mathbf{N} through the couplings $O^{ff'b}$ appearing in Feynman rules (see, appendix D) [27]. This is because, the self energies $\tilde{\Sigma}_{ij}$ and $\tilde{\Pi}_{ij}$ in general contain products of couplings of the form $O_{i..}^{ff'b} O_{j..}^{ff'b}$ (see, appendix E [27] for detailed expressions of $\tilde{\Sigma}_{ij}^V$ and $\tilde{\Pi}_{ij}^V$). The matrix \mathbf{N} , on the other hand, contains the expansion parameter ξ in the leading order (see eqn.(4.34)). This observation, together with the help of eqn.(C.1), help us to express the effective structure of the one-loop corrected neutrino mass matrix as [27],

$$[(\mathcal{M}^{\nu'})_{eff}]_{ij} = A_1 a_i a_j + A_2 c_i c_j + A_3 (a_i c_j + a_j c_i), \quad (4.60)$$

where a_i and c_i are given by eqn.(4.24) and A_i 's are functions of our model parameters and the Passarino-Veltman functions (B_0, B_1) [61, 63, 70] defined in appendix F. The form of the loop corrected mass matrix thus obtained is identical to the tree level one (see, eqn.(4.32)) with different coefficients A_1, A_2 and A_3 arising due to one-loop corrections.

Note that the one-loop diagrams in figure 4.7, contributing to the neutrino mass matrix are very similar to those obtained in bilinear R-parity violating scenario [62, 71–75]. However, it has been pointed out in ref. [26], that there is a new significant contribution coming from the loops containing the neutral scalar and pseudoscalar with dominant singlet component. This contribution is proportional to the mass-splitting between the singlet scalar and pseudoscalar states [76–78]. The corresponding mass splittings for the doublet sneutrinos are much smaller [26]. In fact the sum of contributions of the singlet scalar ($\tilde{\nu}_{n\mathcal{R}}^c$) and pseudoscalar states ($\tilde{\nu}_{n\mathcal{I}}^c$) (see diagrams one and two of the top row of figure 4.7) is $\propto \kappa^2 v c^2$, squared mass difference between the singlet scalar and pseudoscalar mass eigenstates [26]. The effect of one-loop correction to light neutrino masses and mixing has been considered in ref. [26] for one and two generations of right-handed neutrinos.

To conclude this section we finally concentrate on the one-loop contributions to light neutrino mixing. The tree level 3×3 orthogonal matrix U diagonalizes the tree level seesaw matrix M_ν^{seesaw} as shown in eqn.(4.35). In a similar fashion the 3×3 orthogonal matrix (in the limit of all phases equal to zero) that diagonalizes the one-loop corrected neutrino mass matrix $(M^{\nu'})_{\text{eff}}$ (eqn.(4.56)), can be denoted as U' . Mathematically

$$U'^T (M^{\nu'})_{\text{eff}} U' = \text{diag}(m'_1, m'_2, m'_3), \quad (4.61)$$

with m'_1, m'_2, m'_3 as the three one-loop corrected light neutrino masses. The matrix U' now can be used (see eqn.(4.36)) to extract the one loop corrected light neutrino mixing angles, $\theta'_{23}, \theta'_{12}, \theta'_{13}$.

In the next section we will discuss the effect of one-loop corrections to the light neutrino masses and mixing in $\mu\nu$ SMS for different light neutrino mass hierarchy.

4.8 One-loop corrections and mass hierarchies

Analytical forms for the tree level and the one-loop corrected light neutrino mass matrices are given by eqn.(4.22) and eqn.(4.60), respectively. Note that in both of the equations the first two terms ($\propto a_i a_j, \propto c_i c_j$) individually can generate only one neutrino mass, $\propto \sum a_i^2$ and $\propto \sum c_i^2$, respectively. These terms are the effect of the *ordinary* and the *gaugino* seesaw, as already discussed in section 4.5. Together, they can generate two neutrino masses which is sufficient to satisfy the neutrino oscillation data without the cross term ($a_i c_j + a_j c_i$). However, it is the effect of the mixing terms ($a_i c_j + a_j c_i$) which together with the first two terms along with different co-efficients for each term give masses to all three light neutrinos [25, 27].

In the following three consecutive subsections we will analyze the effect of one-loop radiative corrections on the light neutrino masses and mixing when the mass orderings are (1) normal, (2) inverted and (3) quasi-degenerate in nature. The choice of model parameters are given in table 4.6 [25, 27]. Apart from the right-handed sneutrino VEVs other variables are chosen to be the left sneutrino VEVs

Parameter	Chosen Value	Parameter	Chosen Value
λ	0.10	$(A_\lambda \lambda)$	-100 GeV
κ	0.45	$(A_\kappa \kappa)$	450 GeV
$m_{\tilde{e}^c}^2$	300^2 GeV^2	v^c	-895 to -565 GeV
$(A_\nu Y_\nu)^{ii}$	$Y_\nu^{ii} \times 1 \text{ TeV}$	$\tan \beta$	10
M_1	110 GeV	M_2	220 GeV

Table 4.6: Choice of parameters for numerical analysis consistent with the EWSB conditions. These choices are according to the eqn.(4.8). The gaugino soft masses M_1 and M_2 are assumed to be GUT (grand unified theory) motivated, so that, at the electroweak scale, we have $M_1 : M_2 = 1 : 2$.

(v'_i) and the flavour diagonal neutrino Yukawa couplings (Y_ν^{ii}). These are given in table 4.7 [25, 27]. To fit the three flavour global data we consider not only the oscillation constraints (see table 3.1) but

	$Y_\nu^{ii} \times 10^7$			$v'_i \times 10^5 (\text{GeV})$		
	Y_ν^{11}	Y_ν^{22}	Y_ν^{33}	v'_1	v'_2	v'_3
Normal hierarchy	3.550	5.400	1.650	0.730	10.100	12.450
Inverted hierarchy	12.800	3.300	4.450	8.350	8.680	6.400
Quasi-degenerate-I	19.60	19.94	19.99	9.75	10.60	11.83
Quasi-degenerate-II	18.50	18.00	18.00	9.85	10.50	10.10

Table 4.7: Values of the neutrino Yukawa couplings and the left-handed sneutrino VEVs, used as sample parameter points for numerical calculations. These are the values around which the corresponding parameters were varied. Other parameter choices are given in table 4.6.

also constraints from various non-oscillation experiments like Tritium beta decay, neutrinoless double beta decay and cosmology both for the tree level and the one-loop combined analysis.

4.8.1 Normal hierarchy

In the normal hierarchical pattern of the three light neutrino masses (individual masses are denoted by m_i , $i = 1, 2, 3$), the atmospheric and the solar mass squared differences, given by $\Delta m_{atm}^2 = m_3^2 - m_2^2$ and $\Delta m_{solar}^2 = m_2^2 - m_1^2$, are largely governed by the higher mass squared in each case, namely, m_3^2 and m_2^2 , respectively. Before going into the discussion of the variation of the mass-squared values with the model parameter, some general remarks are in order. First of all, note that in eqn.(4.24), if we choose v'_i such that $v'_i \gg \frac{Y_\nu^{ii} v_1}{3\lambda}$, then $b_i \approx c_i$ [28]. Second, both the tree level and the one-loop corrected light neutrino mass matrix have similar structure as shown in eqn.(4.32) and eqn.(4.60). Due to this structural similarity we expect both the tree and the one-loop corrected masses and mixing to show similar type of variations with certain relevant quantities, however with some modifications, because of the inclusion of the one-loop corrections. This similarity also indicates that the light neutrino masses and mixing are entirely controlled by a_i and c_i .

In this subsection, we show the variation of the neutrino squared masses (m_i^2) and the atmospheric and solar mass squared differences with the square of the seesaw parameters $\frac{c_i^2}{M}$ and $\frac{a_i^2}{m_{\nu^c}}$ for normal ordering in light neutrino masses. Results are shown for the tree level as well as the one-loop corrected neutrino masses. These plots also demonstrate the importance of one-loop corrections to neutrino masses compared to the tree level results [27].

Typical mass spectra are shown in figure 4.8. Note that a particular model parameter has been varied while the others are fixed at values given in tables 4.6 and 4.7. The effective light neutrino mass matrix given in eqn.(4.31) suggests that as long as $v'_i \gg \frac{Y_\nu^{ii} v_1}{3\lambda}$ and $\kappa \gg \lambda$, the second term on the

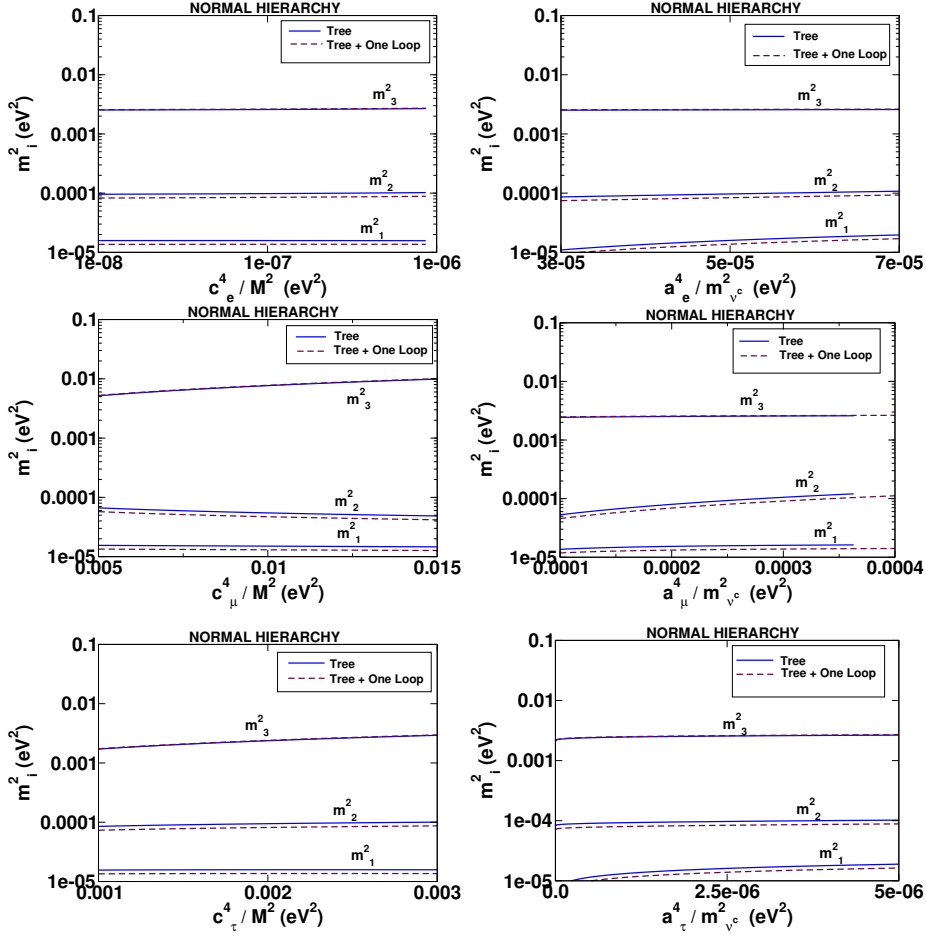


Figure 4.8: Neutrino mass squared values (m_i^2) versus $\frac{c_i^4}{M^2}$ (left panel) and versus $\frac{a_i^4}{m_{\nu c}^2}$ (right panel) plots for the *normal hierarchical* pattern of light neutrino masses, $i = e, \mu, \tau$. Parameter choices are shown in tables 4.6 and 4.7.

right hand side of eqn.(4.31) dominates over the first term and as a result the heaviest neutrino mass scale (m_3) is controlled mainly by the gaugino seesaw effect. This is because in this limit $b_i \approx c_i$, and, as discussed earlier, a neutrino mass matrix with a structure $\sim \frac{c_i c_j}{M}$ can produce only one non-zero neutrino mass. This feature is evident in figure 4.8, where we see that m_3^2 increases as a function of c_i^4/M^2 . The other two masses are almost insensitive to c_i^2/M . A mild variation to m_2^2 comes from the combined effect of gaugino and ordinary seesaw (see the $(a_i c_j + a_j c_i)$ terms in eqns.(4.32), (4.60)). On the other hand, the two lighter neutrino mass scales (m_2^2 and m_1^2) are controlled predominantly by the ordinary seesaw parameters $a_i^2/m_{\nu c}$. This behaviour is observed in the right panel figures of figure 4.8. The heaviest neutrino mass scale is not much affected by the quantities $a_i^2/m_{\nu c}$.

One can also see from these plots that the inclusion of one-loop corrections, for the chosen values of the soft SUSY breaking parameters, reduces the values of m_2^2 and m_1^2 , while increasing the value of m_3^2 only mildly. This is because, with such a choice, the one-loop corrections cause partial cancellation in the generation of m_1 and m_2 . For the heaviest state, it is just the opposite, since the diagonalization of the tree-level mass matrix already yields a negative mass eigenvalue, on which the loop correction has an additive effect. If, with all other parameters fixed, the signs of λ and A_λ are reversed (leading to a positive μ in the place of a negative one), m_1 , m_2 and m_3 are all found to decrease through loop corrections. A flip in the sign of κ and the corresponding soft breaking terms, on the other hand, causes a rise in all the mass eigenvalues, notably for m_1 and m_2 .

In the light of the discussion above, we now turn to explain the variation of Δm_{atm}^2 and Δm_{solar}^2 with c_i^4/M^2 and $a_i^4/m_{\nu c}^2$ shown in figure 4.9 and figure 4.10. For our numerical analysis, in order to set

the scale of the normal hierarchical spectrum, we choose $m_2|_{max} < 0.011$ eV. The left panel in figure 4.9 shows that Δm_{atm}^2 increases more rapidly with $c_{\mu,\tau}^4/M^2$, whereas the variation with c_e^4/M^2 is much slower as expected from figure 4.8. Similar behaviour is shown for the one-loop corrected Δm_{atm}^2 . The small increase in the one-loop corrected result compared to the tree level one is essentially due to the splitting in m_2^2 value as shown earlier. The variation of Δm_{solar}^2 with c_i^4/M^2 can be explained in a similar manner. Obviously, in this case the one-loop corrected result is smaller compared to the tree level one (see, figure 4.8). However, one should note that Δm_{solar}^2 falls off with c_μ^4/M^2 as opposed to the variation with respect to the other two gaugino seesaw parameters. This is due to the fact that m_2^2 slightly decreases with c_μ^4/M^2 but show a slow increase with respect to c_e^4/M^2 and c_τ^4/M^2 . The dark solid lines in all these figures show the allowed values of various parameters where all the neutrino mass and mixing constraints are satisfied.

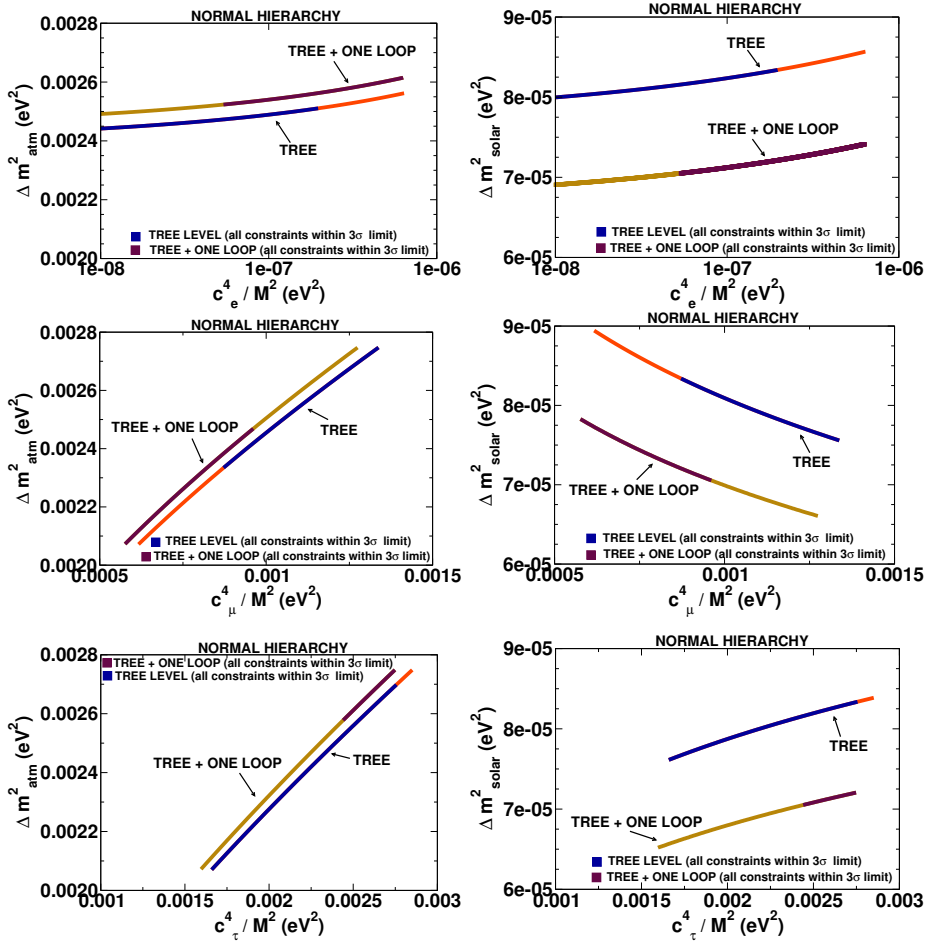


Figure 4.9: Atmospheric and solar mass squared differences (Δm_{atm}^2 , Δm_{solar}^2) vs $\frac{c_i^4}{M^2}$ plots for the normal hierarchical pattern of light neutrino masses, $i = e, \mu, \tau$. The full lines are shown for which only the constraints on Δm_{solar}^2 is not within the 3σ limit (see table 3.1). The dark coloured portions on these lines are the values of parameters for which all the neutrino constraints are within the 3σ limit. The red (yellow) coloured lines in the plots correspond to the tree (one-loop corrected) regions where all the constraints except Δm_{solar}^2 are within 3σ allowed region. Parameter choices are shown in tables 4.6 and 4.7.

The variation of Δm_{atm}^2 and Δm_{solar}^2 with $a_i^4/m_{\nu^c}^2$ in figure 4.10 can be understood in a similar way by looking at the right panel plots of figure 4.8. Δm_{atm}^2 shows a very little increase with $a_{e,\mu}^4/m_{\nu^c}^2$ as expected, whereas the change is more rapid with $a_\tau^4/m_{\nu^c}^2$ for the range of values considered along the x-axis. As in the case of figure 4.9, the solid dark lines correspond to the allowed values of parameters where all the neutrino mass and mixing constraints are satisfied.

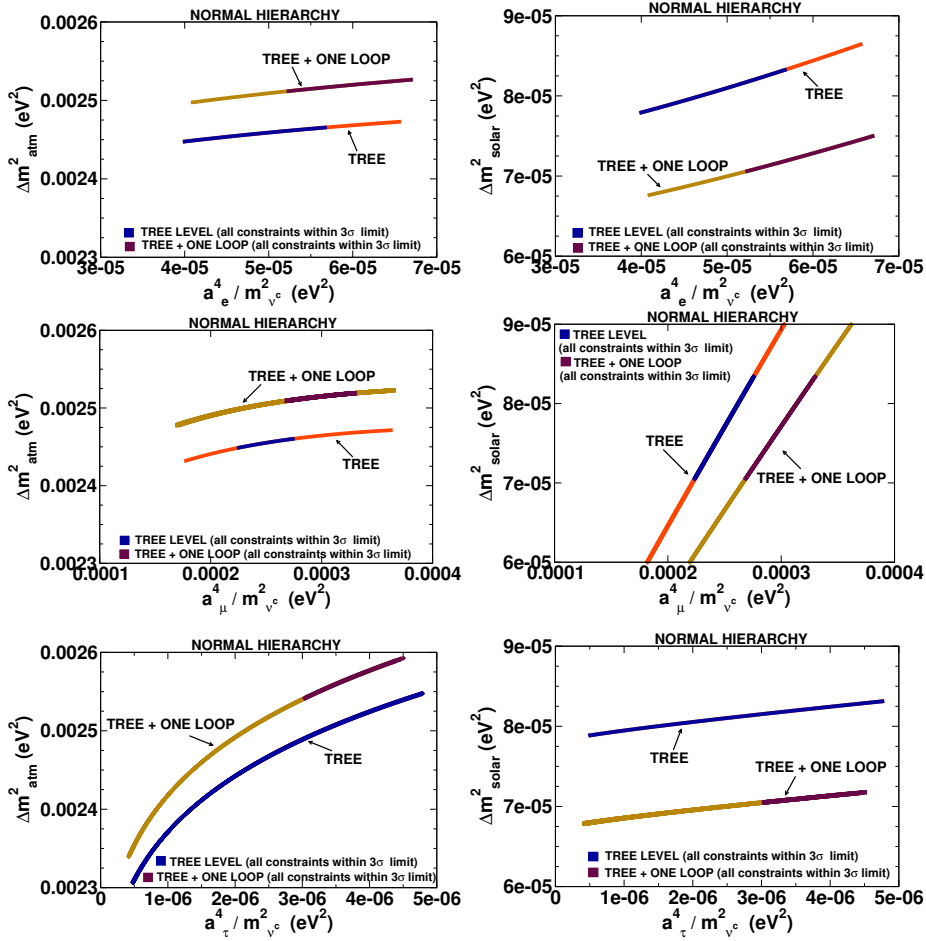


Figure 4.10: Atmospheric and solar mass squared differences (Δm_{atm}^2 , Δm_{solar}^2) vs $a_i^4/m_{\nu^c}^2$ plots for the *normal hierarchical* pattern of light neutrino masses with $i = e, \mu, \tau$. Colour specification is same as described in the context of figure 4.9. Parameter choices are shown in tables 4.6 and 4.7.

For higher values of $a_{e,\tau}^4/m_{\nu^c}^2$, m_2^2 increases very slowly with these parameters (see, figure 4.8) and this is reflected in the right panel plots of figure 4.10, where Δm_{solar}^2 shows a very slow variation with $a_{e,\tau}^4/m_{\nu^c}^2$. On the other hand, m_2^2 increases more rapidly with $a_{\mu}^4/m_{\nu^c}^2$, giving rise to a faster variation of Δm_{solar}^2 . The plots of figure 4.10 show that larger values of Yukawa couplings are required in order to satisfy the global three flavour neutrino data, when one considers one-loop corrected neutrino mass matrix. However, there are allowed ranges of the parameters $a_i^4/m_{\nu^c}^2$, where the neutrino data can be satisfied with both tree and one-loop corrected analysis.

We have also considered the variation of light neutrino mass squared differences with the effective bilinear R_P violating parameter, $\varepsilon_i = Y^{ij}v_j^c$. For this particular numerical study we vary both Y_{ν}^{ii} and the right-handed sneutrino VEVs (v_i^c) simultaneously, in the suitable ranges around the values given in tables 4.6 and 4.7. Δm_{atm}^2 is found to increase with ε_i , whereas the solar mass squared difference decreases with increasing ε_i . The 3σ allowed region for the solar and atmospheric mass squared differences were obtained for the lower values of ε_i s. In addition, we have noticed that the correlations of Δm_{atm}^2 with ε_i is sharper compared to the correlations seen in the case of Δm_{solar}^2 .

Next let us discuss the dependence of Δm_{atm}^2 and Δm_{solar}^2 on two specific model parameters, λ and κ , consistent with EWSB conditions. The loop corrections shift the allowed ranges of κ to lower values with some amount of overlap with the tree level result. On the other hand, the allowed ranges of λ shrinks towards higher values when one-loop corrections are included. These results are shown in figure 4.11. We note in passing that the mass of the lightest CP-even scalar decreases with increasing λ . For example, $\lambda = 0.15$ can produce a lightest scalar mass of 40 GeV, for suitable choices of other

parameters. This happens because with increasing λ , the lightest scalar state picks up more and more right-handed sneutrino admixture. This phenomena as discussed earlier has serious consequence in the mass of the lightest Higgs boson in $\mu\nu$ SSM (see section 4.3 and also eqn.(4.9)).

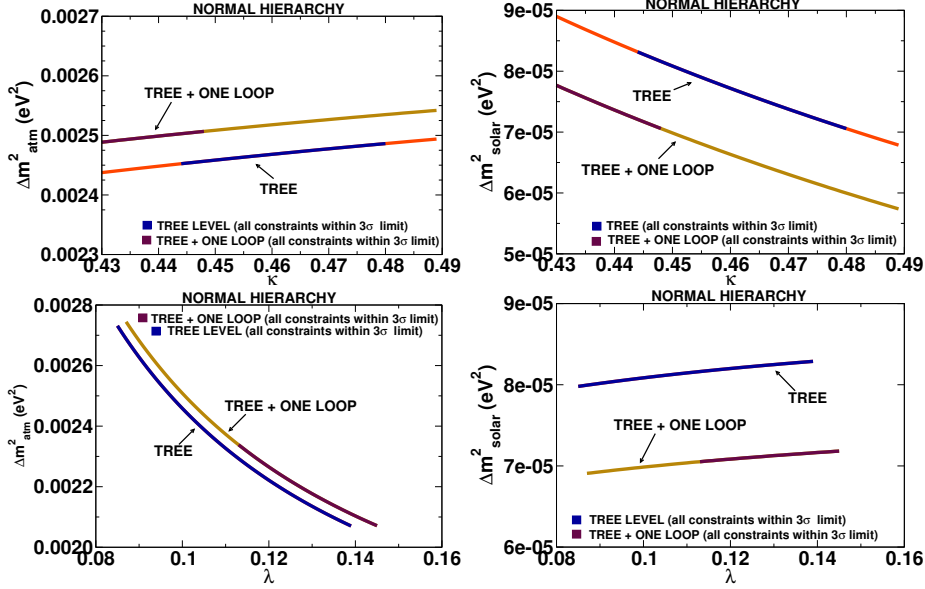


Figure 4.11: Plots showing the variations of Δm_{atm}^2 , Δm_{solar}^2 with model parameters λ and κ for *normal hierarchy*. Colour specification is same as described in the context of figure 4.9. Parameter choices are shown in tables 4.6 and 4.7.

Finally, we will discuss the $\tan\beta$ dependence of Δm_{atm}^2 and Δm_{solar}^2 . These plots are shown in figure 4.12. The quantity Δm_{atm}^2 decreases with the increasing values of $\tan\beta$ and nearly saturates for larger values of $\tan\beta$. However, the one-loop corrected result for Δm_{atm}^2 is not much different from that at the tree level for a particular value of $\tan\beta$. On the other hand, the solar mass squared difference initially increases with $\tan\beta$ and for higher values of $\tan\beta$ the variation slows down and tends to saturate. The one-loop corrections result in lower values of Δm_{solar}^2 for a particular $\tan\beta$. The darker and bigger points on both the plots of figure 4.12 are the allowed values of $\tan\beta$, where all the neutrino experimental data are satisfied. Note that only a very small range of $\tan\beta$ (~ 10 – 14) is allowed. This is a very important observation of this analysis.

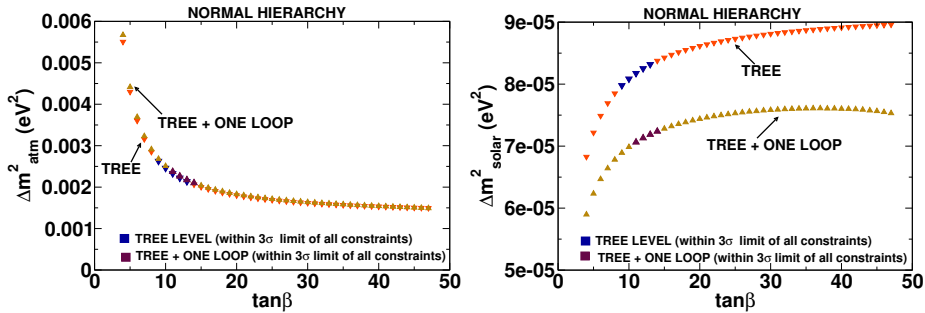


Figure 4.12: Δm_{atm}^2 , Δm_{solar}^2 vs $\tan\beta$ plots for the *normal hierarchical* pattern of light neutrino masses. The allowed values of $\tan\beta$ are shown by bold points. Other parameter choices are shown in tables 4.6 and 4.7.

Next we will discuss the light neutrino mixing and the effect of one-loop corrections on the mixing angles. It was shown in ref. [25] that for the normal hierarchical pattern of neutrino masses, when the parameter $b_i \sim a_i$ (see subsection 4.5.1), the neutrino mixing angles θ_{23} and θ_{13} can be written as (with the tree level analysis), (see eqns.(4.39), (4.38))

$$\sin^2 \theta_{23} \approx \frac{b_\mu^2}{b_\mu^2 + b_\tau^2}, \quad (4.62)$$

and

$$\sin^2 \theta_{13} \approx \frac{b_e^2}{b_\mu^2 + b_\tau^2}. \quad (4.63)$$

On the other hand, the mixing angle θ_{12} is a much more complicated function of the parameters b_i and a_i and we do not show it here. Now, when $b_i \sim a_i$, we can easily see from eqn.(4.24), that

$$v'_i \sim \frac{Y_\nu^{ii} v_1}{3\lambda} (\tan \beta - 1). \quad (4.64)$$

This implies that for $\tan \beta \gg 1$ (recall that the allowed range of $\tan \beta$ is ~ 10 – 14),

$$v'_i \gg \frac{Y_\nu^{ii} v_1}{3\lambda}. \quad (4.65)$$

As we have discussed earlier, for such values of v'_i , the quantities $b_i \approx c_i$. Hence, the mixing angles θ_{23} and θ_{13} can be approximately written as

$$\sin^2 \theta_{23} \approx \frac{c_\mu^2}{c_\mu^2 + c_\tau^2}, \quad (4.66)$$

and

$$\sin^2 \theta_{13} \approx \frac{c_e^2}{c_\mu^2 + c_\tau^2}. \quad (4.67)$$

Naively, one would also expect that $\sin^2 \theta_{12}$ should show some correlation with the quantity c_e^2/c_μ^2 . However, as mentioned earlier, this is a very simple minded expectation since $\sin^2 \theta_{12}$ has a more complicated dependence on the model parameters (see eqn.(4.40)).

The variation of all three mixing angles with the corresponding parameters are shown in figure 4.13. Note that in order to generate these plots, we vary only the quantities c_i and all the other parameters are fixed at the values given in tables 4.6 and 4.7. We have chosen the range of parameters in such a way that the 3-flavour global neutrino data are satisfied. The mixing angles have been calculated numerically by diagonalizing the neutrino mass matrix in eqn.(4.31) and in eqn.(4.60). As expected from our approximate analytical expressions, these plots show very nice correlations of the mixing angles θ_{23} and θ_{13} with the relevant parameters as discussed in eqns.(4.66) and (4.67). For example, note that when $c_\mu \approx c_\tau$, $\sin^2 \theta_{23}$ is predicted to be ≈ 0.5 and that is what we observe in the tree level plot in figure 4.13. However, when one-loop corrections are considered, the value of $\sin^2 \theta_{23}$ is predicted to be somewhat on the lower side of the 3σ allowed region. This can be understood by looking at the left panel plots of figure 4.9, where one can see that the one-loop corrected results prefer lower values of c_μ^2 and higher values of c_τ^2 . Obviously, this gives smaller $\sin^2 \theta_{23}$. On the other hand, the tree level analysis prefers higher values of c_μ^2 and both lower and higher values of c_τ^2 . This gives rise to large as well as small values of $\sin^2 \theta_{23}$.

If one looks at the plot of $\sin^2 \theta_{13}$ in figure 4.13, then it is evident that the amount of ν_e flavour in the heaviest state (ν_3) decreases a little bit with the inclusion of one-loop corrections for a fixed value of the quantity $\frac{c_e^2}{(c_\mu^2 + c_\tau^2)}$. Very small $\sin^2 \theta_{13}$ demands $c_e^2 \ll c_\mu^2, c_\tau^2$. This feature is also consistent with the plots in figure 4.9. The correlation of $\sin^2 \theta_{12}$ with the ratio c_e^2/c_μ^2 is not very sharp as expected from the discussion given above. However, a large θ_{12} mixing angle requires a larger value of this ratio. The effect of one-loop correction is more pronounced in this case and predicts a smaller value of $\sin^2 \theta_{12}$ compared to the tree level result. There is no specific correlation of the mixing angles with the quantities a_i^2 and we do not show them here.

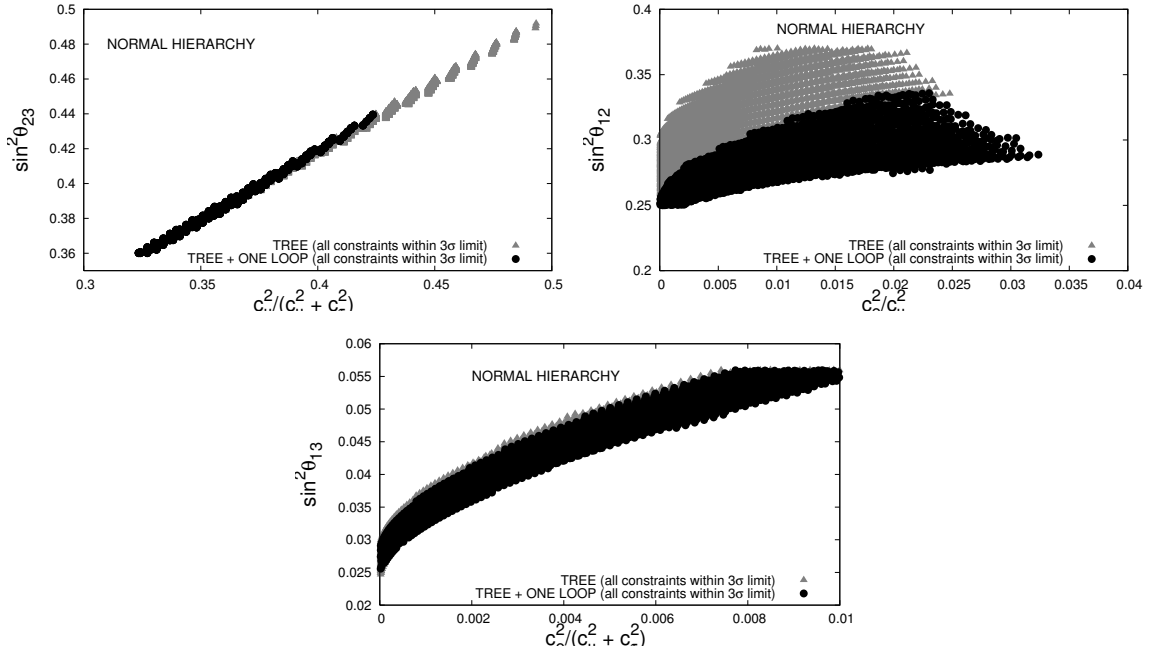


Figure 4.13: Variation of $\sin^2\theta_{23}$ with $\frac{c_e^2}{(c_e^2+c_\tau^2)}$, $\sin^2\theta_{12}$ with $\frac{c_e^2}{c_\mu^2}$, $\sin^2\theta_{13}$ with $\frac{c_e^2}{(c_e^2+c_\tau^2)}$ for normal hierarchy of light neutrino masses. Parameter choices are shown in tables 4.6 and 4.7.

4.8.2 Inverted hierarchy

In this subsection we perform a similar numerical analysis for the inverted hierarchical scheme of three light neutrino masses. Recall that for the inverted hierarchical pattern of light neutrino masses, the absolute values of the mass eigenvalues are such that $m_2 > m_1 \gg m_3$. Thus the solar and the atmospheric mass squared differences are defined as $\Delta m_{atm}^2 = m_1^2 - m_3^2$ and $\Delta m_{solar}^2 = m_2^2 - m_1^2$. In order to generate such a mass pattern, the choices of neutrino Yukawa couplings Y_ν^{ii} and the left-handed sneutrino VEVs v_i^c are shown in table 4.7. However, these are just sample choices and other choices also exist as we will see during the course of this discussion. The choices of other parameters are shown in table 4.6. The effect of one-loop corrections to the mass eigenvalues are such that the absolute values of masses m_3 and m_1 become smaller whereas m_2 grows in magnitude. This effect of increasing the absolute value of m_2 while decreasing that of m_1 makes it extremely difficult to account for the present 3σ limits on Δm_{solar}^2 .

Typical mass spectra are shown in figure 4.14. Once again note that a particular model parameter has been varied while the others are fixed at values given in tables 4.6 and 4.7. As it is evident from these plots, the masses m_1 and m_3 are controlled mainly by the parameters a_i^2/m_ν^c , whereas the mass m_2 is controlled by the seesaw parameters c_i^2/M though there is a small contribution coming from a_i^2/m_ν^c as well.

Let us now turn our attention to the variation of $|\Delta m_{atm}^2|$ and Δm_{solar}^2 with c_i^4/M^2 and a_i^4/m_ν^c shown in figure 4.15 and figure 4.16. For our numerical analysis, we have set the scale of m_3 as $|m_3|_{max} < 0.011$ eV. The left panel in figure 4.15 shows that $|\Delta m_{atm}^2|$ increases with $c_{\mu,\tau}^4/M^2$ and decreases with c_e^4/M^2 . This is essentially the behaviour shown by m_1^2 with the variation of c_i^4/M^2 . Similar behaviour is obtained for the one-loop corrected Δm_{atm}^2 . The decrease in the one-loop corrected result compared to the tree level one is due to the splitting in m_1^2 value as shown in figure 4.14.

The variation of Δm_{solar}^2 with c_i^4/M^2 can be understood in a similar manner by looking at figure 4.14. As explained earlier, in the case of Δm_{solar}^2 , the one-loop corrected result is larger compared to the tree level one. The range of parameters satisfying all the three flavour global neutrino data are shown by the fewer dark points on the plots. Note that the increase of Δm_{solar}^2 at the one-loop level is such that we do not even see any allowed range of parameters when looking at the variation with respect to $c_{e,\tau}^4/M^2$. Once again, the behaviour of Δm_{atm}^2 and Δm_{solar}^2 with the change in the

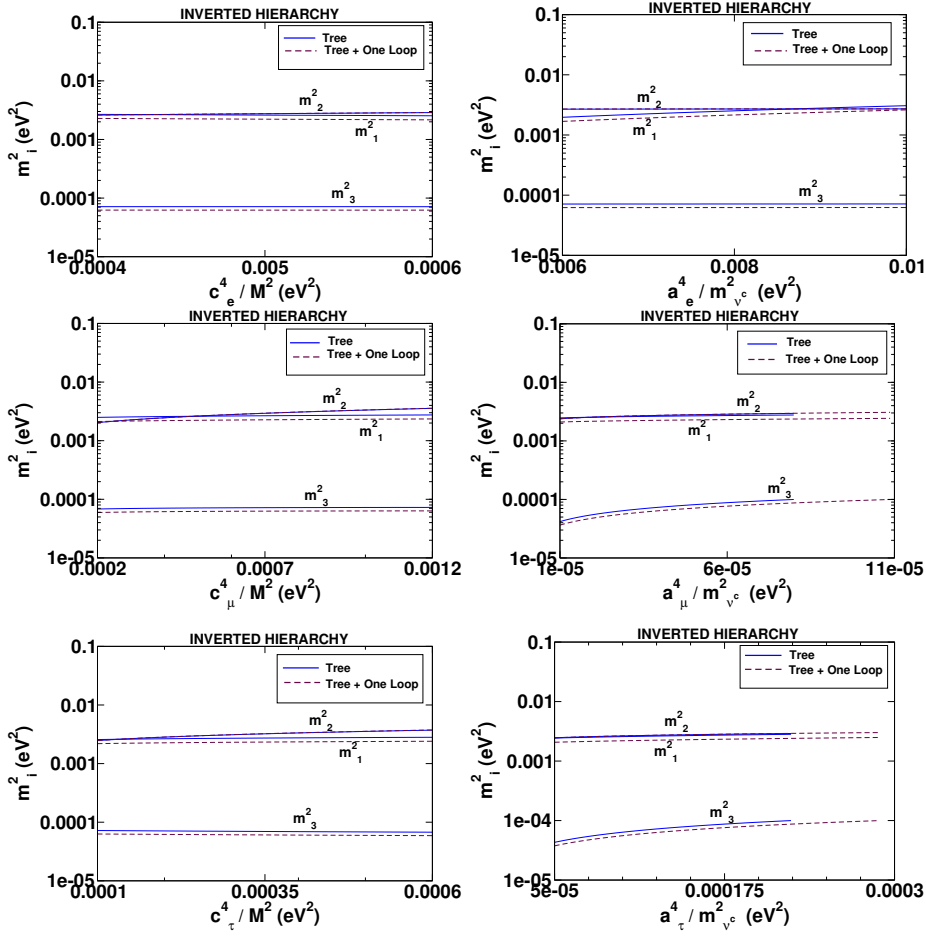


Figure 4.14: Neutrino mass squared values (m_i^2) vs $\frac{c_i^4}{M^2}$ (left panel) and vs $\frac{a_i^4}{m_{\nu^c}^2}$ (right panel) plots for the *inverted hierarchical* pattern of light neutrino masses, $i = e, \mu, \tau$. Parameter choices are shown in tables 4.6 and 4.7.

parameters $a_i^4/m_{\nu^c}^2$ (shown in figure 4.16) can be explained by looking at the right panel plots of figure 4.14.

We have also investigated the nature of variation of $|\Delta m_{atm}^2|$ and Δm_{solar}^2 with ε_i^2 , the squared effective bilinear R_P -violating parameters. $|\Delta m_{atm}^2|$ was found to increase with ε_i^2 (the increase is sharper for ε_1^2), whereas Δm_{solar}^2 initially increases very sharply with ε_i^2 (particularly for ε_1^2 and ε_2^2) and then becomes flat. In the one-loop corrected results we do not find any range of values for parameters where the neutrino data are satisfied. These plots are not shown here.

The variation of mass squared differences with λ and κ have also been analyzed. The variation of $|\Delta m_{atm}^2|$ and Δm_{solar}^2 with λ and κ are found to be opposite to those of normal hierarchical scenario. The one-loop corrected results do not show any allowed ranges of λ and κ (for the chosen values of other parameters) where the neutrino data can be satisfied.

The $\tan\beta$ dependence of $|\Delta m_{atm}^2|$ and Δm_{solar}^2 is shown in figure 4.17. One can see from these two figures that $|\Delta m_{atm}^2|$ initially increases and then start decreasing at a value of $\tan\beta$ around 10. On the other hand, Δm_{solar}^2 initially decreases and then start increasing around the same value of $\tan\beta$. Note that the one-loop corrected result for $|\Delta m_{atm}^2|$ is lower than the corresponding tree level result for $\tan\beta < 10$ whereas the one-loop corrected result for Δm_{solar}^2 is lower than the corresponding tree level result for $\tan\beta > 10$. For the chosen values of other parameters we see that the one-loop corrected analysis does not provide any value of $\tan\beta$ where the neutrino data can be satisfied.

We conclude the discussion on inverted hierarchy by addressing the dependence of neutrino mixing angles with the relevant parameters. In figure 4.18 we show the variation of the neutrino mixing angles

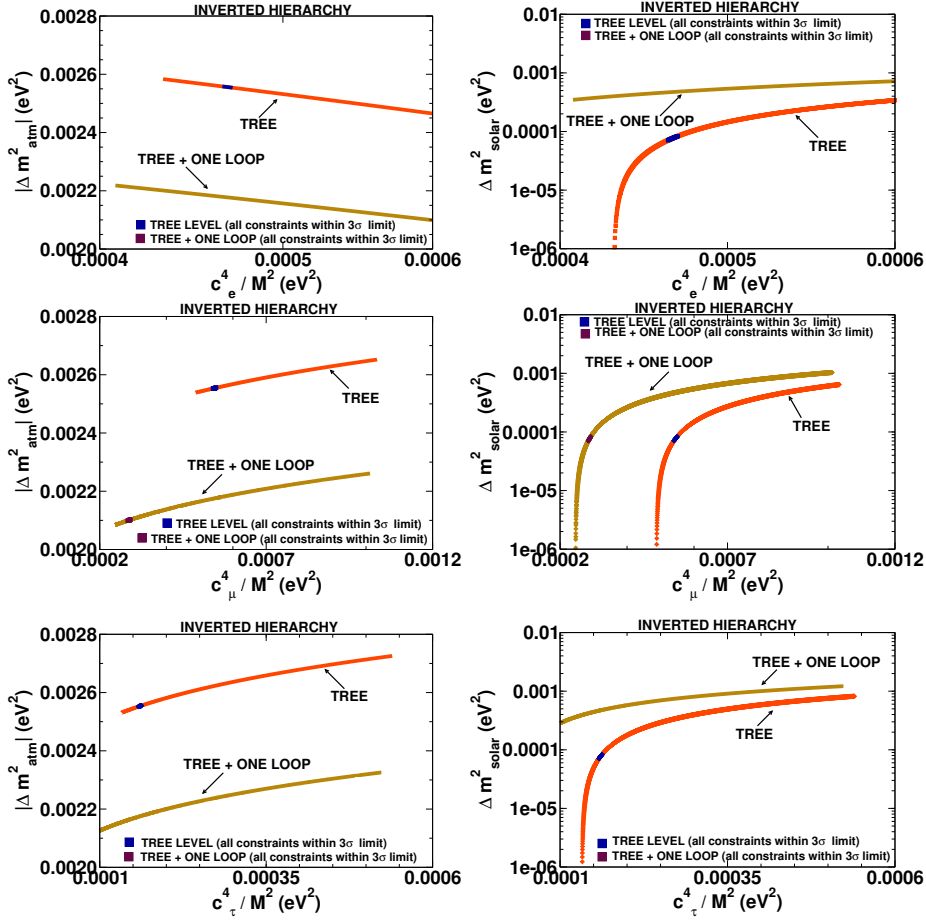


Figure 4.15: Atmospheric and solar mass squared differences ($|\Delta m_{atm}^2|$, Δm_{solar}^2) vs $\frac{c_i^4}{M^2}$ plots for the *inverted hierarchical* pattern of light neutrino masses with $i = e, \mu, \tau$. Colour specification is same as described in the context of figure 4.9. Parameter choices are shown in tables 4.6 and 4.7.

with the same set of parameters as chosen for the normal hierarchical scenario. We notice that for inverted hierarchy the quantity $\sin^2 \theta_{23}$ decreases with increasing $\frac{c_\mu^2}{(c_\mu^2 + c_\tau^2)}$ which is just opposite to that of the normal hierarchy (see, figure 4.13). Nevertheless, the correlation of $\sin^2 \theta_{23}$ with $\frac{c_\mu^2}{(c_\mu^2 + c_\tau^2)}$ is as sharp as in the case of normal hierarchy. A similar feature is obtained for the variation with $\frac{a_\mu^2}{(a_\mu^2 + a_\tau^2)}$.

On the other hand, the correlations of $\sin^2 \theta_{12}$ with $\frac{c_e^2}{c_\mu^2}$ and $\frac{a_e^2}{a_\mu^2}$ and the correlations of $\sin^2 \theta_{13}$ with $\frac{c_e^2}{(c_\mu^2 + c_\tau^2)}$ and $\frac{a_e^2}{(a_\mu^2 + a_\tau^2)}$ are not very sharp and we do not show them here. There are allowed values of relevant parameters where all neutrino data can be satisfied. Remember that, for the plots with c_i s, we varied all the c_i s simultaneously, keeping the values of a_i s fixed at the ones determined by the parameters in table 4.7. Similarly, for the variation of a_i s, the quantities c_i s were kept fixed. The inclusion of one-loop corrections restrict the allowed values of parameter points significantly compared to the tree level results.

4.8.3 Quasi-degenerate spectra

The discussion on the light neutrino mass spectrum remains incomplete without a note on the so-called “quasi-degenerate” scenario. A truly degenerate scenario of three light neutrino masses is, however, inconsistent with the oscillation data. Hence, the quasi-degenerate scenario of light neutrino masses is defined in such a way that in this case all the three individual neutrino masses are much larger compared

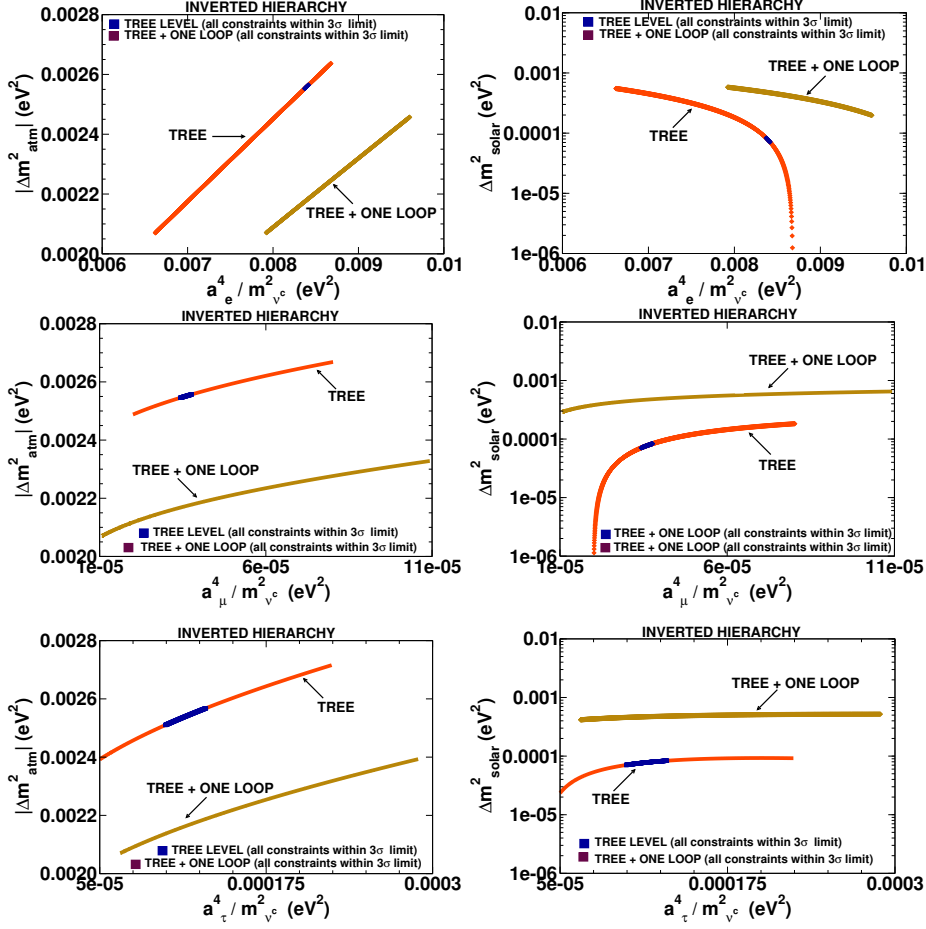


Figure 4.16: Atmospheric and solar mass squared differences ($|\Delta m_{atm}^2|$, Δm_{solar}^2) vs $a_i^4/m_{\nu c}^2$ plots for the *inverted hierarchical* pattern of light neutrino masses with $i = e, \mu, \tau$. Colour specification is same as described in the context of figure 4.9. Parameter choices are shown in tables 4.6 and 4.7.

to the atmospheric neutrino mass scale. Mathematically, one writes $m_1 \approx m_2 \approx m_3 \gg \sqrt{|\Delta m_{atm}^2|}$. Obviously, the oscillation data suggest that even in such a situation there must be a mild hierarchy among the degenerate neutrinos. It is important to note that unlike the normal or inverted hierarchical scheme of light neutrino masses, in the case of quasi-degenerate neutrinos all three neutrinos must be massive in order to satisfy oscillation data (see table 3.1). In the case of normal or inverted hierarchical neutrino masses it is possible to accommodate the three flavour neutrino data even with two massive neutrinos.

In this subsection we have shown that the huge parameter space of $\mu\nu$ SJM always leaves us with enough room to accommodate quasi-degenerate spectrum. For our numerical analysis, we called a set of light neutrino masses to be quasi-degenerate if the lightest among them is greater than 0.1 eV. We choose two sets of sample parameter points which are given below in tabular form (values of other parameters are same as in table 4.6). For these two sets of neutrino Yukawa couplings (Y_{ν}^{ii}) and the left-handed sneutrino VEVs (v_i') we observe the following patterns of light neutrino masses at the tree level

- (i) Quasi-degenerate-I: $m_3 \gtrsim m_2 \gtrsim m_1 \gg \sqrt{|\Delta m_{atm}^2|}$
- (ii) Quasi-degenerate-II: $m_2 \gtrsim m_1 \gtrsim m_3 \gg \sqrt{|\Delta m_{atm}^2|}$.

For case (i), we have varied the parameters around the values in table 4.7 and identified a few extremely fine-tuned points in the parameter space where either the tree level or the one-loop corrected result is consistent with the three flavour global neutrino data. Two representative spectrum as function of $\frac{c_e^4}{M^2}$ and $\frac{a_e^4}{m_{\nu c}^2}$ are shown in figure 4.19. The mass spectrum for Quasi-degenerate-I case is analogous to

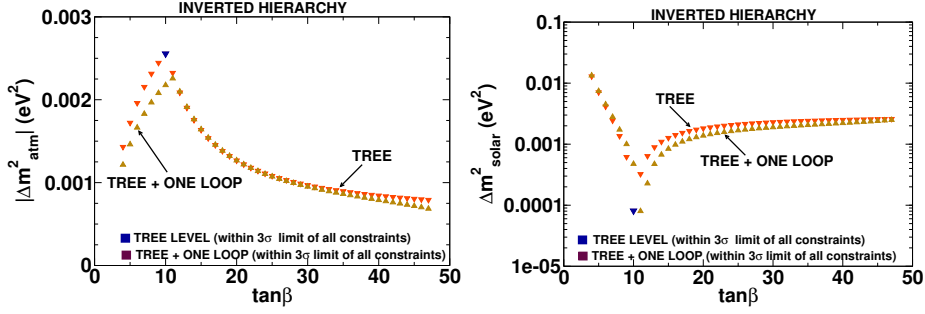


Figure 4.17: $|\Delta m_{atm}^2|$, Δm_{solar}^2 vs $\tan\beta$ plots for the *inverted hierarchical* pattern of light neutrino masses. Colour specification is same as described in the context of figure 4.9. Parameter choices are shown in tables 4.6 and 4.7.

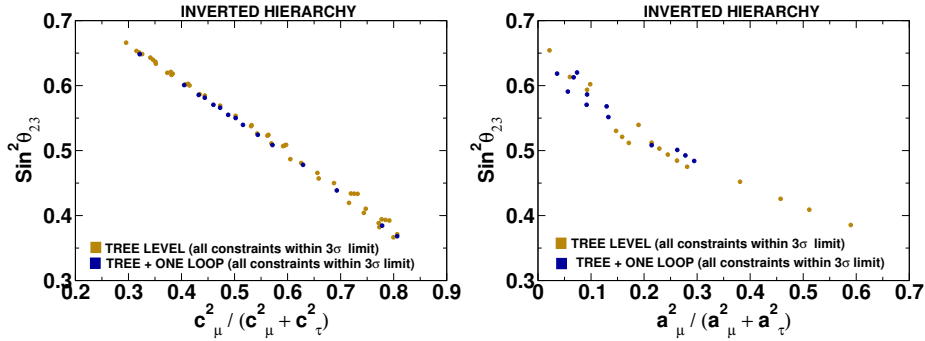


Figure 4.18: Variation of $\sin^2 \theta_{23}$ with $\frac{c_\mu^2}{(c_\mu^2 + c_\tau^2)}$ and $\frac{a_\mu^2}{(a_\mu^2 + a_\tau^2)}$ for inverted hierarchy of light neutrino masses. Parameter choices are shown in tables 4.6 and 4.7.

a normal hierarchical scenario whereas that for Quasi-degenerate-II resembles a inverted spectrum.

As mentioned earlier, one can play with the model parameters and obtain a spectrum with a different ordering of masses termed as “Quasi-degenerate-II” in table 4.7. However, for such an ordering of masses, we found that it was rather impossible to find any region of parameter space where the one-loop corrected result satisfies all the constraints on neutrino masses and mixing. Nevertheless, we must emphasize here that it is not a completely generic conclusion and for other choices of soft SUSY breaking and other parameters it could be possible to have a spectrum like that shown in “Quasi degenerate II” with neutrino constraints satisfied even at the one-loop level. On the other hand, there exist regions where neutrino data are satisfied at the tree level with this ordering of masses.

4.9 Summary

So in a nutshell in $\mu\nu$ SSM it is possible to account for three flavour global neutrino data itself at the tree level even with the choice of flavour diagonal neutrino Yukawa couplings. Besides, different hierarchical (normal, inverted, quasi-degenerate) scheme of light neutrino mass can be accommodated by playing with the hierarchy in Yukawa couplings. The tree level results of neutrino masses and mixing show appreciable variation with the inclusion of the one-loop radiative corrections, depending on the light neutrino mass hierarchy.

It seems so far that the $\mu\nu$ SSM is extremely successful in accommodating massive neutrinos both with tree level and one-loop combined analysis, consistent with the three flavour global data (see

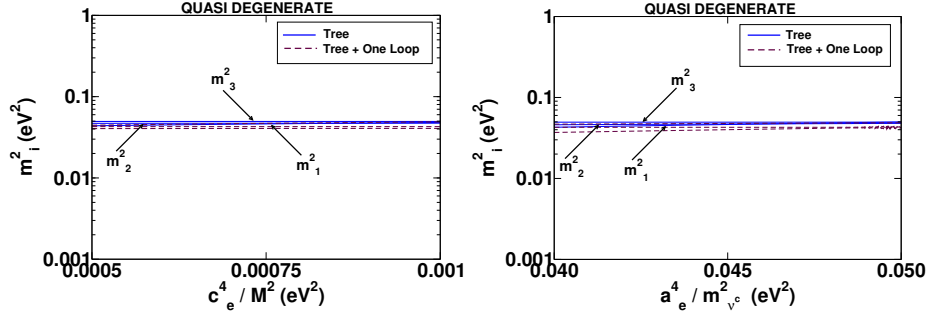


Figure 4.19: Neutrino mass squared values (m_i^2) vs $\frac{c_e^4}{M^2}$ (left panel) and vs $\frac{a_e^4}{m_{\nu e}^2}$ (right panel) plots for the *quasi-degenerate* pattern of light neutrino masses. Parameter choices are shown in tables 4.6 and 4.7.

table 3.1). But how to test these neutrino physics information in a collider experiment, which can give additional checks for the $\mu\nu$ SSM model? Fortunately for us certain ratios of the decay branching ratios of the lightest neutralino (which is also the LSP for a large region of the parameter space) show nice correlations with certain light neutrino mixing angle [25,26]. These correlations could act as excellent probes to the $\mu\nu$ SSM model in the ongoing era of the colliders. These issues will be considered in details in the next chapter.

Bibliography

- [1] Kim J E and Nilles H P 1984 *Phys. Lett.* **B138** 150
- [2] Abada A and Moreau G 2006 *JHEP* **08** 044
- [3] Abada A, Bhattacharyya G and Moreau G 2006 *Phys. Lett.* **B642** 503–509
- [4] Hundi R S, Pakvasa S and Tata X 2009 *Phys. Rev.* **D79** 095011
- [5] Jean-Louis C C and Moreau G 2010 *J. Phys.* **G37** 105015
- [6] Pandita P N and Paulraj P F 1999 *Phys. Lett.* **B462** 294–301
- [7] Pandita P N 2001 *Phys. Rev.* **D64** 056002
- [8] Chemtob M and Pandita P N 2006 *Phys. Rev.* **D73** 055012
- [9] Kitano R and Oda K y 2000 *Phys. Rev.* **D61** 113001
- [10] Nilles H P and Polonsky N 1997 *Nucl. Phys.* **B484** 33–62
- [11] Frank M, Huitu K and Ruppell T 2007 *Eur. Phys. J.* **C52** 413–423
- [12] Das D and Roy S 2010 *Phys. Rev.* **D82** 035002
- [13] Abada A, Bhattacharyya G, Das D and Weiland C 2010 (*Preprint* 1011.5037)
- [14] Lopez-Fogliani D E and Munoz C 2006 *Phys. Rev. Lett.* **97** 041801
- [15] Ellis J R, Gunion J F, Haber H E, Roszkowski L and Zwirner F 1989 *Phys. Rev.* **D39** 844
- [16] Ellis J R *et al.* 1986 *Phys. Lett.* **B176** 403
- [17] Rai B and Senjanovic G 1994 *Phys. Rev.* **D49** 2729–2733
- [18] Abel S A, Sarkar S and White P L 1995 *Nucl. Phys.* **B454** 663–684
- [19] Abel S A 1996 *Nucl. Phys.* **B480** 55–72
- [20] Panagiotakopoulos C and Tamvakis K 1999 *Phys. Lett.* **B446** 224–227
- [21] Panagiotakopoulos C and Tamvakis K 1999 *Phys. Lett.* **B469** 145–148
- [22] Escudero N, Lopez-Fogliani D E, Munoz C and de Austri R R 2008 *JHEP* **12** 099
- [23] Mukhopadhyaya B and Srikanth R 2006 *Phys. Rev.* **D74** 075001
- [24] Farzan Y and Valle J W F 2006 *Phys. Rev. Lett.* **96** 011601
- [25] Ghosh P and Roy S 2009 *JHEP* **04** 069
- [26] Bartl A, Hirsch M, Vicente A, Liebler S and Porod W 2009 *JHEP* **05** 120
- [27] Ghosh P, Dey P, Mukhopadhyaya B and Roy S 2010 *JHEP* **05** 087

- [28] Fidalgo J, Lopez-Fogliani D E, Munoz C and Ruiz de Austri R 2009 *JHEP* **08** 105
- [29] Drees M 1989 *Int. J. Mod. Phys.* **A4** 3635
- [30] Binetruy P and Savoy C A 1992 *Phys. Lett.* **B277** 453–458
- [31] Espinosa J R and Quiros M 1992 *Phys. Lett.* **B279** 92–97
- [32] Espinosa J R and Quiros M 1993 *Phys. Lett.* **B302** 51–58
- [33] Espinosa J R and Quiros M 1998 *Phys. Rev. Lett.* **81** 516–519
- [34] Daikoku Y and Suematsu D 2000 *Prog. Theor. Phys.* **104** 827–833
- [35] Ellwanger U and Hugonie C 2007 *Mod. Phys. Lett.* **A22** 1581–1590
- [36] Pontecorvo B 1957 *Sov. Phys. JETP* **6** 429
- [37] Pontecorvo B 1958 *Sov. Phys. JETP* **7** 172–173
- [38] Maki Z, Nakagawa M and Sakata S 1962 *Prog. Theor. Phys.* **28** 870–880
- [39] Pontecorvo B 1968 *Sov. Phys. JETP* **26** 984–988
- [40] Nowakowski M and Pilaftsis A 1996 *Nucl. Phys.* **B461** 19–49
- [41] Gunion J F and Haber H E 1986 *Nucl. Phys.* **B272** 1
- [42] Schechter J and Valle J W F 1982 *Phys. Rev.* **D25** 774
- [43] Hirsch M and Valle J W F 1999 *Nucl. Phys.* **B557** 60–78
- [44] Hirsch M, Romao J C and Valle J W F 2000 *Phys. Lett.* **B486** 255–262
- [45] Minkowski P 1977 *Phys. Lett.* **B67** 421
- [46] Yanagida T In Proceedings of the Workshop on the Baryon Number of the Universe and Unified Theories, Tsukuba, Japan, 13-14 Feb 1979
- [47] Glashow S L 1980 *NATO Adv. Study Inst. Ser. B Phys.* **59** 687
- [48] Mohapatra R N and Senjanovic G 1980 *Phys. Rev. Lett.* **44** 912
- [49] Gell-Mann M, Ramond P and Slansky R Print-80-0576 (CERN)
- [50] Schechter J and Valle J W F 1980 *Phys. Rev.* **D22** 2227
- [51] Foot R, Lew H, He X G and Joshi G C 1989 *Z. Phys.* **C44** 441
- [52] Ma E 1998 *Phys. Rev. Lett.* **81** 1171–1174
- [53] Wolfram S 5th ed. (Wolfram media, 2003)
- [54] Schwetz T, Tortola M A and Valle J W F 2008 *New J. Phys.* **10** 113011
- [55] Gonzalez-Garcia M C, Maltoni M and Salvado J 2010 *JHEP* **04** 056
- [56] Siegel W 1979 *Phys. Lett.* **B84** 193
- [57] Capper D M, Jones D R T and van Nieuwenhuizen P 1980 *Nucl. Phys.* **B167** 479
- [58] Avdeev L V, Chochia G A and Vladimirov A A 1981 *Phys. Lett.* **B105** 272
- [59] Avdeev L V and Vladimirov A A 1983 *Nucl. Phys.* **B219** 262
- [60] Jack I and Jones D R T 1997 (*Preprint hep-ph/9707278*)

- [61] Passarino G and Veltman M J G 1979 *Nucl. Phys.* **B160** 151
- [62] Hirsch M, Diaz M A, Porod W, Romao J C and Valle J W F 2000 *Phys. Rev.* **D62** 113008
- [63] 't Hooft G and Veltman M J G 1979 *Nucl. Phys.* **B153** 365–401
- [64] Pierce D and Papadopoulos A 1994 *Phys. Rev.* **D50** 565–570
- [65] Pierce D and Papadopoulos A 1994 *Nucl. Phys.* **B430** 278–294
- [66] Hall L J and Suzuki M 1984 *Nucl. Phys.* **B231** 419
- [67] Hempfling R 1996 *Nucl. Phys.* **B478** 3–30
- [68] Liebler S and Porod W 2011 (*Preprint* 1106.2921)
- [69] Atre A, Han T, Pascoli S and Zhang B 2009 *JHEP* **05** 030
- [70] Hahn T and Perez-Victoria M 1999 *Comput. Phys. Commun.* **118** 153–165
- [71] Davidson S and Losada M 2000 *JHEP* **05** 021
- [72] Davidson S and Losada M 2002 *Phys. Rev.* **D65** 075025
- [73] Diaz M A, Hirsch M, Porod W, Romao J C and Valle J W F 2003 *Phys. Rev.* **D68** 013009
- [74] Grossman Y and Rakshit S 2004 *Phys. Rev.* **D69** 093002
- [75] Dedes A, Rimmer S and Rosiek J 2006 *JHEP* **08** 005
- [76] Hirsch M, Klapdor-Kleingrothaus H V and Kovalenko S G 1997 *Phys. Lett.* **B398** 311–314
- [77] Grossman Y and Haber H E 1997 *Phys. Rev. Lett.* **78** 3438–3441
- [78] Dedes A, Haber H E and Rosiek J 2007 *JHEP* **11** 059

Chapter 5

$\mu\nu$ S \overline{S} M: decay of the LSP

5.1 A decaying LSP

We have learned already in section 2.6 that the lightest supersymmetric particle (LSP) is absolutely stable so long as R_p is conserved. Besides, as argued in section 3.4 that the LSP has to be charge and colour neutral [1–3] so long it preserves its stability. Consequently, only the electrically neutral colourless sparticles remain to be the only possible choice for the LSP. Interestingly, when R_p is broken (figure 2.5, see also section 2.6), any sparticle (the lightest neutralino, chargino [4], squark, gluino [5–7], sneutrino [8], (see also ref. [3])) can be the LSP. In a supersymmetric model with broken R_p the LSP will decay into further lighter states namely, into the SM particles. Apart from the neutrinos rest of these decay products are easily detectable in a collider experiment and thus can act as a potential probe for the underlying model. Since $\mu\nu$ S \overline{S} M is an R_p -violating supersymmetric model, the LSP for this model is also unstable and can yield striking signatures at the collider which we aim to discuss in this chapter. This remarkable feature is absent in the conventional R_p conserving supersymmetric models, where any sparticle decay ends with LSP in the final state and hence yield large missing energy signatures. For example if the lightest neutralino ($\tilde{\chi}_1^0$) is the LSP then the following two and three body decay modes are kinematically possible

$$\begin{aligned}\tilde{\chi}_1^0 &\rightarrow W^\pm \ell^\mp, Z^0 \nu_k, h^0 \nu_k, \\ &\rightarrow b\bar{b}\nu_k, \ell_i^+ \ell_j^- \nu_k, q_i \bar{q}_i \nu_k, q_i \bar{q}_j' \ell_k^\mp, \nu_i \bar{\nu}_j \nu_k.\end{aligned}\tag{5.1}$$

The lightest neutralino ($\tilde{\chi}_1^0$) can be the LSP in a large region of the parameter space. The three body decay modes become dominant when mass of the LSP ($m_{\tilde{\chi}_1^0}$) is less than that of the W -boson (m_W). The corresponding Feynman diagrams are given in appendix G, section G.1 (figures G.1, G.2). It is also interesting to note that apart from these tree level two and three body decays the LSP can also decay into a neutrino and a photon radiatively [9–12].

One more important aspect in the decays of the lightest supersymmetric particle through R_p -violating channel is the appearance of the displaced vertices [13–17]. The displaced vertices appear to be macroscopic (\sim a few mm or larger) due to the smallness of the associated R_p -violating couplings. A displaced vertex is defined as the distance traversed by a neutral particle between the primary and the secondary interaction points. The displaced vertices are extremely useful to remove undesired backgrounds in case of a collider analysis. The length of the displaced vertices also vary with the nature of the lightest neutralino or the LSP. Thus, before proceeding further it is important to discuss about the various LSP scenario in $\mu\nu$ S \overline{S} M. We note in passing that in this chapter we concentrate on the two-body decays only and in the next chapter we will discuss about the three body decays.

5.2 Different LSP scenarios in $\mu\nu$ S \overline{S} M

In the $\mu\nu$ S \overline{S} M the neutralino sector is highly enriched compared to that of the MSSM due to R_p -violating mixing of the MSSM neutralinos with the three generations of left-handed and right-handed

neutrinos. So mathematically in $\mu\nu$ SSM with gaugino mass unification at the GUT scale (that is at the electroweak scale $M_2 = 2M_1$), possible LSP natures are described by

1. $\chi_1^0 \approx \mathbf{N}_{11}\tilde{B}^0$, $|\mathbf{N}_{11}|^2 \sim 1 \Rightarrow$ bino like $\tilde{\chi}_1^0$.
2. $\chi_1^0 \approx \mathbf{N}_{13}\tilde{H}_d^0 + \mathbf{N}_{14}\tilde{H}_u^0$, $|\mathbf{N}_{13}|^2 + |\mathbf{N}_{14}|^2 \sim 1 \Rightarrow$ higgsino like $\tilde{\chi}_1^0$.
3. $\chi_1^0 \approx \sum \mathbf{N}_{i,\alpha+4}\nu_\alpha^c$, $|\mathbf{N}_{15}|^2 + |\mathbf{N}_{16}|^2 + |\mathbf{N}_{17}|^2 \sim 1 \Rightarrow$ right-handed neutrino (ν^c) like $\tilde{\chi}_1^0$.

In terms of the model ingredients the LSP nature in $\mu\nu$ SSM depends on the relative dominance of three parameters, (1) the $U(1)$ gaugino soft mass M_1 (see eqn.(4.2)), (2) the higgsino mass parameter or the μ -term ($= 3\lambda v^c$) (see eqns.(4.6), (4.8)) and (3) the right-chiral neutrino Majorana mass term, m_{ν^c} ($= 2\kappa v^c$) (using eqn.(4.8), see eqn.(C.2)) [18–20]. Thus we can write

I. $\mu, m_{\nu^c} > M_1 \Rightarrow$ LSP bino (gaugino) like.

II. $M_1, m_{\nu^c} > \mu \Rightarrow$ LSP higgsino like.

III. $M_1, \mu > m_{\nu^c} \Rightarrow$ LSP right-handed neutrino like. Since right-handed neutrinos are singlet under the SM gauge group, a right-handed neutrino like LSP is often called a “*singlino*” LSP.

It is important to mention that the right sneutrinos ($\tilde{\nu}^c$) are also eligible candidate for the LSP in $\mu\nu$ SSM [18, 21]. Also as a continuation of the discussion of the last section, the length of the displaced vertices can vary from a few mm to a few cm for a bino like LSP to a higgsino like LSP [18, 19]. On the other hand, for a singlino LSP the length of the displaced vertices can be as large as a few meters [19, 20]. None of these are unexpected since a bino like LSP, being a gaugino, has gauge interactions and the gauge couplings are $\sim \mathcal{O}(1)$ couplings whereas a higgsino like LSP involves smaller Yukawa couplings which is responsible for a smaller decay width and consequently a larger (\sim a few cm) displaced vertices. A singlino LSP on the other hand is mostly a gauge singlet fermion by nature and thus couples to other particles via very small R_p -violating couplings, which finally yield a large displaced vertex.

5.3 Decays of the lightest neutralino in $\mu\nu$ SSM

In this section we aim to calculate a few tree level two-body decays of the lightest neutralino $\tilde{\chi}_1^0$ in $\mu\nu$ SSM model [18]. As stated earlier we denote the lightest neutralino as $\tilde{\chi}_1^0$ when the seven neutralino masses (see eqn.(4.16)) are arranged in the increasing order of magnitude ($\tilde{\chi}_1^0$ being the lightest and $\tilde{\chi}_7^0$ being the heaviest). However, for this chapter from now on, we follow the convention of ref. [18] where the eigenvalues are arranged in reverse order so that $\tilde{\chi}_7^0$ denotes the lightest neutralino. The lightest neutralino considered here is either the LSP or the next-to LSP (NLSP). The lightest neutralino mass is set to be more than m_W such that two-body decays dominate. Two-body and three-body decays of the LSP in $\mu\nu$ SSM has been discussed in a recent ref. [19] with one generation of right handed neutrino superfield. Three-body decays of a singlino like lightest neutralino (which is also the LSP) for $\mu\nu$ SSM also has been addressed in ref. [20].

In this section we mainly concentrate on the two-body decays like

$$\begin{aligned}\tilde{\chi}_7^0 &\longrightarrow W^\pm + \ell_k^\mp \\ \tilde{\chi}_7^0 &\longrightarrow Z + \nu_k, ,\end{aligned}\tag{5.2}$$

where $k = 1, 2, 3 \equiv e, \mu, \tau$. The required Feynman rules are given in appendix D. Let us also remark that the lightest neutralino can also decay to $h^0 + \nu_k$, if it is kinematically allowed, where h^0 is the MSSM-like lightest Higgs boson (this is true if the amount of admixture of the MSSM Higgses with the right-handed sneutrinos are very small). However, for our illustration purposes we have considered the mass of the lightest neutralino in such a way that this decay is either kinematically forbidden or very much suppressed (assuming a lower bound on the mass of h to be 114 GeV). Even if this decay branching ratio is slightly larger, it is usually smaller than the branching ratios in the $(\ell_i^\pm + W^\mp)$ channel. Hence, this will not affect our conclusions regarding the ratios of branching ratios in the charged lepton channel ($\ell_i + W$), to be discussed later. The lightest neutralino decay $\tilde{\chi}_7^0 \rightarrow \nu + \tilde{\nu}^c$, where $\tilde{\nu}^c$ is the scalar partner of the gauge singlet neutrino ν^c , is always very suppressed. We will discuss more on this when we consider a ν^c dominated lightest neutralino in subsection 5.4.3.

Consider the following decay process

$$\tilde{\chi}_i \longrightarrow \tilde{\chi}_j + V,\tag{5.3}$$

where $\tilde{\chi}_{i(j)}$ is either a neutralino¹ or chargino, with mass $m_{i(j)}$ and V is the gauge boson which is either W^\pm or Z , with mass m_v . The masses m_i and m_j are positive.

The decay width for this process in eqn.(5.3) is given by [22–24]

$$\Gamma(\tilde{\chi}_i \longrightarrow \tilde{\chi}_j + V) = \frac{g^2 \mathcal{K}^{1/2}}{32 \pi m_i^3 m_W^2} \times \{(G_L^2 + G_R^2) \mathcal{F} - G_L^* G_R \mathcal{G}\}, \quad (5.4)$$

where \mathcal{F} , \mathcal{G} are functions of m_i, m_j, m_v and given by

$$\begin{aligned} \mathcal{F}(m_i, m_j, m_v) &= \mathcal{K} + 3 m_v^2 (m_i^2 + m_j^2 - m_v^2), \\ \mathcal{G}(m_i, m_j, m_v) &= 12 \epsilon_i \epsilon_j m_i m_j m_v^2, \end{aligned} \quad (5.5)$$

with $\epsilon_i(j)$ carrying the actual signs (± 1) of the neutralino masses [25]. The chargino masses must be positive. The kinematical factor \mathcal{K} is given by

$$\mathcal{K}(m_i^2, m_j^2, m_v^2) = (m_i^2 + m_j^2 - m_v^2)^2 - 4 m_i^2 m_j^2. \quad (5.6)$$

In order to derive eqn.(5.4), we have used the relation $m_W^2 = m_Z^2 \cos^2 \theta_W$ and since $v'_i \ll v_1, v_2$, some of the MSSM relations still hold good. The factors G_L, G_R are given here for some possible decay modes

$$\begin{aligned} \text{For } \tilde{\chi}_i^0 &\longrightarrow \tilde{\chi}_j^0 Z \\ G_L &= O_{ji}^{\prime L}, \quad G_R = O_{ji}^{\prime R}, \\ \text{For } \tilde{\chi}_i^0 &\longrightarrow \tilde{\chi}_j^+ W^- \\ G_L &= O_{ij}^L, \quad G_R = O_{ij}^R, \end{aligned} \quad (5.7)$$

where $O_{ji}^{\prime L(R)}$ and $O_{ij}^{L(R)}$ are given by (using eqns.(D.8),(D.13) without the sign factors ϵ_i, η_j)

$$\begin{aligned} O_{ij}^{\prime L} &= -\frac{1}{2} \mathbf{N}_{i3} \mathbf{N}_{j3}^* + \frac{1}{2} \mathbf{N}_{i4} \mathbf{N}_{j4}^* - \frac{1}{2} \mathbf{N}_{i,k+7} \mathbf{N}_{j,k+7}^*, \\ O_{ij}^{\prime R} &= -O_{ij}^{\prime L*}, \quad k = 1, 2, 3, \\ O_{ij}^L &= \mathbf{N}_{i2} \mathbf{V}_{j1}^* - \frac{1}{\sqrt{2}} \mathbf{N}_{i4} \mathbf{V}_{j2}^*, \\ O_{ij}^R &= \mathbf{N}_{i2}^* \mathbf{U}_{j1} + \frac{1}{\sqrt{2}} \mathbf{N}_{i3}^* \mathbf{U}_{j2} + \frac{1}{\sqrt{2}} \mathbf{N}_{i,k+7}^* \mathbf{U}_{j,k+2}. \end{aligned} \quad (5.8)$$

Now consider the decays shown in eqn.(5.2). At this stage let us discuss our notation and convention for calculating these decays [18]. The neutralino mass matrix is a 10×10 mass matrix which includes three generations of the left-handed as well as the gauge-singlet neutrinos (eqns.(4.13), (4.14)). If the mass eigenvalues of this matrix are arranged in the descending order then the three lightest eigenvalues of this 10×10 neutralino mass matrix would correspond to the three light neutrinos. Out of the remaining seven heavy eigenvalues, the lightest one is denoted as the lightest neutralino. Thus, as argued earlier in our notation $\tilde{\chi}_7^0$ is the lightest neutralino (LN) and $\tilde{\chi}_{j+7}^0$, where $j = 1, 2, 3$ correspond to the three light neutrinos [18]. Similarly, for the chargino masses, $\tilde{\chi}_{l+2}^\pm$ ($l = 1, 2, 3$) corresponds to the charged leptons e, μ, τ . Immediately, with this choice, we can write down different natures of the lightest neutralino as

- A. $\chi_7^0 \approx \mathbf{N}_{71} \tilde{B}^0$, $|\mathbf{N}_{71}|^2 \sim 1 \Rightarrow$ bino like LN.
- B. $\chi_7^0 \approx \mathbf{N}_{73} \tilde{H}_d^0 + \mathbf{N}_{74} \tilde{H}_u^0$, $|\mathbf{N}_{73}|^2 + |\mathbf{N}_{74}|^2 \sim 1 \Rightarrow$ higgsino like LN.
- C. $\chi_7^0 \approx \sum \mathbf{N}_{7,\alpha+4} \nu_\alpha^c$, $|\mathbf{N}_{75}|^2 + |\mathbf{N}_{76}|^2 + |\mathbf{N}_{77}|^2 \sim 1 \Rightarrow \nu^c$ like LN.

So for $\tilde{\chi}_{LN}^0 \rightarrow Z + \nu_k$, which is also equivalent to $\tilde{\chi}_7^0 \rightarrow Z + \tilde{\chi}_{j+7}^0$ ($j = 1, 2, 3$), one gets from eqn.(5.7) and eqn.(5.8)

$$\begin{aligned} G_L &= -\frac{1}{2} \mathbf{N}_{j+7,3} \mathbf{N}_{73}^* + \frac{1}{2} \mathbf{N}_{j+7,4} \mathbf{N}_{74}^* - \frac{1}{2} \mathbf{N}_{j+7,k+7} \mathbf{N}_{7,k+7}^*, \\ G_R &= -G_L^*, \end{aligned} \quad (5.9)$$

¹Remember that the neutrinos are also a part of the extended neutralino matrix (eqn.(4.10)).

where $j, k = 1, 2, 3$ and this in turn modifies eqn.(5.4) as

$$\Gamma(\tilde{\chi}_7^0 \rightarrow Z + \tilde{\chi}_{j+\tau}^0) = \frac{g^2 \mathcal{K}^{1/2}}{32 \pi m_{\tilde{\chi}_7^0}^3 m_W^2} \times \left\{ 2 G_L^2 \mathcal{F} + G_L^{*2} \mathcal{G} \right\}, \quad (5.10)$$

with $m_i = m_{\tilde{\chi}_7^0}$, $m_j = m_{\nu_j} \approx 0$ (eqn.(4.16)) and $m_v = m_Z$.

Let us now consider the other decay which is $\tilde{\chi}_{LN}^0 \rightarrow W^\pm + \ell^\mp$ or equivalently $\tilde{\chi}_7^0 \rightarrow W^\pm + \tilde{\chi}_j^\mp$ ($j = 3, 4, 5$).

For the process $\tilde{\chi}_7^0 \rightarrow W^- + \tilde{\chi}_j^+$

$$\begin{aligned} \Gamma(\tilde{\chi}_7^0 \rightarrow W^- + \tilde{\chi}_j^+) &= \frac{g^2 \mathcal{K}^{1/2}}{32 \pi m_{\tilde{\chi}_7^0}^3 m_W^2} \times \left\{ (G_L^2 + G_R^2) \mathcal{F} - G_L^* G_R \mathcal{G} \right\}, \\ G_L &= \mathbf{N}_{72} \mathbf{V}_{j1}^* - \frac{1}{\sqrt{2}} \mathbf{N}_{74} \mathbf{V}_{j2}^*, \\ G_R &= \mathbf{N}_{72}^* \mathbf{U}_{j1} + \frac{1}{\sqrt{2}} \mathbf{N}_{73}^* \mathbf{U}_{j2} + \frac{1}{\sqrt{2}} \mathbf{N}_{7,k+\tau}^* \mathbf{U}_{j,k+2}, \\ (k &= 1, 2, 3), \end{aligned} \quad (5.11)$$

where eqn.(5.7) and eqn.(5.8) have been used. The process $\tilde{\chi}_7^0 \rightarrow W^+ + \tilde{\chi}_j^-$ is obtained by charge conjugation of the process in eqn.(5.11).

Note that the neutralino mixing matrix \mathbf{N} contains the expansion parameter ξ (eqn.(4.23)) which as shown in appendix C can be expressed as a function of the quantities a_i, b_i, c_i (eqn.(4.24)). On the other hand as shown in eqns.(5.10), (5.11) the decay widths (for $\tilde{\chi}_7^0 \rightarrow Z + \nu_j$ and $\tilde{\chi}_7^0 \rightarrow W^\pm + \ell_j^\mp$) contain quadratic power of \mathbf{N} , that is, these decay widths are quadratic in ξ or even more precisely quadratic in a_i, b_i, c_i . This information will be explored further in the next section.

5.4 Light neutrino mixing and the neutralino decay

In $\mu\nu$ SSM, the light neutrino mixing angles are expressible in terms of the parameters a_i, b_i, c_i (see eqn.(4.24)). These relations were also verified numerically, as shown in figures 4.3, 4.4, 4.5. Now it has been already argued in the last section that the two-body decays of the lightest neutralino are also quadratic in a_i, b_i, c_i parameters. Combining these two pictures we found that in $\mu\nu$ SSM the light neutrino mixing angles are correlated with the lightest neutralino (or LSP) decays, to be more precise with the ratios of the decay branching ratio (Br) [18].

These correlations are well studied in the context of the R_p -violating supersymmetric model of light neutrino mass generation [13–17]. Nevertheless, one should note certain differences in these two cases. In $\mu\nu$ SSM lepton number is broken explicitly in the superpotential by terms which are trilinear as well as linear in singlet neutrino superfields. In addition to that there are lepton number conserving terms involving the singlet neutrino superfields with dimensionless neutrino Yukawa couplings. After the electroweak symmetry breaking these terms can generate the effective bilinear R-parity violating terms as well as the $\Delta L = 2$ Majorana mass terms for the singlet neutrinos in the superpotential. In general, there are corresponding soft supersymmetry breaking terms in the scalar potential. Thus the parameter space of this model is much larger compared to the bilinear R_p violating model. Hence, in general, one would not expect a very tight correlation between the neutrino mixing angles and the ratios of decay branching ratios of the LSP. However, under certain simplifying assumptions [18], one can reduce the number of free parameters and in those cases it is possible that the above correlations reappear. This issue has been studied in great detail for the two body $\ell^\pm - W^\mp$ final states in ref. [18] and for all possible two and three body final states in ref. [19]. Let us note in passing that such a nice correlation is lost in the general scenario of bilinear-plus-trilinear R-parity violation [15].

Another important difference between $\mu\nu$ SSM and the bilinear R-parity violating model in the context of the decay of the LSP (assumed to be the lightest neutralino in this case) is that in $\mu\nu$ SSM the lightest neutralino can have a significant singlet neutrino (ν^c) contribution. In this case, the correlation between neutrino mixing angles and decay branching ratios of the LSP is different [18, 19] compared to the cases when the dominant component of the LSP is either a bino, or a higgsino or a

Wino. This gives us a possibility of distinguishing between different R-parity violating models through the observation of the decay branching ratios of the LSP in collider experiments [18,19]. In addition, the decay of the lightest neutralino will show displaced vertices in collider experiments and when the lightest neutralino is predominantly a singlet neutrino, the decay length can be of the order of several meters for a lightest neutralino mass in the neighbourhood of 50 GeV [19]. This is very different from the bilinear R-parity violating model where for a Bino LSP of similar mass the decay length is less than or of the order of a meter or so [16].

In references [13,16,26] this correlation was studied for a bino like neutralino LSP. However, the correlations appear for other natures of the lightest supersymmetric particle as well [27–29]. These inter-relations reflect the predictive power of a model where the light neutrino mass generation as well as the lightest neutralino/LSP decays are governed by a common set of small number of parameters. These correlations are also addressed in a recent review [30]. So in conclusion, with the help of these nice correlations neutrino mixing angles can be indirectly measured in colliders by comparing the branching ratios of the lightest neutralino or the LSP decay modes.

We observe that the correlations between the lightest neutralino decays and neutrino mixing angles depend on the nature of the lightest neutralino as well as on the mass hierarchies of the neutrinos, i.e. whether we have a normal hierarchical pattern of neutrino masses or an inverted one [18]. In this section we look into these possibilities in details with three different natures of the lightest neutralino. We consider that the lightest neutralino to be either (1) bino dominated or (2) higgsino dominated or (3) right-handed neutrino dominated. For each of these cases we consider both the normal and the inverted hierarchical pattern of neutrino masses. In the case of a bino or a higgsino like lightest neutralino, they are also the LSP but for a right-handed neutrino dominated lightest neutralino it is the NLSP with right handed sneutrino as the LSP [18]. The possibility for a right-handed neutrino or singlino like lightest neutralino LSP has also been addressed in references [19,20]. We show that for the different natures of the lightest neutralino, the ratio of branching ratios of certain decays of the lightest neutralino correlates with certain neutrino mixing angle. In some cases the correlation is with the atmospheric angle (θ_{23}) and the reactor angle (θ_{13}) and in other cases the ratio of the branching ratios correlates with the solar mixing angle (θ_{12}). Nevertheless, there also exists scenarios with no correlations at all. Let us now study these possibilities case by case [18] in three subsequent subsections. As already mentioned, that the interesting difference between this study and similar studies with R_p violating scenario [13–16,31] in the MSSM is the presence of a gauge singlet neutrino dominated lightest neutralino. We will see later that in this case the results can be very different from a bino or higgsino dominated lightest neutralino. The lightest neutralino decays in neutrino mass models with spontaneous R-parity violation have been studied in ref. [32]. Our parameter choices for the next three subsections are consistent with the constraints of the scalar sector (section 4.3).

5.4.1 Bino dominated lightest neutralino

According to our choice, at the EW scale the ratio of the $U(1)$ and $SU(2)$ gaugino masses are $M_1 : M_2 = 1 : 2$. If in addition, $M_1 < \mu$ and the value of κ is large (so that the effective gauge singlet neutrino mass $2\kappa v^c$ is large), the lightest neutralino is essentially bino dominated and it is the LSP. First we consider the case when the composition of the lightest neutralino is such that, the bino-component $|N_{71}|^2 > 0.92$ and neutrino masses follow the normal hierarchical pattern. We have observed that for the bino dominated case, the lightest neutralino ($\tilde{\chi}_7^0$) couplings to $\ell^\pm - W^\mp$ pair (where $\ell = e, \mu$ or τ) depend on the quantities b_i along with a factor which is independent of various lepton generations. Naturally, we would expect that the ratios of various decay branching ratios such as $\text{BR}(\tilde{\chi}_7^0 \rightarrow e + W)$, $\text{BR}(\tilde{\chi}_7^0 \rightarrow \mu + W)$, and $\text{BR}(\tilde{\chi}_7^0 \rightarrow \tau + W)$ show nice correlations with the quantities b_i^2/b_j^2 with i, j being e, μ or τ . This feature is evident from figure 5.1. Here we have scanned the parameter space of the three neutrino Yukawa couplings with random values for a particular choice of the couplings λ, κ and the associated soft SUSY breaking trilinear parameters, as well as other MSSM parameters. The trilinear soft parameters A_ν corresponding to Y_ν s also vary randomly in a certain range. In addition we have imposed the condition that the lightest neutralino (which is the LSP) is bino dominated and neutrino mass pattern is normal hierarchical.

We have checked that the correlations between the ratios of the lightest neutralino decay branching ratios and b_i^2/b_j^2 is more prominent with increasing bino component of the lightest neutralino. Note

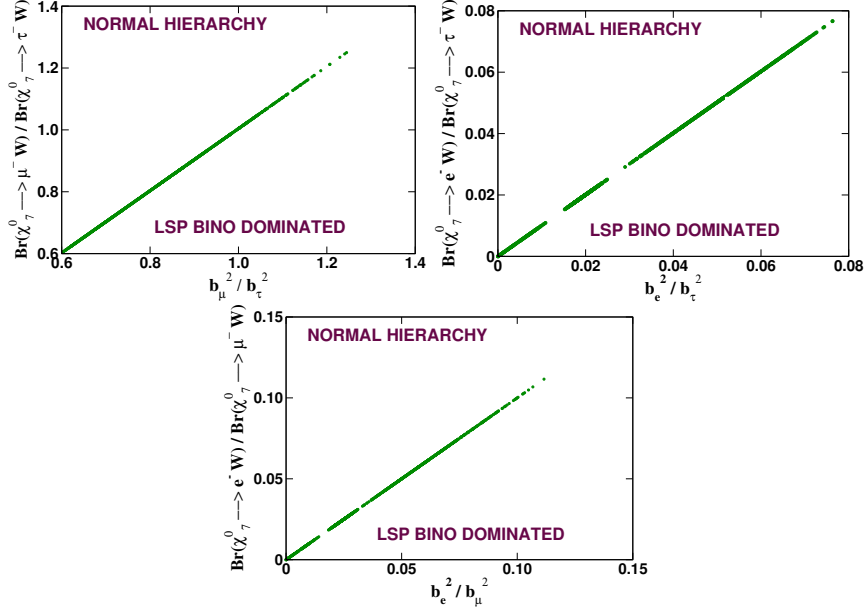


Figure 5.1: Ratio $\frac{Br(\tilde{\chi}_7^0 \rightarrow \ell_i W)}{Br(\tilde{\chi}_7^0 \rightarrow \ell_j W)}$ versus $\frac{b_i^2}{b_j^2}$ plot for a binomial lightest neutralino (the LSP) with binomial component, $|N_{71}|^2 > 0.92$, where $i, j, k = e, \mu, \tau$. Neutrino mass pattern is taken to be normal hierarchical. Choice of parameters are $M_1 = 110$ GeV, $\lambda = 0.13$, $\kappa = 0.65$, $m_{\tilde{\nu}e} = 300$ GeV and $m_{\tilde{L}} = 400$ GeV. Mass of the LSP is 106.9 GeV. The value of the μ parameter comes out to be -228.9 GeV.

that when $(b_i/b_j)^2 \rightarrow 1$ the ratios of branching ratios shown in figure 5.1 also tend to 1. We have seen earlier that the neutrino mixing angles θ_{23} and θ_{13} also show nice correlation with the ratios b_μ^2/b_τ^2 and b_e^2/b_τ^2 , respectively (see figure 4.3). Hence we would expect that the ratios of the branching ratios $\frac{BR(\tilde{\chi}_7^0 \rightarrow \mu W)}{BR(\tilde{\chi}_7^0 \rightarrow \tau W)}$ and $\frac{BR(\tilde{\chi}_7^0 \rightarrow e W)}{\sqrt{BR(\tilde{\chi}_7^0 \rightarrow \mu W)^2 + BR(\tilde{\chi}_7^0 \rightarrow \tau W)^2}}$ show correlations with $\tan^2 \theta_{23}$ and $\tan^2 \theta_{13}$. These correlations are shown in figure 5.2. We have seen earlier (see eqn. (C.6)) that with the normal hierarchical pattern of the neutrino masses, the atmospheric mass scale is determined by the quantity $\Omega_b = \sqrt{b_e^2 + b_\mu^2 + b_\tau^2}$. Naturally one would expect that the atmospheric and the reactor angles are correlated with the $\ell + W$ final states of the lightest neutralino decays and no correlation is expected for the solar angle. This is what we have observed numerically. Here we have considered the regions of the parameter space where the neutrino mass-squared differences and mixing angles are within the 3σ allowed range as shown in table 3.1. Figures 5.2 also shows the model prediction for the ratios of branching ratios where the neutrino experimental data are satisfied. For our sample choice of parameters in figure 5.2, one would expect that the ratio $\frac{BR(\tilde{\chi}_7^0 \rightarrow \mu W)}{BR(\tilde{\chi}_7^0 \rightarrow \tau W)}$ should be in the range 0.45 to 1.25. Similarly, the other ratio $\frac{BR(\tilde{\chi}_7^0 \rightarrow e W)}{\sqrt{BR(\tilde{\chi}_7^0 \rightarrow \mu W)^2 + BR(\tilde{\chi}_7^0 \rightarrow \tau W)^2}}$ is expected in this case to be less than 0.07. We can also see from figure 5.2 that the ratio of branching ratios in the $(\mu + W)$ and $(\tau + W)$ channels becomes almost equal for the maximal value of the atmospheric mixing angle ($\theta_{23} = 45^\circ$). On the other hand, we do not observe any correlation with the solar mixing angle θ_{12} since it is a complicated function of a_i^2 and b_i^2 (see eqn. (4.40)).

In the case of inverted hierarchical mass pattern of the light neutrinos, the $\tilde{\chi}_7^0 - \ell_i - W$ coupling is still controlled by the quantities b_i^2 . Hence the ratios of the branching ratios discussed earlier, show nice correlations with b_i^2/b_j^2 (see figure 5.3). However, in this case the solar mixing angle shows some correlation with the ratio $\frac{BR(\tilde{\chi}_7^0 \rightarrow e W)}{\sqrt{\sum BR(\tilde{\chi}_7^0 \rightarrow \ell_i W)^2}}$ with $\ell_i = \mu, \tau$. This is shown in figure 5.4. The correlation is not very sharp and some dispersion occurs due to the fact that the two heavier neutrino masses controlling the atmospheric mass scale and solar mass-squared difference are not completely determined by the quantities b_i^2 and there is some contribution of the quantities a_i^2 , particularly for

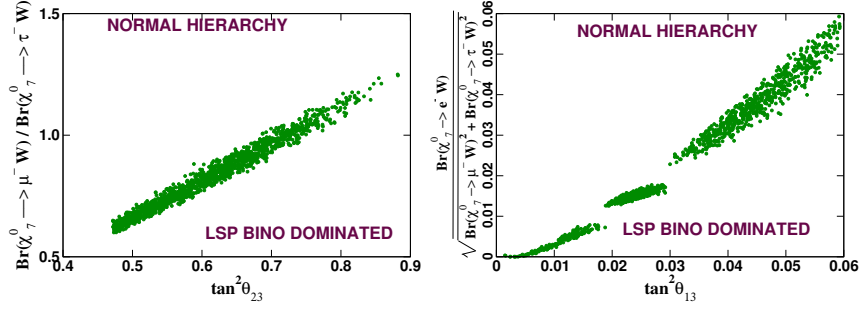


Figure 5.2: Ratio $\frac{Br(\tilde{\chi}_7^0 \rightarrow \mu W)}{Br(\tilde{\chi}_7^0 \rightarrow \tau W)}$ versus $\tan^2 \theta_{23}$ (left), $\frac{Br(\tilde{\chi}_7^0 \rightarrow e W)}{\sqrt{Br(\tilde{\chi}_7^0 \rightarrow \mu W)^2 + Br(\tilde{\chi}_7^0 \rightarrow \tau W)^2}}$ with $\tan^2 \theta_{13}$ (right) plot for a bino dominated lightest neutralino (the LSP) with bino component, $|N_{71}|^2 > 0.92$. Neutrino mass pattern is normal hierarchical. Choice of parameters are same as that of figure 5.1.

the second heavy neutrino mass eigenstate.

The correlation of the ratio $\frac{BR(\tilde{\chi}_7^0 \rightarrow \mu W)}{BR(\tilde{\chi}_7^0 \rightarrow \tau W)}$ with $\tan^2 \theta_{23}$ shows a different behaviour compared to what we have seen in the case of normal hierarchical scenario. This is because in the case of inverted hierarchical mass pattern of the neutrinos, $\tan^2 \theta_{23}$ decreases with increasing b_μ^2/b_τ^2 . One can observe from Figures 5.2 and 5.4 that if the experimental value of the ratio $\frac{BR(\tilde{\chi}_7^0 \rightarrow e W)}{\sqrt{BR(\tilde{\chi}_7^0 \rightarrow \mu W)^2 + BR(\tilde{\chi}_7^0 \rightarrow \tau W)^2}}$ is $\ll 1$ then that indicates a normal hierarchical neutrino mass pattern for a bino-dominated lightest neutralino LSP whereas a higher value (~ 1) of this ratio measured in experiments might indicate that the neutrino mass pattern is inverted hierarchical. Similarly a measurement of the ratio $\frac{BR(\tilde{\chi}_7^0 \rightarrow \mu W)}{BR(\tilde{\chi}_7^0 \rightarrow \tau W)}$ can also give an indication regarding the particular hierarchy of the neutrino mass pattern in the case of a bino dominated LSP.

5.4.2 Higgsino dominated lightest neutralino

When one considers higher values of the $U(1)$ gaugino mass M_1 , i.e. $M_1 > \mu$ and large value of κ (so that the effective gauge singlet neutrino mass $2\kappa v^c$ is large), the lightest neutralino is essentially higgsino dominated and it is the LSP. Naturally one needs to consider a small value of the coupling λ so that the effective μ parameter ($\mu = 3\lambda v^c$) is smaller. In order to look at the lightest neutralino decay branching ratios in this case, we consider a situation where the higgsino component in $\tilde{\chi}_7^0$ is $|N_{73}|^2 + |N_{74}|^2 > 0.90$. As in the case of a bino dominated LSP, the generation dependence of the $\tilde{\chi}_7^0 - \ell_i - W$ couplings comes through the quantities b_i^2 . However, because of the large value of the τ Yukawa coupling, the higgsino- τ mixing is larger and as a result the partial decay width of $\tilde{\chi}_7^0$ into $(W + \tau)$ is larger than into $(W + \mu)$ and $(W + e)$. This feature is shown in figure 5.5, where the ratios of branching ratios are plotted against the quantities b_i^2/b_j^2 . The domination of $BR(\tilde{\chi}_7^0 \rightarrow \tau + W)$ over the other two is clearly evident. Nevertheless, all the three ratios of branching ratios show sharp correlations with the corresponding b_i^2/b_j^2 . In this figure the normal hierarchical pattern of the neutrino masses has been considered. As in the case of a bino LSP, here also the ratios $\frac{BR(\tilde{\chi}_7^0 \rightarrow \mu W)}{BR(\tilde{\chi}_7^0 \rightarrow \tau W)}$ and $\frac{BR(\tilde{\chi}_7^0 \rightarrow e W)}{\sqrt{BR(\tilde{\chi}_7^0 \rightarrow \mu W)^2 + BR(\tilde{\chi}_7^0 \rightarrow \tau W)^2}}$ show nice correlations with neutrino mixing angles θ_{23} and θ_{13} , respectively. This is shown in figure 5.6. However, in this case the predictions for these two ratios are very different from the bino LSP case. The expected value of the ratio $\frac{BR(\tilde{\chi}_7^0 \rightarrow \mu W)}{BR(\tilde{\chi}_7^0 \rightarrow \tau W)}$ is approximately between 0.05 and 0.10 in a region where one can accommodate the experimental neutrino data. Similarly, the predicted value of the ratio $\frac{BR(\tilde{\chi}_7^0 \rightarrow e W)}{\sqrt{BR(\tilde{\chi}_7^0 \rightarrow \mu W)^2 + BR(\tilde{\chi}_7^0 \rightarrow \tau W)^2}}$ is ≤ 0.006 . On the other hand, there is no such correlations with the solar mixing angle θ_{12} .

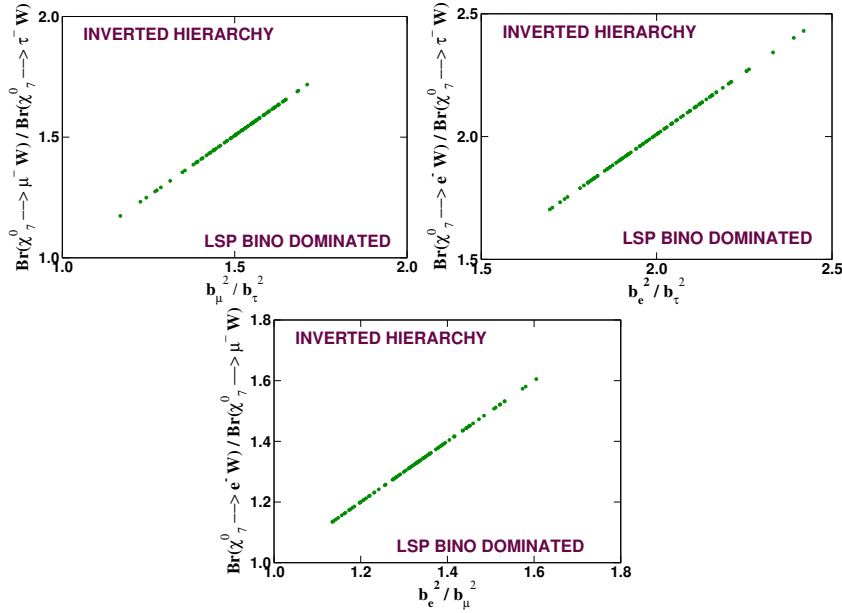


Figure 5.3: Ratio $\frac{BR(\tilde{\chi}_7^0 \rightarrow \ell_i^- W)}{BR(\tilde{\chi}_7^0 \rightarrow \ell_j^- W)}$ versus $\frac{b_i^2}{b_j^2}$ plot for a bino like lightest neutralino (the LSP) with bino component $|N_{71}|^2 > 0.95$, where $i, j, k = e, \mu, \tau$. Neutrino mass pattern is inverted hierarchical. Choice of parameters are $M_1 = 105$ GeV, $\lambda = 0.15$, $\kappa = 0.65$, $m_{\tilde{\nu}^c} = 300$ GeV and $m_{\tilde{L}} = 445$ GeV. Mass of the LSP is 103.3 GeV. The value of the μ parameter comes out to be -263.7 GeV.

Similar correlations of the ratios of branching ratios with b_i^2/b_j^2 are also obtained for a higgsino dominated LSP in the case where the neutrino mass pattern is inverted hierarchical. Once again it shows that the $\tilde{\chi}_7^0$ decays to $(\tau + W)$ channel is dominant over the channels $(e + W)$ and $(\mu + W)$ for any values of b_i^2/b_j^2 because of the larger τ Yukawa coupling. On the other hand, the correlations with the neutrino mixing angles show a behaviour similar to that of a bino LSP with inverted neutrino mass hierarchy though with much smaller values for the ratios $\frac{BR(\tilde{\chi}_7^0 \rightarrow \mu W)}{BR(\tilde{\chi}_7^0 \rightarrow \tau W)}$ and $\frac{BR(\tilde{\chi}_7^0 \rightarrow e W)}{\sqrt{BR(\tilde{\chi}_7^0 \rightarrow \mu W)^2 + BR(\tilde{\chi}_7^0 \rightarrow \tau W)^2}}$. These are shown in figure 5.7. Note that the correlations in this case are not very sharp, especially with $\tan^2 \theta_{12}$. Thus we see that small values of these ratios (for both normal and inverted hierarchy) are characteristic features of a higgsino dominated LSP in this model.

5.4.3 Right-handed neutrino dominated lightest neutralino

Because of our choice of parameters i.e., a generation independent coupling κ of the gauge singlet neutrinos and a common VEV v^c (see eqn.(4.8)), the three neutralino mass eigenstates which are predominantly gauge singlet neutrinos are essentially mass degenerate. There is a very small mass splitting due to mixing. However, unlike the case of a bino or higgsino dominated lightest neutralino, these ν^c dominated lightest neutralino states cannot be considered as the LSP. This is because in this case the lightest scalar (which is predominantly a gauge singlet sneutrino $\tilde{\nu}^c$) is the lightest supersymmetric particle. This is very interesting since usually one does not get a $\tilde{\nu}^c$ as an LSP in a model where the gauge singlet neutrino superfield has a large Majorana mass term in the superpotential. However, in this case the effective Majorana mass term is at the EW scale and there is also a contribution from the trilinear scalar coupling $A_\kappa \kappa$ which keeps the mass of the singlet scalar sneutrino smaller. It is also very interesting to study the decay patterns of the lightest neutralino in this case since here one can probe the gauge singlet neutrino mass scales at the colliders.

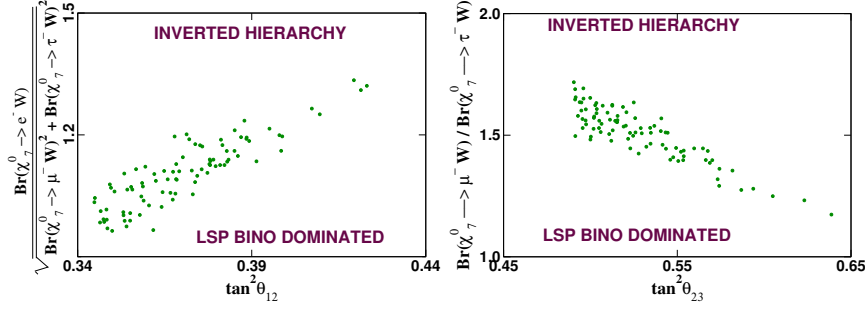


Figure 5.4: Ratio $\frac{\text{Br}(\tilde{\chi}_7^0 \rightarrow e W)}{\sqrt{\text{Br}(\tilde{\chi}_7^0 \rightarrow \mu W)^2 + \text{Br}(\tilde{\chi}_7^0 \rightarrow \tau W)^2}}$ with $\tan^2 \theta_{12}$ (left) plot for a bino dominated lightest neutralino (LSP) with bino component $|N_{71}|^2 > 0.95$. In the right figure the ratio $\frac{\text{Br}(\tilde{\chi}_7^0 \rightarrow \mu W)}{\text{Br}(\tilde{\chi}_7^0 \rightarrow \tau W)}$ versus $\tan^2 \theta_{23}$ is plotted. Neutrino mass pattern is assumed to be inverted hierarchical. Choice of parameters are same as that of figure 5.3.

Before discussing the decay patterns of the lightest neutralino which is ν^c dominated, let us say a few words regarding their production at the LHC. The direct production of ν^c (by ν^c we mean the ν^c dominated lightest neutralino in this subsection) is negligible because of the very small mixing with the MSSM neutralinos. Nevertheless, they can be produced at the end of the cascade decay chains of the squarks and gluinos at the LHC. For example, if the next-to-next-to-lightest SUSY particle (NNLSP) is higgsino dominated (this is the state above the three almost degenerate lightest neutralinos) and it has a non-negligible mixing with ν^c (remember that the higgsino- ν^c mixing occurs mainly because of the term $\lambda \hat{\nu}^c \hat{H}_d \hat{H}_u$ in the superpotential, eqn.(4.1)), then the branching ratio of the decay $\hat{H} \rightarrow Z + \nu^c$ can be larger than the branching ratios in the ℓW and νZ channels. This way one can produce ν^c dominated lightest neutralino. Similarly, a higgsino dominated lighter chargino can also produce gauge singlet neutrinos. Another way of producing ν^c is through the decay of an NNLSP $\tilde{\tau}_1$, such as $\tilde{\tau}_1 \rightarrow \tau + \nu^c$.

When one considers higher value of the gaugino mass, i.e. $M_1 > \mu$ and a small value of the coupling κ (so that the effective Majorana mass of ν^c is small, i.e. $m_{\nu^c} = 2\kappa v^c < \mu$), the lightest neutralino is essentially ν^c dominated. As we have mentioned earlier, in this case the LSP is the scalar partner of ν^c , i.e. $\tilde{\nu}^c$. However, the decay of ν^c into $\nu + \tilde{\nu}^c$ is suppressed compared to the decays $\nu^c \rightarrow \ell_i + W$ and $\nu^c \rightarrow \nu_i + Z$ that we have considered so far. Because of this, in this section we will neglect the decay $\nu^c \rightarrow \nu + \tilde{\nu}^c$ while discussing the correlation of the lightest neutralino ($\tilde{\chi}_7^0$) decays with the neutrino mixing angles.

In this case the coupling of the lightest neutralino ($\tilde{\chi}_7^0$) with ℓ_i - W pair depends on the ν^c content of $\tilde{\chi}_7^0$. Note that the ν^c has a very small mixing with the MSSM neutralino states. However, in some cases the ν^c dominated lightest neutralino can have a non-negligible higgsino component. In such cases the coupling $\tilde{\chi}_7^0$ - ℓ_i - W depends mainly on the quantities b_i . On the other hand, if $\tilde{\chi}_7^0$ is very highly dominated by ν^c , then the coupling $\tilde{\chi}_7^0$ - ℓ_i - W has a nice correlation with the quantities a_i . So in order to study the decay correlations of the ν^c dominated lightest neutralino, we consider two cases (i) ν^c component is > 0.99 , and (ii) ν^c component is > 0.97 with some non-negligible higgsino admixture.

The correlations of the decay branching ratio $\frac{\text{Br}(\tilde{\chi}_7^0 \rightarrow \mu W)}{\text{Br}(\tilde{\chi}_7^0 \rightarrow \tau W)}$ are shown in figure 5.8 for the cases (i) and (ii) mentioned above. As we have explained already, this figure demonstrates that in case (i) the ratio of the branching ratio is dependent on the quantity a_μ^2/a_τ^2 whereas in case (ii) this ratio is correlated with b_μ^2/b_τ^2 though there is some suppression due to large τ Yukawa coupling.

Similar calculations were performed also for the other ratios discussed earlier. For example, in figure 5.9 we have shown the variations of the ratio $\frac{\text{Br}(\tilde{\chi}_7^0 \rightarrow e W)}{\text{Br}(\tilde{\chi}_7^0 \rightarrow \mu W)}$ as functions of $\frac{a_e^2}{a_\mu^2}$ and $\frac{b_e^2}{b_\mu^2}$ for the cases (i) and (ii), respectively. The variation with $\frac{a_e^2}{a_\mu^2}$ is not sharp and dispersive in nature whereas

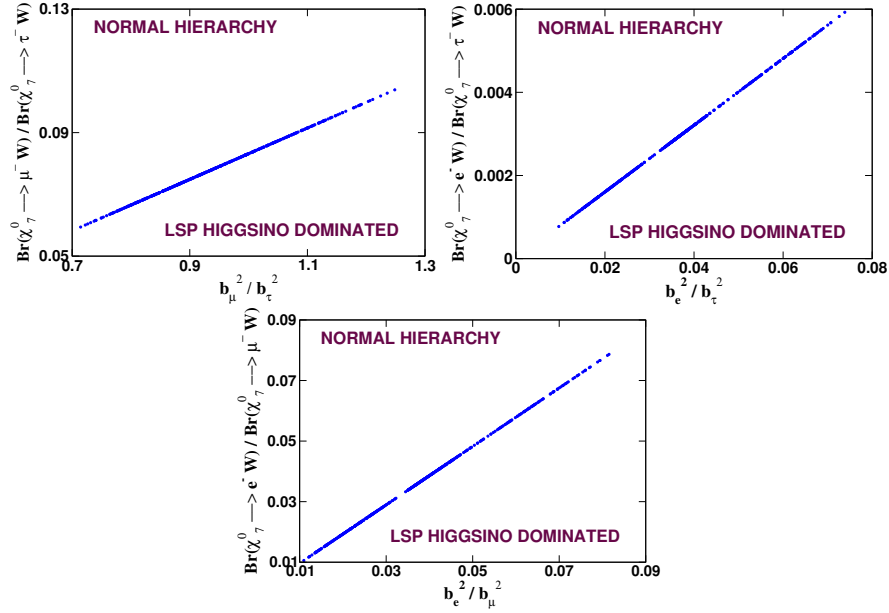


Figure 5.5: Ratio $\frac{BR(\tilde{\chi}_7^0 \rightarrow l_i W)}{BR(\tilde{\chi}_7^0 \rightarrow l_j W)}$ versus $\frac{b_i^2}{b_j^2}$ plot for a higgsino like LSP with higgsino component ($|N_{73}|^2 + |N_{74}|^2 > 0.95$, where $i, j, k = e, \mu, \tau$). Neutrino mass pattern is normal hierarchical. Choice of parameters are $M_1 = 325$ GeV, $\lambda = 0.06$, $\kappa = 0.65$, $m_{\tilde{\nu}^c} = 300$ GeV and $m_{\tilde{L}} = 400$ GeV. Mass of the LSP is 98.6 GeV. The value of the μ parameter comes out to be -105.9 GeV.

the variation with $\frac{b_e^2}{b_\mu^2}$ is very sharp and shows that in this case the relevant couplings are proportional to b_e and b_μ , respectively.

On the other hand, in case (i) only $\tan^2 \theta_{23}$ shows a nice correlation with the ratio $\frac{BR(\tilde{\chi}_7^0 \rightarrow \mu W)}{BR(\tilde{\chi}_7^0 \rightarrow \tau W)}$ (see figure 5.10) and $\tan^2 \theta_{12}$ or $\tan^2 \theta_{13}$ does not show any correlation with the other ratio. The non-linear behaviour of the ratios of branching ratios in case(i) is due to the fact that the parameters $Y_{\nu s}$ (which control the a_i) appear both in the neutralino and chargino mass matrices. The charged lepton Yukawa couplings also play a role in determining the ratios. One can also see that the prediction for this ratio of branching ratio for case (i), as shown in figure 5.10, is in the range $0.5 - 3.5$, which is larger compared to the bino dominated or higgsino dominated cases for both normal and inverted hierarchical pattern of neutrino masses. Also, the nature of this variation is similar to what we see with the inverted hierarchical pattern of neutrino masses in the bino or higgsino dominated cases.

In case (ii) none of the neutrino mixing angles show very good correlations with the ratios of branching ratios that we have been discussing. However, one can still observe some kind of correlation between $\tan^2 \theta_{12}$ and the ratio $\frac{BR(\tilde{\chi}_7^0 \rightarrow e W)}{\sqrt{BR(\tilde{\chi}_7^0 \rightarrow \mu W)^2 + BR(\tilde{\chi}_7^0 \rightarrow \tau W)^2}}$. The prediction for this ratio from the neutrino data is on the smaller side (~ 0.07).

With the inverted hierarchical neutrino mass pattern, in case (i) one observes a sharp correlation of the ratio $\frac{BR(\tilde{\chi}_7^0 \rightarrow \mu W)}{BR(\tilde{\chi}_7^0 \rightarrow \tau W)}$ with $\frac{a_\mu^2}{a_\tau^2}$ (see figure 5.11). The other two ratios $\frac{BR(\tilde{\chi}_7^0 \rightarrow e W)}{BR(\tilde{\chi}_7^0 \rightarrow \mu W)}$ and $\frac{BR(\tilde{\chi}_7^0 \rightarrow e W)}{BR(\tilde{\chi}_7^0 \rightarrow \tau W)}$

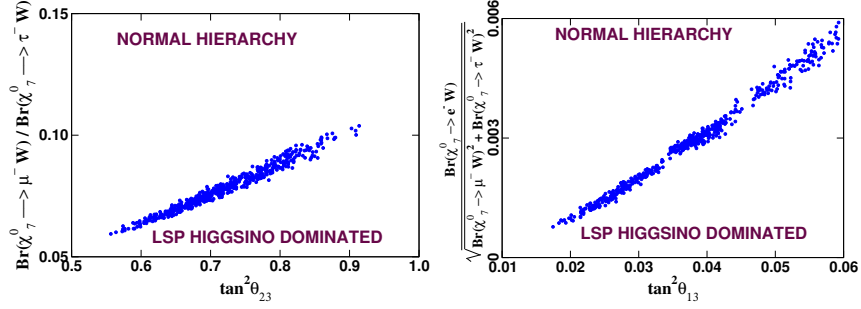


Figure 5.6: Ratio $\frac{BR(\tilde{\chi}_7^0 \rightarrow \mu^- W)}{BR(\tilde{\chi}_7^0 \rightarrow \tau^- W)}$ versus $\tan^2 \theta_{23}$ (left), $\frac{BR(\tilde{\chi}_7^0 \rightarrow e W)}{\sqrt{BR(\tilde{\chi}_7^0 \rightarrow \mu^- W)^2 + BR(\tilde{\chi}_7^0 \rightarrow \tau^- W)^2}}$ with $\tan^2 \theta_{13}$ (right) plot for a higgsino LSP with higgsino component ($|N_{73}|^2 + |N_{74}|^2 > 0.95$). Neutrino mass pattern is normal hierarchical. Choice of parameters are same as that of figure 5.5.

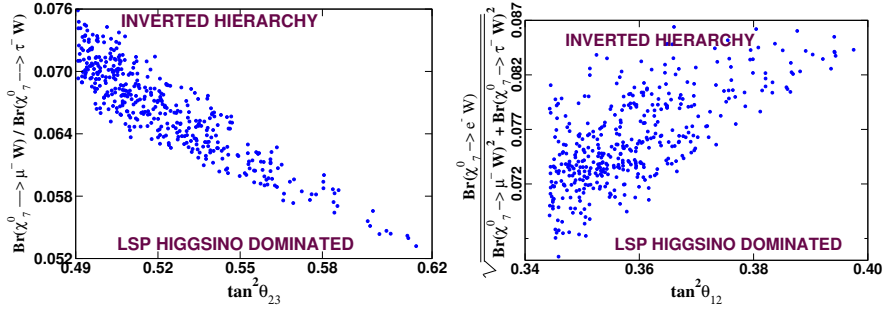


Figure 5.7: Ratio $\frac{BR(\tilde{\chi}_7^0 \rightarrow \mu^- W)}{BR(\tilde{\chi}_7^0 \rightarrow \tau^- W)}$ versus $\tan^2 \theta_{23}$ (left), $\frac{BR(\tilde{\chi}_7^0 \rightarrow e W)}{\sqrt{BR(\tilde{\chi}_7^0 \rightarrow \mu^- W)^2 + BR(\tilde{\chi}_7^0 \rightarrow \tau^- W)^2}}$ with $\tan^2 \theta_{12}$ (right) plot for a higgsino LSP with higgsino component ($|N_{73}|^2 + |N_{74}|^2 > 0.95$). Neutrino mass pattern is inverted hierarchical. Choice of parameters are $M_1 = 490$ GeV, $\lambda = 0.07$, $\kappa = 0.65$, $m_{\tilde{\nu}^c} = 320$ GeV and $m_{\tilde{L}} = 430$ GeV. Mass of the LSP is 110.8 GeV. The value of the μ parameter comes out to be -115.3 GeV.

do not show very sharp correlations with $\frac{a_e^2}{a_\mu^2}$ and $\frac{a_e^2}{a_\tau^2}$, respectively and we do not plot them here. However, in case (ii) all the three ratios show nice correlations with the corresponding b_i^2/b_j^2 . We have shown this in figure 5.11 only for b_μ^2/b_τ^2 . In this case the variations of the ratios of branching ratios with neutrino mixing angles are shown in figure 5.12.

For the case (i), only $\tan^2 \theta_{13}$ shows certain correlation with the ratio of branching ratio shown in figure 5.12 (right), but we do not show it here.

Finally, we would like to reemphasize that in all these different cases discussed above, the lightest neutralino can have a finite decay length which can produce displaced vertices (also discussed earlier in sections 5.1, 5.2) in the vertex detectors. Depending on the composition of the lightest neutralino, one can have different decay lengths. For example, a bino-dominated lightest neutralino can produce a displaced vertex \sim a few mm. Similarly, for a higgsino dominated lightest neutralino, decay vertices of the order of a few cms can be observed [18, 19]. On the other hand, if the lightest neutralino is ν^c dominated, then the decay lengths can be of the order of a few meters [18–20]. These are very unique predictions of this model which can, in principle, be tested at the LHC [20].

The advantage of having large displaced vertices for a singlino like lightest neutralino makes it easier to kill all of the SM backgrounds unambiguously. Additionally, it is also difficult to achieve a reasonably large (\sim a few meter) displaced vertex in the conventional R_p -violating model [13, 15, 16]. As a consequence it is rather difficult for the R_p -violating supersymmetric models to mimic a specific

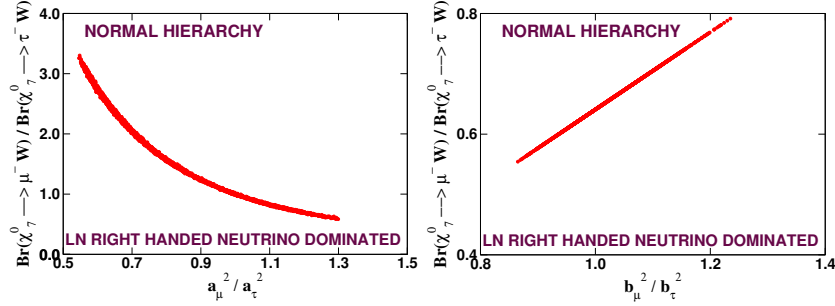


Figure 5.8: Ratio $\frac{BR(\tilde{\chi}_7^0 \rightarrow \mu^- W)}{BR(\tilde{\chi}_7^0 \rightarrow \tau^- W)}$ versus $\frac{a_\mu^2}{a_\tau^2}$ (left) and versus $\frac{b_\mu^2}{b_\tau^2}$ (right) plot for a ν^c like lightest neutralino ($\tilde{\chi}_7^0$) with ν^c component ($|N_{75}|^2 + |N_{76}|^2 + |N_{77}|^2 > 0.99$, (left) and > 0.97 (right)). Neutrino mass pattern is normal hierarchical. Choice of parameters are for (left) $M_1 = 405$ GeV, $\lambda = 0.29$, $\kappa = 0.07$, $(A_\lambda \lambda) = -8.2$ TeV $\times \lambda$, $(A_\kappa \kappa) = 165$ GeV $\times \kappa$, $m_{\tilde{\nu}^c} = 50$ GeV and $m_{\tilde{L}} = 825$ GeV and for (right) $M_1 = 405$ GeV, $\lambda = 0.10$, $\kappa = 0.07$, $(A_\lambda \lambda) = -2$ TeV $\times \lambda$, $(A_\kappa \kappa) = 165$ GeV $\times \kappa$, $m_{\tilde{\nu}^c} = 50$ GeV and $m_{\tilde{L}} = 825$ GeV. Mass of the lightest neutralino is 129.4 GeV (left) and 119.8 GeV (right) respectively. The values of the μ parameter are -803.9 GeV and -258.8 GeV, respectively.

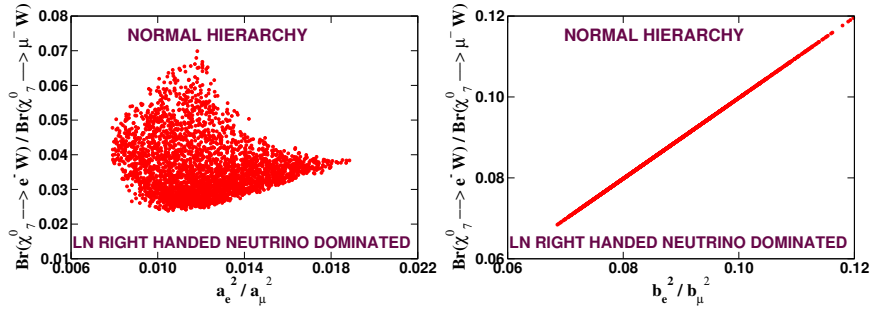


Figure 5.9: Ratio $\frac{BR(\tilde{\chi}_7^0 \rightarrow e^- W)}{BR(\tilde{\chi}_7^0 \rightarrow \mu^- W)}$ versus $\frac{a_e^2}{a_\mu^2}$ (left) and versus $\frac{b_e^2}{b_\mu^2}$ (right) plot for a ν^c like lightest neutralino ($\tilde{\chi}_7^0$) with ν^c component ($|N_{75}|^2 + |N_{76}|^2 + |N_{77}|^2 > 0.99$ (left), and > 0.97 (right)). Neutrino mass pattern is normal hierarchical. Choice of parameters are same as that of figure 5.8.

collider signatures of $\mu\nu$ SSM, particularly when a gauge singlet LSP is involved in the process. We will use the favour of large displaced vertex associated with a singlino like LSP to describe an unconventional signal of the lightest Higgs boson of $\mu\nu$ SSM [20] in the next chapter.

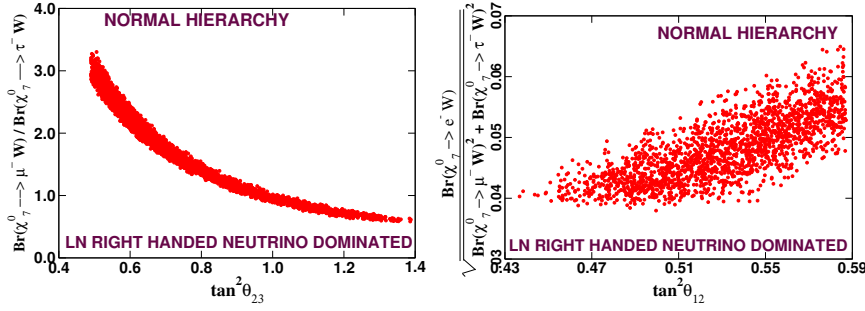


Figure 5.10: Ratio $\frac{BR(\tilde{\chi}_7^0 \rightarrow \mu W)}{BR(\tilde{\chi}_7^0 \rightarrow \tau W)}$ versus $\tan^2 \theta_{23}$ (left), $\frac{BR(\tilde{\chi}_7^0 \rightarrow e W)}{\sqrt{BR(\tilde{\chi}_7^0 \rightarrow \mu W)^2 + BR(\tilde{\chi}_7^0 \rightarrow \tau W)^2}}$ with $\tan^2 \theta_{12}$ (right) plot for a ν^c dominated lightest neutralino with ν^c component ($|N_{75}|^2 + |N_{76}|^2 + |N_{77}|^2 > 0.99$ (left) and > 0.97 (right)). Neutrino mass pattern is normal hierarchical. Choice of parameters are same as that of figure 5.8.

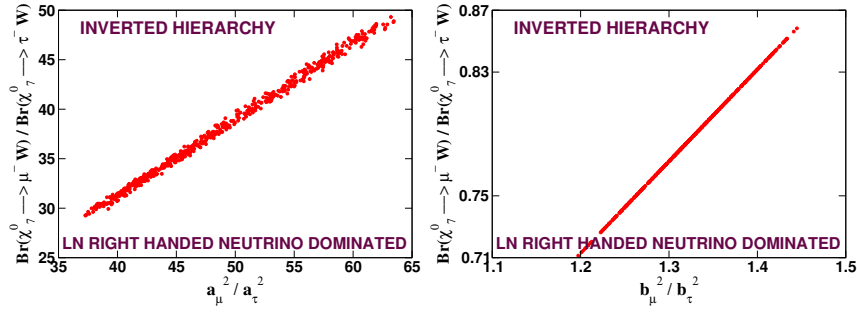


Figure 5.11: Ratio $\frac{BR(\tilde{\chi}_7^0 \rightarrow \mu W)}{BR(\tilde{\chi}_7^0 \rightarrow \tau W)}$ versus $\frac{a_\mu^2}{a_\tau^2}$ (left) and versus $\frac{b_\mu^2}{b_\tau^2}$ (right) plot for a ν^c like lightest neutralino ($\tilde{\chi}_7^0$) with ν^c component ($|N_{75}|^2 + |N_{76}|^2 + |N_{77}|^2 > 0.99$ (left), and > 0.97 (right)). Neutrino mass pattern is inverted hierarchical. Choice of parameters are for (left) $M_1 = 445$ GeV, $\lambda = 0.29$, $\kappa = 0.07$, $(A_\lambda \lambda) = -8.2$ TeV $\times \lambda$, $(A_\kappa \kappa) = 165$ GeV $\times \kappa$, $m_{\tilde{\nu}^c} = 50$ GeV and $m_{\tilde{L}} = 835$ GeV and for (right) $M_1 = 445$ GeV, $\lambda = 0.10$, $\kappa = 0.07$, $(A_\lambda \lambda) = -2$ TeV $\times \lambda$, $(A_\kappa \kappa) = 165$ GeV $\times \kappa$, $m_{\tilde{\nu}^c} = 50$ GeV and $m_{\tilde{L}} = 835$ GeV. Mass of the lightest neutralino is 129.4 GeV (left) and 119.8 GeV (right) respectively.

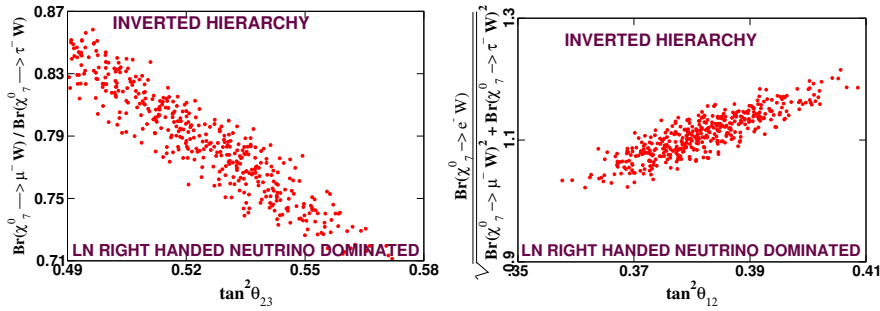


Figure 5.12: Ratio $\frac{BR(\tilde{\chi}_7^0 \rightarrow \mu W)}{BR(\tilde{\chi}_7^0 \rightarrow \tau W)}$ versus $\tan^2 \theta_{23}$ (left), $\frac{BR(\tilde{\chi}_7^0 \rightarrow e W)}{\sqrt{BR(\tilde{\chi}_7^0 \rightarrow \mu W)^2 + BR(\tilde{\chi}_7^0 \rightarrow \tau W)^2}}$ with $\tan^2 \theta_{12}$ (right) plot for a ν^c dominated lightest neutralino with ν^c component ($|N_{75}|^2 + |N_{76}|^2 + |N_{77}|^2 > 0.97$). Neutrino mass pattern is inverted hierarchical. Choice of parameters are same as that of figure 5.11.

Bibliography

- [1] Wolfram S 1979 *Phys. Lett.* **B82** 65
- [2] Dover C B, Gaisser T K and Steigman G 1979 *Phys. Rev. Lett.* **42** 1117
- [3] Ellis J R, Hagelin J S, Nanopoulos D V, Olive K A and Srednicki M 1984 *Nucl. Phys.* **B238** 453–476
- [4] Feng J L, Moroi T, Randall L, Strassler M and Su S f 1999 *Phys. Rev. Lett.* **83** 1731–1734
- [5] Raby S 1998 *Phys. Lett.* **B422** 158–162
- [6] Baer H, Cheung K m and Gunion J F 1999 *Phys. Rev.* **D59** 075002
- [7] Raby S and Tobe K 1999 *Nucl. Phys.* **B539** 3–22
- [8] Hagelin J S, Kane G L and Raby S 1984 *Nucl. Phys.* **B241** 638
- [9] Hall L J and Suzuki M 1984 *Nucl. Phys.* **B231** 419
- [10] Dawson S 1985 *Nucl. Phys.* **B261** 297
- [11] Hempfling R 1997 (*Preprint* hep-ph/9702412)
- [12] Mukhopadhyaya B and Roy S 1999 *Phys. Rev.* **D60** 115012
- [13] Mukhopadhyaya B, Roy S and Vissani F 1998 *Phys. Lett.* **B443** 191–195
- [14] Chun E J and Lee J S 1999 *Phys. Rev.* **D60** 075006
- [15] Choi S Y, Chun E J, Kang S K and Lee J S 1999 *Phys. Rev.* **D60** 075002
- [16] Porod W, Hirsch M, Romao J and Valle J W F 2001 *Phys. Rev.* **D63** 115004
- [17] De Campos F *et al.* 2010 *Phys. Rev.* **D82** 075002
- [18] Ghosh P and Roy S 2009 *JHEP* **04** 069
- [19] Bartl A, Hirsch M, Vicente A, Liebler S and Porod W 2009 *JHEP* **05** 120
- [20] Bandyopadhyay P, Ghosh P and Roy S 2010 (*Preprint* 1012.5762)
- [21] Chang S and de Gouvea A 2009 *Phys. Rev.* **D80** 015008
- [22] Franke F and Fraas H 1996 *Z. Phys.* **C72** 309–325
- [23] Franke F and Fraas H 1997 *Int. J. Mod. Phys.* **A12** 479–534
- [24] Gunion J F and Haber H E 1988 *Phys. Rev.* **D37** 2515
- [25] Gunion J F and Haber H E 1986 *Nucl. Phys.* **B272** 1
- [26] Chun E J, Jung D W, Kang S K and Park J D 2002 *Phys. Rev.* **D66** 073003

- [27] Hirsch M, Porod W, Romao J C and Valle J W F 2002 *Phys. Rev.* **D66** 095006
- [28] Hirsch M and Porod W 2003 *Phys. Rev.* **D68** 115007
- [29] Aristizabal Sierra D, Hirsch M and Porod W 2005 *JHEP* **09** 033
- [30] Nath P *et al.* 2010 *Nucl. Phys. Proc. Suppl.* **200-202** 185–417
- [31] Romao J C, Diaz M A, Hirsch M, Porod W and Valle J W F 2000 *Phys. Rev.* **D61** 071703
- [32] Hirsch M, Vicente A and Porod W 2008 *Phys. Rev.* **D77** 075005

Chapter 6

$\mu\nu$ SSM: Unusual signal of Higgs boson at LHC

6.1 Higgs boson in $\mu\nu$ SSM

In $\mu\nu$ SSM R_p is violated through lepton number violation both in the superpotential and in the soft terms. In this model neutral Higgs bosons of the MSSM mix with three generations of left and right-handed sneutrinos and thus the neutral scalar and pseudoscalar squared mass matrices are enhanced (8×8) over their 2×2 MSSM structures [1, 2]. In a similar fashion the charged Higgs scalar squared mass matrix is also a 8×8 matrix for $\mu\nu$ SSM due to mixing between charged Higgs of the MSSM and charged sleptons [1, 2]. In general the nature of the lightest neutral scalar state can be very different from that of the MSSM due to the presence of the gauge singlet right-handed sneutrino component. It has been already shown that $\mu\nu$ SSM is capable of accommodating neutrino data both from tree level [2] and one loop combined analysis [3]. With the initiation of the LHC experiment at CERN it is naturally tempting to see whether this is capable of producing interesting collider signatures apart from accommodating the neutrino data.

The issues of Higgs boson discovery have been studied extensively over years in the literature (see for example [4]). In this chapter we propose a prodigious signal of Higgs boson in supersymmetry, having dilepton and four hadronic jets along with large displaced vertices ($\gtrsim 3 m$) [5]. Most of the usual signal of Higgs boson are impaired by undesired backgrounds and one has to remove them somehow for claiming a discovery. Often the procedures for background subtraction in turn weaken the desired signal significantly. On the other hand, it was well known that the advantage of displaced vertices are always extremely useful to kill all of the SM backgrounds and also some of the possible backgrounds arising from the R_p violating MSSM. Displaced vertices arising from MSSM with \mathcal{R}_p are usually much smaller [6–9]

Now in the last chapter we have learned that in $\mu\nu$ SSM, with suitable choice of parameters, a right-handed neutrino like lightest neutralino can be a viable candidate for the LSP. It was also discussed that since a right-handed neutrino is singlet under the SM gauge group it can decay only in R_p -violating channels through small R_p -violating couplings and consequently the associated displaced vertices can be very large (\sim meter) [5, 10]. Indeed these displaced vertices can kill all of the SM backgrounds as well as backgrounds arising from MSSM with \mathcal{R}_p [6–9]. Furthermore, imprint of this signal is different from that of the cosmic muons which have definite entry and exit point in the detector. So this is apparently a clean signal and a discovery, thus is definite even with small number of signal events. In the next section we will discuss how to use the favour of these large displaced vertices associated with a singlino like LSP for proposing a new kind of signal of Higgs boson [5].

6.2 The Signal

There are essentially two key features of our analysis, which collectively can lead to an unusual signal of the Higgs boson in supersymmetry

1. The lightest neutralino LSP ($\tilde{\chi}_1^0$) in the $\mu\nu$ SSM with the parameter choice $M_1, \mu \gg m_{\nu^c}$ (see section 5.2) can be predominantly composed of right-handed neutrinos which, as argued earlier will be called a ν^c -like or a singlino like LSP [5,10]. For the analysis of ref. [5] we choose $|\mathbf{N}_{15}|^2 + |\mathbf{N}_{16}|^2 + |\mathbf{N}_{17}|^2 \geq 0.70$.
2. A pair of singlino like LSP can couple to a Higgs boson in $\mu\nu$ SSM mainly through couplings like $\nu^c H_u H_d$ (see fig 6.1).

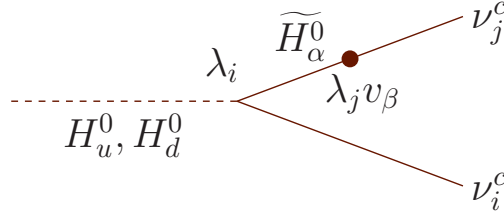


Figure 6.1: Feynman diagram for the singlino singlino Higgs couplings. $\beta = 2/1$ for $\alpha = d/u$.

The neutralino LSP, $\tilde{\chi}_1^0$ in $\mu\nu$ SSM can be predominantly ($\gtrsim 70\%$) ν^c -like (also known as a *singlino* LSP). $\tilde{\chi}_1^0$ being singlet, $\tilde{\chi}_1^0 \tilde{\chi}_1^0 Z$ or $\tilde{\chi}_1^0 q \bar{q}$ couplings [3] are vanishingly small, which in turn results in very small cross-section for direct $\tilde{\chi}_1^0$ pair production. On the contrary, the coupling $\lambda \nu^c H_u H_d$ may produce a large $\tilde{\chi}_1^0 \tilde{\chi}_1^0 S_i^0$ [3] coupling with $\lambda \sim \mathcal{O}(1)$, where S_i^0 are the scalar states. With the chosen set of parameters (see Table 6.1) we obtained $S_4^0 \equiv h^0$, where h^0 is the lightest Higgs boson of MSSM. In addition with heavy squark/gluino masses as indicated in Table 6.1 for different benchmark points, production of a singlino LSP through cascade decays is suppressed. In the backdrop of such a scenario, production of h^0 in gluon fusion channel followed by the decay process $h^0 \rightarrow \tilde{\chi}_1^0 \tilde{\chi}_1^0$ will be the leading production channel for the singlino LSP at the LHC. We want to emphasize here that for the present analysis we choose to work with the tree level mass of the lightest CP-even Higgs boson ($S_4^0 \equiv h^0$) of the $\mu\nu$ SSM. With loop corrections the Higgs boson mass can be higher [1,10]. For loop corrected Higgs boson mass, the process $h^0 \rightarrow \tilde{\chi}_1^0 \tilde{\chi}_1^0$ will yield heavy singlino like LSPs with smaller decay lengths [10]. However, our general conclusions will not change for a singlino LSP in the mass range 20 – 60 GeV, as long as the decay branching ratio for the process $h^0 \rightarrow \tilde{\chi}_1^0 \tilde{\chi}_1^0$ is substantial.

A set of four benchmark points (BP) used for collider studies compatible with neutrino data [11], upto one-loop level analysis [3] are given in Table 6.1. These are sample points and similar spectra can be obtained in a reasonably large region of the parameter space even after satisfying all the constraints from neutrino experiments.

For the set of specified benchmark points (table 6.1), we observe, the process $h^0 \rightarrow \tilde{\chi}_1^0 \tilde{\chi}_1^0$ to be one of the dominant decay modes of h^0 (branching fraction within 35-65%), while the process $h^0 \rightarrow b\bar{b}$ remains the main competitor. Different Feynman rules concerning Higgs decays are given in appendix H. With a suitable choice of benchmark points (table 6.1) two body decays of h^0 into lighter scalar or pseudoscalar states were kept kinematically disfavoured. Squared matrix elements for the processes $h^0 \rightarrow b\bar{b}$ and $h^0 \rightarrow \tilde{\chi}_1^0 \tilde{\chi}_1^0$ are also given in appendix H.

The pair produced singlino like $\tilde{\chi}_1^0$ will finally decay into standard model particles as shown in eqn.(5.1). For a lightest Higgs boson mass m_{h^0} as shown in table 6.1, mass of a singlino like $\tilde{\chi}_1^0$ ($m_{\tilde{\chi}_1^0}$) arising from h^0 decay (see figure 6.1) is $< m_W$, and thus three body decays dominate. Out of the five possible three body final states we choose to work with the specific decay mode $\tilde{\chi}_1^0 \rightarrow q_i \bar{q}'_j \ell_k^\pm$ to yield a signal $pp \rightarrow 2\ell + 4j + X$ in the final state¹. This particular final state is free from neutrinos and thus a reliable invariant mass reconstruction is very much possible. It has to be emphasized here that as suggested in ref. [4], a reliable mass reconstruction is possible even for the final states with a single neutrino, thus apart from the $2\ell + 4j + X$ final state there also exist other equally interesting final states like $3\ell + 2j + X$ ($\tilde{\chi}_1^0 \rightarrow q_i \bar{q}'_j \ell_k^\pm, \tilde{\chi}_1^0 \rightarrow \ell_i^+ \ell_j^- \nu_k$), $1\ell + 4j + X$ ($\tilde{\chi}_1^0 \rightarrow q_i \bar{q}'_j \ell_k^\pm, \tilde{\chi}_1^0 \rightarrow q_i \bar{q}_i \nu_k$) etc. For the chosen benchmark points, $Br(\tilde{\chi}_1^0 \rightarrow q_i \bar{q}'_j \ell_k^\pm)$ lies within 8 – 10%. Squared matrix elements for all possible three body decays of $\tilde{\chi}_1^0$ (see eqn.(5.1)) are given in appendix I. At this point the importance of a singlino $\tilde{\chi}_1^0$ becomes apparent. Since all the leptons and jets are originating from the decays of a

¹The dilepton have same sign on 50% occurrence since $\tilde{\chi}_1^0$ is a Majorana particle.

	BP-1	BP-2	BP-3	BP-4
μ	177.0	196.68	153.43	149.12
$\tan\beta$	10	10	30	30
$m_{h^0} (\equiv m_{S_4^0})$	91.21	91.63	92.74	92.83
$m_{S_1^0}$	48.58	49.33	47.27	49.84
$m_{P_2^0}$	47.21	49.60	59.05	49.45
$m_{S_2^\pm}$	187.11	187.10	187.21	187.21
$m_{\tilde{b}_1}$	831.35	831.33	830.67	830.72
$m_{\tilde{b}_2}$	875.03	875.05	875.72	875.67
$m_{\tilde{t}_1}$	763.41	763.63	761.99	761.98
$m_{\tilde{t}_2}$	961.38	961.21	962.46	962.48
$m_{\tilde{\chi}_1^0}$	43.0	44.07	44.20	44.24
$m_{\tilde{\chi}_2^0}$	55.70	57.64	61.17	60.49
$m_{\tilde{\chi}_4^\pm}$	151.55	166.61	133.69	130.77

Table 6.1: μ -parameter and relevant mass spectrum (GeV) for chosen benchmark points. $m_{\tilde{\chi}_{1,2,3}^\pm} \equiv m_{e,\mu,\tau}$. Only the relevant masses are shown here. Squark masses of first two generations are ~ 800 GeV, which are not shown here. For our parameter choices the fourth CP-even scalar state $S_4^0 \equiv h^0$ [5]. The quantities $S^0, P^0, S^\pm, \tilde{\chi}^0, \tilde{\chi}^\pm$ represent physical scalar, pseudoscalar, charged scalar, neutralino and chargino states, respectively. [1–3]. The heavy quarks namely, bottom, charm and top masses are computed at the m_Z mass scale or at the electroweak scale (see ref. [12] and references therein).

gauge singlet fermion, the associated displaced vertices are very large $\sim 3-4$ meter, which simply wash out any possible backgrounds. Detection of these displaced as well as isolated leptons and hadronic jets can lead to reliable mass reconstruction for $\tilde{\chi}_1^0$ and Higgs boson in the absence of missing energy in the final state. There is one more merit of this analysis, i.e., invariant mass reconstruction for a singlino LSP can give us an estimation of the seesaw scale, since the right-handed neutrinos are operational in light neutrino mass generation through a TeV scale seesaw mechanism [2, 13] in $\mu\nu$ SSM.

It is important to note that in the real experimental ambience, extra jets can arise from initial state radiation (ISR) and final state radiation (FSR). Likewise semi-leptonic decays of quarks can accrue extra leptons. Also from the experimental point of view one cannot have zero missing p_T in the final state. With this set of information we optimize our chosen signal as

$$(n_j \geq 4) + (n_\ell \geq 2) + (p_T \leq 30 \text{ GeV}), \quad (6.1)$$

where $n_{j(\ell)}$ represents the number of jets(leptons).

It should also be noted that, similar final states can appear from the decay of heavier scalar or pseudoscalar states in the model. Obviously, their production cross section will be smaller compared to h^0 and the invariant mass distribution (some other distributions also) should be different in those cases. So, in a sense it is possible to discriminate this signal (eqn.(6.1)) from the model backgrounds. Another possible source of backgrounds can arise from the cosmic muons. However as discussed earlier, cosmic muons have definite entry and exit points inside a detector and thus their signatures are different from the proposed signal.

6.3 Collider analysis and detection

PYTHIA (version 6.4.22) [14] has been used for the purpose of event generation. The corresponding mass spectrum and decay branching fractions are fed to PYTHIA by using the SLHA interface [15]. Subsequent decays of the produced particles, hadronization and the collider analysis were performed using PYTHIA. We used CTEQ5L parton distribution function (PDF) [16, 17] for the analysis. The renormalization/factorization scale Q was chosen to be the parton level center-of-mass energy, $\sqrt{\hat{s}}$. We also kept ISR, FSR and multiple interaction on for the analysis. The production cross-section of h^0 via gluon fusion channel for different benchmark points (table 6.1) is shown in table 6.2.

\sqrt{s}	BP-1	BP-2	BP-3	BP-4
7 TeV	6837	7365	6932	6948
14 TeV	23150	25000	23580	23560

Table 6.2: Hard scattering cross-section in fb for the process $gg \rightarrow h^0$ for PDF CTEQ5L with $Q = \sqrt{\hat{s}}$.

- We have used PYCELL, the toy calorimeter simulation provided in PYTHIA, with the following criteria:
- I. The calorimeter coverage is $|\eta| < 4.5$ and the segmentation is given by $\Delta\eta \times \Delta\phi = 0.09 \times 0.09$ which resembles a generic LHC detector.
 - II. $\Delta R \equiv \sqrt{(\Delta\eta)^2 + (\Delta\phi)^2} = 0.5$ has been used in cone algorithm for jet finding.
 - III. $p_{T,min}^{jet} = 10$ GeV.
 - IV. No jet matches with a hard lepton in the event.

In addition, the following set of standard kinematic cuts were incorporated throughout:

1. $p_T^\ell \geq 5$ GeV and $|\eta|_\ell \leq 2.5$,
2. $|\eta|_j \leq 2.5$, $\Delta R_{\ell j} \geq 0.4$, $\Delta R_{\ell\ell} \geq 0.2$,

where $\Delta R_{\ell j}$ and $\Delta R_{\ell\ell}$ measure the lepton-jet and lepton-lepton isolation, respectively. Events with isolated leptons, having $p_T \geq 5$ GeV are taken for the final state analysis.

Now depending on the distribution of the transverse decay length it is possible to study the behaviour of this spectacular signal in different regions of a generic LHC detector like CMS or ATLAS. For the purpose of illustration we present a slice like picture of the CMS detector in figure 6.2 to describe this novel signal in more details.

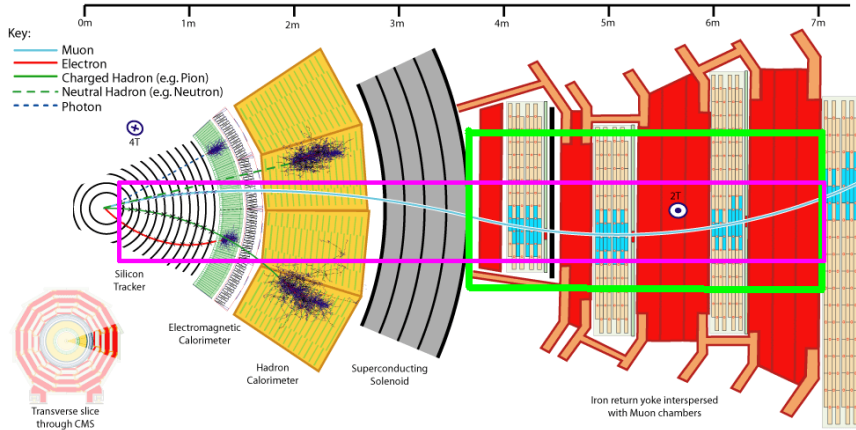


Figure 6.2: Transverse slice from the CMS detector. The maroon square corresponds to the global muons which travel throughout the detector starting from the interaction point. The light green square on the other hand corresponds to the stand-alone muons which leave their imprints only in the muon chamber.

Let us now analyze this rare signal (see eqn.(6.1)) piece wise for the CMS detector as shown by figure 6.2. We choose BP-2 as the sample benchmark point. To start with we divide the entire detector in five different regions on the basis of different transverse decay lengths (L_T) and conduct our analysis. The decay length (L) is given by

$$L = c\tau(\beta\gamma), \quad (6.2)$$

where c is the speed of light in vacuum ($= 1$ in natural unit system), τ is the proper life time and the kinematical factor $\beta\gamma = \frac{|\vec{p}|}{m}$. Here $|\vec{p}|$ is the magnitude of the three momentum $= \sqrt{|p_x|^2 + |p_y|^2 + |p_z|^2}$ and m is the mass of the decaying particle. Now it is in general difficult to measure the longitudinal component of the momentum (p_z) which lies along the beam axis, thus we choose to work with the

transverse decay length given by

$$L_T = c\tau(\beta\gamma)_T, \quad (6.3)$$

where $(\beta\gamma)_T = \frac{\sqrt{|p_x|^2 + |p_y|^2}}{m}$.

I. $L_T \leq 1 \text{ cm}$ ► Roughly 10% to 15% of the total number of events appear in this region. These events are close to the interaction point and may be mimicked by MSSM models with \mathcal{R}_p . Thus we do not consider these points in our analysis though these are also free from the SM backgrounds.

II. $1 \text{ cm} < L_T \leq 50 \text{ cm}$ ► There exist reasonable number of events ($\sim 30\%$ of the total events) with decay length in between 1 cm and 50 cm . For these events the associated electrons and muons² will leave charged tracks in the inner silicon tracker as well as the electrons will deposit their energy at the electronic calorimeter (ECAL). Associated hadronic jets will also deposit their energy at the hadronic calorimeter (HCAL). The associated muons are *global* in nature and leave their marks throughout, upto the muon chamber starting from few layers on the inner tracker. It is easy for the conventional triggers to work for this kind of signal and a reliable mass reconstruction of these displaced hadronic jets and leptons can lead to a discovery. The number of signal events in this region are shown in table 6.3.

III. $50 \text{ cm} < L_T \leq 3 \text{ m}$ ► Almost 40% of the total events appear in this region. The associated electrons and hadronic jets may or may not get detected in this situation depending on the length of the displaced vertices. However, the associated muons will leave tracks either in the muon chamber only or in the muon chamber along with matching tracks in the inner detector also. The number of signal events in this region are also given in table 6.3.

IV. $3 \text{ m} < L_T \leq 6 \text{ m}$ ► There exist some number of events ($\sim 10\%$ of the total number of events) which appear only in the territory of the muon chamber. In this case the associated electrons get absorbed in the thick iron yoke of the muon chamber and thus escape detection. Besides, it is also difficult to identify the hadronic jets as jets in the muon chamber, rather they appear as noise. The muons are, however leave visible tracks in the muon chamber *only* indicating their *stand-alone* natures. It is indeed difficult for the conventional triggers to work for this specific signal, rather this asks for a dedicated special trigger which we believe is a challenging task for experimentalists. The corresponding number of events in this region for BP-2 are shown in table 6.3.

V. $L_T \geq 7 \text{ m}$ ► There also exist a small number of events ($\sim 4\%$) where decays occur outside the detector and yield conventional missing energy signature.

\sqrt{s}	signal	No. of events		
		L_{T_1}	L_{T_2}	L_{T_3}
7 TeV	$\geq 4j + \geq 2\ell + \cancel{p}_T \leq 30 \text{ GeV}$	45	69	17
	$\geq 4j + \geq 2\mu + \cancel{p}_T \leq 30 \text{ GeV}$	27	38	11
	$\geq 4j + \geq 2e + \cancel{p}_T \leq 30 \text{ GeV}$	6	10	2
	$\geq 4j + 1e + 1\mu + \cancel{p}_T \leq 30 \text{ GeV}$	12	21	4
14 TeV	$\geq 4j + \geq 2\ell + \cancel{p}_T \leq 30 \text{ GeV}$	234	373	98
	$\geq 4j + \geq 2\mu + \cancel{p}_T \leq 30 \text{ GeV}$	128	218	58
	$\geq 4j + \geq 2e + \cancel{p}_T \leq 30 \text{ GeV}$	37	45	16
	$\geq 4j + +1e + 1\mu + \cancel{p}_T \leq 30 \text{ GeV}$	69	113	24

Table 6.3: Number of signal events for $\mathcal{L} = 5 \text{ fb}^{-1}$ for $\sqrt{s} = 7$ and 14 TeV at different ranges of the decay length for BP-2 with $1 \text{ cm} < L_{T_1} \leq 50 \text{ cm}$, $50 \text{ cm} < L_{T_2} \leq 3 \text{ m}$ and $3 \text{ m} < L_{T_3} \leq 6 \text{ m}$. L_{T_i} s are different transverse decay lengths.

The number of events for different length of displaced vertices as addressed earlier are shown in table 6.3 both for center-of-mass energy 7 and 14 TeV with an integrated luminosity of 5 fb^{-1} . Since this is a background free signal, even with this number of events this spectacular signal can lead to

² τ 's are dropped out for poor detection efficiency.

discovery at 14 TeV run of the LHC with $\mathcal{L} = 5 \text{ fb}^{-1}$. At 7 TeV the situation looks less promising and higher luminosity might be required for discovering such an event. Distribution of the transverse decay length is shown by figure 6.3.

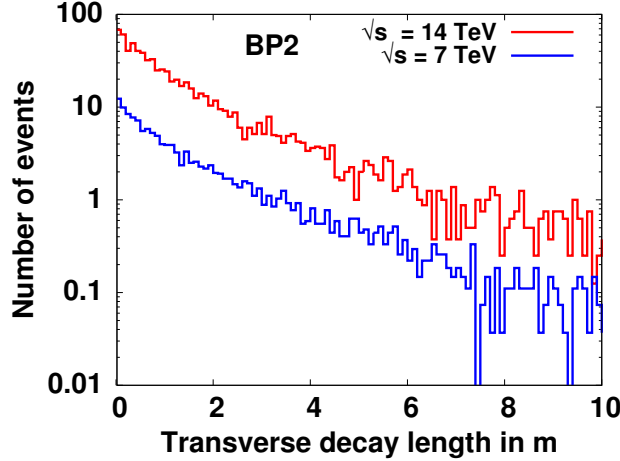


Figure 6.3: Transverse decay length distribution of $\tilde{\chi}_1^0$ for $\sqrt{s} = 7$ and 14 TeV with BP-2 for a typical detector size $\sim 10 \text{ m}$ with $\mathcal{L} = 5 \text{ fb}^{-1}$. Minimum bin size is 10 cm. The signal is given by eqn.(6.1).

In summary, this signal can give rise to non-standard activities in the muon chamber with two muons and four hadronic jets. There are, however, number of events which can leave their imprints not only at the muon chamber but also in the inner tracker and calorimeters concurrently. Integrating these two signatures can lead to discovery of an unusual signal of Higgs boson at the 14 TeV run of the LHC. Though with higher luminosity discovery at $\sqrt{s} = 7 \text{ TeV}$ is also possible. Indubitably, development of new triggers and event reconstruction tools are essential.

It is also important to note that the average decay length for a singlino like LSP is determined by the LSP mass as well as by a set of parameters $(\lambda, \kappa, v^c, Y_\nu^{ii}, v_i')$ so that the constraints on neutrino masses and mixing are satisfied. Here v^c and v_i' stand for the vacuum expectation values of the right and left-handed sneutrino fields.

6.4 Correlations with neutrino mixing angles

One of the striking features in $\mu\nu$ SSM is that certain ratios of branching fractions of the LSP decay modes are correlated with the neutrino mixing angles [2, 10]. These correlations have been explored in details in chapter 5. A consequence of the correlation with solar mixing angle θ_{12} implies $n_\mu > n_e$ in the final state. Figure 6.4 shows the lepton multiplicity distribution for inclusive $\geq 2\ell$ ($\geq 2\mu + \geq 2e + 1\mu, 1e$) and exclusive ($\geq 2\mu, \geq 2e$) for BP-2, without the signal criteria (eqn.(6.1)). Muon dominance of the higher histograms (without any isolation cuts) continues to the lower ones even after the application of $\Delta R_{\ell j}, \Delta R_{\ell\ell}$ cuts. Consequently we observe that the correlation between n_e and n_μ also appears in the lower histograms (figure 6.4) with a ratio $n_e : n_\mu \sim 1 : 3$.

We present number of events for final state signal (eqn.(6.1)) in table 6.4 both for $\sqrt{s} = 7$ and 14 TeV for $\mathcal{L} = 5 \text{ fb}^{-1}$, without a cut on the actual $\tilde{\chi}_1^0$ decay position (like table 6.3). It is important to note from table 6.4 that the correlation between n_e and n_μ in the final state is still well maintained, similar to what was shown in the lower histograms of figure 6.4 even with the final state signal topology (eqn.(6.1)).

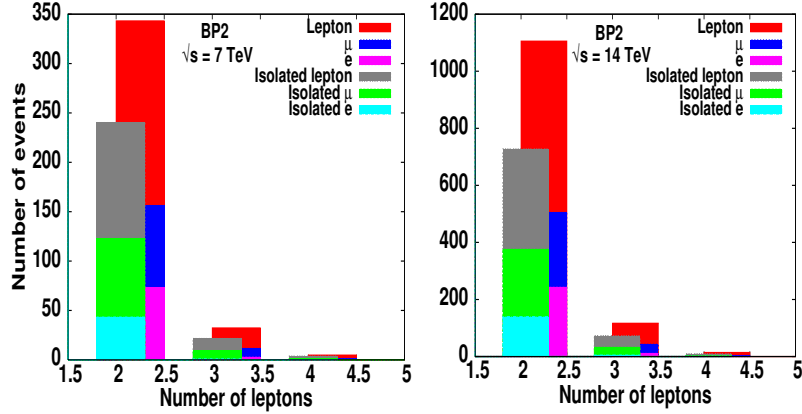


Figure 6.4: Lepton multiplicity distribution of signal for $\sqrt{s} = 7$ and 14 TeV with 1 fb^{-1} of integrated luminosity.

\sqrt{s}	signal	BP-1	BP-2	BP-3	BP-4
7 TeV	$\geq 4j + \geq 2\ell + \cancel{p}_T \leq 30 \text{ GeV}$	181	153	170	173
	$\geq 4j + \geq 2\mu + \cancel{p}_T \leq 30 \text{ GeV}$	100	85	97	100
	$\geq 4j + \geq 2e + \cancel{p}_T \leq 30 \text{ GeV}$	27	23	21	23
	$\geq 4j + 1e + 1\mu + \cancel{p}_T \leq 30 \text{ GeV}$	54	46	52	50
14 TeV	$\geq 4j + \geq 2\ell + \cancel{p}_T \leq 30 \text{ GeV}$	1043	878	951	929
	$\geq 4j + \geq 2\mu + \cancel{p}_T \leq 30 \text{ GeV}$	580	463	533	513
	$\geq 4j + \geq 2e + \cancel{p}_T \leq 30 \text{ GeV}$	160	139	121	129
	$\geq 4j + +1e + 1\mu + \cancel{p}_T \leq 30 \text{ GeV}$	306	279	300	290

Table 6.4: Expected number of events of signals for $\mathcal{L} = 5 \text{ fb}^{-1}$ for $\sqrt{s} = 7$ and 14 TeV.

6.5 Invariant mass

It has been already argued in section 6.3 that with a trustworthy detection of the two isolated and displaced muons and(or) electrons and four associated hadronic jets a background free signal of this kind can lead to definite discovery. We have already discussed about the possibility for invariant mass reconstruction using those leptons and jets, not only for a singlino like LSP but also for h^0 . Results of invariant mass reconstruction for $\tilde{\chi}_1^0$ and h^0 for BP-2 are shown in figure 6.5. We choose $jj\ell$ invariant mass $M(jj\ell)$ for $m_{\tilde{\chi}_1^0}$ reconstruction. Reconstruction of m_{h^0} was achieved through $M(jjj\ell\ell)$, invariant mass of $jjj\ell\ell$ (see eqn.(6.1)). We take the jets and leptons from the window of $35 \text{ GeV} \leq M(jj\ell) \leq 45 \text{ GeV}$ to construct $M(jjj\ell\ell)$. Even a narrow window like this cannot kill all the combinatorial backgrounds. As a corollary, effect of combinatorial background for $m_{\tilde{\chi}_1^0}$ reconstruction (4C_2 for j and 2C_1 for ℓ) also causes long tail for Higgs mass distribution.

In conclusion, we have studied an unusual but spectacular signal of Higgs boson in supersymmetry. This signal can give rise to non-standard activities in the muon chamber with two muons and four hadronic jets. There are, however, number of events which can leave their imprints not only at the muon chamber but also in the inner tracker and calorimeters concurrently. Integrating these two signatures can lead to discovery of an unusual signal of Higgs boson at the 14 TeV run of the LHC. Though with higher luminosity discovery at $\sqrt{s} = 7$ TeV is also possible. Indubitably, development of new triggers and event reconstruction tools are essential. This signal is generic to a class of models where gauge-singlet neutrinos and R_p take part simultaneously in generating neutrino masses and mixing. Another interesting feature of this study is that the number of muonic events in the final state is larger than the number of electron events and the ratio of these two numbers can be predicted from the study of the neutrino mixing angles.

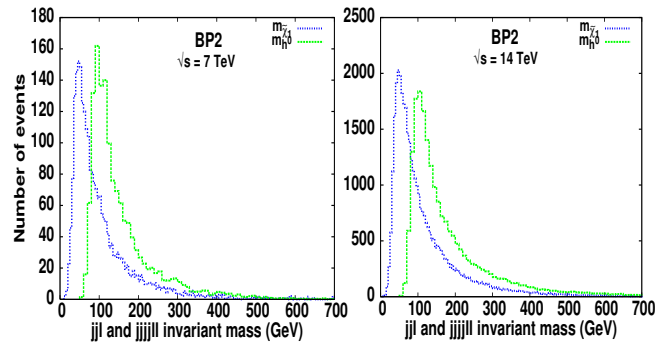


Figure 6.5: Invariant mass distribution for (a) $\tilde{\chi}_1^0$ ($jj\ell$) and (b) the Higgs boson ($jjjj\ell\ell$). Plots are shown for $\sqrt{s} = 7$ and 14 TeV with 1 fb^{-1} of integrated luminosity. Number of events for reconstructing $m_{\tilde{\chi}_1^0}$ for $\sqrt{s} = 7(14)$ TeV are scaled by a multiplicative factor 4(7).

Bibliography

- [1] Escudero N, Lopez-Fogliani D E, Munoz C and de Austri R R 2008 *JHEP* **12** 099
- [2] Ghosh P and Roy S 2009 *JHEP* **04** 069
- [3] Ghosh P, Dey P, Mukhopadhyaya B and Roy S 2010 *JHEP* **05** 087
- [4] Barger V D and Phillips R J N Redwood City, USA: Addison-Wesley (1987) 592 P. (Frontiers in Physics, 71)
- [5] Bandyopadhyay P, Ghosh P and Roy S 2010 (*Preprint* 1012.5762)
- [6] Mukhopadhyaya B, Roy S and Vissani F 1998 *Phys. Lett.* **B443** 191–195
- [7] Choi S Y, Chun E J, Kang S K and Lee J S 1999 *Phys. Rev.* **D60** 075002
- [8] J. C. Romao *et al.*, *Phys. Rev. D* **61**, 071703 (2000).
- [9] Porod W, Hirsch M, Romao J and Valle J W F 2001 *Phys. Rev.* **D63** 115004
- [10] Bartl A, Hirsch M, Vicente A, Liebler S and Porod W 2009 *JHEP* **05** 120
- [11] Schwetz T, Tortola M A and Valle J W F 2008 *New J. Phys.* **10** 113011
- [12] Djouadi A, Kalinowski J and Spira M 1998 *Comput. Phys. Commun.* **108** 56–74
- [13] Lopez-Fogliani D E and Munoz C 2006 *Phys. Rev. Lett.* **97** 041801
- [14] Sjostrand T, Mrenna S and Skands P Z 2006 *JHEP* **05** 026
- [15] Skands P Z *et al.* 2004 *JHEP* **07** 036
- [16] Lai H L *et al.* (CTEQ) 2000 *Eur. Phys. J.* **C12** 375–392
- [17] Pumplin J *et al.* 2002 *JHEP* **07** 012

Chapter 7

Summary and Conclusion

The standard model (SM) of particle physics has already been firmly established as one of the very successful theories in physics as revealed by a host of experiments. However, there are issues where the SM is an apparent failure. Perhaps the severe most problem of the SM is that the scalar mass is not protected by any symmetry arguments. Thus the Higgs boson mass (only scalar in the SM) can be as large as the Planck scale with radiative corrections. It appears that in the SM an unnatural fine-tuning in the Higgs sector is essential for a Higgs boson mass consistent with the requirements of theory and experiment. On the other side, non-vanishing neutrino masses as have been confirmed by experiments, are impossible to explain with the SM alone. These shortcomings, as discussed in chapter 1, ask for some new physics requirement at and beyond the TeV scale.

As a candidate theory to explain new physics beyond the TeV scale together with solutions to the drawbacks of the SM, supersymmetry has sought tremendous attention for the last few decades. A supersymmetric theory includes new particles having spin difference of half-integral unit with that of the SM members. The scalar masses are no longer unprotected and consequently the Higgs boson mass remains free from quadratic divergences under radiative corrections. However, missing experimental evidences for sparticles have confirmed that supersymmetry must be broken in nature so that sparticles remain heavier compared to their SM partners. It was pointed out in chapter 2 that supersymmetry must be broken softly, so that only logarithmic divergences appear in the Higgs boson mass which requires sparticle masses around the TeV scale. This is the prime reason why the discovery of TeV scale superpartners are highly envisaged at the LHC. The definite mechanism for supersymmetry breaking remains yet a debatable issue and consequently different mechanisms exist in literature. Turning our attention to the neutrino sector it appears that it is possible to accommodate massive neutrinos in supersymmetric theories either through R -parity violation or using seesaw mechanisms with extra particle content. It must be emphasized here that in spite of being successful in solving some of the drawbacks of the SM, supersymmetric theories are also not free from shortcomings, which in turn result in a wide variant of models. To mention one, as briefly reviewed in chapter 2, the non-minimal supersymmetric standard model was required to propose a solution to the μ -problem of the minimal version.

Issues of the neutrino masses and mixing remain the prime focus of this thesis. Requirement of massive neutrinos were essential to explain phenomena like atmospheric and solar neutrino problem as observed in oscillation experiments. From experimental constraints, a neutrino mass is expected to be very small. So it remains to be answered how one can generate tiny neutrino masses consistent with the oscillation data. Moreover, it also remains to be answered whether the neutrinos are Dirac or Majorana particles by nature. We review these issues in chapter 3 along with different mechanism of light neutrino mass generation both in supersymmetric and non-supersymmetric theories. The seesaw mechanisms turn out to be the simple most ways to generate small neutrino masses both in supersymmetric and non-supersymmetric theories at the cost of enhanced particle content. But there also exists models of neutrino mass generation through radiative effects. On the contrary, neutrino mass generation through the violation of R -parity is a pure supersymmetric phenomena without any SM analogue. Sources of R -parity violation can be either spontaneous or explicit. In the conventional R -parity violating (bilinear and trilinear) models loop corrections are unavoidable to accommodate

neutrino data. Bilinear R -parity violating models of neutrino mass generation have one more striking feature, that is the existence of nice correlations between the neutrino mixing angles and the lightest supersymmetric particle decay modes. In addition decays of the lightest supersymmetric particle for these class of models produce measurable displaced vertices which together with the fore stated correlations can act as a very promising probe for these models at the colliders. All of these spectacular features of the R -parity violating models have made them perhaps the most well studied models in the context of supersymmetry.

Apart from inevitable loop corrections to satisfy three flavour neutrino data, models with bilinear R -parity violation suffer from the naturalness problem similar to the μ -problem, which is better known as the ϵ -problem. A new kind of supersymmetric model of neutrino mass generation with a simultaneous solution to the μ -problem has been introduced in chapter 4. This model is known as the $\mu\nu$ SSM which by virtue of an imposed Z_3 symmetry is completely free from naturalness problem like μ or ϵ -problem. $\mu\nu$ SSM introduces the gauge singlet right-handed neutrino superfields ($\hat{\nu}_i^c$) to solve the μ problem in a way similar to that of NMSSM. These right-handed neutrinos are also instrumental for light neutrino mass generation in $\mu\nu$ SSM. The terms in the superpotential involving the $\hat{\nu}_i^c$ include the neutrino Yukawa couplings, the trilinear interaction terms among the singlet neutrino superfields as well as a term which couples the Higgs superfields to the $\hat{\nu}_i^c$. In addition, there are corresponding soft SUSY breaking terms in the scalar potential. When the scalar components of $\hat{\nu}_i^c$ get VEVs through the minimization conditions of the scalar potential, an effective μ term with an EW scale magnitude is generated. Explicit \mathcal{R}_p in $\mu\nu$ SSM through lepton number violation both in the superpotential and in the soft supersymmetry breaking Lagrangian result in enlarged (8×8) scalar, pseudoscalar and charged scalar squared mass matrix. Also the neutralino and chargino mass matrices are enhanced. Small Majorana masses of the active neutrinos are generated due to the mixing with the neutralinos as well as due to the seesaw mechanism involving the gauge singlet neutrinos. In such a scenario, we show that it is possible to provide a theory of neutrino masses and mixing explaining the experimental data, even with a flavour diagonal neutrino Yukawa coupling matrix, without resort to an arbitrary flavour structure in the neutrino sector. This essentially happens because of the mixing involved in the neutralino-neutrino (both doublet and singlet) system mentioned above. Light neutrino mass generation in $\mu\nu$ SSM is a combined effect of R -parity violation and a TeV scale seesaw mechanism using right handed neutrinos. Alternatively, as shown in chapter 4 a combined effect of Type-I and Type-III seesaw mechanisms are instrumental for neutrino mass generation in the $\mu\nu$ SSM. The TeV scale seesaw mechanism itself is very interesting since it may provide a direct way to probe the gauge singlet neutrino mass scale at the LHC and does not need to introduce a very high energy scale in the theory, as in the case of GUT seesaw. We present a detailed analytical and numerical work and show that the three flavour neutrino data can be accommodated in such a scenario. In addition, we observe that in this model different neutrino mass hierarchies can also be obtained with correct mixing pattern, at the tree level.

Though all three neutrinos acquire masses at the tree level, it is always important to judge the stability of tree level analysis in the exposure of radiative corrections. In chapter 4 effect of the complete set of one-loop corrections to the light neutrino masses and mixing are considered. The tree level and the one-loop corrected neutrino mass matrix are observed to possess similar structure but with different coefficients arising from the loop corrections. The effects of one-loop corrections are found to be capable of altering the tree level analysis in an appreciable manner depending on the concerned mass hierarchy. We also explore different regions in the SUSY parameter space, which can accommodate the three patterns in turn.

In conclusion, $\mu\nu$ SSM can accommodate neutrino masses and mixing consistent with the three flavour global neutrino data for different mass hierarchies at the tree level itself even with the choice of flavour diagonal neutrino Yukawa couplings. Inclusion of one-loop radiative corrections to light neutrino masses and mixing can alter the results of tree level analysis in a significant manner, depending on the concerned mass orderings.

Correlations between the light neutrino mixing angles with the ratios of certain decay branching ratios of the lightest supersymmetric particle (usually the lightest neutralino for a large region of the parameter space) in $\mu\nu$ SSM have been explored in chapter 5. These correlations are very similar to the bilinear \mathcal{R}_p models and have drawn immense attention as a test of neutrino mixing at a collider experiment. However, there exist certain differences between these two scenarios. In $\mu\nu$ SSM lepton

number is broken explicitly in the superpotential by terms which are trilinear as well as linear in singlet neutrino superfields. In addition to that there are lepton number conserving terms involving the singlet neutrino superfields with dimensionless neutrino Yukawa couplings. After the electroweak symmetry breaking these terms can generate the effective bilinear R-parity violating terms as well as the $\Delta L = 2$ Majorana mass terms for the singlet neutrinos in the superpotential. In general, there are corresponding soft supersymmetry breaking terms in the scalar potential. Thus the parameter space of this model is much larger compared to the bilinear R-parity violating model. Hence, in general, one would not expect a very tight correlation between the neutrino mixing angles and the ratios of decay branching ratios of the LSP. However, under certain simplifying assumptions one can reduce the number of free parameters and in those cases it is possible that the above correlations reappear. As mentioned earlier, we have studied these correlations in great detail for the two body $\ell^\pm W^\mp$ final states. These nice correlations are lost in the general scenario of bilinear-plus-trilinear R-parity violation.

Another important difference between $\mu\nu$ SSM and the bilinear R-parity violating model in the context of the decay of the LSP (assumed to be the lightest neutralino in this case) is that in $\mu\nu$ SSM the lightest neutralino can have a significant singlet neutrino (ν^c) contribution. In this case, the correlation between neutrino mixing angles and decay branching ratios of the LSP is different compared to the cases when the dominant component of the LSP is either a bino, or a higgsino or a Wino. This gives us a possibility of distinguishing between different R-parity violating models through the observation of the decay branching ratios of the LSP in collider experiments. In addition, the decay of the lightest neutralino will show displaced vertices in collider experiments and when the lightest neutralino is predominantly a singlet neutrino, the decay length can be of the order of a few meters for a lightest neutralino mass in the neighbourhood of 50 GeV. This is very different from the bilinear R-parity violating model where for a Bino LSP of similar mass the decay length is less than or of the order of a meter or so.

In a nutshell we have studied the correlations among the ratio of the branching ratios of the lightest supersymmetric particle decays into W -boson and a charged lepton with different relevant parameters. These correlations are analysed for different natures of the lightest neutralino which is usually the lightest supersymmetric particle for a novel region of the parameter space. Besides, effect of different light neutrino mass hierarchies in the correlation study are also taken into account. These spectacular and nice correlations together with a measurement of the displaced vertices can act as an important experimental signature for the $\mu\nu$ SSM.

We shift our attention to a different aspect of the $\mu\nu$ SSM in chapter 6, where a new kind of unconventional signal for the Higgs boson in supersymmetry has been advocated. The basic idea lies in the fact that with suitable choice of model parameters a right handed neutrino like lightest supersymmetric particle is possible in the $\mu\nu$ SSM and a pair of such gauge singlet fermions can couple to a MSSM like Higgs boson. We show that with heavy squark and gluino masses, pair production of the right handed neutrino like lightest supersymmetric particles from the decay of a MSSM like Higgs boson, produced in the gluon fusion channel at the LHC can be the dominant source for singlino pair production.

We analyze a specific final state signal with two isolated and displaced leptons (electron and(or) muon) and four isolated and displaced hadronic jets arising from the three body decay of a pair of right handed neutrino like lightest supersymmetric particles. This particular final state has the advantage of zero missing energy since no neutrinos appear in the process and thus a reliable Higgs boson mass reconstruction as well as the same for a right handed neutrino are highly envisaged. Appearance of reasonably large displaced vertices associated with the gauge singlet nature of a right handed neutrino are extremely useful to abate any SM backgrounds for this proposed signal. Besides, presence of the definite entry and the exit points for the cosmic muons also helps to discriminate this signal from the cosmic muon signature. Depending on the length of the associated displaced vertices this rare signal can either leave its imprints in the entire detector, starting from the tracker to the muon chamber with conventional global muon signature or can leave visible tracks in the muon chamber only from stand alone muons. The latter case also requires development of special kind of triggers. Combining the two fore mentioned scenarios a discovery with this signal criteria is expected with the 14 TeV run of the LHC. This unusual signal is also testable in the 7 TeV LHC run but requires much higher luminosity compared to the 14 TeV scenario. Ratio of the number of electrons to that of the muons in the final state signal is again observed to show correlation with the concerned neutrino mixing angle. We present

a set of four benchmark points where the neutrino data are satisfied up to one-loop level. Apart from the Higgs discovery, a signal of this kind with a faithful mass reconstruction for right handed neutrino like lightest supersymmetric particle offers a possibility to probe the seesaw scale which is one more appealing feature of the $\mu\nu$ SSM. It must be emphasized here that though we performed this analysis with tree level Higgs boson mass in $\mu\nu$ SSM, but even for loop corrected Higgs boson mass our general conclusions will not change for a singlino LSP in the mass range 20 – 60 GeV.

To conclude, $\mu\nu$ SSM is a potential candidate for explaining physics beyond the standard model. Not only this model can accommodate massive neutrinos consistent with the three flavour global data but at the same time also offers a solution to the μ -problem of supersymmetry with the use of same set of right handed neutrino superfields. This model is also phenomenologically very rich and can yield new kind of signatures at collider experiments. Diverse interesting aspects of the $\mu\nu$ SSM have been addressed in this thesis and more studies are expected to reveal more phenomenological wonders in the near future. There are a host of areas yet to be explored for this model like the effect of complete one-loop corrections in the scalar sector, more detailed analysis of new kind of Higgs signal at the colliders, a comparative study of different lightest supersymmetric particle scenarios in the context of an accelerator experiment and many more. In a nutshell, with the LHC running at the corner we expect to explore more wonders of the $\mu\nu$ SSM.

Appendix A

A.1 Scalar mass squared matrices in MSSM

✦ *Neutral scalar*, $(\mathcal{M}_{MSSM\text{-}scalar}^2)_{2\times 2}$ in the basis $(\Re H_d^0, \Re H_u^0) \Rightarrow$

$$\begin{pmatrix} B_\mu \tan\beta - \frac{\mu}{v_1} \varepsilon^\alpha v'_\alpha + 2\gamma_g v_1^2 & -2\gamma_g v_1 v_2 + B_\mu \\ -2\gamma_g v_1 v_2 + B_\mu & B_\mu \cot\beta + B_{\varepsilon_\alpha} \frac{v'_\alpha}{v_2} + 2\gamma_g v_2^2 \end{pmatrix}. \quad (\text{A.1})$$

✦ *Neutral pseudoscalar* $(\mathcal{M}_{MSSM\text{-}pseudoscalar}^2)_{2\times 2}$ in the basis $(\Im H_d^0, \Im H_u^0) \Rightarrow$

$$\begin{pmatrix} B_\mu \tan\beta - \mu \varepsilon^\alpha \frac{v'_\alpha}{v_1} & B_\mu \\ B_\mu & B_\mu \cot\beta + B_{\varepsilon_\alpha} \frac{v'_\alpha}{v_2} \end{pmatrix}. \quad (\text{A.2})$$

✦ *Charged scalar* $(\mathcal{M}_{MSSM\text{-}charged}^2)_{2\times 2}$ in the basis $(H_d^+, H_u^+) \Rightarrow$

$$(\mathcal{M}_{MSSM\text{-}charged}^2)_{2\times 2} = \begin{pmatrix} C_{11}^2 & C_{12}^2 \\ C_{21}^2 & C_{22}^2 \end{pmatrix}, \quad (\text{A.3})$$

where

$$\begin{aligned} C_{11}^2 &= B_\mu \tan\beta - \mu \varepsilon^\alpha \frac{v'_\alpha}{v_1} + Y_e^{\alpha\rho} Y_e^{\beta\rho} v'_\alpha v'_\beta - \frac{g_2^2}{2} \{v_\alpha'^2 - v_2^2\}, \\ C_{12}^2 &= B_\mu + \frac{g_2^2}{2} v_1 v_2, \quad C_{21}^2 = C_{12}^2, \\ C_{22}^2 &= B_\mu \cot\beta + B_{\varepsilon_\alpha} \frac{v'_\alpha}{v_2} + \frac{g_2^2}{2} \{v_\alpha'^2 + v_1^2\}. \end{aligned} \quad (\text{A.4})$$

In these derivations minimization equations for H_u, H_d has been used, which are given by

$$\begin{aligned} \varepsilon_\alpha^2 v_2 - B_{\varepsilon_\alpha} v'_\alpha - B_\mu v_1 + (m_{H_u}^2 + \mu^2) v_2 - \gamma_g \xi_v v_2 &= 0, \\ \mu \varepsilon^\alpha v'_\alpha - B_\mu v_2 + (m_{H_d}^2 + \mu^2) v_1 + \gamma_g \xi_v v_1 &= 0, \end{aligned} \quad (\text{A.5})$$

with $\gamma_g = \frac{1}{4}(g_1^2 + g_2^2)$ and $\xi_v = \sum v_\alpha'^2 + v_1^2 - v_2^2$.

A.2 Fermionic mass matrices in MSSM

✦ *Chargino mass matrix* $(M_{MSSM}^{chargino})_{2\times 2}$ in the basis $-i\tilde{\lambda}_2^+, \tilde{H}_u^+$ (column) and $-i\tilde{\lambda}_2^-, \tilde{H}_d^-$ (row) \Rightarrow

$$(M_{MSSM}^{chargino})_{2\times 2} = \begin{pmatrix} M_2 & g_2 v_2 \\ g_2 v_1 & \mu \end{pmatrix}. \quad (\text{A.6})$$

✠ *Neutralino mass matrix* $(M_{MSSM}^{neutralino})_{4 \times 4}$ in the basis $-i\tilde{B}^0, -i\tilde{W}_3^0, \tilde{H}_d^0, \tilde{H}_u^0 \Rightarrow$

$$(M_{MSSM}^{neutralino})_{4 \times 4} = \begin{pmatrix} M_1 & 0 & -\frac{g_1}{\sqrt{2}}v_1 & \frac{g_1}{\sqrt{2}}v_2 \\ 0 & M_2 & \frac{g_2}{\sqrt{2}}v_1 & -\frac{g_2}{\sqrt{2}}v_2 \\ -\frac{g_1}{\sqrt{2}}v_1 & \frac{g_2}{\sqrt{2}}v_1 & 0 & -\mu \\ \frac{g_1}{\sqrt{2}}v_2 & -\frac{g_2}{\sqrt{2}}v_2 & -\mu & 0 \end{pmatrix}. \quad (\text{A.7})$$

Appendix B

B.1 Scalar mass squared matrices in $\mu\nu$ SSM

Decomposition of various neutral scalar fields of $\mu\nu$ SSM in real (\Re) and imaginary (\Im) parts are as follows

$$\begin{aligned}
H_d^0 &= \Re H_d^0 + \Im H_d^0 = H_{d\mathcal{R}}^0 + iH_{d\mathcal{I}}^0, \\
H_u^0 &= \Re H_u^0 + \Im H_u^0 = H_{u\mathcal{R}}^0 + iH_{u\mathcal{I}}^0, \\
\tilde{\nu}_k^c &= \Re \tilde{\nu}_k^c + \Im \tilde{\nu}_k^c = \tilde{\nu}_{k\mathcal{R}}^c + i\tilde{\nu}_{k\mathcal{I}}^c, \\
\tilde{\nu}_k &= \Re \tilde{\nu}_k + \Im \tilde{\nu}_k = \tilde{\nu}_{k\mathcal{R}} + i\tilde{\nu}_{k\mathcal{I}}.
\end{aligned} \tag{B.1}$$

Only the real components get VEVs as indicated in eqn.(4.3).

The entries of the scalar and pseudoscalar mass-squared matrices are defined as

$$(M_S^2)^{\alpha\beta} = \left\langle \frac{1}{2} \frac{\partial^2 V_{neutral}}{\partial \phi_{\mathcal{R}}^\alpha \partial \phi_{\mathcal{R}}^\beta} \right\rangle, \quad (M_P^2)^{\alpha\beta} = \left\langle \frac{1}{2} \frac{\partial^2 V_{neutral}}{\partial \phi_{\mathcal{I}}^\alpha \partial \phi_{\mathcal{I}}^\beta} \right\rangle, \tag{B.2}$$

where

$$\begin{aligned}
\phi_{\mathcal{R}}^\alpha &= H_{d\mathcal{R}}^0, H_{u\mathcal{R}}^0, \tilde{\nu}_{k\mathcal{R}}^c, \tilde{\nu}_{k\mathcal{R}}, \\
\phi_{\mathcal{I}}^\alpha &= H_{d\mathcal{I}}^0, H_{u\mathcal{I}}^0, \tilde{\nu}_{k\mathcal{I}}^c, \tilde{\nu}_{k\mathcal{I}}.
\end{aligned} \tag{B.3}$$

Note that the Greek indices α, β are used to refer various scalar and pseudoscalar Higgs and both $SU(2)_L$ doublet and singlet sneutrinos, that is $H_d^0, H_u^0, \tilde{\nu}_k^c, \tilde{\nu}_k$, whereas k is used as a subscript to specify various flavours of doublet and singlet sneutrinos i.e., $k = e, \mu, \tau$ in the flavour (weak interaction) basis.

✂ Neutral scalar ►

In the flavour basis or weak interaction basis $\Phi_S^T = (H_{d\mathcal{R}}^0, H_{u\mathcal{R}}^0, \tilde{\nu}_{n\mathcal{R}}^c, \tilde{\nu}_{n\mathcal{R}})$,¹ the scalar mass term in the Lagrangian is of the form

$$\mathcal{L}_{scalar}^{mass} = \Phi_S^T M_S^2 \Phi_S, \tag{B.4}$$

where M_S^2 is an 8×8 symmetric matrix. The mass eigenvectors are

$$S_\alpha^0 = \mathbf{R}_{\alpha\beta}^{S^0} \Phi_{S\beta}, \tag{B.5}$$

with the diagonal mass matrix

$$(\mathcal{M}_S^{diag})_{\alpha\beta}^2 = \mathbf{R}_{\alpha\gamma}^{S^0} M_S^2 \mathbf{R}_{\gamma\delta}^{S^0}. \tag{B.6}$$

✂ Neutral pseudoscalar ►

In the weak interaction basis $\Phi_P^T = (H_{d\mathcal{I}}^0, H_{u\mathcal{I}}^0, \tilde{\nu}_{n\mathcal{I}}^c, \tilde{\nu}_{n\mathcal{I}})$, the pseudoscalar mass term in the Lagrangian is of the form

$$\mathcal{L}_{pseudoscalar}^{mass} = \Phi_P^T M_P^2 \Phi_P, \tag{B.7}$$

¹In refs. [1, 2] $H_{1\mathcal{R}}^0, H_{2\mathcal{R}}^0$ was used in lieu of $H_{d\mathcal{R}}^0, H_{u\mathcal{R}}^0$.

where M_P^2 is an 8×8 symmetric matrix. The mass eigenvectors are defined as

$$P_\alpha^0 = \mathbf{R}_{\alpha\beta}^{P^0} \Phi_{P\beta}, \quad (\text{B.8})$$

with the diagonal mass matrix

$$(\mathcal{M}_P^{diag})_{\alpha\beta}^2 = \mathbf{R}_{\alpha\gamma}^{P^0} M_{P\gamma\delta}^2 \mathbf{R}_{\beta\delta}^{P^0}. \quad (\text{B.9})$$

✦ Charged scalar ►

In the weak basis $\Phi_C^{+T} = (H_d^+, H_u^+, \tilde{e}_{Rn}^+, \tilde{e}_{Ln}^+)^2$ the charged scalar mass term in the Lagrangian is of the form

$$\mathcal{L}_{charged\ scalar}^{mass} = \Phi_C^{-T} M_{C\pm}^2 \Phi_C^+, \quad (\text{B.10})$$

where $M_{C\pm}^2$ is an 8×8 symmetric matrix. The mass eigenvectors are

$$S_\alpha^\pm = \mathbf{R}_{\alpha\beta}^{S^\pm} \Phi_{C\beta}^\pm, \quad (\text{B.11})$$

with the diagonal mass matrix

$$(\mathcal{M}_{C\pm}^{diag})_{\alpha\beta}^2 = \mathbf{R}_{\alpha\gamma}^{S^\pm} M_{C\gamma\delta}^2 \mathbf{R}_{\beta\delta}^{S^\pm}. \quad (\text{B.12})$$

The independent entries of the 8×8 symmetric matrix M_S^2 (eqn. (B.4)) using eqn. (4.5) and eqn.

²In refs. [1, 2] $\Phi_C^{+T} = (H_1^+, H_2^+, \tilde{e}_{Rn}^+, \tilde{e}_{Ln}^+)$ basis was used.

(4.6)³ are given by

$$\begin{aligned}
(M_S^2)^{H_{d\mathcal{R}}^0 H_{d\mathcal{R}}^0} &= \frac{1}{v_1} \left[\sum_j \lambda^j v_2 \left(\sum_{ik} \kappa^{ijk} v_i^c v_k^c \right) + \sum_j \lambda^j r^j v_2^2 + \mu \sum_j r_c^j v_j' \right. \\
&\quad \left. + \sum_i (A_\lambda \lambda)^i v_i^c v_2 \right] + 2\gamma_g v_1^2, \\
(M_S^2)^{H_{d\mathcal{R}}^0 H_{u\mathcal{R}}^0} &= -2 \sum_j \lambda^j \rho^j v_2 - \sum_{i,j,k} \lambda^j \kappa^{ijk} v_i^c v_k^c - 2\gamma_g v_1 v_2 - \sum_i (A_\lambda \lambda)^i v_i^c, \\
(M_S^2)^{H_{u\mathcal{R}}^0 H_{u\mathcal{R}}^0} &= \frac{1}{v_2} \left[-\sum_j \rho^j \left(\sum_{l,k} \kappa^{ljk} v_l^c v_k^c \right) - \sum_{i,j} (A_\nu Y_\nu)^{ij} v_i' v_j^c \right. \\
&\quad \left. + \sum_i (A_\lambda \lambda)^i v_i^c v_1 \right] + 2\gamma_g v_2^2, \\
(M_S^2)^{H_{d\mathcal{R}}^0 \tilde{\nu}_m^c \mathcal{R}} &= -2 \sum_j \lambda^j u_c^{mj} v_2 + 2\mu v_1 \lambda^m - \lambda^m \sum_i r_c^i v_i' - \mu r^m - (A_\lambda \lambda)^m v_2, \\
(M_S^2)^{H_{d\mathcal{R}}^0 \tilde{\nu}_m \mathcal{R}} &= -\sum_j \lambda^j Y_\nu^{mj} v_2^2 - \mu r_c^m + 2\gamma_g v_m' v_1, \\
(M_S^2)^{H_{u\mathcal{R}}^0 \tilde{\nu}_m^c \mathcal{R}} &= 2 \sum_j u_c^{mj} \rho^j + 2\lambda^m \mu v_2 + 2 \sum_i Y_\nu^{im} r_c^i v_2 + \sum_i (A_\nu Y_\nu)^{im} v_i' \\
&\quad - (A_\lambda \lambda)^m v_1, \\
(M_S^2)^{H_{u\mathcal{R}}^0 \tilde{\nu}_m \mathcal{R}} &= 2 \sum_j Y_\nu^{mj} \rho^j v_2 + \sum_{i,j,k} Y_\nu^{mj} \kappa^{ijk} v_i^c v_k^c - 2\gamma_g v_m' v_2 + \sum_j (A_\nu Y_\nu)^{mj} v_j^c, \\
(M_S^2)^{\tilde{\nu}_n^c \mathcal{R} \tilde{\nu}_m^c \mathcal{R}} &= 2 \sum_j \kappa^{jnm} \zeta^j + 4 \sum_j u_c^{mj} u_c^{nj} + \rho^m \rho^n + h^{nm} v_2^2 \\
&\quad + (m_{\tilde{\nu}_c}^2)^{mn} + 2 \sum_i (A_\kappa \kappa)^{imn} v_i^c, \\
(M_S^2)^{\tilde{\nu}_n^c \mathcal{R} \tilde{\nu}_m \mathcal{R}} &= 2 \sum_j Y_\nu^{nj} u_c^{mj} v_2 + Y_\nu^{nm} \sum_i r_c^i v_i' + r_c^n r^m - \mu v_1 Y_\nu^{nm} \\
&\quad - \lambda^m r_c^n v_1 + (A_\nu Y_\nu)^{nm} v_2, \\
(M_S^2)^{\tilde{\nu}_n \mathcal{R} \tilde{\nu}_m \mathcal{R}} &= \sum_j Y_\nu^{nj} Y_\nu^{mj} v_2^2 + r_c^m r_c^n + \gamma_g \xi_\nu \delta_{nm} + 2\gamma_g v_n' v_m' + (m_L^2)^{mn}. \tag{B.13}
\end{aligned}$$

Similarly independent elements of 8×8 symmetric matrix \mathcal{M}_P^2 (eqn. (B.7)) using eqn. (4.5) and

³A typo in $(M_S^2)^{H_{d\mathcal{R}}^0 H_{u\mathcal{R}}^0}$ in ref. [1] has been corrected.

eqn. (4.6) are given by

$$\begin{aligned}
(M_P^2)^{H_{d\mathcal{I}}^0 H_{d\mathcal{I}}^0} &= \frac{1}{v_1} \left[\sum_j \lambda^j v_2 \left(\sum_{ik} \kappa^{ijk} v_i^c v_k^c \right) + \sum_j \lambda^j r^j v_2^2 + \mu \sum_j r_c^j v_j' \right. \\
&\quad \left. + \sum_i (A_\lambda \lambda)^i v_i^c v_2 \right], \\
(M_P^2)^{H_{d\mathcal{I}}^0 H_{u\mathcal{I}}^0} &= \sum_{i,j,k} \lambda^j \kappa^{ijk} v_i^c v_k^c + \sum_i (A_\lambda \lambda)^i v_i^c, \\
(M_P^2)^{H_{u\mathcal{I}}^0 H_{u\mathcal{I}}^0} &= \frac{1}{v_2} \left[-\sum_j \rho^j \left(\sum_{l,k} \kappa^{ljk} v_l^c v_k^c \right) - \sum_{i,j} (A_\nu Y_\nu)^{ij} v_i' v_j^c \right. \\
&\quad \left. + \sum_i (A_\lambda \lambda)^i v_i^c v_1 \right], \\
(M_P^2)^{H_{d\mathcal{I}}^0 \tilde{v}_{m\mathcal{I}}^c} &= -2 \sum_j \lambda^j u_c^{mj} v_2 - \mu r^m + \lambda^m \sum_i r_c^i v_i' + (A_\lambda \lambda)^m v_2, \\
(M_P^2)^{H_{d\mathcal{I}}^0 \tilde{v}_{m\mathcal{I}}} &= -\sum_j \lambda^j Y_\nu^{mj} v_2^2 - \mu r_c^m, \\
(M_P^2)^{H_{u\mathcal{I}}^0 \tilde{v}_{m\mathcal{I}}^c} &= 2 \sum_j u_c^{mj} \rho^j - \sum_i (A_\nu Y_\nu)^{im} v_i' + (A_\lambda \lambda)^m v_1, \\
(M_P^2)^{H_{u\mathcal{I}}^0 \tilde{v}_{m\mathcal{I}}} &= -\sum_{i,j,k} Y_\nu^{mj} \kappa^{ijk} v_i^c v_k^c - \sum_j (A_\nu Y_\nu)^{mj} v_j^c, \\
(M_P^2)^{\tilde{v}_{n\mathcal{I}}^c \tilde{v}_{m\mathcal{I}}^c} &= -2 \sum_j \kappa^{jnm} \zeta^j + 4 \sum_j u_c^{mj} u_c^{nj} + \rho^m \rho^n + h^{nm} v_2^2 \\
&\quad + (m_{\tilde{v}_c}^2)^{nm} - 2 \sum_i (A_\kappa \kappa)^{inm} v_i^c, \\
(M_P^2)^{\tilde{v}_{n\mathcal{I}}^c \tilde{v}_{m\mathcal{I}}} &= 2 \sum_j u_c^{mj} Y_\nu^{nj} v_2 - Y_\nu^{nm} \sum_i r_c^i v_i' + r_c^n r^m + \mu v_1 Y_\nu^{nm} \\
&\quad - \lambda^m r_c^n v_1 - (A_\nu Y_\nu)^{nm} v_2, \\
(M_P^2)^{\tilde{v}_{n\mathcal{I}} \tilde{v}_{m\mathcal{I}}} &= \sum_j Y_\nu^{mj} Y_\nu^{nj} v_2^2 + r_c^m r_c^n + (m_L^2)^{nm} + \gamma_g \xi_\nu \delta_{mn}. \tag{B.14}
\end{aligned}$$

In eqns.(B.13), (B.14) $h^{nm} = \lambda^n \lambda^m + \sum Y_\nu^{in} Y_\nu^{im}$ has been used. One eigenvalue of \mathcal{M}_P^2 matrix is zero which corresponds to the neutral Goldstone boson.

Finally, the independent entries of \mathcal{M}_C^2 using eqn. (4.5) and eqn. (4.6) are given by

$$\begin{aligned}
(M_C^2)^{H_d H_d} &= \frac{1}{v_1} \left[\sum_j \lambda^j \zeta^j v_2 + \mu \sum_j r_c^j v_j' + \sum_i (A_\lambda \lambda)^i v_i^c v_2 \right] \\
&+ \sum_{i,j,k} Y_e^{ij} Y_e^{kj} v_i' v_k' - \frac{g_2^2}{2} (\sum_i v_i'^2 - v_2^2), \\
(M_C^2)^{H_d H_u} &= -\sum_j \lambda^j v_1 v_2 + \sum_j \lambda^j r^j v_2 + \sum_j \lambda^j u_c^{ij} v_i^c + \frac{g_2^2}{2} v_1 v_2 \\
&+ \sum_i (A_\lambda \lambda)^i v_i^c, \\
(M_C^2)^{H_u H_u} &= \frac{1}{v_2} \left[-\sum_j \rho^j \zeta^j - \sum_{i,j} (A_\nu Y_\nu)^{ij} v_i' v_j^c + \sum_i (A_\lambda \lambda)^i v_i^c v_1 \right] \\
&+ \frac{g_2^2}{2} (\sum_i v_i'^2 + v_1^2), \\
(M_C^2)^{H_d \tilde{e} R m} &= -\sum_i r_c^i Y_e^{im} v_2 - \sum_i (A_e Y_e)^{im} v_i', \\
(M_C^2)^{H_d \tilde{e} L m} &= -\mu r_c^m - \sum_{i,j} Y_e^{mj} Y_e^{ij} v_i' v_1 + \frac{g_2^2}{2} v_m' v_1, \\
(M_C^2)^{H_u \tilde{e} R m} &= -\mu \sum_i Y_e^{mi} v_i' - \sum_i Y_e^{im} r_c^i v_1, \\
(M_C^2)^{H_u \tilde{e} L m} &= -\sum_j Y_\nu^{mj} \zeta^j + \frac{g_2^2}{2} v_m' v_2 - \sum_i (A_\nu Y_\nu)^{mi} v_i^c, \\
(M_C^2)^{\tilde{e} R n \tilde{e} R m} &= \sum_{i,j} Y_e^{im} Y_e^{jn} v_i' v_j' + \sum_i Y_e^{im} Y_e^{in} v_1^2 + (m_{\tilde{e}^c}^2)^{mn} - \frac{g_1^2}{2} \xi_\nu \delta_{mn}, \\
(M_C^2)^{\tilde{e} R n \tilde{e} L m} &= -\mu Y_e^{mn} v_2 + (A_e Y_e)^{nm} v_1, \\
(M_C^2)^{\tilde{e} L n \tilde{e} L m} &= r_c^m r_c^n + \sum_j Y_e^{mj} Y_e^{nj} v_1^2 + \gamma_g \xi_\nu \delta_{mn} - \frac{g_2^2}{2} \xi_\nu \delta_{mn} \\
&+ \frac{g_2^2}{2} v_m' v_n' + (m_{\tilde{L}}^2)^{mn}. \tag{B.15}
\end{aligned}$$

For the charged scalar mass-squared matrix, seven out of eight eigenvalues are positive and the remaining one is a massless charged Goldstone boson.

Note that in eqns. (B.13), (B.14), (B.15) we have used v_i^c and v_i' to represent VEV of i -th right handed and left handed sneutrino, respectively. In ref. [1] these were represented by ν_i^c and ν_i , respectively.

✦ Squark mass matrices ▶

In the weak basis, $\tilde{u}'_i = (\tilde{u}_{L_i}, \tilde{u}_{R_i}^*)$ and $\tilde{d}'_i = (\tilde{d}_{L_i}, \tilde{d}_{R_i}^*)$, we get

$$\mathcal{L}_{\text{squark}}^{\text{mass}} = \frac{1}{2} \tilde{u}'_i{}^\dagger M_{\tilde{u}_{ij}}^2 \tilde{u}'_j + \frac{1}{2} \tilde{d}'_i{}^\dagger M_{\tilde{d}_{ij}}^2 \tilde{d}'_j, \tag{B.16}$$

where $\tilde{q} = (\tilde{u}', \tilde{d}')$. Explicitly for up and down type squarks (\tilde{u}, \tilde{d}) , using eqn.(4.6) the entries are

$$\begin{aligned}
(M_{\tilde{u}}^2)^{L_i L_j} &= (m_{\tilde{Q}}^2)^{ij} + \frac{1}{6} \left(\frac{3g_2^2}{2} - \frac{g_1^2}{2} \right) \xi_v \delta^{ij} + \sum_n Y_u^{in} Y_u^{jn} v_2^2, \\
(M_{\tilde{u}}^2)^{R_i R_j} &= (m_{\tilde{u}c}^2)^{ij} + \frac{g_1^2}{3} \xi_v \delta^{ij} + \sum_n Y_u^{ni} Y_u^{nj} v_2^2, \\
(M_{\tilde{u}}^2)^{L_i R_j} &= (A_u Y_u)^{ij} v_2 - Y_u^{ij} v_1 \mu + Y_u^{ij} \sum_l r_c^l v_l', \\
(M_{\tilde{u}}^2)^{R_i L_j} &= (M_{\tilde{u}}^2)^{L_j R_i},
\end{aligned} \tag{B.17}$$

and

$$\begin{aligned}
(M_{\tilde{d}}^2)^{L_i L_j} &= (m_{\tilde{Q}}^2)^{ij} - \frac{1}{6} \left(\frac{3g_2^2}{2} + \frac{g_1^2}{2} \right) \xi_v \delta^{ij} + \sum_n Y_d^{in} Y_d^{jn} v_1^2, \\
(M_{\tilde{d}}^2)^{R_i R_j} &= (m_{\tilde{d}c}^2)^{ij} - \frac{g_1^2}{6} \xi_v \delta^{ij} + \sum_n Y_d^{ni} Y_d^{nj} v_1^2, \\
(M_{\tilde{d}}^2)^{L_i R_j} &= (A_d Y_d)^{ij} v_1 - Y_d^{ij} v_2 \mu, \\
(M_{\tilde{d}}^2)^{R_i L_j} &= (M_{\tilde{d}}^2)^{L_j R_i}.
\end{aligned} \tag{B.18}$$

For the mass eigenstate $\tilde{\mathbf{q}}_i$ we have

$$\tilde{\mathbf{q}}_i = \mathbf{R}_{ij}^{\tilde{q}} \tilde{q}_j, \tag{B.19}$$

with the diagonal mass matrix

$$(\mathcal{M}_{\tilde{q}}^{\text{diag}})^2_{ij} = \mathbf{R}_{il}^{\tilde{q}} M_{\tilde{q}lk}^2 \mathbf{R}_{jk}^{\tilde{q}}. \tag{B.20}$$

B.2 Quark mass matrices in $\mu\nu$ SSM

The mass matrices for up and down quarks are 3×3 and they are diagonalized using bi-unitary transformation. Entries of up and down quark mass matrices $m_{3 \times 3}^u$ and $m_{3 \times 3}^d$ are same as the MSSM and are given below

$$\begin{aligned}
(m_{3 \times 3}^u)_{ij} &= Y_u^{ij} v_2, \\
(m_{3 \times 3}^d)_{ij} &= Y_d^{ij} v_1.
\end{aligned} \tag{B.21}$$

The quark mass matrices are diagonalized as follows

$$\begin{aligned}
\mathbf{R}_L^{u*} m_{3 \times 3}^u \mathbf{R}_R^{u-1} &= \mathcal{M}_U^{\text{diag}}, \\
\mathbf{R}_L^{d*} m_{3 \times 3}^d \mathbf{R}_R^{d-1} &= \mathcal{M}_D^{\text{diag}}.
\end{aligned} \tag{B.22}$$

Appendix C

C.1 Details of expansion matrix ξ

In this appendix the entries of the expansion matrix ξ are given in details

$$\begin{aligned}
\xi_{i1} &\approx \frac{\sqrt{2}g_1\mu m_{\nu^c}^2 M_2 A}{12D} b_i, \\
\xi_{i2} &\approx -\frac{\sqrt{2}g_2\mu m_{\nu^c}^2 M_1 A}{12D} b_i, \\
\xi_{i3} &\approx -\frac{m_{\nu^c}^2 M'}{2D} \left\{ \left(\lambda v_2 v^2 - 4\mu A \frac{M}{v_2} \right) a_i + m_{\nu^c} v_2 v^c b_i \right. \\
&\quad \left. - 3\lambda (\lambda v_1 v^2 - 2m_{\nu^c} v^c v_2) c_i \right\}, \\
\xi_{i4} &\approx -\frac{m_{\nu^c}^2 M'}{2D} \left\{ \lambda v_1 v^2 a_i + m_{\nu^c} v_1 v^c b_i + 3\lambda^2 v_2 v^2 c_i \right\}, \\
\xi_{i,4+i} &\approx \frac{m_{\nu^c} M'}{2D} \left\{ 2\lambda \left(\lambda v^4 (1 - \frac{1}{2} \sin^2 2\beta) + \frac{m_{\nu^c}}{2} v^c v^2 \sin 2\beta \right. \right. \\
&\quad \left. \left. + A v^2 \sin 2\beta - 4\mu M A \right) a_i - \mu m_{\nu^c} v^2 \cos 2\beta b_i \right\}, \\
\xi_{16} \approx \xi_{17} &\approx -\frac{m_{\nu^c} M'}{2D} \left\{ \lambda (\lambda v^4 - 4\mu M A) a_1 + \frac{\mu m_{\nu^c} v^2}{3} b_1 - 2\lambda \mu m_{\nu^c} v_2^2 c_1 \right\}, \\
\xi_{25} \approx \xi_{27} &\approx -\frac{m_{\nu^c} M'}{2D} \left\{ \lambda (\lambda v^4 - 4\mu M A) a_2 + \frac{\mu m_{\nu^c} v^2}{3} b_2 - 2\lambda \mu m_{\nu^c} v_2^2 c_2 \right\}, \\
\xi_{35} \approx \xi_{36} &\approx -\frac{m_{\nu^c} M'}{2D} \left\{ \lambda (\lambda v^4 - 4\mu M A) a_3 + \frac{\mu m_{\nu^c} v^2}{3} b_3 - 2\lambda \mu m_{\nu^c} v_2^2 c_3 \right\},
\end{aligned} \tag{C.1}$$

where using eqn.(4.8)

$$\begin{aligned}
a_i &= Y_{\nu}^{ii} v_2, \quad b_i = (Y_{\nu}^{ii} v_1 + 3\lambda v_i'), \quad c_i = v_i', \\
m_{\nu^c} &= 2\kappa v^c, \quad \mu = 3\lambda v^c, \quad A = (\kappa v^{c^2} + \lambda v_1 v_2), \\
v_2 &= v \sin \beta, \quad v_1 = v \cos \beta, \quad D = \text{Det}[M_{7 \times 7}], \\
\frac{1}{M} &= \frac{g_1^2}{M_1} + \frac{g_2^2}{M_2}, \quad M' = \frac{M_1 M_2}{M},
\end{aligned} \tag{C.2}$$

with $i = e, \mu, \tau \equiv 1, 2, 3$.

C.2 Tree level analysis with perturbative calculation

In the unperturbed basis $\mathcal{B}b_i b_j$ with $\mathcal{B} = \frac{2}{3} \frac{A v^c}{\Delta}$ the eigenvalues and eigenvectors are given by

$$\begin{aligned}
&0, 0, \mathcal{B}(b_e^2 + b_{\mu}^2 + b_{\tau}^2), \\
&\left(-\frac{b_{\tau}}{b_e} \quad 0 \quad 1 \right)^T, \left(-\frac{b_{\mu}}{b_e} \quad 1 \quad 0 \right)^T, \left(\frac{b_e}{b_{\tau}} \quad \frac{b_{\mu}}{b_{\tau}} \quad 1 \right)^T,
\end{aligned} \tag{C.3}$$

where b_i s are given by eqn.(4.24). We choose the co-efficient of $a_i a_j$ term to be $\mathcal{A}(= \frac{1}{6\kappa v^c})$. The set of orthonormal eigenvectors are obtained using Gram-Schmidt orthonormalization procedure. The set of orthonormal eigenvectors obtained in this case are

$$\begin{aligned} y_1 &= \frac{b_e}{\sqrt{b_e^2 + b_\tau^2}} \begin{pmatrix} -\frac{b_\tau}{b_e} \\ 0 \\ 1 \end{pmatrix}, \\ y_2 &= \frac{\sqrt{b_e^2 + b_\tau^2}}{\Omega_b} \begin{pmatrix} -\frac{b_e b_\mu}{b_e^2 + b_\tau^2} \\ 1 \\ -\frac{b_\mu b_\tau}{b_e^2 + b_\tau^2} \end{pmatrix}, \\ y_3 &= \frac{b_\tau}{\Omega_b} \begin{pmatrix} \frac{b_e}{b_\tau} \\ \frac{b_\mu}{b_\tau} \\ 1 \end{pmatrix}, \end{aligned} \quad (\text{C.4})$$

where

$$\Omega_b = \sqrt{b_e^2 + b_\mu^2 + b_\tau^2}. \quad (\text{C.5})$$

Using degenerate perturbation theory for this set of orthonormal eigenvectors, the modified eigenvalues m'_\pm and m'_3 are obtained as

$$\begin{aligned} m'_\pm &= -\frac{\mathcal{A}}{\Omega_b^2} \left\{ \Pi_{ab} \pm \sqrt{[-3\Omega_b^2(\Sigma_{ab})^2 + (\Pi_{ab})^2]} \right\}, \\ m'_3 &= \mathcal{B}\Omega_b^2 - \frac{2\mathcal{A}}{\Omega_b^2} \left\{ (\sum_i a_i b_i)^2 - 3\Lambda_{ab} \right\}, \end{aligned} \quad (\text{C.6})$$

where

$$\Lambda_{ab} = \sum_{i<j} a_i a_j b_i b_j, \quad \Pi_{ab} = \sum_{i<j} (a_i b_j + a_j b_i)^2 - \Lambda_{ab}, \quad \Sigma_{ab} = \sum_{i \neq j \neq k} a_i a_j b_k. \quad (\text{C.7})$$

As one can see from eqn.(C.6), the correction to the eigenvalues are proportional to the coefficient \mathcal{A} appearing in ordinary seesaw (eqn.(4.29)). This is a well expected result since we treat the ordinary seesaw terms as the perturbation. Let us note in passing that this effect is absent if only one generation of left chiral neutrino is considered, whereas for two and three generations of left chiral neutrino the ordinary seesaw effect exists. This can be understood from the most general calculation involving n -generations of left chiral neutrinos, where the coefficients of \mathcal{A} pick up an extra factor $(n-1)$ (see section C.3).

With the set of orthonormal eigenvectors in eqn. (C.4) and the eigenvalues in eqn.(C.6), it is possible to write down the eigenvectors of matrix given by eqn.(4.31) in the following form

$$(\mathcal{Y}_1)_{3 \times 1} = \alpha_1 y_1 + \alpha_2 y_2, \quad (\mathcal{Y}_2)_{3 \times 1} = \alpha'_1 y_1 + \alpha'_2 y_2, \quad (\mathcal{Y}_3)_{3 \times 1} = y_3, \quad (\text{C.8})$$

where $\alpha_1, \alpha_2, \alpha'_1, \alpha'_2$, are calculated using degenerate perturbation theory and their analytical expressions are given by

$$\begin{aligned} \alpha_1 &= \pm \left(\frac{h_{12}}{\sqrt{h_{12}^2 + (h_{11} - m'_+)^2}} \right), \quad \alpha_2 = \mp \left(\frac{h_{11} - m'_+}{\sqrt{h_{12}^2 + (h_{11} - m'_+)^2}} \right), \\ \alpha'_1 &= \pm \left(\frac{h_{12}}{\sqrt{h_{12}^2 + (h_{11} - m'_-)^2}} \right), \quad \alpha'_2 = \mp \left(\frac{h_{11} - m'_-}{\sqrt{h_{12}^2 + (h_{11} - m'_-)^2}} \right). \end{aligned} \quad (\text{C.9})$$

Here m'_+ , m'_- are given by eqn.(C.6) and h_{11} , h_{12} are given by

$$\begin{aligned} h_{11} &= -\frac{2\mathcal{A}(a_\tau^2 b_e^2 + a_e a_\tau b_e b_\tau + a_e^2 b_\tau^2)}{b_+^2}, \\ h_{12} &= \frac{\mathcal{A}[a_\mu(a_\tau b_e - a_e b_\tau)b_+^2 - b_\mu(2b_e b_\tau a_-^2 + a_e a_\tau b_-^2)]}{\Omega_b b_+^2}, \end{aligned} \quad (\text{C.10})$$

where

$$b_\pm^2 = (b_e^2 \pm b_\tau^2), \quad a_\pm^2 = (a_e^2 - a_\tau^2), \quad (\text{C.11})$$

and Ω_b has been defined in eqn.(C.5).

The light neutrino mixing matrix or PMNS matrix U (eqn.(3.9)) can be constructed using the eigenvectors given in eqn.(C.8) and it looks like

$$U = \begin{pmatrix} \mathcal{Y}_1 & \mathcal{Y}_2 & \mathcal{Y}_3 \end{pmatrix}_{3 \times 3}. \quad (\text{C.12})$$

C.3 See-saw masses with n generations

For the sake of completeness we mention the neutrino mass generation in $\mu\nu$ SSM with n generations of lepton family. The most general form of effective neutrino mass matrix is given by

$$(M_\nu^{seesaw})_{ij} = \frac{1}{2n\kappa v^c} a_i a_j (1 - n\delta_{ij}) + \frac{2Av^c}{n\Delta} b_i b_j. \quad (\text{C.13})$$

In this situation eqn.(4.24), eqn.(C.5) and eqn.(C.6) are modified as follows

$$\begin{aligned} \Omega_b &= \sum_m b_m^2 \\ \text{where } b_m &= (Y_\nu^{mm} v_1 + n\lambda\nu_m) \quad m = 1, \dots, n, \end{aligned} \quad (\text{C.14})$$

$$\begin{aligned} m'_r &= -\frac{(n-1)\mathcal{A}}{2\Omega_b^2} \left\{ \Pi_{ab} - (-1)^{n-r} \sqrt{[-3\Omega_b^2(\Sigma_{ab})^2 + (\Pi_{ab})^2]} \right\}, \\ m'_n &= \mathcal{B}\Omega_b^2 - \frac{(n-1)\mathcal{A}}{\Omega_b^2} \left\{ \left(\sum_i a_i^2 b_i^2 \right)^2 - 3(n-2)\Lambda_{ab} \right\}, \end{aligned} \quad (\text{C.15})$$

where $\mathcal{A} = \frac{1}{2n\kappa v^c}$, $\mathcal{B} = \frac{2Av^c}{n\Delta}$, $\mu = n\lambda v^c$, $r = 1, \dots, (n-1)$ and

$$\begin{aligned} \Lambda_{ab} &= \sum_{i < j} a_i a_j b_i b_j, \\ \Pi_{ab} &= \sum_{i < j} (a_i b_j + a_j b_i)^2 - (n-2)\Lambda_{ab}, \\ \Sigma_{ab} &= \sum_{i \neq j \neq k} a_i a_j b_k \end{aligned}$$

where $i, j, k = 1, \dots, n$. (C.16)

Appendix D

D.1 Feynman rules

The relevant Feynman rules required for the calculation of the one-loop contributions to the neutralino masses (see figure 4.7, section 4.7) are shown here [2]. Some of these Feynman rules have been derived also in ref. [1] for calculating two body decays of the lightest neutralino, $\tilde{\chi}_1^0$. Feynman rules for MSSM are given in references [3–5] and in references [6–9] for MSSM with singlet superfields. Feynman rules for R_p -violating MSSM are studied in references [10–12]. The required Feynman rules are (using relations of form *neutralino-fermion-scalar/gauge boson* and they are listed below.

★ Neutralino-neutralino-neutral scalar

The Lagrangian using four component spinor notation can be written as

$$\mathcal{L}^{nnh} = -\frac{\tilde{g}}{\sqrt{2}} \tilde{\chi}_i^0 (O_{Lijk}^{nnh} P_L + O_{Rijk}^{nnh} P_R) \tilde{\chi}_j^0 S_k^0, \quad (\text{D.1})$$

where $\tilde{g} O_{Lijk}^{nnh}$ is given by

$$\begin{aligned} & \eta_j \frac{1}{2} \left[\mathbf{R}_{k1}^{S^0} \left(\frac{g_2}{\sqrt{2}} \mathbf{N}_{i2}^* \mathbf{N}_{j3}^* - \frac{g_1}{\sqrt{2}} \mathbf{N}_{i1}^* \mathbf{N}_{j3}^* - \lambda^m \mathbf{N}_{i4}^* \mathbf{N}_{j,m+4}^* \right) \right. \\ & - \mathbf{R}_{k2}^{S^0} \left(\frac{g_2}{\sqrt{2}} \mathbf{N}_{i2}^* \mathbf{N}_{j4}^* - \frac{g_1}{\sqrt{2}} \mathbf{N}_{i1}^* \mathbf{N}_{j4}^* + \lambda^m \mathbf{N}_{i3}^* \mathbf{N}_{j,m+4}^* - Y_\nu^{mn} \mathbf{N}_{i,n+4}^* \mathbf{N}_{j,m+7}^* \right) \\ & + \mathbf{R}_{k,m+2}^{S^0} \left(Y_\nu^{mn} \mathbf{N}_{i4}^* \mathbf{N}_{j,n+7}^* - \lambda^m \mathbf{N}_{i3}^* \mathbf{N}_{j4}^* + \kappa^{mnp} \mathbf{N}_{i,n+4}^* \mathbf{N}_{j,p+4}^* \right) \\ & \left. + \mathbf{R}_{k,m+5}^{S^0} \left(\frac{g_2}{\sqrt{2}} \mathbf{N}_{i2}^* \mathbf{N}_{j,m+7}^* - \frac{g_1}{\sqrt{2}} \mathbf{N}_{i1}^* \mathbf{N}_{j,m+7}^* + Y_\nu^{mn} \mathbf{N}_{i4}^* \mathbf{N}_{j,n+4}^* \right) \right] \\ & + (i \leftrightarrow j), \end{aligned} \quad (\text{D.2})$$

and¹

$$O_{Rijk}^{nnh} = (O_{Ljik}^{nnh})^*. \quad (\text{D.3})$$

★ Neutralino-neutralino-neutral pseudoscalar

The Lagrangian using four component spinor notation can be written as

$$\mathcal{L}^{nna} = -i \frac{\tilde{g}}{\sqrt{2}} \tilde{\chi}_i^0 (O_{Lijk}^{nna} P_L + O_{Rijk}^{nna} P_R) \tilde{\chi}_j^0 P_k^0, \quad (\text{D.4})$$

¹A typos [2] in the expression of O_{Rijk}^{nnh} has been corrected.

where $\tilde{g}O_{Lijk}^{nna}$ is given as

$$\begin{aligned}
& \eta_j \frac{1}{2} \left[\mathbf{R}_{k1}^{P^0} \left(-\frac{g_2}{\sqrt{2}} \mathbf{N}_{i2}^* \mathbf{N}_{j3}^* + \frac{g_1}{\sqrt{2}} \mathbf{N}_{i1}^* \mathbf{N}_{j3}^* - \lambda^m \mathbf{N}_{i4}^* \mathbf{N}_{j,m+4}^* \right) \right. \\
& + \mathbf{R}_{k2}^{P^0} \left(\frac{g_2}{\sqrt{2}} \mathbf{N}_{i2}^* \mathbf{N}_{j4}^* - \frac{g_1}{\sqrt{2}} \mathbf{N}_{i1}^* \mathbf{N}_{j4}^* - \lambda^m \mathbf{N}_{i3}^* \mathbf{N}_{j,m+4}^* + Y_\nu^{mn} \mathbf{N}_{i,n+4}^* \mathbf{N}_{j,m+7}^* \right) \\
& + \mathbf{R}_{k,m+2}^{P^0} \left(Y_\nu^{mn} \mathbf{N}_{i4}^* \mathbf{N}_{j,n+7}^* - \lambda^m \mathbf{N}_{i3}^* \mathbf{N}_{j4}^* + \kappa^{mnp} \mathbf{N}_{i,n+4}^* \mathbf{N}_{j,p+4}^* \right) \\
& \left. + \mathbf{R}_{k,m+5}^{P^0} \left(-\frac{g_2}{\sqrt{2}} \mathbf{N}_{i2}^* \mathbf{N}_{j,m+7}^* + \frac{g_1}{\sqrt{2}} \mathbf{N}_{i1}^* \mathbf{N}_{j,m+7}^* + Y_\nu^{mn} \mathbf{N}_{i4}^* \mathbf{N}_{j,n+4}^* \right) \right] \\
& + (i \leftrightarrow j),
\end{aligned} \tag{D.5}$$

and²

$$O_{Rijk}^{nna} = -(O_{Ljik}^{nna})^*. \tag{D.6}$$

★ Neutralino-neutralino- Z^0

The Lagrangian using four component spinor notation can be written as

$$\mathcal{L}^{nnz} = -\frac{g_2}{2} \overline{\tilde{\chi}_i} \gamma^\mu (O_{Lij}^{nnz} P_L + O_{Rij}^{nnz} P_R) \tilde{\chi}_j Z_\mu^0, \tag{D.7}$$

where

$$\begin{aligned}
O_{Lij}^{nnz} &= \eta_i \eta_j \frac{1}{2 \cos\theta_W} (\mathbf{N}_{i3} \mathbf{N}_{j3}^* - \mathbf{N}_{i4} \mathbf{N}_{j4}^* + \mathbf{N}_{i,m+7} \mathbf{N}_{j,m+7}^*), \\
O_{Rij}^{nnz} &= \frac{1}{2 \cos\theta_W} (-\mathbf{N}_{i3}^* \mathbf{N}_{j3} + \mathbf{N}_{i4}^* \mathbf{N}_{j4} - \mathbf{N}_{i,m+7}^* \mathbf{N}_{j,m+7}).
\end{aligned} \tag{D.8}$$

★ Neutralino-chargino-charged scalar

The Lagrangian using four component spinor notation can be written as

$$\mathcal{L}^{ncs} = -\tilde{g} \overline{\tilde{\chi}_i} (O_{Lijk}^{ncs} P_L + O_{Rijk}^{ncs} P_R) \tilde{\chi}_j S_k^+ - \tilde{g} \overline{\tilde{\chi}_i} (O_{Lijk}^{ncs} P_L + O_{Rijk}^{ncs} P_R) \tilde{\chi}_j S_k^-, \tag{D.9}$$

where

$$\begin{aligned}
\tilde{g}O_{Lijk}^{ncs} &= \eta_j \left[\mathbf{R}_{k1}^{S^\pm} \left(-\frac{g_2}{\sqrt{2}} \mathbf{U}_{i2}^* \mathbf{N}_{j2}^* - \frac{g_1}{\sqrt{2}} \mathbf{U}_{i2}^* \mathbf{N}_{j1}^* + g_2 \mathbf{U}_{i1}^* \mathbf{N}_{j3}^* \right) \right. \\
& + \mathbf{R}_{k2}^{S^\pm} (\lambda^m \mathbf{U}_{i2}^* \mathbf{N}_{j,m+4}^* - Y_\nu^{mn} \mathbf{U}_{i,m+2}^* \mathbf{N}_{j,n+4}^*) \\
& + \mathbf{R}_{k,m+2}^{S^\pm} (Y_e^{mn} \mathbf{U}_{i,n+2}^* \mathbf{N}_{j3}^* - Y_e^{mn} \mathbf{U}_{i2}^* \mathbf{N}_{j,n+7}^*) \\
& \left. + \mathbf{R}_{k,m+5}^{S^\pm} \left(g_2 \mathbf{U}_{i1}^* \mathbf{N}_{j,m+7}^* - \frac{g_2}{\sqrt{2}} \mathbf{U}_{i,m+2}^* \mathbf{N}_{j2}^* - \frac{g_1}{\sqrt{2}} \mathbf{U}_{i,m+2}^* \mathbf{N}_{j1}^* \right) \right], \\
\tilde{g}O_{Rijk}^{ncs} &= \epsilon_i \left[\mathbf{R}_{k1}^{S^\pm} (\lambda^m \mathbf{V}_{i2} \mathbf{N}_{j,m+4} - Y_e^{mn} \mathbf{V}_{i,n+2} \mathbf{N}_{j,m+7}) \right. \\
& + \mathbf{R}_{k2}^{S^\pm} \left(\frac{g_2}{\sqrt{2}} \mathbf{V}_{i2} \mathbf{N}_{j2} + \frac{g_1}{\sqrt{2}} \mathbf{V}_{i2} \mathbf{N}_{j1} + g_2 \mathbf{V}_{i1} \mathbf{N}_{j4} \right) \\
& + \sqrt{2} g_1 \mathbf{R}_{k,m+2}^{S^\pm} \mathbf{V}_{i,m+2} \mathbf{N}_{j1} \\
& \left. + \mathbf{R}_{k,m+5}^{S^\pm} (Y_e^{mn} \mathbf{V}_{i,n+2} \mathbf{N}_{j3} - Y_\nu^{mn} \mathbf{V}_{i2} \mathbf{N}_{j,n+4}) \right],
\end{aligned} \tag{D.10}$$

and

$$O_{Lijk}^{ncs} = (O_{Rjik}^{ncs})^*, \quad O_{Rijk}^{ncs} = (O_{Ljik}^{ncs})^*. \tag{D.11}$$

²A typos [2] in the expression of O_{Rijk}^{nna} has been corrected.

★ Neutralino-chargino- W

The Lagrangian using four component spinor notation can be written as

$$\mathcal{L}^{ncw} = -g_2 \widetilde{\chi}_i \gamma^\mu (O_{Lij}^{cnw} P_L + O_{Rij}^{cnw} P_R) \widetilde{\chi}_j^0 W_\mu^+ - g_2 \widetilde{\chi}_i^0 \gamma^\mu (O_{Lij}^{ncw} P_L + O_{Rij}^{ncw} P_R) \widetilde{\chi}_j W_\mu^-. \quad (\text{D.12})$$

where

$$\begin{aligned} O_{Lij}^{cnw} &= -\epsilon_i \eta_j \left(\mathbf{V}_{i1} \mathbf{N}_{j2}^* - \frac{1}{\sqrt{2}} \mathbf{V}_{i2} \mathbf{N}_{j4}^* \right), \\ O_{Rij}^{cnw} &= -\mathbf{U}_{i1}^* \mathbf{N}_{j2} - \frac{1}{\sqrt{2}} \mathbf{U}_{i2}^* \mathbf{N}_{j3} - \frac{1}{\sqrt{2}} \mathbf{U}_{i,n+2}^* \mathbf{N}_{j,n+7}, \end{aligned} \quad (\text{D.13})$$

and

$$O_{Lij}^{ncw} = (O_{Lji}^{cnw})^*, \quad O_{Rij}^{ncw} = (O_{Rji}^{cnw})^*. \quad (\text{D.14})$$

The factors η_j and ϵ_i are the proper signs of neutralino and chargino masses [6]. They have values ± 1 .

★ Neutralino-quark-squark

The Lagrangian using four component spinor notation can be written as

$$\mathcal{L}^{nq\tilde{q}} = -\widetilde{g} \widetilde{q}_i (O_{Lijk}^{qn\tilde{q}} P_L + O_{Rijk}^{qn\tilde{q}} P_R) \widetilde{\chi}_j^0 \widetilde{q}_k - \widetilde{g} \widetilde{\chi}_i^0 (O_{Lijk}^{nq\tilde{q}} P_L + O_{Rijk}^{nq\tilde{q}} P_R) q_j \widetilde{q}_k^*. \quad (\text{D.15})$$

where

$$O_{Lijk}^{qn\tilde{q}} = (O_{Rjik}^{nq\tilde{q}})^*, \quad O_{Rijk}^{qn\tilde{q}} = (O_{Ljik}^{nq\tilde{q}})^*, \quad (\text{D.16})$$

and

$$\begin{aligned} \widetilde{g} O_{Lijk}^{nu\tilde{u}} &= \mathbf{R}_{km}^{\tilde{u}} \left(\frac{g_2}{\sqrt{2}} \mathbf{N}_{i2}^* \mathbf{R}_{Ljm}^u + \frac{g_1}{3\sqrt{2}} \mathbf{N}_{i1}^* \mathbf{R}_{Ljm}^u \right) + Y_u^{nm} \mathbf{R}_{k,m+3}^{\tilde{u}} \mathbf{N}_{i4}^* \mathbf{R}_{Ljn}^u, \\ \widetilde{g} O_{Rijk}^{nu\tilde{u}} &= Y_u^{mn*} \mathbf{R}_{km}^{\tilde{u}} \mathbf{N}_{i4} R_{Rjn}^{u*} - \frac{4g_1}{3\sqrt{2}} \mathbf{R}_{k,m+3}^{\tilde{u}} \mathbf{N}_{i1} R_{Rjm}^{u*}, \\ \widetilde{g} O_{Lijk}^{nd\tilde{d}} &= \mathbf{R}_{km}^{\tilde{d}} \left(-\frac{g_2}{\sqrt{2}} \mathbf{N}_{i2}^* \mathbf{R}_{Ljm}^d + \frac{g_1}{3\sqrt{2}} \mathbf{N}_{i1}^* \mathbf{R}_{Ljm}^d \right) + Y_d^{nm} \mathbf{R}_{k,m+3}^{\tilde{d}} \mathbf{N}_{i3}^* \mathbf{R}_{Ljn}^d, \\ \widetilde{g} O_{Rijk}^{nd\tilde{d}} &= Y_d^{mn*} \mathbf{R}_{km}^{\tilde{d}} \mathbf{N}_{i3} R_{Rjn}^{d*} + \frac{2g_1}{3\sqrt{2}} \mathbf{R}_{k,m+3}^{\tilde{d}} \mathbf{N}_{i1} R_{Rjm}^{d*}. \end{aligned} \quad (\text{D.17})$$

Note that for couplings of the type $\widetilde{\chi}^0 \widetilde{\chi}^0 \mathbf{B}$, with \mathbf{B} as either a scalar (CP-even, CP-odd) or a vector boson (Z) the associated Feynman rules must be multiplied by a 2 factor in calculations. This feature is a special property of a Majorana fermion since a Majorana field, being self conjugate (eqn.(3.16)) contains both creation and annihilation operators [3].

We have extensively used a set of relations between weak or flavour eigenbasis and mass eigenbasis, both for the scalars and fermions to derive all these Feynman rules. For the scalars (CP-even scalar, CP-odd scalar, charged scalar and scalar quarks) these relations are given by eqns.(B.5), (B.8), (B.11) and (B.19). Similar relations for the four component neutralinos and charginos (eqn.(4.21)) are given below.

■ Neutralinos

$$\begin{aligned} P_L \widetilde{B}^0 &= P_L N_{i1}^* \widetilde{\chi}_i^0, & P_L \widetilde{W}_3^0 &= P_L N_{i2}^* \widetilde{\chi}_i^0, & P_L \widetilde{H}_j &= P_L N_{i,j+2}^* \widetilde{\chi}_i^0, \\ P_L \nu_k &= P_L N_{i,k+7}^* \widetilde{\chi}_i^0, & P_L \nu_k^c &= P_L N_{i,k+4}^* \widetilde{\chi}_i^0, \\ P_R \widetilde{B}^0 &= P_R N_{i1} \widetilde{\chi}_i^0, & P_R \widetilde{W}_3^0 &= P_R N_{i2} \widetilde{\chi}_i^0, & P_R \widetilde{H}_j &= P_R N_{i,j+2}, \\ P_R \nu_k &= P_R N_{i,k+7} \widetilde{\chi}_i^0, & P_R \nu_k^c &= P_R N_{i,k+4} \widetilde{\chi}_i^0, \end{aligned} \quad (\text{D.18})$$

where $j = 1, 2$ $k = 1, 2, 3$, $i = 1, 2, \dots, 10$

and

$$P_L = \left(\frac{1 - \gamma^5}{2} \right), \quad P_R = \left(\frac{1 + \gamma^5}{2} \right). \quad (\text{D.19})$$

■ *Charginos*

$$\begin{aligned}
P_L \widetilde{W} &= P_L V_{i1}^* \widetilde{\chi}_i, & P_L \widetilde{H} &= P_L V_{i2}^* \widetilde{\chi}_i, & P_L l_k &= P_L U_{i,k+2}^* \widetilde{\chi}_i^c, \\
P_R \widetilde{W} &= P_R U_{i1} \widetilde{\chi}_i, & P_R \widetilde{H} &= P_R U_{i2} \widetilde{\chi}_i, & P_R l_k &= P_R V_{i,k+2} \widetilde{\chi}_i^c, \\
P_L \widetilde{W}^c &= P_L U_{i1}^* \widetilde{\chi}_i^c, & P_L \widetilde{H}^c &= P_L U_{i2}^* \widetilde{\chi}_i^c, & P_L l_k^c &= P_L V_{i,k+2}^* \widetilde{\chi}_i, \\
P_R \widetilde{W}^c &= P_R V_{i1} \widetilde{\chi}_i^c, & P_R \widetilde{H}^c &= P_R V_{i2} \widetilde{\chi}_i^c, & P_R l_k^c &= P_R U_{i,k+2} \widetilde{\chi}_i,
\end{aligned}
\tag{D.20}$$

where $k = 1, 2, 3$, and i varies from 1 to 5.

Appendix E

In this appendix we give the detail expressions for the renormalized self energy functions $\tilde{\Sigma}_{ij}^V$ and $\tilde{\Pi}_{ij}^V$. Different $(Of f' b)$ ¹ couplings are given in appendix D.

E.1 The $\tilde{\Sigma}_{ij}^V$ function

The regularized function $\tilde{\Sigma}_{ij}^V$ is given as

$$\begin{aligned}
& -\frac{1}{16\pi^2} \left[\frac{\tilde{g}^2}{2} \sum_{r=1}^8 \sum_{k=1}^{10} (O_{Lkir}^{nnh} O_{Rjkr}^{nnh} + O_{Ljkr}^{nnh} O_{Rkir}^{nnh}) B_1(p^2, m_{\chi_k^0}^2, m_{S_r^0}^2) \right. \\
& - \frac{\tilde{g}^2}{2} \sum_{r=1}^7 \sum_{k=1}^{10} (O_{Lkir}^{nna} O_{Rjkr}^{nna} + O_{Ljkr}^{nna} O_{Rkir}^{nna}) B_1(p^2, m_{\chi_k^0}^2, m_{P_r^0}^2) \\
& + g_2^2 \sum_{k=1}^{10} (O_{Lki}^{nnz} O_{Ljk}^{nnz} + O_{Rki}^{nnz} O_{Rjk}^{nnz}) B_1(p^2, m_{\chi_k^0}^2, m_{Z_\mu^0}^2) \\
& + 2g_2^2 \sum_{k=1}^5 (O_{Lki}^{cnw} O_{Ljk}^{cnw} + O_{Rki}^{cnw} O_{Rjk}^{cnw}) B_1(p^2, m_{\tilde{\chi}_k^\mp}^2, m_{W_\mu^\pm}^2) \\
& + \tilde{g}^2 \sum_{r=1}^7 \sum_{k=1}^5 (O_{Lkir}^{cns} O_{Rjkr}^{cns} + O_{Ljkr}^{cns} O_{Rkir}^{cns}) B_1(p^2, m_{\tilde{\chi}_k^\mp}^2, m_{S_r^\pm}^2) \\
& + 3\tilde{g}^2 \sum_{r=1}^6 \sum_{k=1}^3 (O_{Lkir}^{un\tilde{u}} O_{Rjkr}^{un\tilde{u}} + O_{Ljkr}^{un\tilde{u}} O_{Rkir}^{un\tilde{u}}) B_1(p^2, m_{u_k}^2, m_{\tilde{u}_r}^2) \\
& \left. + 3\tilde{g}^2 \sum_{r=1}^6 \sum_{k=1}^3 (O_{Lkir}^{dn\tilde{d}} O_{Rjkr}^{dn\tilde{d}} + O_{Ljkr}^{dn\tilde{d}} O_{Rkir}^{dn\tilde{d}}) B_1(p^2, m_{d_k}^2, m_{\tilde{d}_r}^2) \right]. \tag{E.1}
\end{aligned}$$

¹ f is a neutralino, f' is either a neutralino or a chargino or a quark and b is either a scalar (CP-even or CP-odd or charged or squark) or a vector boson (W^{\pm}, Z).

E.2 The $\tilde{\Pi}_{ij}^V$ function

In similar fashion $\tilde{\Pi}_{ij}^V$ looks like

$$\begin{aligned}
& -\frac{1}{16\pi^2} \left[\tilde{g}^2 \sum_{r=1}^8 \sum_{k=1}^{10} \frac{m_{\tilde{\chi}_k^0}}{2} (O_{Lk\tilde{i}r}^{nnh} O_{Ljkr}^{nnh} + O_{Rk\tilde{i}r}^{nnh} O_{Rjkr}^{nnh}) B_0(p^2, m_{\tilde{\chi}_k^0}^2, m_{S_r^0}^2) \right. \\
& - \tilde{g}^2 \sum_{r=1}^7 \sum_{k=1}^{10} \frac{m_{\tilde{\chi}_k^0}}{2} (O_{Lk\tilde{i}r}^{nna} O_{Ljkr}^{nna} + O_{Rk\tilde{i}r}^{nna} O_{Rjkr}^{nna}) B_0(p^2, m_{\tilde{\chi}_k^0}^2, m_{P_r^0}^2) \\
& - 2g_2^2 \sum_{k=1}^{10} m_{\tilde{\chi}_k^0} (O_{Lki}^{nnz} O_{Rjk}^{nnz} + O_{Ljk}^{nnz} O_{Rki}^{nnz}) B_0(p^2, m_{\tilde{\chi}_k^0}^2, m_{Z_\mu^0}^2) \\
& - 4g_2^2 \sum_{k=1}^5 m_{\tilde{\chi}_k^\pm} (O_{Lki}^{cnw} O_{Rjk}^{cnw} + O_{Rki}^{cnw} O_{Ljk}^{cnw}) B_0(p^2, m_{\tilde{\chi}_k^\pm}^2, m_{W_\mu^\pm}^2) \\
& + \tilde{g}^2 \sum_{r=1}^7 \sum_{k=1}^5 m_{\tilde{\chi}_k^\pm} (O_{Lk\tilde{i}r}^{cns} O_{Ljkr}^{cns} + O_{Rjkr}^{cns} O_{Rk\tilde{i}r}^{cns}) B_0(p^2, m_{\tilde{\chi}_k^\pm}^2, m_{S_r^\pm}^2) \\
& + 3\tilde{g}^2 \sum_{r=1}^6 \sum_{k=1}^3 m_{u_k} (O_{Lk\tilde{i}r}^{un\tilde{u}} O_{Ljkr}^{un\tilde{u}} + O_{Rk\tilde{i}r}^{un\tilde{u}} O_{Rjkr}^{un\tilde{u}}) B_0(p^2, m_{u_k}^2, m_{\tilde{u}_r}^2) \\
& \left. + 3\tilde{g}^2 \sum_{r=1}^6 \sum_{k=1}^3 m_{d_k} (O_{Lk\tilde{i}r}^{dn\tilde{d}} O_{Ljkr}^{dn\tilde{d}} + O_{Rk\tilde{i}r}^{dn\tilde{d}} O_{Rjkr}^{dn\tilde{d}}) B_0(p^2, m_{d_k}^2, m_{\tilde{d}_r}^2) \right]. \tag{E.2}
\end{aligned}$$

Note that the quark - squark loops (second row, right most diagram of figure 4.7) receive an extra enhancement by a factor of 3 from *three* different quark colours. The Passarino-Veltman functions (B_0, B_1) are given in appendix F.

Appendix F

F.1 The B_0 , B_1 functions

The B_0 and B_1 functions are Passarino-Veltman [13, 14] functions defined in the notation of [15] as

$$\begin{aligned}\frac{i}{16\pi^2}B_0(p^2, m_{f'_k}^2, m_{b_r}^2) &= (\mu^2)^{4-D} \int \frac{d^D q}{(2\pi)^D} \frac{1}{(q^2 - m_{f'_k}^2)((q+p)^2 - m_{b_r}^2)}, \\ \frac{i}{16\pi^2}B_\mu(p^2, m_{f'_k}^2, m_{b_r}^2) &= (\mu^2)^{4-D} \int \frac{d^D q}{(2\pi)^D} \frac{q_\mu}{(q^2 - m_{f'_k}^2)((q+p)^2 - m_{b_r}^2)}, \\ B_\mu(p^2, m_{f'_k}^2, m_{b_r}^2) &= p_\mu B_1(p^2, m_{f'_k}^2, m_{b_r}^2).\end{aligned}\tag{F.1}$$

D is the dimension of the integral. In the D dimension mass dimension $[M]$ for a fermion is $[M]^{\frac{D-1}{2}}$ and that of a scalar is $[M]^{\frac{D-2}{2}}$. Consequently, the 4-dimensional couplings are scaled by a factor $(\mu^2)^{4-D}$, where $[\mu] = [M]$.

Appendix G

G.1 Feynman diagrams for the tree level $\tilde{\chi}_1^0$ decay

Possible two-body and three-body final states (at the tree level) arising from the R_p -violating decays of a lightest neutralino, $\tilde{\chi}_1^0$ are shown here

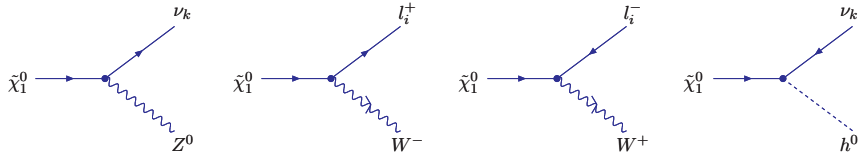


Figure G.1: Feynman diagrams for the possible two body decays of the lightest neutralino. h^0 is the lightest Higgs boson of the MSSM which is similar to the SM Higgs boson.

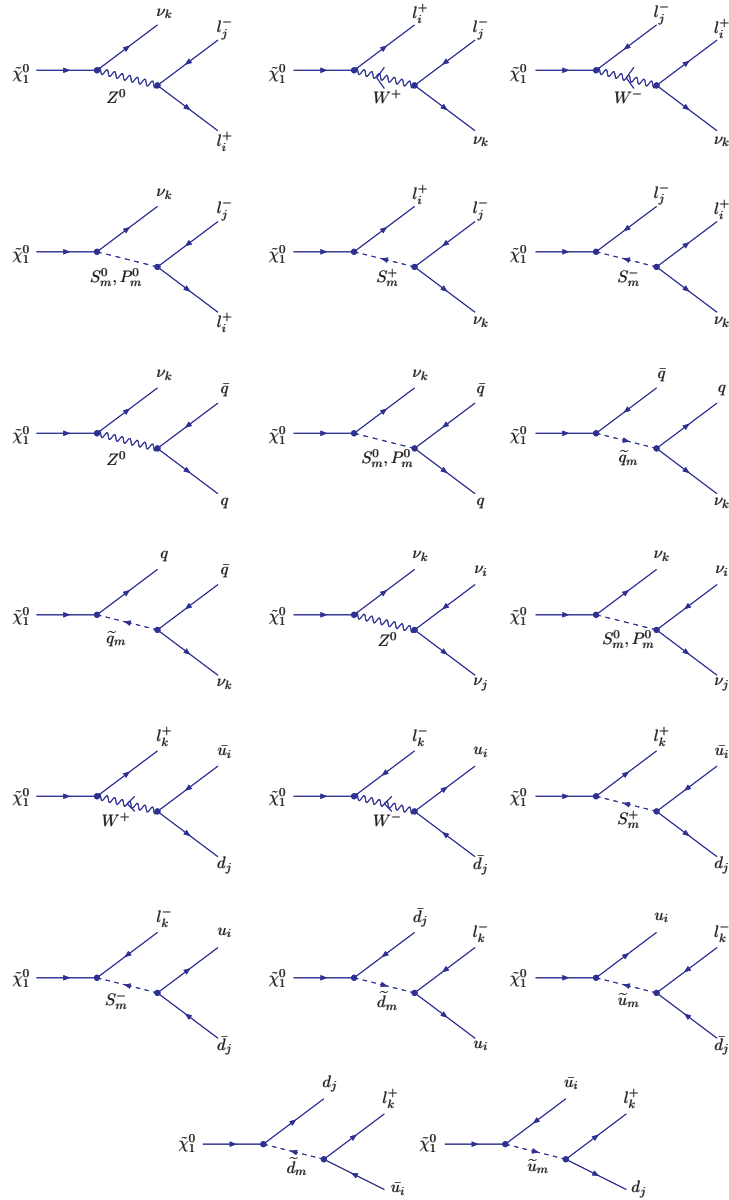


Figure G.2: Feynman diagrams for the possible three body decays of the lightest neutralino. S^0, P^0, S^\pm represent the scalar, the pseudoscalar and the charged scalar states, respectively.

Appendix H

H.1 Feynman rules

The relevant Feynman rules required for the calculation of the possible two-decays of the scalar and pseudoscalar states are shown in this appendix. The factors η_i, η_j and ϵ_i, ϵ_j are the proper signs of neutralino and chargino masses [6].

★ Chargino-chargino-neutral scalar

The Lagrangian using four component spinor notation can be written as

$$\mathcal{L}^{cch} = -\frac{\tilde{g}}{\sqrt{2}} \overline{\tilde{\chi}_i} (O_{Lijk}^{cch} P_L + O_{Rijk}^{cch} P_R) \tilde{\chi}_j S_k^0, \quad (\text{H.1})$$

where

$$\begin{aligned} \tilde{O}_{Lijk}^{cch} = & \epsilon_j \left[\mathbf{R}_{k1}^{S^0} (Y_e^{mn} \mathbf{U}_{i,m+2}^* \mathbf{V}_{j,n+2}^* + g_2 \mathbf{U}_{i2}^* \mathbf{V}_{j1}^*) \right. \\ & + g_2 \mathbf{R}_{k2}^{S^0} \mathbf{U}_{i1}^* \mathbf{V}_{j2}^* \\ & + \mathbf{R}_{k,m+2}^{S^0} (\lambda^m \mathbf{U}_{i2}^* \mathbf{V}_{j2}^* - Y_\nu^{mn} \mathbf{U}_{i,n+2}^* \mathbf{V}_{j2}^*) \\ & \left. + \mathbf{R}_{k,m+5}^{S^0} (g_2 \mathbf{U}_{i,m+2}^* \mathbf{V}_{j1}^* - Y_e^{mn} \mathbf{U}_{i2}^* \mathbf{V}_{j,n+2}^*) \right], \end{aligned} \quad (\text{H.2})$$

and

$$\tilde{O}_{Rijk}^{cch} = (\tilde{O}_{Ljik}^{cch})^*. \quad (\text{H.3})$$

★ Chargino-chargino-neutral pseudoscalar

The Lagrangian using four component spinor notation can be written as

$$\mathcal{L}^{cch} = -i \frac{\tilde{g}}{\sqrt{2}} \overline{\tilde{\chi}_i} (O_{Lijk}^{cca} P_L + O_{Rijk}^{cca} P_R) \tilde{\chi}_j P_k^0, \quad (\text{H.4})$$

where

$$\begin{aligned} \tilde{O}_{Lijk}^{cca} = & \epsilon_j \left[\mathbf{R}_{k1}^{P^0} (Y_e^{mn} \mathbf{U}_{i,m+2}^* \mathbf{V}_{j,n+2}^* - g_2 \mathbf{U}_{i2}^* \mathbf{V}_{j1}^*) \right. \\ & - g_2 \mathbf{R}_{k2}^{P^0} \mathbf{U}_{i1}^* \mathbf{V}_{j2}^* \\ & + \mathbf{R}_{k,m+2}^{P^0} (\lambda^m \mathbf{U}_{i2}^* \mathbf{V}_{j2}^* - Y_\nu^{mn} \mathbf{U}_{i,n+2}^* \mathbf{V}_{j2}^*) \\ & \left. - \mathbf{R}_{k,m+5}^{P^0} (g_2 \mathbf{U}_{i,m+2}^* \mathbf{V}_{j1}^* + Y_e^{mn} \mathbf{U}_{i2}^* \mathbf{V}_{j,n+2}^*) \right], \end{aligned} \quad (\text{H.5})$$

and

$$\tilde{O}_{Rijk}^{cca} = -(\tilde{O}_{Ljik}^{cca})^*. \quad (\text{H.6})$$

★ Down-quark-down-quark-neutral scalar

The Lagrangian using four component spinor notation can be written as

$$\mathcal{L}^{ddh} = -\tilde{g}\bar{d}_i(O_{Lijk}^{ddh}P_L + O_{Rijk}^{ddh}P_R)d_jS_k^0, \quad (\text{H.7})$$

where

$$\begin{aligned} \tilde{g}O_{Lijk}^{ddh} &= \frac{1}{\sqrt{2}}Y_d^{mn}\mathbf{R}_{k1}^{S^0}\mathbf{R}_{Lim}^d\mathbf{R}_{Ljn}^d, \\ \tilde{g}O_{Rijk}^{ddh} &= (\tilde{g}O_{Lijk}^{ddh})^*. \end{aligned} \quad (\text{H.8})$$

★ Down-quark-down-quark-neutral pseudoscalar

The Lagrangian using four component spinor notation can be written as

$$\mathcal{L}^{dda} = -i\tilde{g}\bar{d}_i(O_{Lijk}^{dda}P_L + O_{Rijk}^{dda}P_R)d_jP_k^0, \quad (\text{H.9})$$

where

$$\begin{aligned} \tilde{g}O_{Lijk}^{dda} &= \frac{1}{\sqrt{2}}Y_d^{mn}\mathbf{R}_{k1}^{P^0}\mathbf{R}_{Lim}^d\mathbf{R}_{Ljn}^d, \\ \tilde{g}O_{Rijk}^{dda} &= -(\tilde{g}O_{Lijk}^{dda})^*. \end{aligned} \quad (\text{H.10})$$

★ Up-quark-up-quark-neutral scalar

The Lagrangian using four component spinor notation can be written as

$$\mathcal{L}^{uuh} = -\tilde{g}\bar{u}_i(O_{Lijk}^{uuh}P_L + O_{Rijk}^{uuh}P_R)u_jS_k^0, \quad (\text{H.11})$$

where

$$\begin{aligned} \tilde{g}O_{Lijk}^{uuh} &= \frac{1}{\sqrt{2}}Y_u^{mn}\mathbf{R}_{k2}^{S^0}\mathbf{R}_{Lim}^u\mathbf{R}_{Ljn}^u, \\ \tilde{g}O_{Rijk}^{uuh} &= (\tilde{g}O_{Lijk}^{uuh})^*. \end{aligned} \quad (\text{H.12})$$

★ Up-quark-up-quark-neutral pseudoscalar

The Lagrangian using four component spinor notation can be written as

$$\mathcal{L}^{uua} = -i\tilde{g}\bar{u}_i(O_{Lijk}^{uua}P_L + O_{Rijk}^{uua}P_R)u_jP_k^0, \quad (\text{H.13})$$

where

$$\begin{aligned} \tilde{g}O_{Lijk}^{uua} &= \frac{1}{\sqrt{2}}Y_u^{mn}\mathbf{R}_{k2}^{P^0}\mathbf{R}_{Lim}^u\mathbf{R}_{Ljn}^u, \\ \tilde{g}O_{Rijk}^{uua} &= -(\tilde{g}O_{Lijk}^{uua})^*. \end{aligned} \quad (\text{H.14})$$

★ Quark-squark-chargino

The Lagrangian using four component spinor notation can be written as

$$\mathcal{L}^{q\tilde{q}c} = -\tilde{g}\bar{\chi}_i^c(O_{Lijk}^{cdu}P_L + O_{Rijk}^{cdu}P_R)d_j\tilde{u}_k^* - \tilde{g}\bar{u}_i(O_{Lijk}^{ucd}P_L + O_{Rijk}^{ucd}P_R)\tilde{\chi}_j\tilde{d}_k + h.c., \quad (\text{H.15})$$

where

$$\begin{aligned} \tilde{g}O_{Lijk}^{cdu} &= -Y_u^{mn}\mathbf{V}_{i2}^*\mathbf{R}_{Ljm}^d\mathbf{R}_{k,n+3}^{\tilde{u}} + g_2\mathbf{V}_{i1}^*\mathbf{R}_{Ljm}^d\mathbf{R}_{km}^{\tilde{u}}, \\ \tilde{g}O_{Rijk}^{cdu} &= -Y_d^{mn}\mathbf{U}_{i2}\mathbf{R}_{Rjn}^{d*}\mathbf{R}_{km}^{\tilde{u}}, \\ \tilde{g}O_{Lijk}^{ucd} &= -Y_u^{mn}\mathbf{V}_{j2}^*\mathbf{R}_{Lin}^u\mathbf{R}_{km}^{\tilde{d}*}, \\ \tilde{g}O_{Rijk}^{ucd} &= -Y_d^{mn}\mathbf{U}_{j2}\mathbf{R}_{Lim}^{u*}\mathbf{R}_{k,n+3}^{\tilde{d}*} + g_2\mathbf{U}_{j1}\mathbf{R}_{Lim}^{u*}\mathbf{R}_{km}^{\tilde{d}*}. \end{aligned} \quad (\text{H.16})$$

The charge conjugated chargino spinor $\tilde{\chi}^c$ is defined by eqn.(4.21).

★ Quark-quark-charged scalar

The Lagrangian is written as

$$\mathcal{L}^{qq^s} = -\tilde{g}\bar{u}_i (O_{Lijk}^{uds} P_L + O_{Rijk}^{uds} P_R) d_j S_k^+ + h.c., \quad (\text{H.17})$$

where

$$\begin{aligned} \tilde{g}O_{Lijk}^{uds} &= -Y_u^{mn} \mathbf{R}_{Rin}^u \mathbf{R}_{Ljm}^d \mathbf{R}_{k2}^{S^\pm}, \\ \tilde{g}O_{Rijk}^{uds} &= -Y_d^{mn} \mathbf{R}_{Lim}^{u*} \mathbf{R}_{Rjn}^{d*} \mathbf{R}_{k1}^{S^\pm}. \end{aligned} \quad (\text{H.18})$$

H.2 Squared matrix elements for $h^0 \rightarrow \tilde{\chi}_i^0 \tilde{\chi}_j^0, b\bar{b}$

$$\begin{aligned} \bullet |M|^2(h^0 \rightarrow \tilde{\chi}_i^0 \tilde{\chi}_j^0) &= 2\tilde{g}^2(m_{h^0}^2 - (m_{\tilde{\chi}_i^0}^2 + m_{\tilde{\chi}_j^0}^2)) \left(O_{Lij4}^{nnh^*} O_{Lij4}^{nnh} + O_{Rij4}^{nnh^*} O_{Rij4}^{nnh} \right) \\ &\quad - 4\tilde{g}^4 m_{\tilde{\chi}_i^0} m_{\tilde{\chi}_j^0} \left(O_{Rij4}^{nnh^*} O_{Lij4}^{nnh} + O_{Lij4}^{nnh^*} O_{Rij4}^{nnh} \right), \end{aligned} \quad (\text{H.19})$$

where we have used the favour of an extra 2 factor for $\tilde{\chi}_i^0 - \tilde{\chi}_j^0 - h^0$ vertex [3] (also see appendix D).

$$\begin{aligned} \bullet |M|^2(h^0 \rightarrow b\bar{b}) &= 3\tilde{g}^2(m_{h^0}^2 - 2m_b^2) \left(O_{L334}^{ddh^*} O_{L334}^{ddh} + O_{R334}^{ddh^*} O_{R334}^{ddh} \right) \\ &\quad - 6\tilde{g}^4 m_b^2 \left(O_{R334}^{ddh^*} O_{L334}^{ddh} + O_{L334}^{ddh^*} O_{R334}^{ddh} \right), \end{aligned} \quad (\text{H.20})$$

where we have used relations from appendix D, section H.1 and put 3 for the colour factor.

Appendix I

I.1 Three body decays of the $\tilde{\chi}_1^0$ LSP

In this appendix we write down the spin-averaged (sum over spins of the final state particles and average over the spin of initial particle) matrix element square ($|\overline{\mathbb{M}}|^2$) for possible three body decays of a neutralino LSP $\tilde{\chi}_1^0$. The possible decays are given by eqn. (5.1). Since neutralinos are fermion by nature, an average over the initial particle spin will yield a factor of $\frac{1}{2}$, that is, mathematically,

$$|\overline{\mathbb{M}}|^2 = \frac{N_c X_1 X_2}{(2 \cdot \frac{1}{2} + 1)} \left[\sum_i M_i^\dagger M_i + 2\Re \left(\sum_{i \neq j} M_i^\dagger M_j \right) \right], \quad (\text{I.1})$$

where we put spin of the neutralino, $S_{\tilde{\chi}_i^0} = \frac{1}{2}$ in the factor $\frac{1}{(2 \cdot S_{\tilde{\chi}_i^0} + 1)}$. The second terms of eqn.(I.1) represent interference terms in case multiple Feynman diagrams exist for a given process. M_i represents amplitude of the i -th Feynman Diagram of a given process. N_c is the colour factor which is 3(1) for processes involving quarks(leptons). The quantities $X_{1,2}$ are associated with two vertices of a three body decay process (see figure I.1 for example). These factors are 2 for a $\tilde{\chi}_1^0 - \nu -$ neutral boson vertex¹ since $\tilde{\chi}_1^0, \nu$ are Majorana particles [3] and equal to 1 for all other vertices. All processes are calculated using 't-Hooft-Feynman gauge.

I.2 Process $\tilde{\chi}_1^0 \rightarrow q\bar{q}\nu$

We start with the processes involving down type quarks ($q = d, s, b$) first and later for $q = u, c$. We represent different down and up type quarks generically by d and u , respectively. We write down all possible $M_i^\dagger M_j$ for the five diagrams shown in figure I.1. The four-momentum assignments are as follows

$$\tilde{\chi}_1^0(P) \rightarrow q(k) + \bar{q}(k') + \nu_i(p), \quad (\text{I.2})$$

where i stands for i -th neutrino flavour. $i = 1, 2, 3$ or e, μ, τ . $\tilde{\chi}_1^0$ is the lightest of the seven heavy neutralino states (see eqn.(4.16)).

$$\begin{aligned} \bullet M_1^\dagger M_1(\tilde{\chi}_1^0 \rightarrow q\bar{q} \sum \nu_i) &= \frac{4g_2^4}{\cos_{\theta_w}^2 [(k+k')^2 - m_Z^2] + m_Z^2 \Gamma_Z^2} \\ &\sum_i [(P.k)(p.k') A_{11}^{qq\nu_i} + (P.k')(p.k) B_{11}^{qq\nu_i} + m_q^2 (P.p) C_{11}^{qq\nu_i}], \end{aligned} \quad (\text{I.3})$$

¹Also true for $\nu - \nu -$ neutral boson vertex, appears in $\tilde{\chi}_1^0 \rightarrow \nu\nu\bar{\nu}$ process.

where $q = d(u)$, Γ_Z is the Z -boson decay width and

$$\begin{aligned}
A_{11}^{qq\nu_i} &= \left(O_{Li1}^{1iZ^*} O_{Li1}^{1iZ} + O_{Ri1}^{1iZ^*} O_{Ri1}^{1iZ} \right) \left(\frac{1(4)}{9} \sin^4 \theta_W - \frac{1(2)}{6} \sin^2 \theta_W + \frac{1}{8} \right) \\
&+ \left(O_{Li1}^{1iZ^*} O_{Li1}^{1iZ} - O_{Ri1}^{1iZ^*} O_{Ri1}^{1iZ} \right) \left(\frac{1(2)}{6} \sin^2 \theta_W - \frac{1}{8} \right), \\
B_{11}^{qq\nu_i} &= \left(O_{Li1}^{1iZ^*} O_{Li1}^{1iZ} + O_{Ri1}^{1iZ^*} O_{Ri1}^{1iZ} \right) \left(\frac{1(4)}{9} \sin^4 \theta_W - \frac{1(2)}{6} \sin^2 \theta_W + \frac{1}{8} \right) \\
&- \left(O_{Li1}^{1iZ^*} O_{Li1}^{1iZ} - O_{Ri1}^{1iZ^*} O_{Ri1}^{1iZ} \right) \left(\frac{1}{6} \sin^2 \theta_W - \frac{1}{8} \right), \\
C_{11}^{qq\nu_i} &= \left(O_{Li1}^{1iZ^*} O_{Li1}^{1iZ} + O_{Ri1}^{1iZ^*} O_{Ri1}^{1iZ} \right) \left(\frac{1(4)}{9} \sin^4 \theta_W - \frac{1(2)}{6} \sin^2 \theta_W \right). \tag{I.4}
\end{aligned}$$

$$\begin{aligned}
\bullet M_2^\dagger M_2 (\tilde{\chi}_1^0 \rightarrow q\bar{q} \sum \nu_i) &= \sum_{r,s=1}^2 \frac{4\tilde{g}^4}{\left[((k'+p)^2 - m_{\tilde{q}_r}^2)((k'+p)^2 - m_{\tilde{q}_s}^2) \right]} \\
&\sum_i \left[(P.k)(p.k') A_{22}^{qq\nu_i} + m_q m_{\tilde{\chi}_1^0} (p.k') B_{22}^{qq\nu_i} \right], \tag{I.5}
\end{aligned}$$

where

$$\begin{aligned}
A_{22}^{qq\nu_i} &= \left(O_{Lq1\tilde{q}_s}^{q1\tilde{q}} O_{Lq1\tilde{q}_r}^{q1\tilde{q}^*} + O_{Rq1\tilde{q}_s}^{q1\tilde{q}} O_{Rq1\tilde{q}_r}^{q1\tilde{q}^*} \right) \left(O_{Li\tilde{q}_s}^{iq\tilde{q}} O_{Li\tilde{q}_r}^{iq\tilde{q}^*} + O_{Ri\tilde{q}_s}^{iq\tilde{q}} O_{Ri\tilde{q}_r}^{iq\tilde{q}^*} \right), \\
B_{22}^{qq\nu_i} &= \left(O_{Lq1\tilde{q}_s}^{q1\tilde{q}} O_{Rq1\tilde{q}_r}^{q1\tilde{q}^*} + O_{Rq1\tilde{q}_s}^{q1\tilde{q}} O_{Lq1\tilde{q}_r}^{q1\tilde{q}^*} \right) \left(O_{Li\tilde{q}_s}^{iq\tilde{q}} O_{Li\tilde{q}_r}^{iq\tilde{q}^*} + O_{Ri\tilde{q}_s}^{iq\tilde{q}} O_{Ri\tilde{q}_r}^{iq\tilde{q}^*} \right). \tag{I.6}
\end{aligned}$$

$$\begin{aligned}
\bullet M_3^\dagger M_3 (\tilde{\chi}_1^0 \rightarrow q\bar{q} \sum \nu_i) &= \sum_{r,s=1}^2 \frac{4\tilde{g}^4}{\left[((k+p)^2 - m_{\tilde{q}_r}^2)((k+p)^2 - m_{\tilde{q}_s}^2) \right]} \\
&\sum_i \left[(P.k')(p.k) A_{33}^{qq\nu_i} + m_q m_{\tilde{\chi}_1^0} (p.k) B_{33}^{qq\nu_i} \right], \tag{I.7}
\end{aligned}$$

where

$$\begin{aligned}
A_{33}^{qq\nu_i} &= \left(O_{L1q\tilde{q}_s}^{1q\tilde{q}} O_{L1q\tilde{q}_r}^{1q\tilde{q}^*} + O_{R1q\tilde{q}_s}^{1q\tilde{q}} O_{R1q\tilde{q}_r}^{1q\tilde{q}^*} \right) \left(O_{Lqi\tilde{q}_s}^{qi\tilde{q}} O_{Lqi\tilde{q}_r}^{qi\tilde{q}^*} + O_{Rqi\tilde{q}_s}^{qi\tilde{q}} O_{Rqi\tilde{q}_r}^{qi\tilde{q}^*} \right), \\
B_{33}^{qq\nu_i} &= \left(O_{L1q\tilde{q}_s}^{1q\tilde{q}} O_{R1q\tilde{q}_r}^{1q\tilde{q}^*} + O_{R1q\tilde{q}_s}^{1q\tilde{q}} O_{L1q\tilde{q}_r}^{1q\tilde{q}^*} \right) \left(O_{Lqi\tilde{q}_s}^{qi\tilde{q}} O_{Lqi\tilde{q}_r}^{qi\tilde{q}^*} + O_{Rqi\tilde{q}_s}^{qi\tilde{q}} O_{Rqi\tilde{q}_r}^{qi\tilde{q}^*} \right). \tag{I.8}
\end{aligned}$$

$$\begin{aligned}
\bullet M_4^\dagger M_4 (\tilde{\chi}_1^0 \rightarrow q\bar{q} \sum \nu_i) &= \sum_{k,l=1}^8 \frac{2\tilde{g}^4}{\left[((k+k')^2 - m_{S_0^2}^2)((k+k')^2 - m_{S_0^2}^2) \right]} \\
&\sum_i \left[(P.p)(k.k') A_{44}^{qq\nu_i} - m_q^2 (P.p) B_{44}^{qq\nu_i} \right], \tag{I.9}
\end{aligned}$$

where

$$\begin{aligned}
A_{44}^{qq\nu_i} &= \left(O_{Lqqk}^{qqh^*} O_{Lqql}^{qqh} + O_{Rqqk}^{qqh^*} O_{Rqql}^{qqh} \right) \left(O_{Li1k}^{i1h^*} O_{Li1l}^{i1h} + O_{Ri1k}^{i1h^*} O_{Ri1l}^{i1h} \right), \\
B_{44}^{qq\nu_i} &= \left(O_{Lqqk}^{qqh^*} O_{Rqql}^{qqh} + O_{Rqqk}^{qqh^*} O_{Lqql}^{qqh} \right) \left(O_{Li1k}^{i1h^*} O_{Li1l}^{i1h} + O_{Ri1k}^{i1h^*} O_{Ri1l}^{i1h} \right). \tag{I.10}
\end{aligned}$$

$$\begin{aligned}
\bullet M_5^\dagger M_5 (\tilde{\chi}_1^0 \rightarrow q\bar{q} \sum \nu_i) &= \sum_{k,l=1}^8 \frac{2\tilde{g}^4}{\left[((k+k')^2 - m_{P_0^2}^2)((k+k')^2 - m_{P_0^2}^2) \right]} \\
&\sum_i \left[(P.p)(k.k') A_{55}^{qq\nu_i} - m_q^2 (P.p) B_{55}^{qq\nu_i} \right], \tag{I.11}
\end{aligned}$$

where

$$\begin{aligned} A_{55}^{qq\nu_i} &= \left(O_{Lqk}^{qqa*} O_{Lqql}^{qqa} + O_{Rqk}^{qqa*} O_{Rqql}^{qqa} \right) \left(O_{Li1k}^{i1a*} O_{Li1l}^{i1a} + O_{Ri1k}^{i1a*} O_{Ri1l}^{i1a} \right), \\ B_{55}^{qq\nu_i} &= \left(O_{Lqk}^{qqa*} O_{Rqql}^{qqa} + O_{Rqk}^{qqa*} O_{Lqql}^{qqa} \right) \left(O_{Li1k}^{i1a*} O_{Li1l}^{i1a} + O_{Ri1k}^{i1a*} O_{Ri1l}^{i1a} \right). \end{aligned} \quad (\text{I.12})$$

$$\begin{aligned} \bullet M_1^\dagger M_2(\tilde{\chi}_1^0 \rightarrow q\bar{q} \sum \nu_i) &= -(+) \sum_{r=1}^2 \frac{2g_2^2 \tilde{g}^2 \sec\theta_W}{\left[((k+k')^2 - m_Z^2 - im_Z \Gamma_Z)((p+k')^2 - m_{\tilde{q}_r}^2) \right]} \\ &\sum_i \left[2(p.k')(P.k)(A_{12}^{qq\nu_i} C_{12}^{qq\nu_i} + B_{12}^{qq\nu_i} D_{12}^{qq\nu_i}) + m_q m_{\tilde{\chi}_1^0}(p.k)(A_{12}^{qq\nu_i} D_{12}^{qq\nu_i} + B_{12}^{qq\nu_i} C_{12}^{qq\nu_i}) \right. \\ &\left. + 2m_q m_{\tilde{\chi}_1^0}(p.k')(B_{12}^{qq\nu_i} E_{12}^{qq\nu_i} + A_{12}^{qq\nu_i} F_{12}^{qq\nu_i}) + m_q^2(P.p)(A_{12}^{qq\nu_i} E_{12}^{qq\nu_i} + B_{12}^{qq\nu_i} F_{12}^{qq\nu_i}) \right], \end{aligned} \quad (\text{I.13})$$

where

$$\begin{aligned} A_{12}^{qq\nu_i} &= O_{Li1}^{1iZ*} O_{Ri1q_r}^{iq\tilde{q}}, \quad B_{12}^{qq\nu_i} = O_{Ri1}^{1iZ*} O_{Li1q_r}^{iq\tilde{q}}, \quad C_{12}^{qq\nu_i} = \frac{1(2)}{3} \sin^2\theta_W O_{Lq1q_r}^{q1\tilde{q}}, \\ D_{12}^{qq\nu_i} &= \frac{1(2)}{3} \sin^2\theta_W O_{Rq1q_r}^{q1\tilde{q}} - \frac{1}{2} O_{Rq1q_r}^{q1\tilde{q}}, \quad E_{12}^{qq\nu_i} = \frac{1(2)}{3} \sin^2\theta_W O_{Lq1q_r}^{q1\tilde{q}} - \frac{1}{2} O_{Lq1q_r}^{q1\tilde{q}}, \\ F_{12}^{qq\nu_i} &= \frac{1(2)}{3} \sin^2\theta_W O_{Rq1q_r}^{q1\tilde{q}}. \end{aligned} \quad (\text{I.14})$$

$$\begin{aligned} \bullet M_1^\dagger M_3(\tilde{\chi}_1^0 \rightarrow q\bar{q} \sum \nu_i) &= (-) \sum_{r=1}^2 \frac{2g_2^2 \tilde{g}^2 \sec\theta_W}{\left[((k+k')^2 - m_Z^2 - im_Z \Gamma_Z)((p+k)^2 - m_{\tilde{q}_r}^2) \right]} \\ &\sum_i \left[2(p.k)(P.k')(A_{13}^{qq\nu_i} C_{13}^{qq\nu_i} + B_{13}^{qq\nu_i} D_{13}^{qq\nu_i}) + m_q m_{\tilde{\chi}_1^0}(p.k')(A_{13}^{qq\nu_i} D_{13}^{qq\nu_i} + B_{13}^{qq\nu_i} C_{13}^{qq\nu_i}) \right. \\ &\left. + 2m_q m_{\tilde{\chi}_1^0}(p.k)(B_{13}^{qq\nu_i} E_{13}^{qq\nu_i} + A_{13}^{qq\nu_i} F_{13}^{qq\nu_i}) + m_q^2(P.p)(A_{13}^{qq\nu_i} E_{13}^{qq\nu_i} + B_{13}^{qq\nu_i} F_{13}^{qq\nu_i}) \right], \end{aligned} \quad (\text{I.15})$$

where

$$\begin{aligned} A_{13}^{qq\nu_i} &= O_{Ri1}^{1iZ*} O_{Lq1q_r}^{iq\tilde{q}}, \quad B_{13}^{qq\nu_i} = O_{Li1}^{1iZ*} O_{Rq1q_r}^{iq\tilde{q}}, \quad C_{13}^{qq\nu_i} = \frac{1(2)}{3} \sin^2\theta_W O_{R1q\tilde{q}_r}^{1q\tilde{q}}, \\ D_{13}^{qq\nu_i} &= \frac{1(2)}{3} \sin^2\theta_W O_{L1q\tilde{q}_r}^{1q\tilde{q}} - \frac{1}{2} O_{L1q\tilde{q}_r}^{1q\tilde{q}}, \quad E_{13}^{qq\nu_i} = \frac{1(2)}{3} \sin^2\theta_W O_{R1q\tilde{q}_r}^{1q\tilde{q}} - \frac{1}{2} O_{R1q\tilde{q}_r}^{1q\tilde{q}}, \\ F_{13}^{qq\nu_i} &= \frac{1(2)}{3} \sin^2\theta_W O_{L1q\tilde{q}_r}^{1q\tilde{q}}. \end{aligned} \quad (\text{I.16})$$

$$\begin{aligned} \bullet M_1^\dagger M_4(\tilde{\chi}_1^0 \rightarrow q\bar{q} \sum \nu_i) &= -(+) \sum_{k=1}^8 \frac{\sqrt{2}g_2^2 \tilde{g}^2 \sec\theta_W}{\left[((k+k')^2 - m_Z^2 - im_Z \Gamma_Z)((k+k')^2 - m_{\tilde{S}_k^0}^2) \right]} \\ &\sum_i \left[m_q m_{\tilde{\chi}_1^0}(p.k') A_{14}^{qq\nu_i} - m_q m_{\tilde{\chi}_1^0}(p.k) B_{14}^{qq\nu_i} \right], \end{aligned} \quad (\text{I.17})$$

where

$$\begin{aligned} A_{14}^{qq\nu_i} &= \left(O_{Ri1}^{1iZ*} O_{Li1k}^{i1h} + O_{Li1}^{1iZ*} O_{Ri1k}^{i1h} \right) \\ &\times \left\{ \left(\frac{1(2)}{3} \sin^2\theta_W - \frac{1}{2} \right) O_{Lbbk}^{qqh} + \frac{1(2)}{3} \sin^2\theta_W O_{Rbbk}^{qqh} \right\}, \\ B_{14}^{qq\nu_i} &= \left(O_{Ri1}^{1iZ*} O_{Li1k}^{i1h} + O_{Li1}^{1iZ*} O_{Ri1k}^{i1h} \right) \\ &\times \left\{ \left(\frac{1(2)}{3} \sin^2\theta_W - \frac{1}{2} \right) O_{Rbbk}^{qqh} + \frac{1(2)}{3} \sin^2\theta_W O_{Lbbk}^{qqh} \right\}. \end{aligned} \quad (\text{I.18})$$

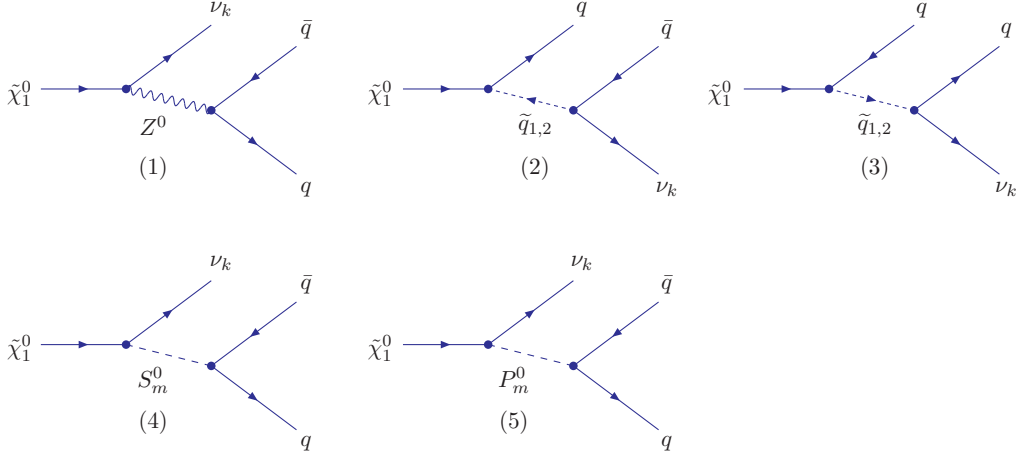


Figure I.1: Feynman diagrams for the possible three body decays of the lightest supersymmetric particle into $q\bar{q}\nu$ final states, with $q \neq t$. $\tilde{q}_{1,2}$ are the squarks in the mass eigenbasis (see eqn.(B.19)). S_m^0, P_m^0 are the neutral scalar and pseudoscalar states of the $\mu\nu$ SMS as shown by eqns.(B.5), (B.8).

$$\bullet M_1^\dagger M_5(\tilde{\chi}_1^0 \rightarrow q\bar{q} \sum \nu_i) = (-) \sum_{k=1}^8 \frac{\sqrt{2}g_2^2\tilde{g}^2 \sec\theta_W}{\left[((k+k')^2 - m_Z^2 - im_Z\Gamma_Z)((k+k')^2 - m_{P_k^0}^2) \right]} \sum_i \left[m_q m_{\tilde{\chi}_1^0}(p.k') A_{15}^{qq\nu_i} - m_q m_{\tilde{\chi}_1^0}(p.k) B_{15}^{qq\nu_i} \right], \quad (\text{I.19})$$

where

$$\begin{aligned} A_{15}^{qq\nu_i} &= \left(O_{Ri1}^{1iZ^*} O_{Li1k}^{i1a} + O_{Li1}^{1iZ^*} O_{Ri1k}^{i1a} \right) \\ &\times \left\{ \left(\frac{1(2)}{3} \sin^2\theta_W - \frac{1}{2} \right) O_{Lbbk}^{qqa} + \frac{1(2)}{3} \sin^2\theta_W O_{Rbbk}^{qqa} \right\}, \\ B_{15}^{qq\nu_i} &= \left(O_{Ri1}^{1iZ^*} O_{Li1k}^{i1a} + O_{Li1}^{1iZ^*} O_{Ri1k}^{i1a} \right) \\ &\times \left\{ \left(\frac{1(2)}{3} \sin^2\theta_W - \frac{1}{2} \right) O_{Rbbk}^{qqa} + \frac{1(2)}{3} \sin^2\theta_W O_{Lbbk}^{qqa} \right\}. \end{aligned} \quad (\text{I.20})$$

$$\begin{aligned} \bullet M_2^\dagger M_3(\tilde{\chi}_1^0 \rightarrow q\bar{q} \sum \nu_i) &= - \sum_{r,s=1}^2 \frac{2\tilde{g}^4}{\left[((p+k')^2 - m_{\tilde{q}_r}^2)((p+k)^2 - m_{\tilde{q}_s}^2) \right]} \\ &\sum_i \left[\{ (P.k)(p.k') - (P.p)(k.k') + (P.k')(p.k) \} (A_{23}^{qq\nu_i} O_{Lq1\tilde{q}_r}^{q1\tilde{q}^*} + B_{23}^{qq\nu_i} O_{Rq1\tilde{q}_r}^{q1\tilde{q}^*}) \right. \\ &+ m_q m_{\tilde{\chi}_1^0}(p.k') (A_{23}^{qq\nu_i} O_{Rq1\tilde{q}_r}^{q1\tilde{q}^*} + B_{23}^{qq\nu_i} O_{Lq1\tilde{q}_r}^{q1\tilde{q}^*}) + m_q m_{\tilde{\chi}_1^0}(p.k) (C_{23}^{qq\nu_i} O_{Rq1\tilde{q}_r}^{q1\tilde{q}^*} + D_{23}^{qq\nu_i} O_{Lq1\tilde{q}_r}^{q1\tilde{q}^*}) \\ &\left. + m_q^2 (P.p) (C_{23}^{qq\nu_i} O_{Lq1\tilde{q}_r}^{q1\tilde{q}^*} + D_{23}^{qq\nu_i} O_{Rq1\tilde{q}_r}^{q1\tilde{q}^*}) \right], \end{aligned} \quad (\text{I.21})$$

where

$$\begin{aligned} A_{23}^{qq\nu_i} &= O_{Lqi\tilde{q}_s}^{qi\tilde{q}} O_{Liq\tilde{q}_r}^{iq\tilde{q}^*} O_{L1q\tilde{q}_s}^{1q\tilde{q}}, & B_{23}^{qq\nu_i} &= O_{Rqi\tilde{q}_s}^{qi\tilde{q}} O_{Riq\tilde{q}_r}^{iq\tilde{q}^*} O_{R1q\tilde{q}_s}^{1q\tilde{q}}, \\ C_{23}^{qq\nu_i} &= O_{Rqi\tilde{q}_s}^{qi\tilde{q}} O_{Riq\tilde{q}_r}^{iq\tilde{q}^*} O_{L1q\tilde{q}_s}^{1q\tilde{q}}, & D_{23}^{qq\nu_i} &= O_{Lqi\tilde{q}_s}^{qi\tilde{q}} O_{Liq\tilde{q}_r}^{iq\tilde{q}^*} O_{R1q\tilde{q}_s}^{1q\tilde{q}}. \end{aligned} \quad (\text{I.22})$$

$$\begin{aligned}
\bullet M_2^\dagger M_4(\tilde{\chi}_1^0 \rightarrow q\bar{q} \sum \nu_i) &= \sum_{r=1}^2 \sum_{k=1}^8 \frac{\sqrt{2}\tilde{g}^4}{\left[((p+k')^2 - m_{\tilde{q}_r}^2)((k+k')^2 - m_{S_k^0}^2) \right]} \\
&\sum_i \left[\{(P.p)(k.k') - (P.k')(p.k) + (p.k')(P.k)\} (A_{24}^{qq\nu_i} O_{Rq1\tilde{q}_r}^{q1\tilde{q}^*} + B_{24}^{qq\nu_i} O_{Lq1\tilde{q}_r}^{q1\tilde{q}^*}) \right. \\
&- i\epsilon_{\mu\nu\rho\sigma} p^\mu P^\nu k^\rho k'^\sigma (A_{24}^{qq\nu_i} O_{Rq1\tilde{q}_r}^{q1\tilde{q}^*} - B_{24}^{qq\nu_i} O_{Lq1\tilde{q}_r}^{q1\tilde{q}^*}) \\
&+ m_q m_{\tilde{\chi}_1^0} (p.k') (A_{24}^{qq\nu_i} O_{Lq1\tilde{q}_r}^{q1\tilde{q}^*} + B_{24}^{qq\nu_i} O_{Rq1\tilde{q}_r}^{q1\tilde{q}^*}) - m_q m_{\tilde{\chi}_1^0} (p.k) (C_{24}^{qq\nu_i} O_{Lq1\tilde{q}_r}^{q1\tilde{q}^*} + D_{24}^{qq\nu_i} O_{Rq1\tilde{q}_r}^{q1\tilde{q}^*}) \\
&\left. - m_q^2 (P.p) (C_{24}^{qq\nu_i} O_{Rq1\tilde{q}_r}^{q1\tilde{q}^*} + D_{24}^{qq\nu_i} O_{Lq1\tilde{q}_r}^{q1\tilde{q}^*}) \right], \tag{I.23}
\end{aligned}$$

where

$$\begin{aligned}
A_{24}^{qq\nu_i} &= O_{Rqk}^{qqh} O_{Riq\tilde{q}_r}^{iq\tilde{q}^*} O_{Ri1k}^{i1h}, & B_{24}^{qq\nu_i} &= O_{Lqk}^{qqh} O_{Liq\tilde{q}_r}^{iq\tilde{q}^*} O_{Li1k}^{i1h}, \\
C_{24}^{qq\nu_i} &= O_{Lqk}^{qqh} O_{Riq\tilde{q}_r}^{iq\tilde{q}^*} O_{Ri1k}^{i1h}, & D_{24}^{qq\nu_i} &= O_{Rqk}^{qqh} O_{Liq\tilde{q}_r}^{iq\tilde{q}^*} O_{Li1k}^{i1h}.
\end{aligned} \tag{I.24}$$

$$\begin{aligned}
\bullet M_2^\dagger M_5(\tilde{\chi}_1^0 \rightarrow q\bar{q} \sum \nu_i) &= - \sum_{r=1}^2 \sum_{k=1}^8 \frac{\sqrt{2}\tilde{g}^4}{\left[((p+k')^2 - m_{\tilde{q}_r}^2)((k+k')^2 - m_{P_k^0}^2) \right]} \\
&\sum_i \left[\{(P.p)(k.k') - (P.k')(p.k) + (p.k')(P.k)\} (A_{25}^{qq\nu_i} O_{Rq1\tilde{q}_r}^{q1\tilde{q}^*} + B_{25}^{qq\nu_i} O_{Lq1\tilde{q}_r}^{q1\tilde{q}^*}) \right. \\
&- i\epsilon_{\mu\nu\rho\sigma} p^\mu P^\nu k^\rho k'^\sigma (A_{25}^{qq\nu_i} O_{Rq1\tilde{q}_r}^{q1\tilde{q}^*} - B_{25}^{qq\nu_i} O_{Lq1\tilde{q}_r}^{q1\tilde{q}^*}) \\
&+ m_q m_{\tilde{\chi}_1^0} (p.k') (A_{25}^{qq\nu_i} O_{Lq1\tilde{q}_r}^{q1\tilde{q}^*} + B_{25}^{qq\nu_i} O_{Rq1\tilde{q}_r}^{q1\tilde{q}^*}) - m_q m_{\tilde{\chi}_1^0} (p.k) (C_{25}^{qq\nu_i} O_{Lq1\tilde{q}_r}^{q1\tilde{q}^*} + D_{25}^{qq\nu_i} O_{Rq1\tilde{q}_r}^{q1\tilde{q}^*}) \\
&\left. - m_q^2 (P.p) (C_{25}^{qq\nu_i} O_{Rq1\tilde{q}_r}^{q1\tilde{q}^*} + D_{25}^{qq\nu_i} O_{Lq1\tilde{q}_r}^{q1\tilde{q}^*}) \right], \tag{I.25}
\end{aligned}$$

where

$$\begin{aligned}
A_{25}^{qq\nu_i} &= O_{Rqk}^{qqa} O_{Riq\tilde{q}_r}^{iq\tilde{q}^*} O_{Ri1k}^{i1a}, & B_{25}^{qq\nu_i} &= O_{Lqk}^{qqa} O_{Liq\tilde{q}_r}^{iq\tilde{q}^*} O_{Li1k}^{i1a}, \\
C_{25}^{qq\nu_i} &= O_{Lqk}^{qqa} O_{Riq\tilde{q}_r}^{iq\tilde{q}^*} O_{Ri1k}^{i1a}, & D_{25}^{qq\nu_i} &= O_{Rqk}^{qqa} O_{Liq\tilde{q}_r}^{iq\tilde{q}^*} O_{Li1k}^{i1a}.
\end{aligned} \tag{I.26}$$

$$\begin{aligned}
\bullet M_3^\dagger M_4(\tilde{\chi}_1^0 \rightarrow q\bar{q} \sum \nu_i) &= \sum_{r=1}^2 \sum_{k=1}^8 \frac{\sqrt{2}\tilde{g}^4}{\left[((p+k)^2 - m_{\tilde{q}_r}^2)((k+k')^2 - m_{S_k^0}^2) \right]} \\
&\sum_i \left[\{(P.k')(p.k) - (P.k)(p.k') + (P.p)(k.k')\} (A_{34}^{qq\nu_i} O_{L1q\tilde{q}_r}^{1q\tilde{q}^*} + B_{34}^{qq\nu_i} O_{R1q\tilde{q}_r}^{1q\tilde{q}^*}) \right. \\
&+ m_q m_{\tilde{\chi}_1^0} (p.k) (A_{34}^{qq\nu_i} O_{R1q\tilde{q}_r}^{1q\tilde{q}^*} + B_{34}^{qq\nu_i} O_{L1q\tilde{q}_r}^{1q\tilde{q}^*}) - m_q m_{\tilde{\chi}_1^0} (p.k') (C_{34}^{qq\nu_i} O_{R1q\tilde{q}_r}^{1q\tilde{q}^*} + D_{34}^{qq\nu_i} O_{L1q\tilde{q}_r}^{1q\tilde{q}^*}) \\
&\left. - m_q^2 (P.p) (C_{34}^{qq\nu_i} O_{L1q\tilde{q}_r}^{1q\tilde{q}^*} + D_{34}^{qq\nu_i} O_{R1q\tilde{q}_r}^{1q\tilde{q}^*}) \right], \tag{I.27}
\end{aligned}$$

where

$$\begin{aligned}
A_{34}^{qq\nu_i} &= O_{Lqk}^{qqh} O_{Lqi\tilde{q}_r}^{qi\tilde{q}^*} O_{Li1k}^{i1h}, & B_{34}^{qq\nu_i} &= O_{Rqk}^{qqh} O_{Rqi\tilde{q}_r}^{qi\tilde{q}^*} O_{Ri1k}^{i1h}, \\
C_{34}^{qq\nu_i} &= O_{Rqk}^{qqh} O_{Lqi\tilde{q}_r}^{qi\tilde{q}^*} O_{Li1k}^{i1h}, & D_{34}^{qq\nu_i} &= O_{Lqk}^{qqh} O_{Rqi\tilde{q}_r}^{qi\tilde{q}^*} O_{Ri1k}^{i1h}.
\end{aligned} \tag{I.28}$$

$$\begin{aligned}
\bullet M_3^\dagger M_5(\tilde{\chi}_1^0 \rightarrow q\bar{q} \sum \nu_i) &= - \sum_{r=1}^2 \sum_{k=1}^8 \frac{\sqrt{2}\tilde{g}^4}{\left[((p+k)^2 - m_{\tilde{q}_r}^2)((k+k')^2 - m_{P_k^0}^2) \right]} \\
&\sum_i \left[\{(P.k')(p.k) - (P.k)(p.k') + (P.p)(k.k')\} (A_{35}^{qq\nu_i} O_{L1q\tilde{q}_r}^{1q\tilde{q}^*} + B_{35}^{qq\nu_i} O_{R1q\tilde{q}_r}^{1q\tilde{q}^*}) \right. \\
&+ m_q m_{\tilde{\chi}_1^0} (p.k) (A_{35}^{qq\nu_i} O_{R1q\tilde{q}_r}^{1q\tilde{q}^*} + B_{35}^{qq\nu_i} O_{L1q\tilde{q}_r}^{1q\tilde{q}^*}) - m_q m_{\tilde{\chi}_1^0} (p.k') (C_{35}^{qq\nu_i} O_{R1q\tilde{q}_r}^{1q\tilde{q}^*} + D_{35}^{qq\nu_i} O_{L1q\tilde{q}_r}^{1q\tilde{q}^*}) \\
&\left. - m_q^2 (P.p) (C_{35}^{qq\nu_i} O_{L1q\tilde{q}_r}^{1q\tilde{q}^*} + D_{35}^{qq\nu_i} O_{R1q\tilde{q}_r}^{1q\tilde{q}^*}) \right], \tag{I.29}
\end{aligned}$$

where

$$\begin{aligned} A_{35}^{qq\nu_i} &= O_{Lqqk}^{qqa} O_{Lqi\tilde{q}_r}^{qi\tilde{q}^*} O_{Li1k}^{i1a}, & B_{35}^{qq\nu_i} &= O_{Rqqk}^{qqa} O_{Rqi\tilde{q}_r}^{qi\tilde{q}^*} O_{Ri1k}^{i1a}, \\ C_{35}^{qq\nu_i} &= O_{Rqqk}^{qqa} O_{Lqi\tilde{q}_r}^{qi\tilde{q}^*} O_{Li1k}^{i1a}, & D_{35}^{qq\nu_i} &= O_{Lqqk}^{qqa} O_{Rqi\tilde{q}_r}^{qi\tilde{q}^*} O_{Ri1k}^{i1a}. \end{aligned} \quad (\text{I.30})$$

$$\begin{aligned} \bullet M_4^\dagger M_5(\tilde{\chi}_1^0 \rightarrow q\bar{q} \sum \nu_i) &= - \sum_{k,l=1}^8 \frac{2\tilde{g}^4}{\left[((k+k')^2 - m_{S_k^0}^2)((k+k')^2 - m_{P_l^0}^2) \right]} \\ &\sum_i \left[(P.p)(k.k') \left(O_{Li1k}^{i1h^*} O_{Li1l}^{i1a} + O_{Ri1k}^{i1h^*} O_{Ri1l}^{i1a} \right) \left(O_{Lqqk}^{qqh^*} O_{Lqql}^{qqa} + O_{Rqqk}^{qqh^*} O_{Rqql}^{qqa} \right) \right. \\ &\left. - m_q^2 (P.p) \left(O_{Li1k}^{i1h^*} O_{Li1l}^{i1a} + O_{Ri1k}^{i1h^*} O_{Ri1l}^{i1a} \right) \left(O_{Rqqk}^{qqh^*} O_{Lqql}^{qqa} + O_{Lqqk}^{qqh^*} O_{Rqql}^{qqa} \right) \right]. \end{aligned} \quad (\text{I.31})$$

Values for Weinberg angle θ_W and Γ_Z are given in ref. [16]. Quark masses are also taken from ref. [16]. All the relevant couplings are given in appendices D and H.

I.3 Process $\tilde{\chi}_1^0 \rightarrow \ell_i^+ \ell_j^- \nu_k$

We represent different leptons (e, μ, τ) generically by ℓ . We write down all possible $M_i^\dagger M_j$ for the seven diagrams shown in figure I.2. We treat the charge conjugate leptons as charginos (see eqn.(4.21)) as shown in eqn.(D.20). The four-momentum assignments are as follows

$$\tilde{\chi}_1^0(P) \rightarrow \ell_i^+(k) + \ell_j^-(k') + \nu_k(p), \quad (\text{I.32})$$

where i, j, k stand for various lepton flavours. $i, j, k = 1, 2, 3$ or e, μ, τ .

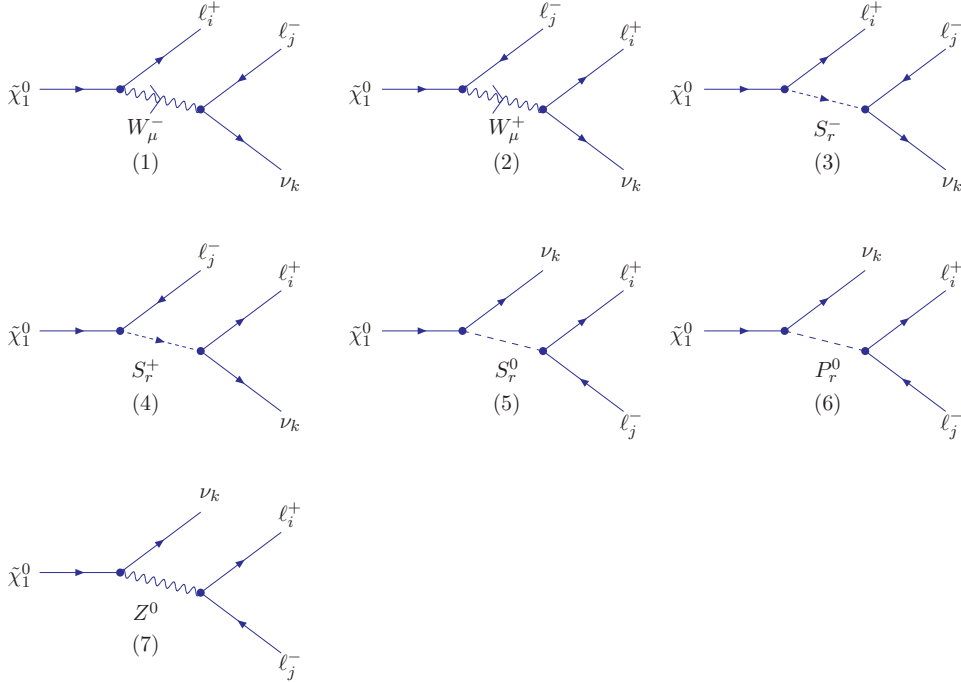


Figure I.2: Feynman diagrams for the possible three body decays of the lightest supersymmetric particle into $\ell_i^+ + \ell_j^- + \nu_k$ final states. S_r^\pm, S_r^0, P_r^0 are the charged scalar, neutral scalar and pseudoscalar states of the $\mu\nu$ SSM as shown by eqns.(B.11), (B.5), (B.8).

$$\begin{aligned}
& \bullet M_1^\dagger M_1(\tilde{\chi}_1^0 \rightarrow \sum \ell_i^+ \ell_j^- \nu_k) = \frac{8g_2^4}{[(p+k')^2 - m_W^2]^2 + m_W^2 \Gamma_W^2} \\
& \sum_{i,j,k} \left[2(P.k')(p.k) A_{11}^{\ell_i^+ \ell_j^- \nu_k} + 2(P.p)(k.k') B_{11}^{\ell_i^+ \ell_j^- \nu_k} - m_{\ell_i} m_{\tilde{\chi}_1^0} (p.k') C_{11}^{\ell_i^+ \ell_j^- \nu_k} \right],
\end{aligned} \tag{I.33}$$

where

$$\begin{aligned}
A_{11}^{\ell_i^+ \ell_j^- \nu_k} &= (O_{Li1}^{cnw*} O_{Li1}^{cnw} O_{Lkj}^{ncw*} O_{Lkj}^{ncw} + O_{Ri1}^{cnw*} O_{Ri1}^{cnw} O_{Rkj}^{ncw*} O_{Rkj}^{ncw}), \\
B_{11}^{\ell_i^+ \ell_j^- \nu_k} &= (O_{Li1}^{cnw*} O_{Li1}^{cnw} O_{Rkj}^{ncw*} O_{Rkj}^{ncw} + O_{Ri1}^{cnw*} O_{Ri1}^{cnw} O_{Lkj}^{ncw*} O_{Lkj}^{ncw}), \\
C_{11}^{\ell_i^+ \ell_j^- \nu_k} &= (O_{Ri1}^{cnw*} O_{Li1}^{cnw} + O_{Li1}^{cnw*} O_{Ri1}^{cnw}) (O_{Lkj}^{ncw*} O_{Lkj}^{ncw} + O_{Rkj}^{ncw*} O_{Rkj}^{ncw}).
\end{aligned} \tag{I.34}$$

$$\begin{aligned}
& \bullet M_2^\dagger M_2(\tilde{\chi}_1^0 \rightarrow \sum \ell_i^+ \ell_j^- \nu_k) = \frac{8g_2^4}{[(p+k)^2 - m_W^2]^2 + m_W^2 \Gamma_W^2} \\
& \sum_{i,j,k} \left[2(P.k)(p.k') A_{22}^{\ell_i^+ \ell_j^- \nu_k} + 2(P.p)(k.k') B_{22}^{\ell_i^+ \ell_j^- \nu_k} - m_{\ell_j} m_{\tilde{\chi}_1^0} (p.k) C_{22}^{\ell_i^+ \ell_j^- \nu_k} \right],
\end{aligned} \tag{I.35}$$

where

$$\begin{aligned}
A_{22}^{\ell_i^+ \ell_j^- \nu_k} &= (O_{L1j}^{ncw*} O_{L1j}^{ncw} O_{L1j}^{cnw*} O_{L1j}^{cnw} + O_{R1j}^{ncw*} O_{R1j}^{ncw} O_{R1j}^{cnw*} O_{R1j}^{cnw}), \\
B_{22}^{\ell_i^+ \ell_j^- \nu_k} &= (O_{L1j}^{ncw*} O_{L1j}^{ncw} O_{R1j}^{cnw*} O_{R1j}^{cnw} + O_{R1j}^{ncw*} O_{R1j}^{ncw} O_{L1j}^{cnw*} O_{L1j}^{cnw}), \\
C_{22}^{\ell_i^+ \ell_j^- \nu_k} &= (O_{R1j}^{ncw*} O_{L1j}^{cnw} + O_{L1j}^{ncw*} O_{R1j}^{cnw}) (O_{L1j}^{cnw*} O_{L1j}^{cnw} + O_{R1j}^{cnw*} O_{R1j}^{cnw}).
\end{aligned} \tag{I.36}$$

$$\begin{aligned}
& \bullet M_3^\dagger M_3(\tilde{\chi}_1^0 \rightarrow \sum \ell_i^+ \ell_j^- \nu_k) = \sum_{r,l=1}^8 \frac{4\tilde{g}^4}{[(p+k')^2 - m_{S_r^\pm}^2][(p+k')^2 - m_{S_l^\pm}^2]} \\
& \sum_{i,j,k} \left[(P.k)(p.k') A_{33}^{\ell_i^+ \ell_j^- \nu_k} + m_{\ell_i} m_{\tilde{\chi}_1^0} (p.k') B_{33}^{\ell_i^+ \ell_j^- \nu_k} \right],
\end{aligned} \tag{I.37}$$

where

$$\begin{aligned}
A_{33}^{\ell_i^+ \ell_j^- \nu_k} &= (O_{Li1r}^{cns*} O_{Li1l}^{cns} + O_{Ri1r}^{cns*} O_{Ri1l}^{cns}) (O_{Lkjr}^{cns*} O_{Lkjl}^{cns} + O_{Rkjr}^{cns*} O_{Rkjl}^{cns}), \\
B_{33}^{\ell_i^+ \ell_j^- \nu_k} &= (O_{Ri1r}^{cns*} O_{Li1l}^{cns} + O_{Li1r}^{cns*} O_{Ri1l}^{cns}) (O_{Lkjr}^{cns*} O_{Lkjl}^{cns} + O_{Rkjr}^{cns*} O_{Rkjl}^{cns}).
\end{aligned} \tag{I.38}$$

$$\begin{aligned}
& \bullet M_4^\dagger M_4(\tilde{\chi}_1^0 \rightarrow \sum \ell_i^+ \ell_j^- \nu_k) = \sum_{r,l=1}^8 \frac{4\tilde{g}^4}{[(p+k)^2 - m_{S_r^\pm}^2][(p+k)^2 - m_{S_l^\pm}^2]} \\
& \sum_{i,j,k} \left[(P.k')(p.k) A_{44}^{\ell_i^+ \ell_j^- \nu_k} + m_{\ell_j} m_{\tilde{\chi}_1^0} (p.k) B_{44}^{\ell_i^+ \ell_j^- \nu_k} \right],
\end{aligned} \tag{I.39}$$

where

$$\begin{aligned}
A_{44}^{\ell_i^+ \ell_j^- \nu_k} &= (O_{L1jr}^{cns*} O_{L1jl}^{cns} + O_{R1jr}^{cns*} O_{R1jl}^{cns}) (O_{Likr}^{cns*} O_{Likl}^{cns} + O_{Rikr}^{cns*} O_{Rikl}^{cns}), \\
B_{44}^{\ell_i^+ \ell_j^- \nu_k} &= (O_{R1jr}^{cns*} O_{L1jl}^{cns} + O_{L1jr}^{cns*} O_{R1jl}^{cns}) (O_{Likr}^{cns*} O_{Likl}^{cns} + O_{Rikr}^{cns*} O_{Rikl}^{cns}).
\end{aligned} \tag{I.40}$$

$$\begin{aligned}
\bullet M_5^\dagger M_5(\tilde{\chi}_1^0 \rightarrow \sum \ell_i^+ \ell_j^- \nu_k) &= \sum_{r,l=1}^8 \frac{\tilde{g}^4}{\left[((k+k')^2 - m_{S^0}^2)((k+k')^2 - m_{S^0}^2) \right]} \\
&\sum_{i,j,k} \left[(P.p)(k.k') A_{55}^{\ell_i^+ \ell_j^- \nu_k} - m_{\ell_i} m_{\ell_j} (P.p) B_{55}^{\ell_i^+ \ell_j^- \nu_k} \right],
\end{aligned} \tag{I.41}$$

where

$$\begin{aligned}
A_{55}^{\ell_i^+ \ell_j^- \nu_k} &= (O_{Lk1r}^{nnh*} O_{Lk1l}^{nnh} + O_{Rk1r}^{nnh*} O_{Rk1l}^{nnh}) (O_{Lijr}^{cch*} O_{Lijl}^{cch} + O_{Rijr}^{cch*} O_{Rijl}^{cch}), \\
B_{55}^{\ell_i^+ \ell_j^- \nu_k} &= (O_{Lk1r}^{nnh*} O_{Lk1l}^{nnh} + O_{Rk1r}^{nnh*} O_{Rk1l}^{nnh}) (O_{Rijr}^{cch*} O_{Lijl}^{cch} + O_{Lijr}^{cch*} O_{Rijl}^{cch}).
\end{aligned} \tag{I.42}$$

$$\begin{aligned}
\bullet M_6^\dagger M_6(\tilde{\chi}_1^0 \rightarrow \sum \ell_i^+ \ell_j^- \nu_k) &= \sum_{r,l=1}^8 \frac{\tilde{g}^4}{\left[((k+k')^2 - m_{P^0}^2)((k+k')^2 - m_{P^0}^2) \right]} \\
&\sum_{i,j,k} \left[(P.p)(k.k') A_{66}^{\ell_i^+ \ell_j^- \nu_k} - m_{\ell_i} m_{\ell_j} (P.p) B_{66}^{\ell_i^+ \ell_j^- \nu_k} \right],
\end{aligned} \tag{I.43}$$

where

$$\begin{aligned}
A_{66}^{\ell_i^+ \ell_j^- \nu_k} &= (O_{Lk1r}^{nna*} O_{Lk1l}^{nna} + O_{Rk1r}^{nna*} O_{Rk1l}^{nna}) (O_{Lijr}^{cca*} O_{Lijl}^{cca} + O_{Rijr}^{cca*} O_{Rijl}^{cca}), \\
B_{66}^{\ell_i^+ \ell_j^- \nu_k} &= (O_{Lk1r}^{nna*} O_{Lk1l}^{nna} + O_{Rk1r}^{nna*} O_{Rk1l}^{nna}) (O_{Rijr}^{cca*} O_{Lijl}^{cca} + O_{Lijr}^{cca*} O_{Rijl}^{cca}).
\end{aligned} \tag{I.44}$$

$$\begin{aligned}
\bullet M_7^\dagger M_7(\tilde{\chi}_1^0 \rightarrow \sum \ell_i^+ \ell_j^- \nu_k) &= \frac{2g_2^4}{\cos^2 \theta_W [(k+k')^2 - m_Z^2]^2 + m_Z^2 \Gamma_Z^2} \\
&\sum_{i,j,k} \left[2(P.k')(p.k) A_{77}^{\ell_i^+ \ell_j^- \nu_k} + 2(P.k)(p.k') B_{77}^{\ell_i^+ \ell_j^- \nu_k} - m_{\ell_i} m_{\ell_j} (P.p) C_{77}^{\ell_i^+ \ell_j^- \nu_k} \right],
\end{aligned} \tag{I.45}$$

where

$$\begin{aligned}
A_{77}^{\ell_i^+ \ell_j^- \nu_k} &= (O_{Lk1}^{nnz*} O_{Lk1}^{nnz} O_{Lij}^{ccz*} O_{Lij}^{ccz} + O_{Rk1}^{nnz*} O_{Rk1}^{nnz} O_{Rij}^{ccz*} O_{Rij}^{ccz}), \\
B_{77}^{\ell_i^+ \ell_j^- \nu_k} &= (O_{Lk1}^{nnz*} O_{Lk1}^{nnz} O_{Rij}^{ccz*} O_{Rij}^{ccz} + O_{Rk1}^{nnz*} O_{Rk1}^{nnz} O_{Lij}^{ccz*} O_{Lij}^{ccz}), \\
C_{77}^{\ell_i^+ \ell_j^- \nu_k} &= (O_{Lk1}^{nnz*} O_{Lk1}^{nnz} + O_{Rk1}^{nnz*} O_{Rk1}^{nnz}) (O_{Rij}^{ccz*} O_{Lij}^{ccz} + O_{Lij}^{ccz*} O_{Rij}^{ccz}).
\end{aligned} \tag{I.46}$$

$$\begin{aligned}
\bullet M_1^\dagger M_2(\tilde{\chi}_1^0 \rightarrow \sum \ell_i^+ \ell_j^- \nu_k) &= \\
&\frac{8g_2^4}{\left[((p+k')^2 - m_W^2) - im_W \Gamma_W \right] \left[((p+k)^2 - m_W^2)^2 + im_W \Gamma_W \right]} \\
&\sum_{i,j,k} \left[-2(P.p)(k.k') (A_{12}^{\ell_i^+ \ell_j^- \nu_k} O_{Li1}^{cnw*} + B_{12}^{\ell_i^+ \ell_j^- \nu_k} O_{Ri1}^{cnw*}) \right. \\
&+ m_{\ell_i} m_{\tilde{\chi}_1^0} (p.k') (A_{12}^{\ell_i^+ \ell_j^- \nu_k} O_{Ri1}^{cnw*} + B_{12}^{\ell_i^+ \ell_j^- \nu_k} O_{Li1}^{cnw*}) \\
&+ m_{\ell_j} m_{\tilde{\chi}_1^0} (p.k) (C_{12}^{\ell_i^+ \ell_j^- \nu_k} O_{Ri1}^{cnw*} + D_{12}^{\ell_i^+ \ell_j^- \nu_k} O_{Li1}^{cnw*}) \\
&\left. + m_{\ell_i} m_{\ell_j} (P.p) (C_{12}^{\ell_i^+ \ell_j^- \nu_k} O_{Li1}^{cnw*} + D_{12}^{\ell_i^+ \ell_j^- \nu_k} O_{Ri1}^{cnw*}) \right],
\end{aligned} \tag{I.47}$$

where

$$\begin{aligned} A_{12}^{\ell_i^+ \ell_j^- \nu_k} &= O_{Rkj}^{ncw^*} O_{L1j}^{ncw} O_{L1k}^{cnw}, & B_{12}^{\ell_i^+ \ell_j^- \nu_k} &= O_{Lkj}^{ncw^*} O_{R1j}^{ncw} O_{R1k}^{cnw}, \\ C_{12}^{\ell_i^+ \ell_j^- \nu_k} &= O_{Lkj}^{ncw^*} O_{L1j}^{ncw} O_{R1k}^{cnw}, & D_{12}^{\ell_i^+ \ell_j^- \nu_k} &= O_{Rkj}^{ncw^*} O_{R1j}^{ncw} O_{L1k}^{cnw}, \end{aligned} \quad (\text{I.48})$$

$$\begin{aligned} \bullet M_1^\dagger M_3(\tilde{\chi}_1^0 \rightarrow \sum \ell_i^+ \ell_j^- \nu_k) &= \sum_{l=1}^8 \frac{4g_2^2 \tilde{g}^2}{\left[(((p+k')^2 - m_W^2) - im_W \Gamma_W)((p+k')^2 - m_{S_l^\pm}^2)\right]} \\ &\quad \sum_{i,j,k} \left[m_{\ell_j} m_{\tilde{\chi}_1^0}(p.k) A_{13}^{\ell_i^+ \ell_j^- \nu_k} + m_{\ell_i} m_{\ell_j}(P.p) B_{13}^{\ell_i^+ \ell_j^- \nu_k} \right], \end{aligned} \quad (\text{I.49})$$

where

$$\begin{aligned} A_{13}^{\ell_i^+ \ell_j^- \nu_k} &= \left(O_{Ri1}^{cnw^*} O_{Li1l}^{cns} + O_{Li1}^{cnw^*} O_{Ri1l}^{cns} \right) \left(O_{Rkj}^{ncw^*} O_{Lkjl}^{ncs} + O_{Lkj}^{ncw^*} O_{Rkjl}^{ncs} \right), \\ B_{13}^{\ell_i^+ \ell_j^- \nu_k} &= \left(O_{Li1}^{cnw^*} O_{Li1l}^{cns} + O_{Ri1}^{cnw^*} O_{Ri1l}^{cns} \right) \left(O_{Rkj}^{ncw^*} O_{Lkjl}^{ncs} + O_{Lkj}^{ncw^*} O_{Rkjl}^{ncs} \right). \end{aligned} \quad (\text{I.50})$$

$$\begin{aligned} \bullet M_1^\dagger M_4(\tilde{\chi}_1^0 \rightarrow \sum \ell_i^+ \ell_j^- \nu_k) &= - \sum_{r=1}^8 \frac{4g_2^2 \tilde{g}^2}{\left[(((p+k')^2 - m_W^2) - im_W \Gamma_W)((p+k)^2 - m_{S_r^\pm}^2)\right]} \\ &\quad \sum_{i,j,k} \left[2(P.k')(p.k) (A_{14}^{\ell_i^+ \ell_j^- \nu_k} O_{Li1}^{cnw^*} + B_{14}^{\ell_i^+ \ell_j^- \nu_k} O_{Ri1}^{cnw^*}) \right. \\ &\quad - m_{\ell_i} m_{\tilde{\chi}_1^0}(p.k') (A_{14}^{\ell_i^+ \ell_j^- \nu_k} O_{Ri1}^{cnw^*} + B_{14}^{\ell_i^+ \ell_j^- \nu_k} O_{Li1}^{cnw^*}) \\ &\quad + 2m_{\ell_j} m_{\tilde{\chi}_1^0}(p.k) (C_{14}^{\ell_i^+ \ell_j^- \nu_k} O_{Ri1}^{cnw^*} + D_{14}^{\ell_i^+ \ell_j^- \nu_k} O_{Li1}^{cnw^*}) \\ &\quad \left. - m_{\ell_i} m_{\ell_j}(P.p) (C_{14}^{\ell_i^+ \ell_j^- \nu_k} O_{Li1}^{cnw^*} + D_{14}^{\ell_i^+ \ell_j^- \nu_k} O_{Ri1}^{cnw^*}) \right], \end{aligned} \quad (\text{I.51})$$

where

$$\begin{aligned} A_{14}^{\ell_i^+ \ell_j^- \nu_k} &= O_{Lkj}^{ncw^*} O_{L1jl}^{ncs} O_{Rikl}^{cns}, & B_{14}^{\ell_i^+ \ell_j^- \nu_k} &= O_{Rkj}^{ncw^*} O_{R1jl}^{ncs} O_{Likl}^{cns}, \\ C_{14}^{\ell_i^+ \ell_j^- \nu_k} &= O_{Rkj}^{ncw^*} O_{L1jl}^{ncs} O_{Likl}^{cns}, & D_{14}^{\ell_i^+ \ell_j^- \nu_k} &= O_{Lkj}^{ncw^*} O_{R1jl}^{ncs} O_{Rikl}^{cns}. \end{aligned} \quad (\text{I.52})$$

$$\begin{aligned} \bullet M_1^\dagger M_5(\tilde{\chi}_1^0 \rightarrow \sum \ell_i^+ \ell_j^- \nu_k) &= - \sum_{r=1}^8 \frac{2g_2^2 \tilde{g}^2}{\left[(((p+k')^2 - m_W^2) - im_W \Gamma_W)((k+k')^2 - m_{S_r^0}^2)\right]} \\ &\quad \sum_{i,j,k} \left[2(P.p)(k.k') (A_{15}^{\ell_i^+ \ell_j^- \nu_k} O_{Li1}^{cnw^*} + B_{15}^{\ell_i^+ \ell_j^- \nu_k} O_{Ri1}^{cnw^*}) \right. \\ &\quad - m_{\ell_i} m_{\tilde{\chi}_1^0}(p.k') (A_{15}^{\ell_i^+ \ell_j^- \nu_k} O_{Ri1}^{cnw^*} + B_{15}^{\ell_i^+ \ell_j^- \nu_k} O_{Li1}^{cnw^*}) \\ &\quad + m_{\ell_j} m_{\tilde{\chi}_1^0}(p.k) (C_{15}^{\ell_i^+ \ell_j^- \nu_k} O_{Ri1}^{cnw^*} + D_{15}^{\ell_i^+ \ell_j^- \nu_k} O_{Li1}^{cnw^*}) \\ &\quad \left. - 2m_{\ell_i} m_{\ell_j}(P.p) (C_{15}^{\ell_i^+ \ell_j^- \nu_k} O_{Li1}^{cnw^*} + D_{15}^{\ell_i^+ \ell_j^- \nu_k} O_{Ri1}^{cnw^*}) \right], \end{aligned} \quad (\text{I.53})$$

where

$$\begin{aligned} A_{15}^{\ell_i^+ \ell_j^- \nu_k} &= O_{Rkj}^{ncw^*} O_{Lk1l}^{nnh} O_{Rijl}^{cch}, & B_{15}^{\ell_i^+ \ell_j^- \nu_k} &= O_{Lkj}^{ncw^*} O_{Rk1l}^{nnh} O_{Lijl}^{cch}, \\ C_{15}^{\ell_i^+ \ell_j^- \nu_k} &= O_{Rkj}^{ncw^*} O_{Lk1l}^{nnh} O_{Lijl}^{cch}, & D_{15}^{\ell_i^+ \ell_j^- \nu_k} &= O_{Lkj}^{ncw^*} O_{Rk1l}^{nnh} O_{Rijl}^{cch}. \end{aligned} \quad (\text{I.54})$$

$$\begin{aligned}
\bullet M_1^\dagger M_6(\tilde{\chi}_1^0 \rightarrow \sum \ell_i^+ \ell_j^- \nu_k) &= \sum_{r=1}^8 \frac{2g_2^2 \tilde{g}^2}{\left[(((p+k')^2 - m_W^2) - im_W \Gamma_W)((k+k')^2 - m_{P^0}^2)\right]} \\
&\sum_{i,j,k} \left[2(P.p)(k.k')(A_{16}^{\ell_i^+ \ell_j^-} \nu_k O_{Li1}^{cnw*} + B_{16}^{\ell_i^+ \ell_j^-} \nu_k O_{Ri1}^{cnw*}) \right. \\
&\quad - m_{\ell_i} m_{\tilde{\chi}_1^0}(p.k')(A_{16}^{\ell_i^+ \ell_j^-} \nu_k O_{Ri1}^{cnw*} + B_{16}^{\ell_i^+ \ell_j^-} \nu_k O_{Li1}^{cnw*}) \\
&\quad + m_{\ell_j} m_{\tilde{\chi}_1^0}(p.k)(C_{16}^{\ell_i^+ \ell_j^-} \nu_k O_{Ri1}^{cnw*} + D_{16}^{\ell_i^+ \ell_j^-} \nu_k O_{Li1}^{cnw*}) \\
&\quad \left. - 2m_{\ell_i} m_{\ell_j}(P.p)(C_{16}^{\ell_i^+ \ell_j^-} \nu_k O_{Li1}^{cnw*} + D_{16}^{\ell_i^+ \ell_j^-} \nu_k O_{Ri1}^{cnw*}) \right], \tag{I.55}
\end{aligned}$$

where

$$\begin{aligned}
A_{16}^{\ell_i^+ \ell_j^-} \nu_k &= O_{Rkj}^{ncw*} O_{Lk1l}^{nna} O_{Rijl}^{cca}, & B_{16}^{\ell_i^+ \ell_j^-} \nu_k &= O_{Lkj}^{ncw*} O_{Rk1l}^{nna} O_{Lijl}^{cca}, \\
C_{16}^{\ell_i^+ \ell_j^-} \nu_k &= O_{Rkj}^{ncw*} O_{Lk1l}^{nna} O_{Lijl}^{cca}, & D_{16}^{\ell_i^+ \ell_j^-} \nu_k &= O_{Lkj}^{ncw*} O_{Rk1l}^{nna} O_{Rijl}^{cca}. \tag{I.56}
\end{aligned}$$

$$\begin{aligned}
\bullet M_1^\dagger M_7(\tilde{\chi}_1^0 \rightarrow \sum \ell_i^+ \ell_j^- \nu_k) &= \frac{4g_2^4 \text{see}\theta_W}{\left[(((p+k')^2 - m_W^2) - im_W \Gamma_W)[((k+k')^2 - m_Z^2) + im_Z \Gamma_Z]\right]} \\
&\sum_{i,j,k} \left[2(P.k')(p.k)(A_{17}^{\ell_i^+ \ell_j^-} \nu_k O_{Li1}^{cnw*} + B_{17}^{\ell_i^+ \ell_j^-} \nu_k O_{Ri1}^{cnw*}) \right. \\
&\quad - m_{\ell_i} m_{\tilde{\chi}_1^0}(p.k')(A_{17}^{\ell_i^+ \ell_j^-} \nu_k O_{Ri1}^{cnw*} + B_{17}^{\ell_i^+ \ell_j^-} \nu_k O_{Li1}^{cnw*}) \\
&\quad + m_{\ell_j} m_{\tilde{\chi}_1^0}(p.k)(C_{17}^{\ell_i^+ \ell_j^-} \nu_k O_{Ri1}^{cnw*} + D_{17}^{\ell_i^+ \ell_j^-} \nu_k O_{Li1}^{cnw*}) \\
&\quad \left. + m_{\ell_i} m_{\ell_j}(P.p)(C_{17}^{\ell_i^+ \ell_j^-} \nu_k O_{Li1}^{cnw*} + D_{17}^{\ell_i^+ \ell_j^-} \nu_k O_{Ri1}^{cnw*}) \right], \tag{I.57}
\end{aligned}$$

where

$$\begin{aligned}
A_{17}^{\ell_i^+ \ell_j^-} \nu_k &= O_{Lkj}^{ncw*} O_{Lk1}^{nnz} O_{Lij}^{ccz}, & B_{17}^{\ell_i^+ \ell_j^-} \nu_k &= O_{Rkj}^{ncw*} O_{Rk1}^{nnz} O_{Rij}^{ccz}, \\
C_{17}^{\ell_i^+ \ell_j^-} \nu_k &= O_{Lkj}^{ncw*} O_{Lk1}^{nnz} O_{Rij}^{ccz}, & D_{17}^{\ell_i^+ \ell_j^-} \nu_k &= O_{Rkj}^{ncw*} O_{Rk1}^{nnz} O_{Lij}^{ccz}. \tag{I.58}
\end{aligned}$$

$$\begin{aligned}
\bullet M_2^\dagger M_3(\tilde{\chi}_1^0 \rightarrow \sum \ell_i^+ \ell_j^- \nu_k) &= \sum_{r=1}^8 \frac{4g_2^2 \tilde{g}^2}{\left[(((p+k)^2 - m_W^2) - im_W \Gamma_W)((p+k')^2 - m_{S_r^\pm}^2)\right]} \\
&\sum_{i,j,k} \left[2(P.k)(p.k')(A_{23}^{\ell_i^+ \ell_j^-} \nu_k O_{L1j}^{ncw*} + B_{23}^{\ell_i^+ \ell_j^-} \nu_k O_{R1j}^{ncw*}) \right. \\
&\quad - m_{\ell_j} m_{\tilde{\chi}_1^0}(p.k)(A_{23}^{\ell_i^+ \ell_j^-} \nu_k O_{R1j}^{ncw*} + B_{23}^{\ell_i^+ \ell_j^-} \nu_k O_{L1j}^{ncw*}) \\
&\quad + 2m_{\ell_i} m_{\tilde{\chi}_1^0}(p.k')(C_{23}^{\ell_i^+ \ell_j^-} \nu_k O_{R1j}^{ncw*} + D_{23}^{\ell_i^+ \ell_j^-} \nu_k O_{L1j}^{ncw*}) \\
&\quad \left. - m_{\ell_i} m_{\ell_j}(P.p)(C_{23}^{\ell_i^+ \ell_j^-} \nu_k O_{L1j}^{ncw*} + D_{23}^{\ell_i^+ \ell_j^-} \nu_k O_{R1j}^{ncw*}) \right], \tag{I.59}
\end{aligned}$$

where

$$\begin{aligned}
A_{23}^{\ell_i^+ \ell_j^-} \nu_k &= O_{Rik}^{cnw*} O_{Li1r}^{cns} O_{Rkjr}^{ncs}, & B_{23}^{\ell_i^+ \ell_j^-} \nu_k &= O_{Lik}^{cnw*} O_{Ri1r}^{cns} O_{Lkjr}^{ncs}, \\
C_{23}^{\ell_i^+ \ell_j^-} \nu_k &= O_{Lik}^{cnw*} O_{Li1r}^{cns} O_{Lkjr}^{ncs}, & D_{23}^{\ell_i^+ \ell_j^-} \nu_k &= O_{Rik}^{cnw*} O_{Ri1r}^{cns} O_{Rkjr}^{ncs}. \tag{I.60}
\end{aligned}$$

$$\begin{aligned}
\bullet M_2^\dagger M_4(\tilde{\chi}_1^0 \rightarrow \sum \ell_i^+ \ell_j^- \nu_k) &= - \sum_{r=1}^8 \frac{4g_2^2 \tilde{g}^2}{\left[\left((p+k)^2 - m_W^2 \right) - im_W \Gamma_W \right] \left((p+k)^2 - m_{S_r^\pm}^2 \right)} \\
&\quad \sum_{i,j,k} \left[m_{\ell_i} m_{\tilde{\chi}_1^0}(p.k') A_{24}^{\ell_i^+ \ell_j^- \nu_k} + m_{\ell_i} m_{\ell_j}(P.p) B_{24}^{\ell_i^+ \ell_j^- \nu_k} \right],
\end{aligned} \tag{I.61}$$

where

$$\begin{aligned}
A_{24}^{\ell_i^+ \ell_j^- \nu_k} &= \left(O_{R1j}^{ncw^*} O_{L1jr}^{ncs} + O_{L1j}^{ncw^*} O_{R1jr}^{ncs} \right) \left(O_{Lik}^{ncw^*} O_{Likr}^{cns} + O_{Rik}^{ncw^*} O_{Rikr}^{cns} \right), \\
B_{24}^{\ell_i^+ \ell_j^- \nu_k} &= \left(O_{L1j}^{ncw^*} O_{L1jr}^{ncs} + O_{R1j}^{ncw^*} O_{R1jr}^{ncs} \right) \left(O_{Lik}^{ncw^*} O_{Likr}^{cns} + O_{Rik}^{ncw^*} O_{Rikr}^{cns} \right).
\end{aligned} \tag{I.62}$$

$$\begin{aligned}
\bullet M_2^\dagger M_5(\tilde{\chi}_1^0 \rightarrow \sum \ell_i^+ \ell_j^- \nu_k) &= \sum_{r=1}^8 \frac{2g_2^2 \tilde{g}^2}{\left[\left((p+k)^2 - m_W^2 \right) - im_W \Gamma_W \right] \left((k+k')^2 - m_{S_r^0}^2 \right)} \\
&\quad \sum_{i,j,k} \left[2(P.p)(k.k') \left(A_{25}^{\ell_i^+ \ell_j^- \nu_k} O_{L1j}^{ncw^*} + B_{25}^{\ell_i^+ \ell_j^- \nu_k} O_{R1j}^{ncw^*} \right) \right. \\
&\quad - m_{\ell_j} m_{\tilde{\chi}_1^0}(p.k) \left(A_{25}^{\ell_i^+ \ell_j^- \nu_k} O_{R1j}^{ncw^*} + B_{25}^{\ell_i^+ \ell_j^- \nu_k} O_{L1j}^{ncw^*} \right) \\
&\quad + m_{\ell_i} m_{\tilde{\chi}_1^0}(p.k') \left(C_{25}^{\ell_i^+ \ell_j^- \nu_k} O_{R1j}^{ncw^*} + D_{25}^{\ell_i^+ \ell_j^- \nu_k} O_{L1j}^{ncw^*} \right) \\
&\quad \left. - 2m_{\ell_i} m_{\ell_j}(P.p) \left(C_{25}^{\ell_i^+ \ell_j^- \nu_k} O_{L1j}^{ncw^*} + D_{25}^{\ell_i^+ \ell_j^- \nu_k} O_{R1j}^{ncw^*} \right) \right],
\end{aligned} \tag{I.63}$$

where

$$\begin{aligned}
A_{25}^{\ell_i^+ \ell_j^- \nu_k} &= O_{Lik}^{cnw^*} O_{Lk1r}^{nnh} O_{Rijr}^{cch}, & B_{25}^{\ell_i^+ \ell_j^- \nu_k} &= O_{Rik}^{cnw^*} O_{Rk1r}^{nnh} O_{Lijr}^{cch}, \\
C_{25}^{\ell_i^+ \ell_j^- \nu_k} &= O_{Lik}^{cnw^*} O_{Lk1r}^{nnh} O_{Lijr}^{cch}, & D_{25}^{\ell_i^+ \ell_j^- \nu_k} &= O_{Rik}^{cnw^*} O_{Rk1r}^{nnh} O_{Rijr}^{cch}.
\end{aligned} \tag{I.64}$$

$$\begin{aligned}
\bullet M_2^\dagger M_6(\tilde{\chi}_1^0 \rightarrow \sum \ell_i^+ \ell_j^- \nu_k) &= - \sum_{r=1}^8 \frac{2g_2^2 \tilde{g}^2}{\left[\left((p+k)^2 - m_W^2 \right) - im_W \Gamma_W \right] \left((k+k')^2 - m_{P_r^0}^2 \right)} \\
&\quad \sum_{i,j,k} \left[2(P.p)(k.k') \left(A_{26}^{\ell_i^+ \ell_j^- \nu_k} O_{L1j}^{ncw^*} + B_{26}^{\ell_i^+ \ell_j^- \nu_k} O_{R1j}^{ncw^*} \right) \right. \\
&\quad - m_{\ell_j} m_{\tilde{\chi}_1^0}(p.k) \left(A_{26}^{\ell_i^+ \ell_j^- \nu_k} O_{R1j}^{ncw^*} + B_{26}^{\ell_i^+ \ell_j^- \nu_k} O_{L1j}^{ncw^*} \right) \\
&\quad + m_{\ell_i} m_{\tilde{\chi}_1^0}(p.k') \left(C_{26}^{\ell_i^+ \ell_j^- \nu_k} O_{R1j}^{ncw^*} + D_{26}^{\ell_i^+ \ell_j^- \nu_k} O_{L1j}^{ncw^*} \right) \\
&\quad \left. - 2m_{\ell_i} m_{\ell_j}(P.p) \left(C_{26}^{\ell_i^+ \ell_j^- \nu_k} O_{L1j}^{ncw^*} + D_{26}^{\ell_i^+ \ell_j^- \nu_k} O_{R1j}^{ncw^*} \right) \right],
\end{aligned} \tag{I.65}$$

where

$$\begin{aligned}
A_{26}^{\ell_i^+ \ell_j^- \nu_k} &= O_{Lik}^{cnw^*} O_{Lk1r}^{nna} O_{Rijr}^{cca}, & B_{26}^{\ell_i^+ \ell_j^- \nu_k} &= O_{Rik}^{cnw^*} O_{Rk1r}^{nna} O_{Lijr}^{cca}, \\
C_{26}^{\ell_i^+ \ell_j^- \nu_k} &= O_{Lik}^{cnw^*} O_{Lk1r}^{nna} O_{Lijr}^{cca}, & D_{26}^{\ell_i^+ \ell_j^- \nu_k} &= O_{Rik}^{cnw^*} O_{Rk1r}^{nna} O_{Rijr}^{cca}.
\end{aligned} \tag{I.66}$$

$$\begin{aligned}
& \bullet M_2^\dagger M_7(\tilde{\chi}_1^0 \rightarrow \sum \ell_i^+ \ell_j^- \nu_k) = \\
& \frac{4g_2^4 \sec\theta_W}{\left[\left((p+k)^2 - m_W^2 \right) - im_W \Gamma_W \right] \left[\left((k+k')^2 - m_Z^2 \right) + im_Z \Gamma_Z \right]} \\
& \sum_{i,j,k} \left[2(P.k)(p.k') (A_{27}^{\ell_i^+ \ell_j^- \nu_k} O_{L1j}^{ncw*} + B_{27}^{\ell_i^+ \ell_j^- \nu_k} O_{R1j}^{ncw*}) \right. \\
& - m_{\ell_j} m_{\tilde{\chi}_1^0}(p.k) (A_{27}^{\ell_i^+ \ell_j^- \nu_k} O_{R1j}^{ncw*} + B_{27}^{\ell_i^+ \ell_j^- \nu_k} O_{L1j}^{ncw*}) \\
& + m_{\ell_i} m_{\tilde{\chi}_1^0}(p.k') (C_{27}^{\ell_i^+ \ell_j^- \nu_k} O_{R1j}^{ncw*} + D_{27}^{\ell_i^+ \ell_j^- \nu_k} O_{L1j}^{ncw*}) \\
& \left. + m_{\ell_i} m_{\ell_j}(P.p) (C_{27}^{\ell_i^+ \ell_j^- \nu_k} O_{L1j}^{ncw*} + D_{27}^{\ell_i^+ \ell_j^- \nu_k} O_{R1j}^{ncw*}) \right], \tag{I.67}
\end{aligned}$$

where

$$\begin{aligned}
A_{27}^{\ell_i^+ \ell_j^- \nu_k} &= O_{Rik}^{cnw*} O_{Lk1}^{nnz} O_{Rij}^{ccz}, & B_{27}^{\ell_i^+ \ell_j^- \nu_k} &= O_{Lik}^{cnw*} O_{Rk1}^{nnz} O_{Lij}^{ccz}, \\
C_{27}^{\ell_i^+ \ell_j^- \nu_k} &= O_{Rik}^{cnw*} O_{Lk1}^{nnz} O_{Lij}^{ccz}, & D_{27}^{\ell_i^+ \ell_j^- \nu_k} &= O_{Lik}^{cnw*} O_{Rk1}^{nnz} O_{Rij}^{ccz}. \tag{I.68}
\end{aligned}$$

$$\begin{aligned}
& \bullet M_3^\dagger M_4(\tilde{\chi}_1^0 \rightarrow \sum \ell_i^+ \ell_j^- \nu_k) = - \sum_{r,l=1}^8 \frac{2\tilde{g}^4}{\left[\left((p+k')^2 - m_{S_\pm^2}^2 \right) \left((p+k)^2 - m_{S_\pm^2}^2 \right) \right]} \\
& \sum_{i,j,k} \left[\{ (P.k)(p.k') - (P.p)(k.k') + (P.k')(p.k) \} (A_{34}^{\ell_i^+ \ell_j^- \nu_k} O_{Li1r}^{cns*} + B_{34}^{\ell_i^+ \ell_j^- \nu_k} O_{Ri1r}^{cns*}) \right. \\
& + m_{\ell_i} m_{\tilde{\chi}_1^0}(p.k) (A_{34}^{\ell_i^+ \ell_j^- \nu_k} O_{Ri1r}^{cns*} + B_{34}^{\ell_i^+ \ell_j^- \nu_k} O_{Li1r}^{cns*}) \\
& + m_{\ell_j} m_{\tilde{\chi}_1^0}(p.k') (C_{34}^{\ell_i^+ \ell_j^- \nu_k} O_{Ri1r}^{cns*} + D_{34}^{\ell_i^+ \ell_j^- \nu_k} O_{Li1r}^{cns*}) \\
& \left. + m_{\ell_i} m_{\ell_j}(P.p) (C_{34}^{\ell_i^+ \ell_j^- \nu_k} O_{Li1r}^{cns*} + D_{34}^{\ell_i^+ \ell_j^- \nu_k} O_{Ri1r}^{cns*}) \right], \tag{I.69}
\end{aligned}$$

where

$$\begin{aligned}
A_{34}^{\ell_i^+ \ell_j^- \nu_k} &= O_{Lkjr}^{ncs*} O_{L1jl}^{ncs} O_{Likl}, & B_{34}^{\ell_i^+ \ell_j^- \nu_k} &= O_{Rkjr}^{ncs*} O_{R1jl}^{ncs} O_{Rikl}, \\
C_{34}^{\ell_i^+ \ell_j^- \nu_k} &= O_{Rkjr}^{ncs*} O_{L1jl}^{ncs} O_{Rikl}, & D_{34}^{\ell_i^+ \ell_j^- \nu_k} &= O_{Lkjr}^{ncs*} O_{R1jl}^{ncs} O_{Likl}. \tag{I.70}
\end{aligned}$$

$$\begin{aligned}
& \bullet M_3^\dagger M_5(\tilde{\chi}_1^0 \rightarrow \sum \ell_i^+ \ell_j^- \nu_k) = \sum_{r,l=1}^8 \frac{\tilde{g}^4}{\left[\left((p+k')^2 - m_{S_\pm^2}^2 \right) \left((k+k')^2 - m_{S_0^2}^2 \right) \right]} \\
& \sum_{i,j,k} \left[\{ (P.k)(p.k') - (P.k')(p.k) + (P.p)(k.k') \} (A_{35}^{\ell_i^+ \ell_j^- \nu_k} O_{Li1r}^{cns*} + B_{35}^{\ell_i^+ \ell_j^- \nu_k} O_{Ri1r}^{cns*}) \right. \\
& + m_{\ell_i} m_{\tilde{\chi}_1^0}(p.k') (A_{35}^{\ell_i^+ \ell_j^- \nu_k} O_{Ri1r}^{cns*} + B_{35}^{\ell_i^+ \ell_j^- \nu_k} O_{Li1r}^{cns*}) \\
& - m_{\ell_j} m_{\tilde{\chi}_1^0}(p.k) (C_{35}^{\ell_i^+ \ell_j^- \nu_k} O_{Ri1r}^{cns*} + D_{35}^{\ell_i^+ \ell_j^- \nu_k} O_{Li1r}^{cns*}) \\
& \left. - m_{\ell_i} m_{\ell_j}(P.p) (C_{35}^{\ell_i^+ \ell_j^- \nu_k} O_{Li1r}^{cns*} + D_{35}^{\ell_i^+ \ell_j^- \nu_k} O_{Ri1r}^{cns*}) \right], \tag{I.71}
\end{aligned}$$

where

$$\begin{aligned}
A_{35}^{\ell_i^+ \ell_j^- \nu_k} &= O_{Lkjr}^{ncs*} O_{Lk1l}^{nnh} O_{Lijl}, & B_{35}^{\ell_i^+ \ell_j^- \nu_k} &= O_{Rkjr}^{ncs*} O_{Rk1l}^{nnh} O_{Rijl}, \\
C_{35}^{\ell_i^+ \ell_j^- \nu_k} &= O_{Lkjr}^{ncs*} O_{Lk1l}^{nnh} O_{Rijl}, & D_{35}^{\ell_i^+ \ell_j^- \nu_k} &= O_{Rkjr}^{ncs*} O_{Rk1l}^{nnh} O_{Lijl}. \tag{I.72}
\end{aligned}$$

$$\begin{aligned}
\bullet M_3^\dagger M_6(\tilde{\chi}_1^0 \rightarrow \sum \ell_i^+ \ell_j^- \nu_k) &= - \sum_{r,l=1}^8 \frac{\tilde{g}^4}{\left[((p+k')^2 - m_{S_r^\pm}^2)((k+k')^2 - m_{P_l^0}^2) \right]} \\
&\sum_{i,j,k} \left[\{ (P.k)(p.k') - (P.k')(p.k) + (P.p)(k.k') \} (A_{36}^{\ell_i^+ \ell_j^- \nu_k} O_{Li1r}^{cns^*} + B_{36}^{\ell_i^+ \ell_j^- \nu_k} O_{Ri1r}^{cns^*}) \right. \\
&+ m_{\ell_i} m_{\tilde{\chi}_1^0}(p.k')(A_{36}^{\ell_i^+ \ell_j^- \nu_k} O_{Ri1r}^{cns^*} + B_{36}^{\ell_i^+ \ell_j^- \nu_k} O_{Li1r}^{cns^*}) \\
&- m_{\ell_j} m_{\tilde{\chi}_1^0}(p.k)(C_{36}^{\ell_i^+ \ell_j^- \nu_k} O_{Ri1r}^{cns^*} + D_{36}^{\ell_i^+ \ell_j^- \nu_k} O_{Li1r}^{cns^*}) \\
&\left. - m_{\ell_i} m_{\ell_j}(P.p)(C_{36}^{\ell_i^+ \ell_j^- \nu_k} O_{Li1r}^{cns^*} + D_{36}^{\ell_i^+ \ell_j^- \nu_k} O_{Ri1r}^{cns^*}) \right], \tag{I.73}
\end{aligned}$$

where

$$\begin{aligned}
A_{36}^{\ell_i^+ \ell_j^- \nu_k} &= O_{Lkjr}^{ncs^*} O_{Lk1l}^{nna} O_{Lijl}^{cca}, & B_{36}^{\ell_i^+ \ell_j^- \nu_k} &= O_{Rkjr}^{ncs^*} O_{Rk1l}^{nna} O_{Rijl}^{cca}, \\
C_{36}^{\ell_i^+ \ell_j^- \nu_k} &= O_{Lkjr}^{ncs^*} O_{Lk1l}^{nna} O_{Rijl}^{cca}, & D_{36}^{\ell_i^+ \ell_j^- \nu_k} &= O_{Rkjr}^{ncs^*} O_{Rk1l}^{nna} O_{Lijl}^{cca}.
\end{aligned} \tag{I.74}$$

$$\begin{aligned}
\bullet M_3^\dagger M_7(\tilde{\chi}_1^0 \rightarrow \sum \ell_i^+ \ell_j^- \nu_k) &= - \sum_{r=1}^8 \frac{2g_2^2 \tilde{g}^2}{\left[((p+k')^2 - m_{S_r^\pm}^2)((k+k')^2 - m_Z^2 + im_Z \Gamma_Z) \right]} \\
&\sum_{i,j,k} \left[2(P.k)(p.k')(A_{37}^{\ell_i^+ \ell_j^- \nu_k} O_{Lij}^{ccz} + B_{37}^{\ell_i^+ \ell_j^- \nu_k} O_{Rij}^{ccz}) \right. \\
&+ m_{\ell_i} m_{\ell_j}(P.p)(A_{37}^{\ell_i^+ \ell_j^- \nu_k} O_{Rij}^{ccz} + B_{37}^{\ell_i^+ \ell_j^- \nu_k} O_{Lij}^{ccz}) \\
&+ 2m_{\ell_i} m_{\tilde{\chi}_1^0}(p.k')(C_{37}^{\ell_i^+ \ell_j^- \nu_k} O_{Rij}^{ccz} + D_{37}^{\ell_i^+ \ell_j^- \nu_k} O_{Lij}^{ccz}) \\
&\left. + m_{\ell_j} m_{\tilde{\chi}_1^0}(p.k)(C_{37}^{\ell_i^+ \ell_j^- \nu_k} O_{Lij}^{ccz} + D_{37}^{\ell_i^+ \ell_j^- \nu_k} O_{Rij}^{ccz}) \right], \tag{I.75}
\end{aligned}$$

where

$$\begin{aligned}
A_{37}^{\ell_i^+ \ell_j^- \nu_k} &= O_{Lkjr}^{ncs^*} O_{Rk1l}^{nnz} O_{Ri1r}^{cns^*}, & B_{37}^{\ell_i^+ \ell_j^- \nu_k} &= O_{Rkjr}^{ncs^*} O_{Lk1l}^{nnz} O_{Li1r}^{cns^*}, \\
C_{37}^{\ell_i^+ \ell_j^- \nu_k} &= O_{Rkjr}^{ncs^*} O_{Lk1l}^{nnz} O_{Ri1r}^{cns^*}, & D_{37}^{\ell_i^+ \ell_j^- \nu_k} &= O_{Lkjr}^{ncs^*} O_{Rk1l}^{nnz} O_{Li1r}^{cns^*}.
\end{aligned} \tag{I.76}$$

$$\begin{aligned}
\bullet M_4^\dagger M_5(\tilde{\chi}_1^0 \rightarrow \sum \ell_i^+ \ell_j^- \nu_k) &= \sum_{r,l=1}^8 \frac{\tilde{g}^4}{\left[((p+k)^2 - m_{S_r^\pm}^2)((k+k')^2 - m_{S_l^0}^2) \right]} \\
&\sum_{i,j,k} \left[\{ (P.k')(p.k) - (P.k)(p.k') + (P.p)(k.k') \} (A_{45}^{\ell_i^+ \ell_j^- \nu_k} O_{L1jr}^{ncs^*} + B_{45}^{\ell_i^+ \ell_j^- \nu_k} O_{R1jr}^{ncs^*}) \right. \\
&+ m_{\ell_j} m_{\tilde{\chi}_1^0}(p.k)(A_{45}^{\ell_i^+ \ell_j^- \nu_k} O_{R1jr}^{ncs^*} + B_{45}^{\ell_i^+ \ell_j^- \nu_k} O_{L1jr}^{ncs^*}) \\
&- m_{\ell_i} m_{\tilde{\chi}_1^0}(p.k')(C_{45}^{\ell_i^+ \ell_j^- \nu_k} O_{R1jr}^{ncs^*} + D_{45}^{\ell_i^+ \ell_j^- \nu_k} O_{L1jr}^{ncs^*}) \\
&\left. - m_{\ell_i} m_{\ell_j}(P.p)(C_{45}^{\ell_i^+ \ell_j^- \nu_k} O_{L1jr}^{ncs^*} + D_{45}^{\ell_i^+ \ell_j^- \nu_k} O_{R1jr}^{ncs^*}) \right], \tag{I.77}
\end{aligned}$$

where

$$\begin{aligned}
A_{45}^{\ell_i^+ \ell_j^- \nu_k} &= O_{Likr}^{cns^*} O_{Lk1l}^{nnh} O_{Lijl}^{cch}, & B_{45}^{\ell_i^+ \ell_j^- \nu_k} &= O_{Rikr}^{cns^*} O_{Rk1l}^{nnh} O_{Rijl}^{cch}, \\
C_{45}^{\ell_i^+ \ell_j^- \nu_k} &= O_{Likr}^{cns^*} O_{Lk1l}^{nnh} O_{Rijl}^{cch}, & D_{45}^{\ell_i^+ \ell_j^- \nu_k} &= O_{Rikr}^{cns^*} O_{Rk1l}^{nnh} O_{Lijl}^{cch}.
\end{aligned} \tag{I.78}$$

$$\begin{aligned}
\bullet M_4^\dagger M_6(\tilde{\chi}_1^0 \rightarrow \sum \ell_i^+ \ell_j^- \nu_k) &= - \sum_{r,l=1}^8 \frac{\tilde{g}^4}{\left[((p+k)^2 - m_{S^\pm}^2)((k+k')^2 - m_{P^0}^2) \right]} \\
&\sum_{i,j,k} \left[\{ (P.k')(p.k) - (P.k)(p.k') + (P.p)(k.k') \} (A_{46}^{\ell_i^+ \ell_j^- \nu_k} O_{L1jr}^{ncs^*} + B_{46}^{\ell_i^+ \ell_j^- \nu_k} O_{R1jr}^{ncs^*}) \right. \\
&+ m_{\ell_j} m_{\tilde{\chi}_1^0}(p.k) (A_{46}^{\ell_i^+ \ell_j^- \nu_k} O_{R1jr}^{ncs^*} + B_{46}^{\ell_i^+ \ell_j^- \nu_k} O_{L1jr}^{ncs^*}) \\
&- m_{\ell_i} m_{\tilde{\chi}_1^0}(p.k') (C_{46}^{\ell_i^+ \ell_j^- \nu_k} O_{R1jr}^{ncs^*} + D_{46}^{\ell_i^+ \ell_j^- \nu_k} O_{L1jr}^{ncs^*}) \\
&\left. - m_{\ell_i} m_{\ell_j}(P.p) (C_{46}^{\ell_i^+ \ell_j^- \nu_k} O_{L1jr}^{ncs^*} + D_{46}^{\ell_i^+ \ell_j^- \nu_k} O_{R1jr}^{ncs^*}) \right], \tag{I.79}
\end{aligned}$$

where

$$\begin{aligned}
A_{46}^{\ell_i^+ \ell_j^- \nu_k} &= O_{Likr}^{cns^*} O_{Lk1l}^{nna} O_{Lijl}^{cca}, & B_{46}^{\ell_i^+ \ell_j^- \nu_k} &= O_{Rikr}^{cns^*} O_{Rk1l}^{nna} O_{Rijl}^{cca}, \\
C_{46}^{\ell_i^+ \ell_j^- \nu_k} &= O_{Likr}^{cns^*} O_{Lk1l}^{nna} O_{Rijl}^{cca}, & D_{46}^{\ell_i^+ \ell_j^- \nu_k} &= O_{Rikr}^{cns^*} O_{Rk1l}^{nna} O_{Lijl}^{cca}.
\end{aligned} \tag{I.80}$$

$$\begin{aligned}
\bullet M_4^\dagger M_7(\tilde{\chi}_1^0 \rightarrow \sum \ell_i^+ \ell_j^- \nu_k) &= \sum_{r=1}^8 \frac{2g_2^2 \tilde{g}^2}{\left[((p+k)^2 - m_{S^\pm}^2)((k+k')^2 - m_Z^2 + im_Z \Gamma_Z) \right]} \\
&\sum_{i,j,k} \left[2(P.k')(p.k) (A_{47}^{\ell_i^+ \ell_j^- \nu_k} O_{Rij}^{ccz} + B_{47}^{\ell_i^+ \ell_j^- \nu_k} O_{Lij}^{ccz}) \right. \\
&+ m_{\ell_i} m_{\ell_j}(P.p) (A_{47}^{\ell_i^+ \ell_j^- \nu_k} O_{Lij}^{ccz} + B_{47}^{\ell_i^+ \ell_j^- \nu_k} O_{Rij}^{ccz}) \\
&+ 2m_{\ell_j} m_{\tilde{\chi}_1^0}(p.k) (C_{47}^{\ell_i^+ \ell_j^- \nu_k} O_{Lij}^{ccz} + D_{47}^{\ell_i^+ \ell_j^- \nu_k} O_{Rij}^{ccz}) \\
&\left. + m_{\ell_i} m_{\tilde{\chi}_1^0}(p.k') (C_{47}^{\ell_i^+ \ell_j^- \nu_k} O_{Rij}^{ccz} + D_{47}^{\ell_i^+ \ell_j^- \nu_k} O_{Lij}^{ccz}) \right], \tag{I.81}
\end{aligned}$$

where

$$\begin{aligned}
A_{47}^{\ell_i^+ \ell_j^- \nu_k} &= O_{Likr}^{cns^*} O_{Rk1l}^{nnz} O_{R1jr}^{ncs^*}, & B_{47}^{\ell_i^+ \ell_j^- \nu_k} &= O_{Rikr}^{cns^*} O_{Lk1l}^{nnz} O_{L1jr}^{ncs^*}, \\
C_{47}^{\ell_i^+ \ell_j^- \nu_k} &= O_{Rikr}^{cns^*} O_{Lk1l}^{nnz} O_{R1jr}^{ncs^*}, & D_{47}^{\ell_i^+ \ell_j^- \nu_k} &= O_{Likr}^{cns^*} O_{Rk1l}^{nnz} O_{L1jr}^{ncs^*}.
\end{aligned} \tag{I.82}$$

$$\begin{aligned}
\bullet M_5^\dagger M_6(\tilde{\chi}_1^0 \rightarrow \sum \ell_i^+ \ell_j^- \nu_k) &= - \sum_{r,l=1}^8 \frac{\tilde{g}^4}{\left[((k+k')^2 - m_{S^0}^2)((k+k')^2 - m_{P^0}^2) \right]} \\
&\sum_{i,j,k} \left[(P.p)(k.k') A_{56}^{\ell_i^+ \ell_j^- \nu_k} - m_{\ell_i} m_{\ell_j}(P.p) B_{56}^{\ell_i^+ \ell_j^- \nu_k} \right], \tag{I.83}
\end{aligned}$$

where

$$\begin{aligned}
A_{56}^{\ell_i^+ \ell_j^- \nu_k} &= \left(O_{Lijr}^{cch^*} O_{Lijl}^{cca} + O_{Rijr}^{cch^*} O_{Rijl}^{cca} \right) \left(O_{Lk1r}^{nnh^*} O_{Lk1l}^{nna} + O_{Rk1r}^{nnh^*} O_{Rk1l}^{nna} \right), \\
B_{56}^{\ell_i^+ \ell_j^- \nu_k} &= \left(O_{Rijr}^{cch^*} O_{Lijl}^{cca} + O_{Lijr}^{cch^*} O_{Rijl}^{cca} \right) \left(O_{Lk1r}^{nnh^*} O_{Lk1l}^{nna} + O_{Rk1r}^{nnh^*} O_{Rk1l}^{nna} \right).
\end{aligned} \tag{I.84}$$

$$\begin{aligned}
\bullet M_5^\dagger M_7(\tilde{\chi}_1^0 \rightarrow \sum \ell_i^+ \ell_j^- \nu_k) &= - \sum_{r=1}^8 \frac{g_2^2 \tilde{g}^2 \text{see}\theta_W}{\left[((k+k')^2 - m_{S^0}^2)((k+k')^2 - m_Z^2 + im_Z \Gamma_Z) \right]} \\
&\sum_{i,j,k} \left[m_{\ell_i} m_{\tilde{\chi}_1^0}(p.k') A_{57}^{\ell_i^+ \ell_j^- \nu_k} - m_{\ell_j} m_{\tilde{\chi}_1^0}(p.k) B_{57}^{\ell_i^+ \ell_j^- \nu_k} \right], \tag{I.85}
\end{aligned}$$

where

$$\begin{aligned} A_{57}^{\ell_i^+ \ell_j^- \nu_k} &= \left(O_{Rijr}^{cch^*} O_{Rij}^{ccz} + O_{Lijr}^{cch^*} O_{Lij}^{ccz} \right) \left(O_{Rk1r}^{nnh^*} O_{Lk1}^{nnz} + O_{Lk1r}^{nnh^*} O_{Rk1}^{nnz} \right), \\ B_{57}^{\ell_i^+ \ell_j^- \nu_k} &= \left(O_{Rijr}^{cch^*} O_{Lij}^{ccz} + O_{Lijr}^{cch^*} O_{Rij}^{ccz} \right) \left(O_{Rk1r}^{nnh^*} O_{Lk1}^{nnz} + O_{Lk1r}^{nnh^*} O_{Rk1}^{nnz} \right). \end{aligned} \quad (\text{I.86})$$

$$\begin{aligned} \bullet M_6^\dagger M_7(\tilde{\chi}_1^0 \rightarrow \sum \ell_i^+ \ell_j^- \nu_k) &= \sum_{r=1}^8 \frac{g_2^2 \tilde{g}^2 \text{see}\theta_W}{\left[((k+k')^2 - m_{P_r^0}^2)((k+k')^2 - m_Z^2 + im_Z \Gamma_Z) \right]} \\ &\quad \sum_{i,j,k} \left[m_{\ell_i} m_{\tilde{\chi}_1^0}(p.k') A_{67}^{\ell_i^+ \ell_j^- \nu_k} - m_{\ell_j} m_{\tilde{\chi}_1^0}(p.k) B_{67}^{\ell_i^+ \ell_j^- \nu_k} \right], \end{aligned} \quad (\text{I.87})$$

where

$$\begin{aligned} A_{67}^{\ell_i^+ \ell_j^- \nu_k} &= \left(O_{Rijr}^{cca^*} O_{Rij}^{ccz} + O_{Lijr}^{cca^*} O_{Lij}^{ccz} \right) \left(O_{Rk1r}^{nna^*} O_{Lk1}^{nnz} + O_{Lk1r}^{nna^*} O_{Rk1}^{nnz} \right), \\ B_{67}^{\ell_i^+ \ell_j^- \nu_k} &= \left(O_{Rijr}^{cca^*} O_{Lij}^{ccz} + O_{Lijr}^{cca^*} O_{Rij}^{ccz} \right) \left(O_{Rk1r}^{nna^*} O_{Lk1}^{nnz} + O_{Lk1r}^{nna^*} O_{Rk1}^{nnz} \right). \end{aligned} \quad (\text{I.88})$$

Γ_W and Γ_Z are the decay width for W and Z -boson, respectively and their values are given in ref. [16]. All the lepton masses are also taken from ref. [16].

I.4 Process $\tilde{\chi}_1^0 \rightarrow \nu_i \bar{\nu}_j \nu_k$

We represent different lepton flavours (e, μ, τ) by i, j, k . We write down all possible $M_i^\dagger M_j$ for the three diagrams shown in figure I.3. The four-momentum assignments are as follows

$$\tilde{\chi}_1^0(P) \rightarrow \nu_i(p) + \bar{\nu}_j(k) + \nu_k(k'). \quad (\text{I.89})$$

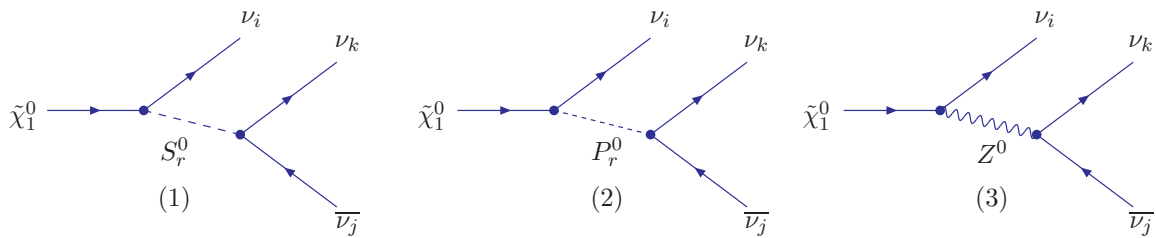


Figure I.3: Feynman diagrams for the possible three body decays of the lightest supersymmetric particle into $\nu_i \bar{\nu}_j \nu_k$ final states. S_r^0, P_r^0 are the neutral scalar and pseudoscalar states of the $\mu\nu$ S SM as shown by eqns.(B.5), (B.8).

$$\begin{aligned} \bullet M_1^\dagger M_1(\tilde{\chi}_1^0 \rightarrow \sum \nu_i \bar{\nu}_j \nu_k) &= \sum_{r,l=1}^8 \frac{\tilde{g}^4}{\left[((k+k')^2 - m_{S_r^0}^2)((k+k')^2 - m_{S_l^0}^2) \right]} \\ &\quad \times \sum_{i,j,k} (P.p)(k.k') \left(O_{Lilr}^{nnh^*} O_{Lil}^{nnh} + O_{Rilr}^{nnh^*} O_{Ril}^{nnh} \right) \left(O_{Lkjr}^{nnh^*} O_{Lkj}^{nnh} + O_{Rkjr}^{nnh^*} O_{Rkj}^{nnh} \right). \end{aligned} \quad (\text{I.90})$$

$$\begin{aligned}
& \bullet M_2^\dagger M_2(\tilde{\chi}_1^0 \rightarrow \sum \nu_i \bar{\nu}_j \nu_k) = \sum_{r,l=1}^8 \frac{\tilde{g}^4}{\left[((k+k')^2 - m_{P^0}^2)((k+k')^2 - m_{l^0}^2) \right]} \\
& \times \sum_{i,j,k} (P.p)(k.k') \left(O_{Li1r}^{nna*} O_{Li1l}^{nna} + O_{Ri1r}^{nna*} O_{Ri1l}^{nna} \right) \left(O_{Lkjr}^{nna*} O_{Lkjl}^{nna} + O_{Rkjr}^{nna*} O_{Rkjl}^{nna} \right).
\end{aligned} \tag{I.91}$$

$$\begin{aligned}
& \bullet M_3^\dagger M_3(\tilde{\chi}_1^0 \rightarrow \sum \nu_i \bar{\nu}_j \nu_k) = \frac{g^4}{\left[((k+k')^2 - m_Z^2)^2 + m_Z^2 \Gamma_Z^2 \right]} \\
& \times \sum_{i,j,k} \left[(P.k)(p.k') \left(O_{Li1}^{nnz*} O_{Li1}^{nnz} O_{Lkj}^{nnz*} O_{Lkj}^{nnz} + O_{Ri1}^{nnz*} O_{Ri1}^{nnz} O_{Rkj}^{nnz*} O_{Rkj}^{nnz} \right) \right. \\
& \left. + (P.k')(p.k) \left(O_{Li1}^{nnz*} O_{Li1}^{nnz} O_{Rkj}^{nnz*} O_{Rkj}^{nnz} + O_{Ri1}^{nnz*} O_{Ri1}^{nnz} O_{Lkj}^{nnz*} O_{Lkj}^{nnz} \right) \right].
\end{aligned} \tag{I.92}$$

$$\begin{aligned}
& \bullet M_1^\dagger M_2(\tilde{\chi}_1^0 \rightarrow \sum \nu_i \bar{\nu}_j \nu_k) = - \sum_{r,l=1}^8 \frac{\tilde{g}^4}{\left[((k+k')^2 - m_{S^0}^2)((k+k')^2 - m_{P^0}^2) \right]} \\
& \times \sum_{i,j,k} (P.p)(k.k') \left(O_{Li1r}^{nnh*} O_{Li1l}^{nna} + O_{Ri1r}^{nnh*} O_{Ri1l}^{nna} \right) \left(O_{Lkjr}^{nnh*} O_{Lkjl}^{nna} + O_{Rkjr}^{nnh*} O_{Rkjl}^{nna} \right).
\end{aligned} \tag{I.93}$$

$$\bullet M_1^\dagger M_3(\tilde{\chi}_1^0 \rightarrow \sum \nu_i \bar{\nu}_j \nu_k) = 0. \tag{I.94}$$

$$\bullet M_2^\dagger M_3(\tilde{\chi}_1^0 \rightarrow \sum \nu_i \bar{\nu}_j \nu_k) = 0. \tag{I.95}$$

I.5 Process $\tilde{\chi}_1^0 \rightarrow \bar{u}_i d_j \ell_k^+$

We represent different lepton flavours (e, μ, τ) by k . $u_i(d_j)$ stands for different up-type and down-type quarks ($u, c(d, s, b)$), except the top. We write down all possible $M_i^\dagger M_j$ for the four diagrams shown in figure I.4. Required couplings are given in appendices D and H. The four-momentum assignments are as follows

$$\tilde{\chi}_1^0(P) \rightarrow \ell_k^+(p) + \bar{u}_i(k) + d_j(k'). \tag{I.96}$$

$$\begin{aligned}
& \bullet M_1^\dagger M_1(\tilde{\chi}_1^0 \rightarrow \sum \bar{u}_i d_j \ell_k^+) = \sum_{i,j,k} \frac{4g^4 |V_{ij}^{CKM}|^2}{\left[(((k+k')^2 - m_W^2)^2 + m_W^2 \Gamma_W^2) \right]} \\
& \left[2(P.k)(p.k') O_{Lk1}^{cnw*} O_{Lk1}^{cnw} + 2(P.k')(p.k) O_{Rk1}^{cnw*} O_{Rk1}^{cnw} \right. \\
& \left. - m_{\ell_k} m_{\tilde{\chi}_1^0}(k.k') \left(O_{Rk1}^{cnw*} O_{Lk1}^{cnw} + O_{Lk1}^{cnw*} O_{Rk1}^{cnw} \right) \right].
\end{aligned} \tag{I.97}$$

$$\begin{aligned}
& \bullet M_2^\dagger M_2(\tilde{\chi}_1^0 \rightarrow \sum \bar{u}_i d_j \ell_k^+) = \sum_{i,j,k} \sum_{r,l=1}^8 \frac{4\tilde{g}^4}{\left[((k+k')^2 - m_{S^\pm}^2)((k+k')^2 - m_{l^\pm}^2) \right]} \\
& \left[(P.p) \left(O_{Lk1r}^{cns*} O_{Lk1l}^{cns} + O_{Rk1r}^{cns*} O_{Rk1l}^{cns} \right) + m_{\ell_k} m_{\tilde{\chi}_1^0} \left(O_{Lk1r}^{cns*} O_{Rk1l}^{cns} + O_{Rk1r}^{cns*} O_{Lk1l}^{cns} \right) \right] \\
& \times \left[(k.k') \left(O_{Lijl}^{uds*} O_{Lijr}^{uds} + O_{Rijl}^{uds*} O_{Rijr}^{uds} \right) - m_{u_i} m_{d_j} \left(O_{Rijl}^{uds*} O_{Lijr}^{uds} + O_{Lijl}^{uds*} O_{Rijr}^{uds} \right) \right].
\end{aligned} \tag{I.98}$$

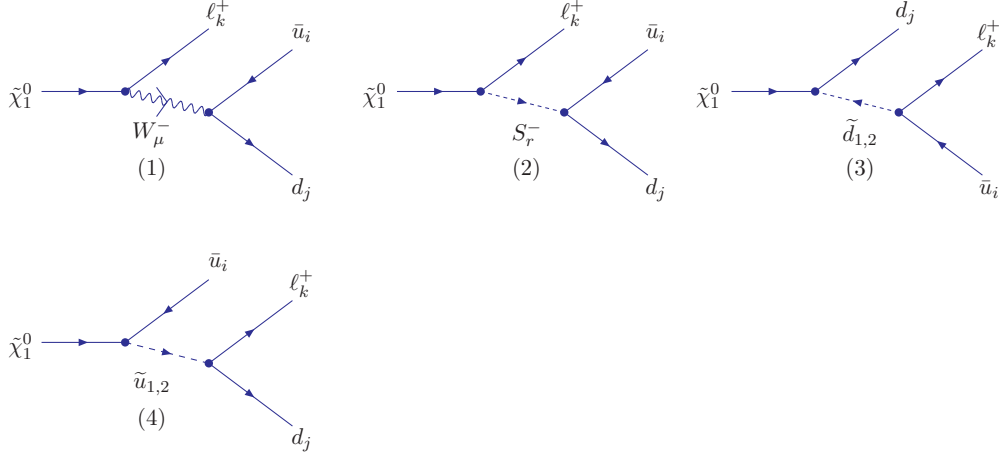


Figure I.4: Feynman diagrams for the possible three body decays of the lightest supersymmetric particle into $\bar{u}_i d_j \ell_k^+$ final states. S_r^- are the charged scalar states of the $\mu\nu$ SSM as shown by eqn.(B.11). $\tilde{u}(\tilde{d})$ are the up and down-type squarks as shown by eqn.(B.19) corresponding to \bar{u}_i and d_j .

$$\begin{aligned}
\bullet M_3^\dagger M_3(\tilde{\chi}_1^0 \rightarrow \sum \bar{u}_i d_j \ell_k^+) &= \sum_{i,j,k} \sum_{r,l=1}^2 \frac{4\tilde{g}^4}{\left[((p+k)^2 - m_{\tilde{d}_r}^2)((p+k)^2 - m_{\tilde{d}_l}^2) \right]} \\
&\left[(P.k') \left(O_{Lj1r}^{dn\tilde{d}^*} O_{Lj1l}^{dn\tilde{d}} + O_{Rj1r}^{dn\tilde{d}^*} O_{Rj1l}^{dn\tilde{d}} \right) + m_{d_j} m_{\tilde{\chi}_1^0} \left(O_{Rj1r}^{dn\tilde{d}^*} O_{Lj1l}^{dn\tilde{d}} + O_{Lj1r}^{dn\tilde{d}^*} O_{Rj1l}^{dn\tilde{d}} \right) \right] \\
&\times \left[(p.k) \left(O_{Likl}^{ucd^*} O_{Likr}^{ucd} + O_{Rikl}^{ucd^*} O_{Rikr}^{ucd} \right) - m_{u_i} m_{\ell_k} \left(O_{Rikl}^{ucd^*} O_{Likr}^{ucd} + O_{Likl}^{ucd^*} O_{Rikr}^{ucd} \right) \right].
\end{aligned} \tag{I.99}$$

$$\begin{aligned}
\bullet M_4^\dagger M_4(\tilde{\chi}_1^0 \rightarrow \sum \bar{u}_i d_j \ell_k^+) &= \sum_{i,j,k} \sum_{r,l=1}^2 \frac{4\tilde{g}^4}{\left[((p+k')^2 - m_{\tilde{u}_r}^2)((p+k')^2 - m_{\tilde{u}_l}^2) \right]} \\
&\left[(P.k) \left(O_{L1ir}^{nu\tilde{u}^*} O_{L1il}^{nu\tilde{u}} + O_{R1ir}^{nu\tilde{u}^*} O_{R1il}^{nu\tilde{u}} \right) + m_{u_i} m_{\tilde{\chi}_1^0} \left(O_{R1ir}^{nu\tilde{u}^*} O_{L1il}^{nu\tilde{u}} + O_{L1ir}^{nu\tilde{u}^*} O_{R1il}^{nu\tilde{u}} \right) \right] \\
&\times \left[(p.k') \left(O_{Lkjl}^{cdu^*} O_{Lkjr}^{cdu} + O_{Rkjl}^{cdu^*} O_{Rkjr}^{cdu} \right) - m_{d_j} m_{\ell_k} \left(O_{Rkjl}^{cdu^*} O_{Lkjr}^{cdu} + O_{Lkjl}^{cdu^*} O_{Rkjr}^{cdu} \right) \right].
\end{aligned} \tag{I.100}$$

$$\begin{aligned}
\bullet M_1^\dagger M_2(\tilde{\chi}_1^0 \rightarrow \sum \bar{u}_i d_j \ell_k^+) &= \\
&\sum_{i,j,k} \sum_{r=1}^8 \frac{2\sqrt{2}g_2^2\tilde{g}^2 V_{ij}^{CKM}}{\left[((k+k')^2 - m_W^2 - im_W\Gamma_W)((k+k')^2 - m_{S_r^\pm}^2) \right]} \\
&\left[m_{u_i} m_{\tilde{\chi}_1^0} (p.k') O_{Lijr}^{uds^*} A_{12}^{\bar{u}_i d_j \ell_k^+} + m_{\ell_k} m_{u_i} (P.k') O_{Lijr}^{uds^*} B_{12}^{\bar{u}_i d_j \ell_k^+} \right. \\
&\left. - m_{d_j} m_{\tilde{\chi}_1^0} (p.k) O_{Rijr}^{uds^*} A_{12}^{\bar{u}_i d_j \ell_k^+} - m_{d_j} m_{\ell_k} (P.k) O_{Rijr}^{uds^*} B_{12}^{\bar{u}_i d_j \ell_k^+} \right].
\end{aligned} \tag{I.101}$$

where

$$A_{12}^{\bar{u}_i d_j \ell_k^+} = \left(O_{Lk1r}^{cnw^*} O_{Rk1r}^{cns} + O_{Rk1r}^{cnw^*} O_{Lk1r}^{cns} \right), \quad B_{12}^{\bar{u}_i d_j \ell_k^+} = \left(O_{Lk1r}^{cnw^*} O_{Lk1r}^{cns} + O_{Rk1r}^{cnw^*} O_{Rk1r}^{cns} \right). \tag{I.102}$$

$$\begin{aligned}
& \bullet M_1^\dagger M_3(\tilde{\chi}_1^0 \rightarrow \sum \bar{u}_i d_j \ell_k^+) = \\
& - \sum_{i,j,k} \sum_{r=1}^2 \frac{2\sqrt{2}g_2^2 \tilde{g}^2 V_{ij}^{CKM}}{\left[((k+k')^2 - m_W^2 - im_W \Gamma_W)((p+k)^2 - m_{\tilde{d}_r}^2) \right]} \\
& \left[2(P.k')(p.k)A_{13}^{\bar{u}_i d_j \ell_k^+} - m_{\ell_k} m_{\tilde{\chi}_1^0}(k.k')B_{13}^{\bar{u}_i d_j \ell_k^+} + m_{u_i} m_{\tilde{\chi}_1^0}(p.k')C_{13}^{\bar{u}_i d_j \ell_k^+} \right. \\
& - 2m_{u_i} m_{\ell_k}(P.k')D_{13}^{\bar{u}_i d_j \ell_k^+} + 2m_{d_j} m_{\tilde{\chi}_1^0}(p.k)E_{13}^{\bar{u}_i d_j \ell_k^+} - m_{d_j} m_{\ell_k}(P.k)F_{13}^{\bar{u}_i d_j \ell_k^+} \\
& \left. + m_{u_i} m_{d_j}(P.p)G_{13}^{\bar{u}_i d_j \ell_k^+} - 2m_{u_i} m_{d_j} m_{\ell_k} m_{\tilde{\chi}_1^0} H_{13}^{\bar{u}_i d_j \ell_k^+} \right], \tag{I.103}
\end{aligned}$$

where

$$\begin{aligned}
A_{13}^{\bar{u}_i d_j \ell_k^+} &= O_{Rk1}^{cnw*} O_{Rikr}^{ucd*} O_{Rj1r}^{dn\tilde{d}}, & B_{13}^{\bar{u}_i d_j \ell_k^+} &= O_{Lk1}^{cnw*} O_{Rikr}^{ucd*} O_{Rj1r}^{dn\tilde{d}}, \\
C_{13}^{\bar{u}_i d_j \ell_k^+} &= O_{Lk1}^{cnw*} O_{Likr}^{ucd*} O_{Rj1r}^{dn\tilde{d}}, & D_{13}^{\bar{u}_i d_j \ell_k^+} &= O_{Rk1}^{cnw*} O_{Likr}^{ucd*} O_{Rj1r}^{dn\tilde{d}}, \\
E_{13}^{\bar{u}_i d_j \ell_k^+} &= O_{Rk1}^{cnw*} O_{Rikr}^{ucd*} O_{Lj1r}^{dn\tilde{d}}, & F_{13}^{\bar{u}_i d_j \ell_k^+} &= O_{Lk1}^{cnw*} O_{Rikr}^{ucd*} O_{Lj1r}^{dn\tilde{d}}, \\
G_{13}^{\bar{u}_i d_j \ell_k^+} &= O_{Lk1}^{cnw*} O_{Likr}^{ucd*} O_{Lj1r}^{dn\tilde{d}}, & H_{13}^{\bar{u}_i d_j \ell_k^+} &= O_{Rk1}^{cnw*} O_{Likr}^{ucd*} O_{Lj1r}^{dn\tilde{d}}. \tag{I.104}
\end{aligned}$$

$$\begin{aligned}
& \bullet M_1^\dagger M_4(\tilde{\chi}_1^0 \rightarrow \sum \bar{u}_i d_j \ell_k^+) = \\
& \sum_{i,j,k} \sum_{r=1}^2 \frac{2\sqrt{2}g_2^2 \tilde{g}^2 V_{ij}^{CKM}}{\left[((k+k')^2 - m_W^2 - im_W \Gamma_W)((p+k')^2 - m_{\tilde{u}_r}^2) \right]} \\
& \left[2(P.k)(p.k')A_{14}^{\bar{u}_i d_j \ell_k^+} - m_{\ell_k} m_{\tilde{\chi}_1^0}(k.k')B_{14}^{\bar{u}_i d_j \ell_k^+} + m_{d_j} m_{\tilde{\chi}_1^0}(p.k)C_{14}^{\bar{u}_i d_j \ell_k^+} \right. \\
& - 2m_{d_j} m_{\ell_k}(P.k)D_{14}^{\bar{u}_i d_j \ell_k^+} + 2m_{u_i} m_{\tilde{\chi}_1^0}(p.k')E_{14}^{\bar{u}_i d_j \ell_k^+} - m_{u_i} m_{\ell_k}(P.k')F_{14}^{\bar{u}_i d_j \ell_k^+} \\
& \left. + m_{u_i} m_{d_j}(P.p)G_{14}^{\bar{u}_i d_j \ell_k^+} - 2m_{u_i} m_{d_j} m_{\ell_k} m_{\tilde{\chi}_1^0} H_{14}^{\bar{u}_i d_j \ell_k^+} \right], \tag{I.105}
\end{aligned}$$

where

$$\begin{aligned}
A_{14}^{\bar{u}_i d_j \ell_k^+} &= O_{Lk1}^{cnw*} O_{Lkjr}^{cdu*} O_{Ll1r}^{nu\tilde{u}}, & B_{14}^{\bar{u}_i d_j \ell_k^+} &= O_{Rk1}^{cnw*} O_{Lkjr}^{cdu*} O_{Ll1r}^{nu\tilde{u}}, \\
C_{14}^{\bar{u}_i d_j \ell_k^+} &= O_{Rk1}^{cnw*} O_{Rkjr}^{cdu*} O_{Ll1r}^{nu\tilde{u}}, & D_{14}^{\bar{u}_i d_j \ell_k^+} &= O_{Lk1}^{cnw*} O_{Rkjr}^{cdu*} O_{Ll1r}^{nu\tilde{u}}, \\
E_{14}^{\bar{u}_i d_j \ell_k^+} &= O_{Lk1}^{cnw*} O_{Lkjr}^{cdu*} O_{Rl1r}^{nu\tilde{u}}, & F_{14}^{\bar{u}_i d_j \ell_k^+} &= O_{Rk1}^{cnw*} O_{Lkjr}^{cdu*} O_{Rl1r}^{nu\tilde{u}}, \\
G_{14}^{\bar{u}_i d_j \ell_k^+} &= O_{Rk1}^{cnw*} O_{Rkjr}^{cdu*} O_{Rl1r}^{nu\tilde{u}}, & H_{14}^{\bar{u}_i d_j \ell_k^+} &= O_{Lk1}^{cnw*} O_{Rkjr}^{cdu*} O_{Rl1r}^{nu\tilde{u}}. \tag{I.106}
\end{aligned}$$

$$\begin{aligned}
\bullet M_2^\dagger M_3(\tilde{\chi}_1^0 \rightarrow \sum \bar{u}_i d_j \ell_k^+) &= \sum_{i,j,k} \sum_{r=1}^8 \sum_{l=1}^2 \frac{2\tilde{g}^4}{\left[((k+k')^2 - m_{S_\mp}^2)((p+k)^2 - m_{d_l}^2) \right]} \\
&\left[\{ (P.p)(k.k') - (P.k)(p.k') + (P.k')(p.k) \} \left(A_{23}^{\bar{u}_i d_j \ell_k^+} O_{Lk1r}^{cns*} + B_{23}^{\bar{u}_i d_j \ell_k^+} O_{Rk1r}^{cns*} \right) \right. \\
&+ m_{\ell_k} m_{\tilde{\chi}_1^0}(k.k') \left(A_{23}^{\bar{u}_i d_j \ell_k^+} O_{Rk1r}^{cns*} + B_{23}^{\bar{u}_i d_j \ell_k^+} O_{Lk1r}^{cns*} \right) \\
&- m_{u_i} m_{\tilde{\chi}_1^0}(p.k') \left(C_{23}^{\bar{u}_i d_j \ell_k^+} O_{Rk1r}^{cns*} + D_{23}^{\bar{u}_i d_j \ell_k^+} O_{Lk1r}^{cns*} \right) \\
&- m_{u_i} m_{\ell_k}(P.k') \left(C_{23}^{\bar{u}_i d_j \ell_k^+} O_{Lk1r}^{cns*} + D_{23}^{\bar{u}_i d_j \ell_k^+} O_{Rk1r}^{cns*} \right) \\
&+ m_{d_j} m_{\tilde{\chi}_1^0}(p.k) \left(E_{23}^{\bar{u}_i d_j \ell_k^+} O_{Rk1r}^{cns*} + F_{23}^{\bar{u}_i d_j \ell_k^+} O_{Lk1r}^{cns*} \right) \\
&+ m_{d_j} m_{\ell_k}(P.k) \left(E_{23}^{\bar{u}_i d_j \ell_k^+} O_{Lk1r}^{cns*} + F_{23}^{\bar{u}_i d_j \ell_k^+} O_{Rk1r}^{cns*} \right) \\
&- m_{u_i} m_{d_j}(P.p) \left(G_{23}^{\bar{u}_i d_j \ell_k^+} O_{Lk1r}^{cns*} + H_{23}^{\bar{u}_i d_j \ell_k^+} O_{Rk1r}^{cns*} \right) \\
&\left. - m_{u_i} m_{d_j} m_{\ell_k} m_{\tilde{\chi}_1^0} \left(G_{23}^{\bar{u}_i d_j \ell_k^+} O_{Rk1r}^{cns*} + H_{23}^{\bar{u}_i d_j \ell_k^+} O_{Lk1r}^{cns*} \right) \right], \tag{I.107}
\end{aligned}$$

where

$$\begin{aligned}
A_{23}^{\bar{u}_i d_j \ell_k^+} &= O_{Rikl}^{ucd*} O_{Rijr}^{uds} O_{Lj1l}^{dn\tilde{d}}, & B_{23}^{\bar{u}_i d_j \ell_k^+} &= O_{Likl}^{ucd*} O_{Lijr}^{uds} O_{Rj1l}^{dn\tilde{d}}, \\
C_{23}^{\bar{u}_i d_j \ell_k^+} &= O_{Likl}^{ucd*} O_{Rijr}^{uds} O_{Lj1l}^{dn\tilde{d}}, & D_{23}^{\bar{u}_i d_j \ell_k^+} &= O_{Rikl}^{ucd*} O_{Lijr}^{uds} O_{Rj1l}^{dn\tilde{d}}, \\
E_{23}^{\bar{u}_i d_j \ell_k^+} &= O_{Likl}^{ucd*} O_{Lijr}^{uds} O_{Lj1l}^{dn\tilde{d}}, & F_{23}^{\bar{u}_i d_j \ell_k^+} &= O_{Rikl}^{ucd*} O_{Rijr}^{uds} O_{Rj1l}^{dn\tilde{d}}, \\
G_{23}^{\bar{u}_i d_j \ell_k^+} &= O_{Rikl}^{ucd*} O_{Lijr}^{uds} O_{Lj1l}^{dn\tilde{d}}, & H_{23}^{\bar{u}_i d_j \ell_k^+} &= O_{Likl}^{ucd*} O_{Rijr}^{uds} O_{Rj1l}^{dn\tilde{d}}. \tag{I.108}
\end{aligned}$$

$$\begin{aligned}
\bullet M_2^\dagger M_4(\tilde{\chi}_1^0 \rightarrow \sum \bar{u}_i d_j \ell_k^+) &= \sum_{i,j,k} \sum_{r=1}^8 \sum_{l=1}^2 \frac{2\tilde{g}^4}{\left[((k+k')^2 - m_{S_\mp}^2)((p+k')^2 - m_{u_l}^2) \right]} \\
&\left[\{ (P.p)(k.k') - (P.k')(p.k) + (P.k)(p.k') \} \left(A_{24}^{\bar{u}_i d_j \ell_k^+} O_{Lk1r}^{cns*} + B_{24}^{\bar{u}_i d_j \ell_k^+} O_{Rk1r}^{cns*} \right) \right. \\
&+ m_{\ell_k} m_{\tilde{\chi}_1^0}(k.k') \left(A_{24}^{\bar{u}_i d_j \ell_k^+} O_{Rk1r}^{cns*} + B_{24}^{\bar{u}_i d_j \ell_k^+} O_{Lk1r}^{cns*} \right) \\
&- m_{d_j} m_{\tilde{\chi}_1^0}(p.k) \left(C_{24}^{\bar{u}_i d_j \ell_k^+} O_{Rk1r}^{cns*} + D_{24}^{\bar{u}_i d_j \ell_k^+} O_{Lk1r}^{cns*} \right) \\
&- m_{d_j} m_{\ell_k}(P.k) \left(C_{24}^{\bar{u}_i d_j \ell_k^+} O_{Lk1r}^{cns*} + D_{24}^{\bar{u}_i d_j \ell_k^+} O_{Rk1r}^{cns*} \right) \\
&+ m_{u_i} m_{\tilde{\chi}_1^0}(p.k') \left(E_{24}^{\bar{u}_i d_j \ell_k^+} O_{Rk1r}^{cns*} + F_{24}^{\bar{u}_i d_j \ell_k^+} O_{Lk1r}^{cns*} \right) \\
&+ m_{u_i} m_{\ell_k}(P.k') \left(E_{24}^{\bar{u}_i d_j \ell_k^+} O_{Lk1r}^{cns*} + F_{24}^{\bar{u}_i d_j \ell_k^+} O_{Rk1r}^{cns*} \right) \\
&- m_{u_i} m_{d_j}(P.p) \left(G_{24}^{\bar{u}_i d_j \ell_k^+} O_{Lk1r}^{cns*} + H_{24}^{\bar{u}_i d_j \ell_k^+} O_{Rk1r}^{cns*} \right) \\
&\left. - m_{u_i} m_{d_j} m_{\ell_k} m_{\tilde{\chi}_1^0} \left(G_{24}^{\bar{u}_i d_j \ell_k^+} O_{Rk1r}^{cns*} + H_{24}^{\bar{u}_i d_j \ell_k^+} O_{Lk1r}^{cns*} \right) \right], \tag{I.109}
\end{aligned}$$

where

$$\begin{aligned}
A_{24}^{\bar{u}_i d_j \ell_k^+} &= O_{Rkjl}^{cdu*} O_{Rijr}^{uds} O_{Ll1l}^{nu\tilde{u}}, & B_{24}^{\bar{u}_i d_j \ell_k^+} &= O_{Lkjl}^{cdu*} O_{Lijr}^{uds} O_{Rl1l}^{nu\tilde{u}}, \\
C_{24}^{\bar{u}_i d_j \ell_k^+} &= O_{Lkjl}^{cdu*} O_{Rijr}^{uds} O_{Ll1l}^{nu\tilde{u}}, & D_{24}^{\bar{u}_i d_j \ell_k^+} &= O_{Rkjl}^{cdu*} O_{Lijr}^{uds} O_{Rl1l}^{nu\tilde{u}}, \\
E_{24}^{\bar{u}_i d_j \ell_k^+} &= O_{Lkjl}^{cdu*} O_{Lijr}^{uds} O_{Ll1l}^{nu\tilde{u}}, & F_{24}^{\bar{u}_i d_j \ell_k^+} &= O_{Rkjl}^{cdu*} O_{Rijr}^{uds} O_{Rl1l}^{nu\tilde{u}}, \\
G_{24}^{\bar{u}_i d_j \ell_k^+} &= O_{Rkjl}^{cdu*} O_{Lijr}^{uds} O_{Ll1l}^{nu\tilde{u}}, & H_{24}^{\bar{u}_i d_j \ell_k^+} &= O_{Lkjl}^{cdu*} O_{Rijr}^{uds} O_{Rl1l}^{nu\tilde{u}}. \tag{I.110}
\end{aligned}$$

$$\begin{aligned}
\bullet M_3^\dagger M_4(\tilde{\chi}_1^0 \rightarrow \sum \bar{u}_i d_j \ell_k^+) &= - \sum_{i,j,k} \sum_{r,l=1}^2 \frac{2\tilde{g}^4}{\left[((p+k)^2 - m_{\tilde{d}_r}^2)((p+k')^2 - m_{\tilde{u}_l}^2) \right]} \\
&\left[\{ (P.k')(p.k) - (P.p)(k.k') + (P.k)(p.k') \} \left(A_{34}^{\bar{u}_i d_j \ell_k^+} O_{Lj1r}^{dn\tilde{d}^*} + B_{34}^{\bar{u}_i d_j \ell_k^+} O_{Rj1r}^{dn\tilde{d}^*} \right) \right. \\
&+ m_{d_j} m_{\tilde{\chi}_1^0}(p.k) \left(A_{34}^{\bar{u}_i d_j \ell_k^+} O_{Rj1r}^{dn\tilde{d}^*} + B_{34}^{\bar{u}_i d_j \ell_k^+} O_{Lj1r}^{dn\tilde{d}^*} \right) \\
&- m_{\ell_k} m_{\tilde{\chi}_1^0}(k.k') \left(C_{34}^{\bar{u}_i d_j \ell_k^+} O_{Rj1r}^{dn\tilde{d}^*} + D_{34}^{\bar{u}_i d_j \ell_k^+} O_{Lj1r}^{dn\tilde{d}^*} \right) \\
&- m_{d_j} m_{\ell_k}(P.k) \left(C_{34}^{\bar{u}_i d_j \ell_k^+} O_{Lj1r}^{dn\tilde{d}^*} + D_{34}^{\bar{u}_i d_j \ell_k^+} O_{Rj1r}^{dn\tilde{d}^*} \right) \\
&+ m_{u_i} m_{\tilde{\chi}_1^0}(p.k') \left(E_{34}^{\bar{u}_i d_j \ell_k^+} O_{Rj1r}^{dn\tilde{d}^*} + F_{34}^{\bar{u}_i d_j \ell_k^+} O_{Lj1r}^{dn\tilde{d}^*} \right) \\
&+ m_{u_i} m_{d_j}(P.p) \left(E_{34}^{\bar{u}_i d_j \ell_k^+} O_{Lj1r}^{dn\tilde{d}^*} + F_{34}^{\bar{u}_i d_j \ell_k^+} O_{Rj1r}^{dn\tilde{d}^*} \right) \\
&- m_{u_i} m_{\ell_k}(P.k') \left(G_{34}^{\bar{u}_i d_j \ell_k^+} O_{Lj1r}^{dn\tilde{d}^*} + H_{34}^{\bar{u}_i d_j \ell_k^+} O_{Rj1r}^{dn\tilde{d}^*} \right) \\
&\left. - m_{u_i} m_{d_j} m_{\ell_k} m_{\tilde{\chi}_1^0} \left(G_{34}^{\bar{u}_i d_j \ell_k^+} O_{Rj1r}^{dn\tilde{d}^*} + H_{34}^{\bar{u}_i d_j \ell_k^+} O_{Lj1r}^{dn\tilde{d}^*} \right) \right], \tag{I.111}
\end{aligned}$$

where

$$\begin{aligned}
A_{34}^{\bar{u}_i d_j \ell_k^+} &= O_{Rkjl}^{cdu^*} O_{Rikr}^{ucd} O_{L1il}^{nu\tilde{u}}, & B_{34}^{\bar{u}_i d_j \ell_k^+} &= O_{Lkjl}^{cdu^*} O_{Likr}^{ucd} O_{R1il}^{nu\tilde{u}}, \\
C_{34}^{\bar{u}_i d_j \ell_k^+} &= O_{Lkjl}^{cdu^*} O_{Rikr}^{ucd} O_{L1il}^{nu\tilde{u}}, & D_{34}^{\bar{u}_i d_j \ell_k^+} &= O_{Rkjl}^{cdu^*} O_{Likr}^{ucd} O_{R1il}^{nu\tilde{u}}, \\
E_{34}^{\bar{u}_i d_j \ell_k^+} &= O_{Lkjl}^{cdu^*} O_{Likr}^{ucd} O_{L1il}^{nu\tilde{u}}, & F_{34}^{\bar{u}_i d_j \ell_k^+} &= O_{Rkjl}^{cdu^*} O_{Rikr}^{ucd} O_{R1il}^{nu\tilde{u}}, \\
G_{34}^{\bar{u}_i d_j \ell_k^+} &= O_{Rkjl}^{cdu^*} O_{Likr}^{ucd} O_{L1il}^{nu\tilde{u}}, & H_{34}^{\bar{u}_i d_j \ell_k^+} &= O_{Lkjl}^{cdu^*} O_{Rikr}^{ucd} O_{R1il}^{nu\tilde{u}}. \tag{I.112}
\end{aligned}$$

I.6 Process $\tilde{\chi}_1^0 \rightarrow u_i \bar{d}_j \ell_k^-$

We represent different lepton flavours (e, μ, τ) by k . $u_i(d_j)$ stands for different up-type and down-type quarks ($u, c(d, s, b)$), except the top. We write down all possible $M_i^\dagger M_j$ for the four diagrams shown in figure I.5. Required couplings are given in appendices D and H. The four-momentum assignments are as follows

$$\tilde{\chi}_1^0(P) \rightarrow \ell_k^-(p) + u_i(k) + \bar{d}_j(k'). \tag{I.113}$$

$$\bullet M_1^\dagger M_1(\tilde{\chi}_1^0 \rightarrow \sum u_i \bar{d}_j \ell_k^-) = M_1^\dagger M_1(\tilde{\chi}_1^0 \rightarrow \sum \bar{u}_i d_j \ell_k^+) \tag{I.114}$$

$$\bullet M_2^\dagger M_2(\tilde{\chi}_1^0 \rightarrow \sum u_i \bar{d}_j \ell_k^-) = M_2^\dagger M_2(\tilde{\chi}_1^0 \rightarrow \sum \bar{u}_i d_j \ell_k^+) \tag{I.115}$$

$$\bullet M_3^\dagger M_3(\tilde{\chi}_1^0 \rightarrow \sum u_i \bar{d}_j \ell_k^-) = M_3^\dagger M_3(\tilde{\chi}_1^0 \rightarrow \sum \bar{u}_i d_j \ell_k^+) \tag{I.116}$$

$$\bullet M_4^\dagger M_4(\tilde{\chi}_1^0 \rightarrow \sum u_i \bar{d}_j \ell_k^-) = M_4^\dagger M_4(\tilde{\chi}_1^0 \rightarrow \sum \bar{u}_i d_j \ell_k^+) \tag{I.117}$$

$$\begin{aligned}
\bullet M_1^\dagger M_2(\tilde{\chi}_1^0 \rightarrow \sum u_i \bar{d}_j \ell_k^-) &= \\
&\sum_{i,j,k} \sum_{r=1}^8 \frac{2\sqrt{2}g_2^2\tilde{g}^2 V_{ij}^{CKM^*}}{\left[((k+k')^2 - m_W^2 - im_W\Gamma_W)((k+k')^2 - m_{S_r^\pm}^2) \right]} \\
&\left[m_{d_j} m_{\tilde{\chi}_1^0}(p.k) O_{Rijr}^{uds} A_{12}^{u_i \bar{d}_j \ell_k^-} + m_{\ell_k} m_{d_j}(P.k) O_{Rijr}^{uds} B_{12}^{u_i \bar{d}_j \ell_k^-} \right. \\
&\left. - m_{u_i} m_{\tilde{\chi}_1^0}(p.k') O_{Lijr}^{uds} A_{12}^{u_i \bar{d}_j \ell_k^-} - m_{u_i} m_{\ell_k}(P.k') O_{Lijr}^{uds} B_{12}^{u_i \bar{d}_j \ell_k^-} \right], \tag{I.118}
\end{aligned}$$

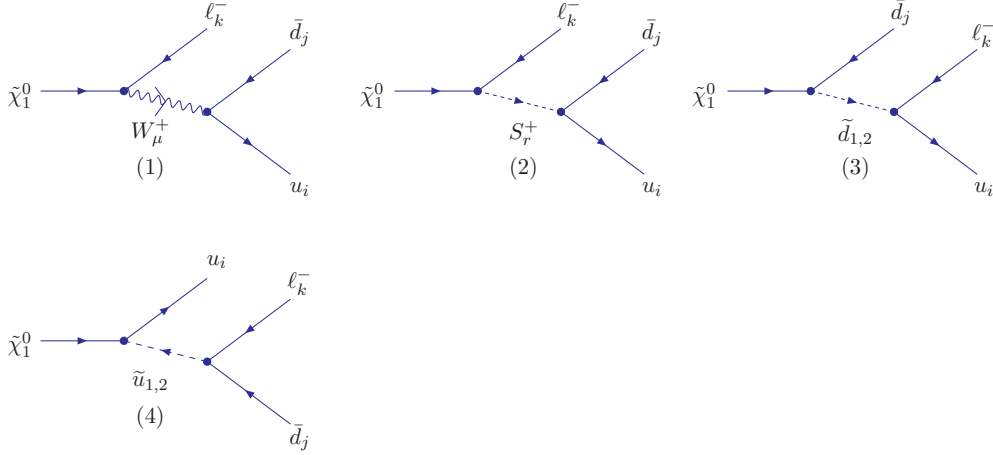


Figure I.5: Feynman diagrams for the possible three body decays of the lightest supersymmetric particle into $u_i \bar{d}_j \ell_k^-$ final states. S_r^+ are the charged scalar states of the $\mu\nu$ SMS as shown by eqn.(B.11). $\tilde{u}(\tilde{d})$ are the up and down-type squarks as shown by eqn.(B.19) corresponding to \bar{u}_i and d_j .

where

$$A_{12}^{u_i \bar{d}_j \ell_k^-} = \left(O_{Rk1}^{cnw} O_{Rk1r}^{cns^*} + O_{Lk1}^{cnw} O_{Lk1r}^{cns^*} \right), \quad B_{12}^{u_i \bar{d}_j \ell_k^-} = \left(O_{Lk1}^{cnw} O_{Rk1r}^{cns^*} + O_{Rk1}^{cnw} O_{Lk1r}^{cns^*} \right). \quad (\text{I.119})$$

$$\begin{aligned} & \bullet M_1^\dagger M_3(\tilde{\chi}_1^0 \rightarrow \sum u_i \bar{d}_j \ell_k^-) = \\ & \sum_{i,j,k} \sum_{r=1}^2 \frac{2\sqrt{2}g_2^2 \tilde{g}^2 V_{ij}^{CKM^*}}{\left[((k+k')^2 - m_W^2 - im_W \Gamma_W)((p+k)^2 - m_{\tilde{d}_r}^2) \right]} \\ & \left[2(P.k)(p.k') A_{13}^{u_i \bar{d}_j \ell_k^-} - m_{\ell_k} m_{\tilde{\chi}_1^0}(k.k') B_{13}^{u_i \bar{d}_j \ell_k^-} + m_{u_i} m_{\tilde{\chi}_1^0}(p.k') C_{13}^{u_i \bar{d}_j \ell_k^-} \right. \\ & - 2m_{u_i} m_{\ell_k}(P.k') D_{13}^{u_i \bar{d}_j \ell_k^-} + 2m_{d_j} m_{\tilde{\chi}_1^0}(p.k) E_{13}^{u_i \bar{d}_j \ell_k^-} - m_{d_j} m_{\ell_k}(P.k) F_{13}^{u_i \bar{d}_j \ell_k^-} \\ & \left. + m_{u_i} m_{d_j}(P.p) G_{13}^{u_i \bar{d}_j \ell_k^-} - 2m_{u_i} m_{d_j} m_{\ell_k} m_{\tilde{\chi}_1^0} H_{13}^{u_i \bar{d}_j \ell_k^-} \right], \quad (\text{I.120}) \end{aligned}$$

where

$$\begin{aligned} A_{13}^{u_i \bar{d}_j \ell_k^-} &= O_{Lk1}^{cnw} O_{Rikr}^{ucd} O_{Rj1r}^{dnd^*}, & B_{13}^{u_i \bar{d}_j \ell_k^-} &= O_{Rk1}^{cnw} O_{Rikr}^{ucd} O_{Rj1r}^{dnd^*}, \\ C_{13}^{u_i \bar{d}_j \ell_k^-} &= O_{Rk1}^{cnw} O_{Likr}^{ucd} O_{Rj1r}^{dnd^*}, & D_{13}^{u_i \bar{d}_j \ell_k^-} &= O_{Lk1}^{cnw} O_{Likr}^{ucd} O_{Rj1r}^{dnd^*}, \\ E_{13}^{u_i \bar{d}_j \ell_k^-} &= O_{Lk1}^{cnw} O_{Rikr}^{ucd} O_{Lj1r}^{dnd^*}, & F_{13}^{u_i \bar{d}_j \ell_k^-} &= O_{Rk1}^{cnw} O_{Rikr}^{ucd} O_{Lj1r}^{dnd^*}, \\ G_{13}^{u_i \bar{d}_j \ell_k^-} &= O_{Rk1}^{cnw} O_{Likr}^{ucd} O_{Lj1r}^{dnd^*}, & H_{13}^{u_i \bar{d}_j \ell_k^-} &= O_{Lk1}^{cnw} O_{Likr}^{ucd} O_{Lj1r}^{dnd^*}. \end{aligned} \quad (\text{I.121})$$

$$\begin{aligned} & \bullet M_1^\dagger M_4(\tilde{\chi}_1^0 \rightarrow \sum u_i \bar{d}_j \ell_k^-) = \\ & - \sum_{i,j,k} \sum_{r=1}^2 \frac{2\sqrt{2}g_2^2 \tilde{g}^2 V_{ij}^{CKM^*}}{\left[((k+k')^2 - m_W^2 - im_W \Gamma_W)((p+k')^2 - m_{\tilde{u}_r}^2) \right]} \\ & \left[2(P.k)(p.k') A_{14}^{u_i \bar{d}_j \ell_k^-} - m_{\ell_k} m_{\tilde{\chi}_1^0}(k.k') B_{14}^{u_i \bar{d}_j \ell_k^-} + m_{d_j} m_{\tilde{\chi}_1^0}(p.k) C_{14}^{u_i \bar{d}_j \ell_k^-} \right. \\ & - 2m_{d_j} m_{\ell_k}(P.k) D_{14}^{u_i \bar{d}_j \ell_k^-} + 2m_{u_i} m_{\tilde{\chi}_1^0}(p.k') E_{14}^{u_i \bar{d}_j \ell_k^-} - m_{u_i} m_{\ell_k}(P.k') F_{14}^{u_i \bar{d}_j \ell_k^-} \\ & \left. + m_{u_i} m_{d_j}(P.p) G_{14}^{u_i \bar{d}_j \ell_k^-} - 2m_{u_i} m_{d_j} m_{\ell_k} m_{\tilde{\chi}_1^0} H_{14}^{u_i \bar{d}_j \ell_k^-} \right], \quad (\text{I.122}) \end{aligned}$$

where

$$\begin{aligned}
A_{14}^{u_i \bar{d}_j \ell_k^-} &= O_{Rk1}^{cnw} O_{Lkjr}^{cdu} O_{L1ir}^{nu\tilde{u}^*}, & B_{14}^{u_i \bar{d}_j \ell_k^-} &= O_{Lk1}^{cnw} O_{Lkjr}^{cdu} O_{L1ir}^{nu\tilde{u}^*}, \\
C_{14}^{u_i \bar{d}_j \ell_k^-} &= O_{Lk1}^{cnw} O_{Rkjr}^{cdu} O_{L1ir}^{nu\tilde{u}^*}, & D_{14}^{u_i \bar{d}_j \ell_k^-} &= O_{Rk1}^{cnw} O_{Rkjr}^{cdu} O_{L1ir}^{nu\tilde{u}^*}, \\
E_{14}^{u_i \bar{d}_j \ell_k^-} &= O_{Rk1}^{cnw} O_{Lkjr}^{cdu} O_{R1ir}^{nu\tilde{u}^*}, & F_{14}^{u_i \bar{d}_j \ell_k^-} &= O_{Lk1}^{cnw} O_{Lkjr}^{cdu} O_{R1ir}^{nu\tilde{u}^*}, \\
G_{14}^{u_i \bar{d}_j \ell_k^-} &= O_{Lk1}^{cnw} O_{Rkjr}^{cdu} O_{R1ir}^{nu\tilde{u}^*}, & H_{14}^{u_i \bar{d}_j \ell_k^-} &= O_{Rk1}^{cnw} O_{Rkjr}^{cdu} O_{R1ir}^{nu\tilde{u}^*}.
\end{aligned} \tag{I.123}$$

$$\bullet M_2^\dagger M_3(\tilde{\chi}_1^0 \rightarrow \sum u_i \bar{d}_j \ell_k^-) \underset{L \leftrightarrow R}{\equiv} M_2^\dagger M_3(\tilde{\chi}_1^0 \rightarrow \sum \bar{u}_i d_j \ell_k^+)^*. \tag{I.124}$$

$$\bullet M_2^\dagger M_4(\tilde{\chi}_1^0 \rightarrow \sum u_i \bar{d}_j \ell_k^-) \underset{L \leftrightarrow R}{\equiv} M_2^\dagger M_4(\tilde{\chi}_1^0 \rightarrow \sum \bar{u}_i d_j \ell_k^+)^*. \tag{I.125}$$

$$\bullet M_3^\dagger M_4(\tilde{\chi}_1^0 \rightarrow \sum u_i \bar{d}_j \ell_k^-) \underset{L \leftrightarrow R}{\equiv} M_3^\dagger M_4(\tilde{\chi}_1^0 \rightarrow \sum \bar{u}_i d_j \ell_k^+)^*. \tag{I.126}$$

V_{ij}^{CKM} are the entries of the CKM matrix and their values are given in ref. [16].

Bibliography

- [1] Ghosh P and Roy S 2009 *JHEP* **04** 069
- [2] Ghosh P, Dey P, Mukhopadhyaya B and Roy S 2010 *JHEP* **05** 087
- [3] Haber H E and Kane G L 1985 *Phys. Rept.* **117** 75–263
- [4] Rosiek J 1990 *Phys. Rev.* **D41** 3464
- [5] Rosiek J 1995 (*Preprint* hep-ph/9511250)
- [6] Gunion J F and Haber H E 1986 *Nucl. Phys.* **B272** 1
- [7] Gunion J F and Haber H E 1986 *Nucl. Phys.* **B278** 449
- [8] Franke F and Fraas H 1996 *Z. Phys.* **C72** 309–325
- [9] Franke F and Fraas H 1997 *Int. J. Mod. Phys.* **A12** 479–534
- [10] Hempfling R 1996 *Nucl. Phys.* **B478** 3–30
- [11] Hirsch M, Diaz M A, Porod W, Romao J C and Valle J W F 2000 *Phys. Rev.* **D62** 113008
- [12] Diaz M A, Hirsch M, Porod W, Romao J C and Valle J W F 2003 *Phys. Rev.* **D68** 013009
- [13] 't Hooft G and Veltman M J G 1979 *Nucl. Phys.* **B153** 365–401
- [14] Passarino G and Veltman M J G 1979 *Nucl. Phys.* **B160** 151
- [15] Hahn T and Perez-Victoria M 1999 *Comput. Phys. Commun.* **118** 153–165
- [16] Nakamura K *et al.* (Particle Data Group) 2010 *J. Phys.* **G37** 075021